PROJECT THERMO - PHASE B PRIME

PREPARED BY
G.O. FREDRICKSON
DEPUTY PROGRAM MANAGER
J.D. SCHWEIKLE
PROGRAM MANAGER

PREPARED FOR NATIONAL AERONAUTICS
AND SPACE ADMINISTRATION,
GEORGE C. MARSHALL SPACE FLIGHT
CENTER, PROPULSION AND VEHICLE
ENGINEERING LABORATORY,
HUNTSVILLE, ALABAMA,
UNDER CONTRACT No. NAS 8-21129

APPROVED BY
P.L. KLEVATT
CHIEF ENGINEER
ADVANCE PROPULSION DEPARTMENT

DOUGLAS
MISSILE & SPACE SYSTEMS DIVISION

PRECEDING PAGE BLANK NOT FILMED.

FOREWORD

This is the Final Report of the Project THERMO Phase B Prime Program that covers the period from 1 April 1967 through 18 September 1967. This work was accomplished for the National Aeronautics and Space Administration, George C. Marshall Space Flight Center, Huntsville, Alabama, under Contract No. NAS8-21129, dated 1 April 1967.

While it is essentially impractical to mention everyone who contributed to this study, the following deserve special credit:

J. B. Blackmon	Interface Stability
Dr. I. Catton	Perturbation Analyses
R. Gershman	Propellant Transfer
L. A. Holmes	Stratification-Destratification
J. J. Hutmacher	Structural Design
D. R. Krause	High-Performance Insulation
Dr. R. A. Madsen	Boilover-Entrainment
R. F. Manoske	Carrier Evaluation
Dr. S. H. Schwartz	Boiling Heat Transfer

PRECEDING PAGE BLANK NOT FILMED.

CONTENTS

PRECEDING PAGE BLANK NOT FILMED.

FIGURES

TABLES

Section 1
INTRODUCTION AND SUMMARY

The Douglas Project THERMO Phase B Study resulted in the definition of a wide range of low gravity experiments to advance space vehicle cryogenic technology and the preliminary design of an orbital research laboratory. This laboratory, orbited with a Saturn-carrier vehicle and manned by three astronauts, was an integrated assembly of experiments from several technological areas.

The Project THERMO Phase B Prime study is intended to explore the possibilities of individual experimentation utilizing smaller carrier vehicles with experiments aimed at providing cryogenic technology required for the future manned planetary fly-by and landing missions.

The five-month program was divided into two study efforts, technology identification and experiment definition. The objective of the technology study was to determine the technology gaps and a program for resolving them in the areas of low gravity fluid mechanics, cryogenic storage, and heat transfer as applied to the manned Mars missions as currently envisioned; the S-IVC and S-IIB, and nuclear stage systems. Technology requirements were to be defined around five of the Phase B experiment areas: Propellant Transfer, Boiling Heat Transfer and Boilover, Interface Stability, Stratification-Destratification, and High-Performance Insulation. The conceptual design of flight experiments, based on the technological needs identified, was the objective of the experiment definition effort. The capabilities of four carrier vehicles, Scout, Thor Delta, Atlas, and the Workshop, were to be used as experiment constraints.

A survey of proposed Mars exploration missions and vehicle development schedules was accomplished to provide a baseline time reference for scheduling THERMO technology development. It was found that the manned flyby missions will be performed during the 1975-1980 time period with the

S-IVC/S-IIB concept. The most promising mission time occurs in 1976. The capture missions (nuclear stage) must be accomplished during the 1982-1988 time period with present vehicle concepts. Design data are needed no later than 1971 and 1973 for the S-IVC/S-IIB and nuclear stages, respectively. The early nuclear stage design start is due to an extensive vehicle development and long-term orbital test period.

Detailed discussion between THERMO and each vehicle design study team was accomplished. Several areas were identified in which the vehicle studies assumed technology, presently inadequate, to be available through AAP or other orbital experimentation by 1970. Critical technology problem areas in order of priority (based on design personnel opinion) are: cryogenic storage tank pressure control; low g venting; propellant slosh control during maneuvers; S-IIB propellant transfer technology, ullage control during propellant outflow and propellant transfer receiver tank thermodynamics; life support system heat transfer; propellant mass gaging; and some orbital engine restart technology. The requirement for orbital experimentation was found in each THERMO technology area. The general information needed for technology development was determined. Information acquisition program schedules were developed to ensure data availability in time for vehicle hardware design.

To ensure the definition of practical, feasible cost effective experiment packages, a carrier definition study was undertaken. Flight and hardware design constraints upon the experiments were delineated.

The assessment of booster costs and in-orbit payload capabilities resulted in the definition of four classes of available experiment payload weights. The nominal weights are: 350 lb, Scout; 765 lb, Atlas E and F, 1,600 lb, Thor-Delta; and 3,200 lb, Thor Agena, or Atlas SLV-3A. Payload varies with altitude, and these listed are for a nominal 200-nmi orbit.

Payload drag in orbit was determined, and a detailed study of tracking station data acquisition and experiment telemetry was accomplished. The time over stations compatible with telemetry and tape recorder dump were defined for 7-day missions originating at both PMR and KSC.

Candidate spacecraft subsystems were defined and used for experiment definition. Available flight-qualified components were emphasized. Batteries were selected for electrical power over solar cells, and a list of those available with capacities ranging from 3 watt-hr to 12 kw-hr was prepared. A building block telemetry system to be used with or without an in-flight recorder was delineated which has a 50-, 100-, or 150-channel capability. Available hardware was found for both single and dual TV camera systems. A basic guidance and ACS (attitude control system) unit was outlined, and a building block mono-propellant hydrazine APS (auxiliary propulsion system) unit resulted from trade-off studies and discussions with engine manufacturers.

An interface stability experiment, quite similar to the Project THERMO Phase B design, was defined. The system, consisting of three transparent tanks, is designed for KSC launch with a Thor-Delta class vehicle. Smaller payloads are incompatible with the requirements on minimum tank size for scaling and the weight of the test fluid, hexane. The TV data acquisition requirements negate the possibility of a PMR launch (Atlas E and F booster).

The recommended HPI conceptual experiment design is also similar to that developed during Phase B. It is a calorimeter-type tank design, which is aimed at providing evacuation, thermal, and structural insulation system performance. The experiment delineates a Goodyear system, but the concept is independent of any specific system. It is compatible with an Atlas E and F in a low Earth orbit. Another experiment design was evaluated and is reported herein. This is a simple framework which supports up to six insulation systems and will provide orbital evacuation and structural data for comparison and selection of vehicle insulation concepts.

For the vehicles surveyed, propellant transfer is incorporated only in the S-IIB design. Experiment definition, therefore, stressed application to this particular vehicle as opposed to the general experimentation of Phase B. Two different experiment packages requiring separate launches are recommended. An experiment in the area of outflow technology is designed around two spherical transparent tanks. Hexane is the experiment fluid. The other experiment, a three-tank system (all metal, no windows), using LOX, investigates receiver tank thermodynamics. The first experiment appears compatible with an Atlas E and F, or the larger Thor Delta. The three-tank experiment requires a Thor Delta or Thor Agena.

Three boiling experiment concept designs were defined and are presented; one each for a 350-, 765-, and 1,600-pound spacecraft. Based on the data derived from each, the 1,600-pound package is recommended. This experiment fulfills most of the Phase B boiling experiment objectives.

An experiment is recommended to measure the liquid level rise and entrainment during venting of fully saturated LH_2 at 15 psia to 35 psia. Data points are proposed for different combinations of depressurization rates and settling acceleration levels that are directly applicable to designing space vehicles. A method is derived for correlating and extrapolating the data to other design conditions. Television coverage of the ullage and liquid space is recommended to study the nature of the process.

An experiment is also suggested for a second orbital flight to investigate the effects of tank diameter, initial thermal stratification, and initial liquid-vapor interface disturbances on level rise and entrainment. Only minor modifications to the equipment are necessary to perform the second experiment. The experiment package conceptual design is similar to that recommended for the boiling experiment, a 1,600-pound-class payload.

Several stratification/destratification experiments are identified based on two separate orbital experiment programs. One is oriented toward the S-IVC/S-IIB inverted dome configuration, and the other to the nuclear stage. Experimentation and tank configuration is similar to the Phase B storage module.

Perturbations caused by the ACS system, variable drag, and on-board equipment was assessed in each experiment area. The experiments were found to be feasible, but some effects will always be present, particularly ACS-induced perturbations. These will be present in the Mars vehicle also. A further effort is recommended to delineate the importance of the effects and include those of importance as experiment objectives.

Similar spacecraft subsystems were utilized wherever possible for the experiment conceptual designs. This leads to a cost-effective overall experimentation program as engineering, development, and testing costs can be shared between the individual experiment packages. This will yield a much lower cost per experiment than the $6.5 million estimated. A study is recommended to ascertain total program costs. Its objective should include an investigation of the details of a plug in-plug out common spacecraft equipment and propulsion section and the definition of a total overall flight program which includes all the experimentation shown necessary to obtain the technology for Mars vehicle design.

Section 2
CRYOGENIC TECHNOLOGY REQUIREMENTS FOR PLANETARY EXPLORATION MISSIONS

Technology necessary to design manned Mars fly-by vehicles was investigated in the areas of propellant tank venting, long-term propellant storage, propellant control, life support, and propellant transfer. Vehicles considered were the S-IIB, S-IVC, and a modular nuclear stage. The nuclear stage is a Martian capture vehicle, but it was included since the current development schedule shows a need for technology existing concurrently with that of the S-IVC/S-IIB fly-by missions.

A survey of candidate missions was performed to provide a basis for determining when data would be required for vehicle design. Discussions of technology requirements between THERMO and vehicle design and management personnel for each of the study vehicles were undertaken. Design problem areas were identified; a list of information requirements was prepared; means of obtaining the information were determined; and a schedule was developed.

Little is known about many of the areas evaluated, and research must proceed in the traditional step-by-step manner. Consequently, a complete definition of data required and a firm schedule for obtaining it must evolve as research proceeds. The plan developed in this study is aimed at providing a foundation for a living program management tool which, through updating, will evolve with the evolving technology.

2.1 SURVEY OF PROPOSED MANNED PLANETARY MISSIONS

The survey showed that manned planetary landing is developing into a major post-Apollo goal with several distinct exploration periods of interest. Typical of current planning is a program relying initially on unmanned probes, and then manned encounter followed by landings. Encounter missions are feasible within the growth capability of existing programs, and new hardware is foreseen for manned landing including a modularized nuclear stage with 200-day to 300-day LH_2 storage. This hardware is also adequate for Venus missions, characteristically one-half the Mars trip time (Reference 2-1).

The manned Mars exploration periods are 1975-1980 (690-day fly-bys) and the interval between the 1981 and 1988 oppositions (capture and landing). Nine one-month launch windows are available with opposition and swingby profiles. Manned stop-over opportunities are greatly reduced in the 1990's. The best fly-by occurs in November 1976; after 1979, fly-bys are undesirable (Reference 2-2). For THERMO planning, target dates assumed were 1976 (fly-by) and 1981 (capture).

2.2 VEHICLE TECHNOLOGY REQUIREMENTS

2.2.1 Saturn S-IVC

The S-IVC study (Reference 2-3) showed that a 1975 Mars Twilight mission could be undertaken with an Orbital Launch Vehicle consisting of three S-IVC stages with design based on an assumed 1970 technology. With existing KSC facilities, the mission involves 30-day orbital cryogenic storage, docking and assembly into an Orbital Launch Vehicle (OLV) unit, and both partial and complete burns of the stages for Earth escape.

Although orbital refueling is not required, long-term orbital storage and the attendant HPI technology is necessary. There is interest in extending storage capability to one year. The Goodyear insulation system was selected. It was assumed that the J-2S engine will start in low g with any propellant condition. The spinning mode for astronaut gravity conditioning is a possibility.

Saturn/Apollo Application investigations recommended in support of the S-IVC are propellant venting schemes, propellant control during docking, and insulation performance. Propellant venting is of particular importance due to the weight involved in the APS units.

2.2.2 Modularized Nuclear Stage

Douglas Nuclear Stage Study personnel were contacted resulting in the identification of the same general technology requirements as for the S-IVC. The study (Reference 2-4) investigated Mars Capture and Landing missions of about 480 days' duration in the 1982-1986 time period.

Five 33 by 70-foot nuclear stages are assembled in orbit; three stages are used for Earth escape; one for Mars deceleration; and one for Mars escape. Propellant storage times vary from 80-120 days for the Earth escape stages to 240-260 days for Mars deceleration and escape stages. There are no transfers of propellant in orbit, and spinning to maintain an artificial gravity is not planned. Provision for an engine after-cooling period is necessary, although restart is not planned.

Because design of the stages will emphasize design optimums as opposed to the modification philosophy characteristic of the approach to the fly-by hardware design, more detailed technological information will be required. Propellant storage and venting are the most severe problems due to the extremely long storage times involved and the pressure stabilized tankage design. The latter necessitates an orbital blowdown operation. Mass gaging in a nuclear environment and nuclear heating of the propellant are problems unique to this stage.

The vehicle development schedule currently envisioned is: Stage Requirements Study - 1969; Program Definition - 1973; First Orbit Flight - 1977; and Planetary Flight - 1982. This indicates that a large part of the design data must be available during 1973, the date used for THERMO planning.

2.2.3 Saturn S-IIB

This study (Reference 2-5) investigated the feasibility of an S-IIB stage to perform the same missions as the S-IVC. Orbital rendezvous and assembly is required along with orbital propellant transfer from three LO_2 tankers. The vehicle then burns all of its propellant for Earth escape. A total of 10 days of LH_2 propellant storage is involved with up to 163 days for a LO_2 tanker. LO_2 will be on board the assembled orbital launch vehicle for 2-1/2 days.

A list of problems requiring further design data was presented to THERMO personnel during discussions with the NAA study team. They are: (1) Low g Storage and Venting (S-IIB and Tanker): thermodynamic separator, direct vent penalties for trade-offs with thermodynamic separator, heat distribution in tank, effects of low g slosh, degree of stratification, choice of transverse or spin mode for settling, mixer requirements, and common bulkhead gas barrier performance; (2) LO_2 Transfer: heat transfer data between gas and liquid to verify nonvent transfer concept, outlet designs to prevent vapor pull-through, length of time to transfer at 10^{-4} g/g_e or less, slosh wave damping during transfer, and methods of dissipating kinetic energy in the receiver tank; (3) Mass Gaging (S-IIB and Tanker); (4) High-Performance Insulation: thermal performance of the Goodyear and Linde systems, purge pressure differential limitations, time to outgas, and absorption and absorption characteristics of insulating material.

2.3 TECHNOLOGY REQUIREMENTS AND DEVELOPMENT PLAN

2.3.1 Technology Gaps

Each of the vehicles will require similar technology with the exception of the S-IIB which adds LO_2 orbital transfer to the list of problems. These requirements in order of priority (Survey consensus) are summarized in Table 2-1.

Propellant storage and low g venting were considered the foremost problems by each vehicle design team with solutions assumed to be available in the early 1970's. Valid insulation performance data is needed, although one S-IVC design prescribes a shadow shield in lieu of HPI, but the resulting short orbital time (110 hours) necessitates rapid launches and launch facilities not presently available. The trade-offs between stratified storage, a mixer, and a thermodynamic separator are of interest. A refrigeration system is a possible requirement for some nuclear stage missions.

The low g venting problem would be circumvented by a thermodynamic separator. However, the nuclear stage mission involves a tank blowdown upon injection into orbit since the structure is pressure-stabilized during launch. Therefore, venting data are required.

Table 2-1

VEHICLE DESIGN TECHNOLOGY REQUIREMENTS

CRYOGENIC STORAGE TANK PRESSURE CONTROL

1. Insulation System Performance
2. Refrigeration and Thermal Control System Performance
3. Fluid Orientation in Low G
4. Thermal Stratification and Effect on Pressure
5. Mixer Design and Performance
6. Thermodynamic Separator Performance

LOW G VENTING

1. Settling Techniques
2. Degree of Boilover During Venting
3. Degree of Entrainment During Venting
4. Performance of Passive Separators

PROPELLANT SLOSH CONTROL DURING MANEUVERS

1. Degree of Induced Slosh
2. Degree of Propellant/Vehicle Dynamic Coupling
3. Ullage Thermodynamics - Pressure Collapse

ULLAGE CONTROL DURING PROPELLANT OUTFLOW

1. Interface Dynamics During Outflow
2. Outlet Configuration
3. Flow and Acceleration Schedule

PROPELLANT TRANSFER RECEIVER TANK THERMODYNAMICS

1. Analytical Models
2. Scaling Procedures
3. Lox Data
4. Inlet Configuration
5. Prediction of Pressure Transients during Inflow
6. Control of Inlet Inertia

LIFE SUPPORT SYSTEM DESIGN

1. Subcritical Storage of Cryogens
2. Boiling Heat Transfer Characteristics

PROPELLANT MASS GAGING

1. Gage System Performance on Chemical and Nuclear Vehicles

ORBITAL RESTART OF ENGINES

1. Settling Technique
2. Low G Tank Repressurization

Propellant slosh control during maneuvers is common to all the vehicles due to the requirement for orbital docking and assembly. The vehicle perturbations, caused by slosh, which must be considered to affect the final rendezvous, are inadequately predicted by current techniques. The propellant outflow and receiver tank thermodynamics problems stem from the S-IIB alone. The efficient transfer of LO_2 is mandatory for the successful completion of the mission.

Long-lifetime crew support systems are required. The THERMO survey could not identify precise (heat transfer and fluid mechanics) technology gaps in these systems which would influence mission feasibility since the requirements of equipment manufacturers were unavailable. Data requirements in this area appear to involve problems similar to propellant storage.

Propellant gaging is common to the three vehicles. The nuclear vehicles will require a gage operable in a radiation field. A requirement for orbital verification of gage performance was indicated.

The orbital engine restart problem is minimized by the J-2S engine capabilities. It appears that some problems may occur in this area during idle-mode operation and for the nuclear vehicles. However, requirements are necessarily vague at this stage of vehicle design.

2.3.2 Technology Development Plan

Table 2-1, Design Technology Requirements, was expanded to list the information needed to adequately develop this technology. This level of detail is somewhat uncertain due to the limited knowledge available in each area and the limitations on the survey scope. The results of this work are presented below, along with data acquisition schedules encompassing the five THERMO areas of interest. Also shown are the methods of information acquisition which may be used.

The schedules are based on three key dates: 1 January 1968, start; 1 January 1971, S-IIB/S-IVC design start; and 1 January 1973, Nuclear Stage design start. The 1971 date appears to be the latest that S-IVC/S-11B design may begin for the preferred 1976 mission with the current 5-year development schedule (Section 2.1). A 1975 mission necessitates that technology be available one year earlier. Another significant ground rule used was an 18-month period for the design and launch of a flight experiment. This approach results in a schedule reflecting the best case; maximum time available for obtaining information with minimum length flight programs. No margin is included for error, delays, or an earlier S-IIB/S-IVC design start date, a possibility difficult to assess at this time. These pads, not included in the schedules, must of necessity be somewhat arbitrary and will vary according to the complexity of the technological problem involved. An area such as propellant storage, of high priority with many uncertainties, should clearly have a higher contingency time factor included than design verification tests.

2.4 CRYOGENIC STORAGE TANK PRESSURE CONTROL

Five general technology gaps were identified for this vehicle problem area.

2.4.1 HPI Insulation System Performance

Figure 2-1 shows the information desired by the vehicle designers surveyed. Although some items are independent of insulation type and configuration, the majority are not, and must be evaluated for a given system. The S-IVC and S-IIB have the MSFC-Goodyear system whereas nuclear stage work has revolved around an NRC-2 and a Lockheed system. Since the Survey vehicles are conceptual, the list was limited as much as possible to configuration-insensitive items.

The interstitial pressure history directly affects insulation system thermal performance. The ability of current designs to evacuate to less than 10^{-4} Torr is uncertain. Also, the effects of rapid external pressure decay during boost is in question. Ground tests suggest that insulation adsorption and absorption properties will significantly affect interstitial pressure and thermal performance. The magnitude of possible increases in tank leakage occurring during boost on ultimate insulation performance is of interest.

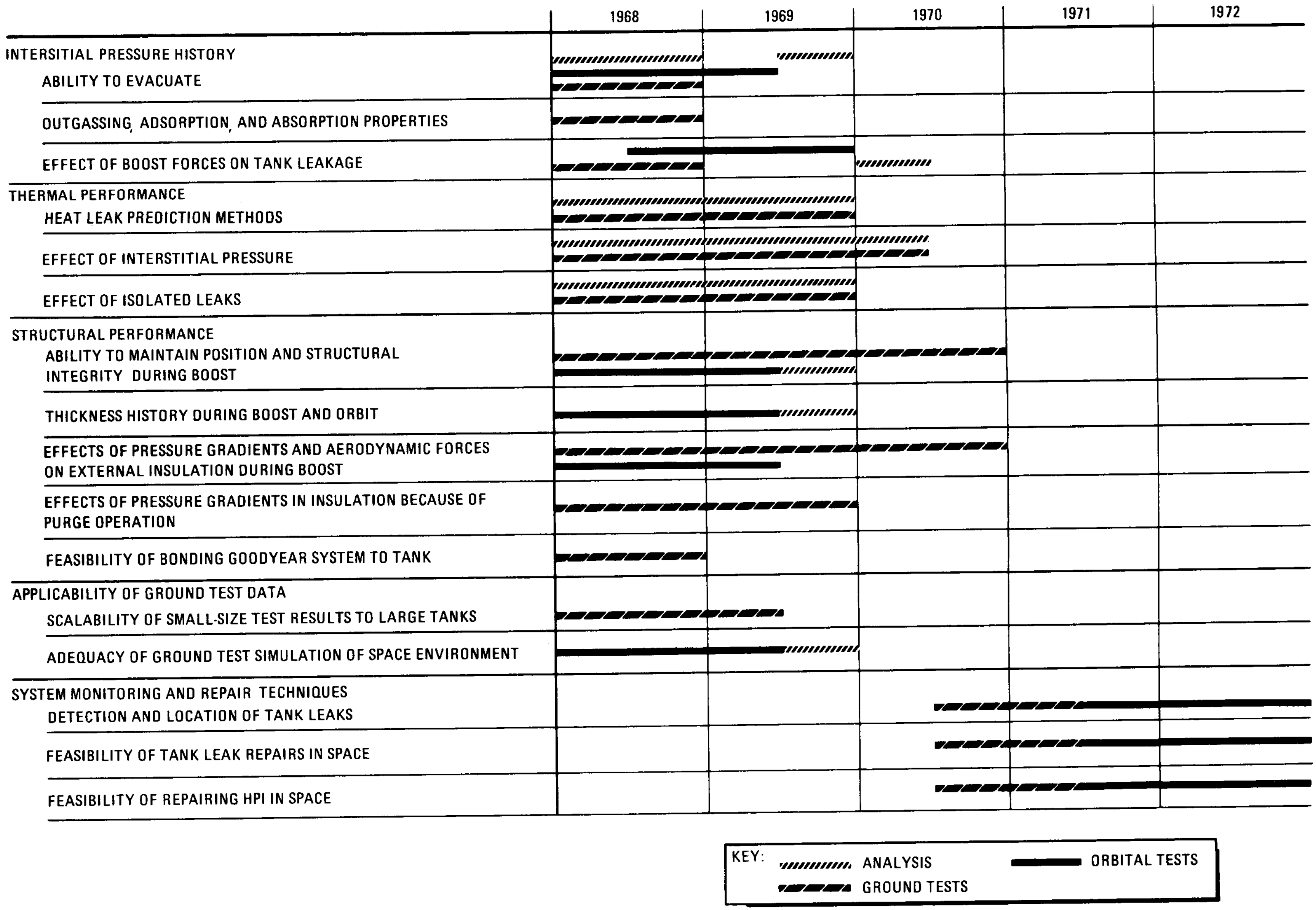

Figure 2-1. Schedule of HPI System Technology Requirements

Extensive thermal performance data on some HPI systems is available indicating the effect on heat transfer of perforated material, placement of insulation away from the tank wall, layer density, blanket joints, and layup methods. More information is needed, but it appears that requirements will evolve from current MSFC studies. The development of improved methods of predicting heat leaks would be valuable. An indication of the effect of interstitial pressure on the thermal performance is available. However, an improvement is necessary. Also, the area of the insulation degraded by an isolated tank leak is not known for the Goodyear insulation.

Structural performance information, the ability of the insulation to maintain structural integrity during boost, is needed. The insulation thickness history during boost and orbit is of interest to determine the effect of fluff or springback on insulation performance. The effect of aerodynamic loads on the externally installed Goodyear system (S-IIB) is desired. Technology appears to be available to avoid excessive purge-gas pressure gradients within the insulation for some HPI types successfully purged on small tanks. However, uncertainties exist for the large Goodyear/S-IIB application. The feasibility of bonding Goodyear HPI to the S-IVC dome is uncertain.

One of the greatest areas of uncertainty encountered was the applicability of ground test data to full-scale tankage/insulation systems. Some ground experiments indicate a discrepancy between large and small test tank data. Scalability of data should be improved over the arbitrary multiplication factor currently available for some systems. The applicability of ground test data to space conditions was questioned.

Interest was expressed in the feasibility of monitoring and repairing the tank/ HPI system for Mars capture stages (see also Reference 2-6). Improved leak detection methods are also needed for preflight checkout.

HPI performance data, scheduled in Figure 2-1, should be available during the S-IIB/S-IVC program definition phase, prior to 1971.

Interstitial pressure and thermal performance are intimately related and can be investigated concurrently for the insulation systems of interest. Ground performance testing in conjunction with existing analytical techniques and tests of panel layups provide the ground work for orbital performance verification testing.

Some structural performance data can be obtained through coupon and subsystem tests, but should be verified by testing through exposure to actual launch conditions; i. e., all environmental factors acting simultaneously. A long period of ground tests is shown to reflect intermittent testing during insulation development and vehicle definition programs.

Early assessment of ground test data validity through orbital test provides important benefits to S-IVB/S-IVC design. Early refinement of vehicle performance expectations and venting penalties will result from the orbital and verified ground test data. More cost effective insulation development test planning should also follow.

Propellant tankage repair technology, relatively unimportant for the fly-by missions but a possible safety consideration for captive missions, is scheduled to coincide with nuclear vehicle development.

2.4.2 Refrigeration and Other Termal Control Systems

Design interest was expressed in four items: (1) degradation characteristics of surface finish optical properties; (2) shadow shields; (3) refrigeration systems; and (4) forced cooling of heat shorts.

2.4.3 Fluid Orientation in Low G

Areas where information is needed are shown in Figure 2-2.

Degree of Fluid Motion Following MECO

Wave amplification at MECO may cause the vent outlet to become covered with liquid and also induce disturbing forces and moments on the vehicle. Wave amplification data is needed as a function of tank and baffle geometry,

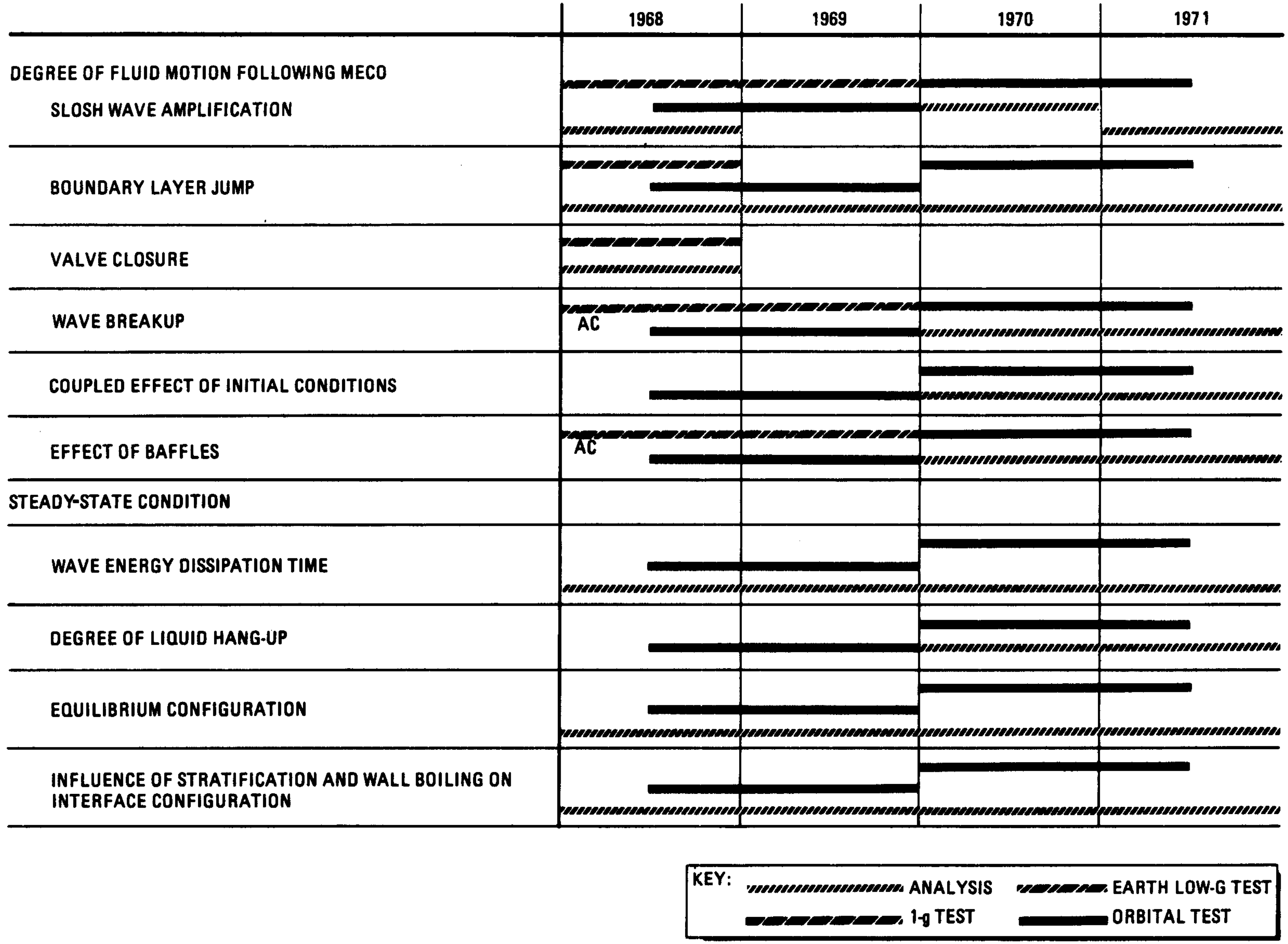

Figure 2-2. Fluid Orientation in Low-G Technology Schedule

g levels, phase angle, and rate of g level change. Boundary layer kinetic energy also causes wave amplification at MECO. Correlated data for baffled tanks is required for vehicle optimization.

Valve closure causes a spike of propellant at the liquid interface which dissipates into a low amplitude wave. Globules may be thrown into the ullage causing pressure collapse if they undergo heat and mass transfer or pressure rise by impinging on a hot tank wall. This may occur in the partial burn S-IVC stage.

At MECO, high amplitude waves may roll up the tank wall. Wave breakup will occur if the waves strike baffles or internal hardware. Information on the degree of wave breakup for the tanks of interest and its effect on tank pressure is needed to assess potential pressure changes.

The fluid motion at MECO affects the steady-state condition of the liquid which in turn influences computations of thermal energy distribution, resettling time and g levels, and slosh forces. The importance of this initial motion on the steady-state configuration should be assessed.

Steady-State Condition

Wave dissipation times are required for optimum sizing of auxiliary propulsion systems and baffles. The designer requires damping factors as a function of amplitude, g level, and internal configuration. Correlated 1-g experimental data and extensive analyses are available. Additional analyses of the nonlinear case and correlated low g wave motion data are necessary.

Liquid may collect on internal hardware or the top of the tank. Subsequent venting may lead to liquid loss. Information on the degree of importance of this problem should be assessed.

Many different steady-state liquid configurations are possible; vapor bubbles in the center of the tank or beneath baffles, portions of the liquid at both the tank top and bottom or all the liquid at one end. Numerical programs are available for the prediction of liquid interface configurations but experimental verification is required.

Scheduling

The initial fluid motion phenomena occurring at MECO, such as wave amplification, break-up, and baffle effects, may be studied in drop tower and aircraft tests. These experiments are scheduled for the 1968-69 time period and are supported by parallel analyses. Based on the preliminary experiments, scaled in-orbit tests are scheduled for 1968-1970 followed by vehicle design analyses. Since the nuclear stage tank geometry will be significantly different from the S-IVC and S-IIB geometries, separate tests are required.

The steady-state condition phenomena can only be tested in orbit. Supporting analyses are scheduled previous to and after the in-orbit tests. These are shown continuously to reflect the intermittent research efforts progressing along with the orbital testing.

2.4.4 Thermal Stratification and Mixer Performance

2.4.4.1 Thermal Stratification

The all-heat-to-vapor model is usable for design, but doubt exists as to the degree of its overconservative results (large number of vents). Reference 2-7 contains a detailed survey of stratification models and their limitations. Figure 2-3 lists data to evaluate these tools and develop accurate prediction techniques.

Identification of Heat Transfer Modes

Stratification strongly depends upon the heat transfer mode. Without convection, stratification is a simple conduction problem. Initiation of convection is defined by stability criteria generally involving a critical Rayleigh number. Those available, for idealized situations, show that convection may not exist in interplanetary mission tankage.

If convection exists, the separation of the convective regimes must be known. For semi-infinite fluid on a vertical wall, three regimes are defined: viscous, and the laminar and turbulent boundary layer. For tankage, this is not

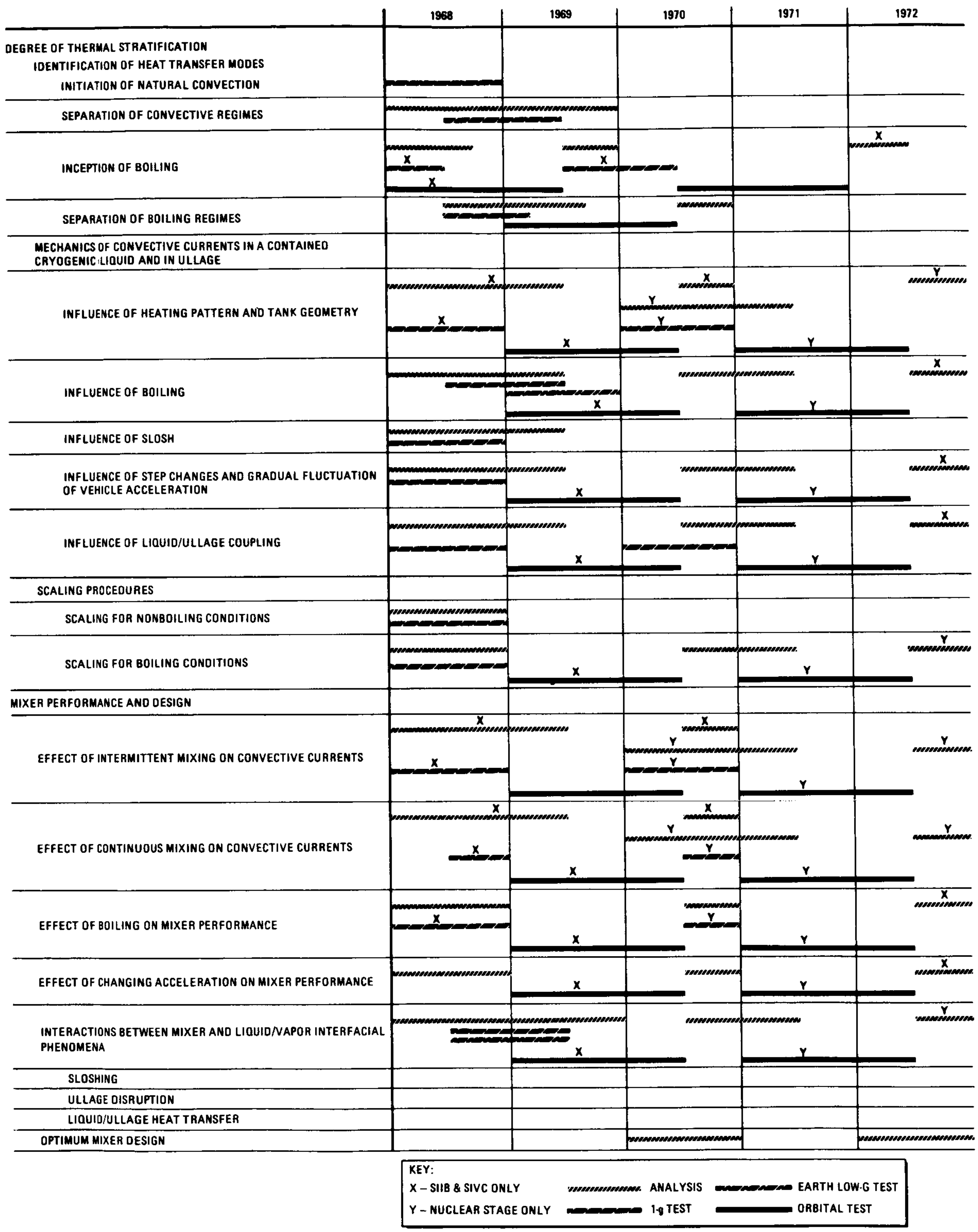

Figure 2-3. Schedule for Stratification and Mixer Performance Technology

always valid. Idealized solutions show a number of circulation modes. In some, near-boundary-layer flow exists and in others, general circulation. To assess design tools, the separation between the regimes must be known.

Validity of nonboiling stratification predictions is dependent upon an understanding of incipient boiling. Boiling may occur in orbiting tanks at low heat fluxes. Correlations of incipience with gravity, pressure, degree of subcooling, and surface conditions are needed.

The effect of boiling on stratification is undetermined. It appears that deviations from nonboiling predictions are less serious at heat fluxes near incipience than in the violent boiling regime. To assess this influence, it is necessary to determine the effect of gravity on boiling, and then the degree of agitation produced. Separations between isolated and nonisolated bubble regimes and film boiling should be made. This may be important if boiling occurs at low heat fluxes. Little energy is available for vaporization; tank wall boiling may be very different than that observed at 1 g/g_e. Low heat flux boiling may not seriously change the nonboiling stratification pattern, greatly simplifying the stratification problem. If this is not the case, boiling data is valuable in developing boiling stratification models.

Analysis of Convective Currents in a Two-Phase Fluid

The tank energy distribution and heat transfer mode are coupled and cannot be entirely separated. By understanding the current mechanisms and magnitude, the energy distribution and tank pressure history can be established.

Convective patterns are a function of tank configuration and heating patterns; localized heat shorts can dominate the flow. Since the vehicles have dissimilar geometry and heating patterns, these parameters must be understood.

Boiling appears likely, hence its influence on the energy distribution must be understood. Experiments indicate that a large portion of heat transferred during boiling goes directly into the ullage and promotes severe stratification.

The effect of sloshing on stratification is unclear. Two sloshing extremes have been observed: laminar (minimal effect) and turbulent (promotes mixing). Since acceleration level changes will be present, an understanding with respect to stratification is required. Also, some sloshing, i. e., boundary layer jump, is coupled to the convection processes and must be understood relative to convection.

In some cases, the tank/acceleration vector will be nearly constant resulting in quasi-steady state convection. However, elliptically orbiting vehicles experience a significant variation in drag. Vehicle maneuvering will result in periodic acceleration step changes. The influence of these variations on convection must be considered.

Ullage foreign gas and the relative heating of the liquid and ullage cause differences in stratification. Liquid/ullage coupling is influenced by convective currents in both the liquid and ullage and the tank wall heat transfer mode. An understanding is required. Surface curvature at low Bond number conditions is an additional factor.

Non-boiling and Boiling Scaling Criteria

It is desirable to employ experimentally devised design data, hence, a need for scaling. This scaling lends itself to a separation into these domains. Scaling for each, including both acceleration variations and free surface sloshing, is required. The importance of the various parameters should be defined.

2.4.4.2 Mixers

An understanding of phenomena associated with mixing (Figure 2-3) is necessary to properly design systems for pressure rise rate reduction. A knowledge of the heat transfer mode, discussed above, is required.

Intermittent mixing has been considered. The convective currents produced as a function of the mixer location, jet configuration, and the initial stratification currents must be understood. Tests show that the thermally stratified layer resists mixing; a low mixing rate will not overcome stratification. Also, a pressure response lag, important to mixing schedules, occurs.

For sizing continuous mixers, the combination of forced convection and natural convection must be understood. Mixing is assured by brute force design, but a severe mixer weight and power penalty may be incurred. The amount of residual stratification as a function of the mixer size, nozzle location and configuration, tank geometry, and heating pattern is needed.

Because boiling is likely, its influence on the convective current produced by mixing is required. No applicable experimental data has been obtained. Concern over the effect of localized vapor pockets on tank pressure has been indicated.

Acceleration variations may be important to the convective processes and their effect on mixing is unclear. As with stratification, the possibility of using an average acceleration level for mixing must be considered.

An important consideration for mixing in space is the influence of forced convective currents on the liquid/vapor interface. The liquid momentum may disrupt the ullage. Sloshing may be significant, and the interface heat transfer may be changed. This heat transfer may also be changed by the forced convective currents at the surface, even without ullage disruption. These effects must be considered.

2.4.4.3 Scheduling

The analyses and tests needed to bridge the stratification/destratification technology gaps are scheduled in Figure 2-3. A design approach was taken with the schedule aimed at solving specific design problems. With this scheme, a requirement for a complete understanding of all of the facets of the problem can be alleviated by using proper scaling techniques in conjunction with subscale tests. A phenomenological approach was ruled out because of the complexity of the problem area. It did not appear that a sufficient understanding could be obtained in time to meet the design needs.

With the design approach, the areas of boiling and scaling become important and require immediate attention. Boiling has been anticipated at very low heat fluxes at low gravity levels, and therefore the assumption of natural convection with high-performance insulation may be erroneous. The inception of boiling must be known to define the wall heat transfer mode.

Because the transient times for the inception of boiling are out of the range of low gravity Earth facilities, orbital testing is necessary. Analyses and Earth-based experimentation should be accomplished to define appropriate scaling parameters for both boiling and nonboiling situations providing the basis for orbital tests. The relative importance of the influencing parameters is required to assess the effects of imperfect scaling.

Because of the difference in geometry between the S-IIB/S-IVC (inverted dome) and the Nuclear Stage (hemispherical dome), the schedule, aside from boiling and scaling, has been separated into two phases. To scale the data, geometric similarity must be maintained; thus, the separation of the two problems. Although the S-IIB and S-IVC may have significantly different heating rates and patterns, both could be simulated with one orbital test through appropriate heater design.

The analyses, ground and drop-tower test periods indicated represent intense effort. The break points shown are periods of logical reduced effort. Drop-tower tests are contingent on analytical and ground test results.

Stratification and mixing low g venting experiments are logical companions of a single system and, therefore, should be scheduled as such. For the S-IIB/S-IVC phase, a single orbital experiment may be sufficient to provide data for both stratification and mixer design. The number of experiments depends on carrier availability and the analytical results.

The Nuclear Stage may require only one orbital experiment. The number required is contingent on the analyses and ground tests as well as the results of the S-IIB/S-IVC orbital experiment. The orbital experiment(s) for the Nuclear Stage must be initiated by January 1971.

2.4.5 Low G Venting

Settled cyclic venting, needed for the nuclear stage orbital blowdown, is the only alternative available for the S-IVC/S-IIB in the absence of a workable thermodynamic separator. Consequently settling, boilover, and entrainment data should be available for use on these stages.

2.4.5.1 Mechanics of Settling

Technology development should be aimed at providing a reduction in ullaging system weight penalties derived with current techniques.

Taylor instability of the interface governs the initial liquid flow, axisymmetric or asymmetric, upon thrust application. The liquid configuration at instability, a function of the Bond number and prior propellant disturbances, influences settling time. The axisymmetric flow case has been determined analytically and experimentally verified. Low g data (employing models) on the asymmetric modes and the effect of initial liquid motion is required.

The resettling flow in large, smooth tanks is approximately inviscid above a critical Bond and visco-gravitational number (Reference 2-7). In baffled tanks, however, the viscous dissipation and liquid flow field will be different. Scale model test data varying Bond number in baffled and unbaffled tanks is required. The significance of viscous dissipation should be determined.

Impact of the liquid causes bubble formation accompanied by turbulent dissipation which eventually subsides to laminar wave motion. Scaling analyses and low g data (baffled and unbaffled tanks) on bubble distribution, coalescence, breakup, and rise times as well as the turbulent dissipation time are required.

Laminar wave dissipation is well understood, but low Bond number nonlinear sloshing requires further study, especially the effects of baffles. Wave energy dissipation rates and wave modes require definition.

Resettling may be accomplished to meet the criteria of minimum propellant consumption or minimum time, or a compromise between the two. The information indicated above should be adequate to optimize system design.

The schedule, Figure 2-4 shows analyses and drop-tower and aircraft tests preceding two in-orbit tests of propellant settling phenomena. In order to design efficient orbital tests and to provide the vehicle designer with an improved preliminary technique for determining resettling time, aircraft tests are required. This information will also be useful in determining

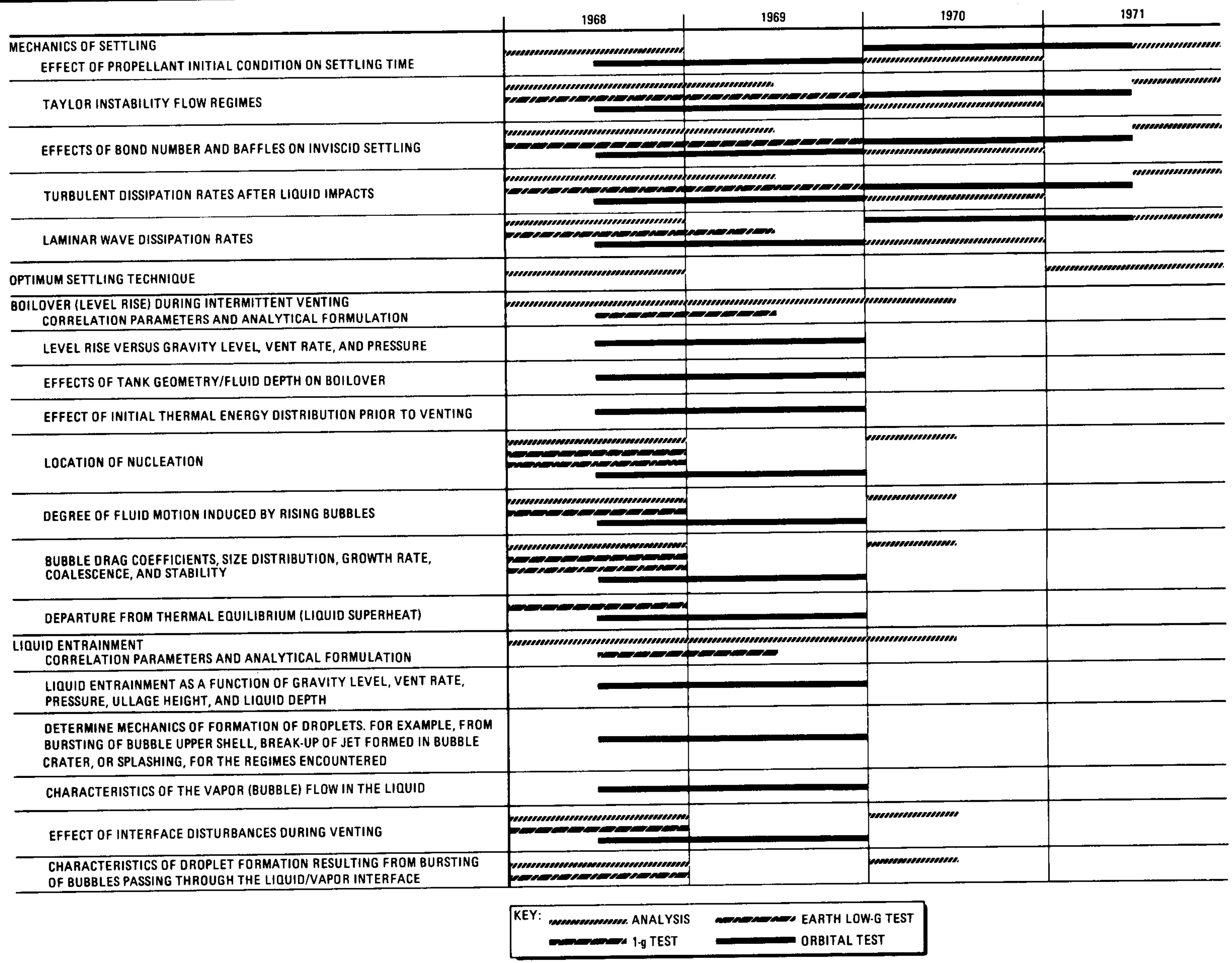

Figure 2-4. Schedule for Low-G Venting Technology

settling times required for other in-orbit experiments such as stratification/ destratification and propellant transfer. Analyses follow the in-orbit experiments which are directed towards solving the specific vehicle settling design problems.

2.4.5.2 Boilover and Entrainment

The S-IVC/S-IIB require venting of essentially full propellant tanks with cyclic direct venting. The problems of liquid loss by boilover due to liquid level rise, and entrainment of liquid in the vented vapor are encountered. These problems may be severe.

There are presently no satisfactory techniques available for predicting level rise and entrainment under conditions of reduced gravity. Present design assumes complete vapor entrainment to determine liquid level rise. A conservatively large acceleration avoids entrainment. These techniques, satisfactory for S-IVB (large ullage volume) result in excessive S-IVC/ S-IIB A. P. S. requirements. It is unlikely that a purely analytical description of level rise and entrainment will evolve, due to problem complexity, but development of dimensionless correlations appears promising. An understanding of the processes involved and the design information desired can only come from orbital experimentation.

<u>Boilover</u>

Figure 2-4 lists the information required to establish the desirability of direct venting for nearly full tanks and accumulate design data.

Several correlations are available to predict the expansion of a bubbly mixture at normal gravity where bubbles are introduced from the bottom of the container. A modification of these might prove satisfactory for the reduced gravity situation. Further investigation is necessary.

Design data required are the level rise as a function of the vent rate, gravity level, and pressure for a prescribed tank geometry. The influence of tank geometry and fluid depth must also be available. Thermal stratification will tend to decrease the level rise compared to fully saturated liquid. Therefore, the effect of the initial temperature profile must be known.

Some understanding of the processes responsible for level rise is necessary to aid in developing analytical correlations and interpreting data. The mechanisms must also be studied to establish the flow regime. Several may be possible for the boilover process. Extrapolation of test results is not possible unless the flow regime under test conditions is identical to that of the vehicle.

A number of the basic mechanisms of the process are listed in Figure 2-4. The location of bubble nucleation defines the location of energy removal by evaporation, and the dispersion of the gaseous phase in the liquid. This information is basic to any analysis. The degree of fluid motion induced by rising bubbles must be accounted for. Large bubbles will stir the liquid resulting in convection and removal of small bubbles that would not otherwise be removed by buoyancy. The velocity of the vapor phase in passing through the liquid is an important entrainment parameter and directly determines level rise. This velocity is determined by the bubble drag coefficient, which is in turn related to bubble size and interaction. Bubble size is related to bubble growth rate, coalescence, and stability (break-up). Bubble growth rate is a direct function of the liquid superheat.

Entrainment

As with the liquid level rise, several correlations are available to predict liquid entrainment for a bubbly mixture at normal gravity where bubbles are introduced from the bottom of the container. If the mechanism of entrainment is not grossly different for reduced gravity situations, these correlations can probably be modified for design use. More investigation is necessary.

The design information desired is the entrainment as a function of vent rate, gravity level, pressure, tank geometry, and fluid depth. It appears that the height between the liquid interface and the vent outlet is very important. It is desirable to know the effect of initial disturbances of the liquid-vapor interface (e. g., sloshing) because it is desirable to initiate venting as soon after settling as possible.

The basic mechanisms responsible for entrainment should be studied for the same reasons as for boilover. Basic mechanisms of importance are listed in Figure 2-4. Studies indicate that there are several mechanisms responsible for the formation of entrained droplets. The entrainment is significantly more severe if the droplets are formed by splashing or jet breakup than bursting of the bubble shell. The analytical description applicable also varies with the mechanism responsible. Also, the nature of the vapor flow through the liquid significantly influences entrainment. The most predominant mechanism of droplet formation at normal gravity is the breakup of the jet formed in the crater of a bursted bubble. Therefore, it seems desirable to study the influence of gravity on this process.

2.4.5.3 Scheduling

A schedule for this technology is presented in Figure 2-4. An understanding of these processes and the design information desired can only come from orbital experimentation.

The objective of the program (Figure 2-4) is to fly an orbital experiment as soon as possible to determine the desirability of cyclic venting nearly full tanks, and to determine the nature of the process so that additional analysis and experimentation can be planned. Sufficient time is available for a second orbital experiment after the initial experiment. Ground testing is concerned with studying fundamental mechanisms of the process to aid orbital experiment planning and establishing analytical descriptions.

There are several reasons supporting orbital experimentation. It is important that the flow regime, i.e., the nature and distribution of the flow of the two phases within one another, be established under the actual conditions of operation. Flow characteristics can change drastically with transition to a different regime. Data from one flow regime cannot be scaled to another. Two flow regimes have been observed in level rise studies at normal gravity and three for entrainment. It is quite possible that gravity reductions might cause the existence of others. Further, it has been estimated that the transient times involved in boilover and entrainment under reduced gravity are in the order of 15 sec to 100 sec, a time not available with ground test techniques. Once flow regimes and transient times of the processes have been determined in orbit, it can be ascertained if ground tests are useful.

Boilover

It has been considered that some analytical appreciation of the boilover/entrainment problem is necessary to plan a logical orbital experiment. Therefore, effort should begin immediately to establish correlation parameters for liquid level rise and entrainment. Since these should be valid both at normal and reduced gravity, testing at normal gravity should be performed for initial verification. Ultimately, however, the correlation techniques must be verified under actual reduced gravity conditions of operation. Once the validity of the correlations has been established, it can be ascertained if useful data can be obtained under conditions of normal gravity.

Normal gravity testing has been proposed in Figure 2-4 to study the basic mechanisms of the process to aid in developing correlations. In addition, low-gravity ground tests could prove useful to study the location of nucleation and bubble characteristics which will be influenced by the gravity level. Liquid hydrogen should be employed to study the location of nucleation and departure from thermal equilibrium. Other fluids can be employed elsewhere.

Liquid Entrainment

Evaluation of techniques to correlate data on liquid entrainment during venting, and the effect of interface disturbances on entrainment should begin immediately. Ground testing should be conducted to verify these techniques. Additional analysis and testing should be performed to study the most likely mechanism of droplet formation. Analyses are necessary to plan the orbital experiment. As with boilover, evaluation of correlation techniques must be accomplished by orbital testing.

2.5 PROPELLANT SLOSH CONTROL DURING MANEUVERS

The problem of predicting the behavior of the large Mars vehicles subjected to internal propellant slosh (orbital docking) is encountered. Figure 2-5 lists information required to develop design tools.

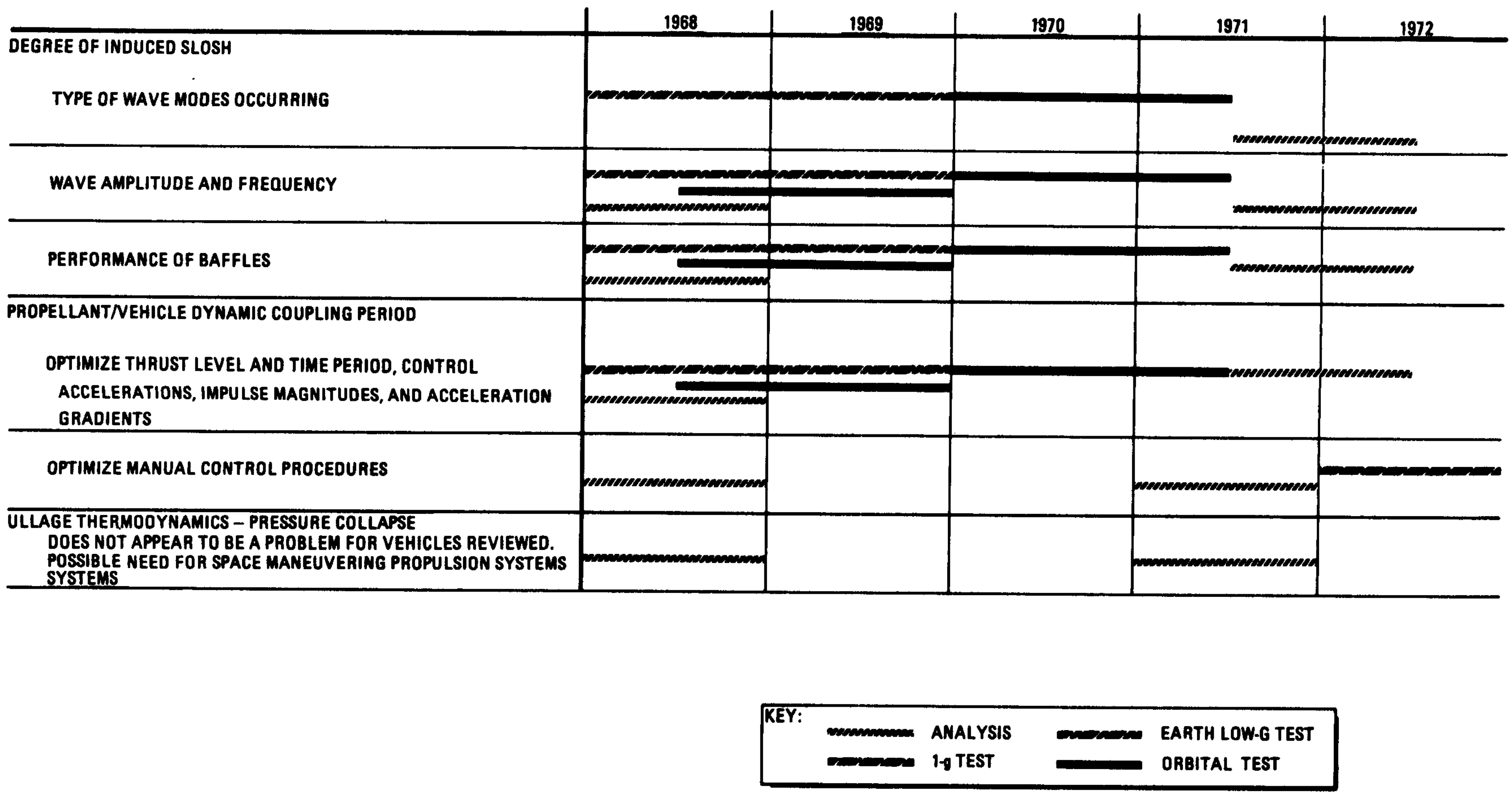

Figure 2-5. Propellant Slosh Control Technology Schedule

2. 5. 1 Degree of Induced Liquid Slosh

Docking accelerations can cause a high degree of sloshing which may be nonlinear, nonplanar, and/or rotating waves accompanied by bubble ingestion and globule production. The propellant and ullage could become completely mixed.

Liquid motion in low g due to high impulse forces is one of the least understood areas of low g fluid dynamics. An understanding must rely on low g tests with tanks and accelerations simulating the vehicle conditions. Data on bubble formation, globule production, wave modes, and baffle effects are needed.

2. 5. 2 Propellant/Vehicle Dynamic Coupling

Liquid movement causes the position of the vehicle to shift, inducing corrective maneuvers, aggravating the docking problem. The increased ACS demands may exceed the available propellant since estimates are based on total impulse changes only. Also, the ACS attempting continuous control, may cause even greater liquid motions.

Propellant/vehicle dynamic coupling must be assessed. Thrust levels, control accelerations, impulse acceleration magnitudes, acceleration gradients, and thrust application time periods must be defined.

During final rendezvous, manual control may be used. The magnitude of the manual control problem should be assessed in light of propellant/vehicle dynamic coupling.

2. 5. 3 Scheduling

Figure 2-5 schedules preliminary information on low g liquid sloshing obtained from drop tower and aircraft tests. This data and the supporting analyses will provide the foundation for efficient orbital experiments. Further analysis will then be required, especially numerical programs, in order for the vehicle designer to optimize baffle geometry and control accelerations. These problems appear to be especially critical with docking and assembly of large, off-loaded stages.

2.6 ULLAGE CONTROL DURING PROPELLANT OUTFLOW

Ullage control during outflow, particularly in regard to suction dip, has been designated a significant technology gap by the S-IIB study. The study estimated that technology improvements in outlet configuration and flow scheduling can reduce the transfer ullaging propellant required by an order of magnitude. Furthermore, it was assumed that a Bond number of 100 is needed during bulk transfer. The ullaging propellant could be further reduced if lower Bond numbers are found acceptable. The suction dip problem may also be encountered in the nuclear stage where propellant flow must be ensured during shutdown transients to cool the engine. Figure 2-6 lists the information desired.

Interface shape is a function of Froude number, Bond number, outlet diameter/tank diameter, percent ullage, and tank geometry. Extensive analyses are available. Detailed solutions for inviscid models have been determined (References 2-8, 2-9) as well as functional relationships for the general case (Reference 2-10). A more general analysis of viscous effects is needed and existing analyses must be extended to cover practical tanker geometries. The analytical models have been verified experimentally in small tanks with relatively high Bond number. Experimentation must be extended to large tanks and to practical Bond numbers.

In the S-IIb, propellant transfer occurs shortly after docking of the tanker with the orbital launch vehicle. It is expected that docking will cause significant sloshing of propellants which will damp out very slowly in low g and thus may influence the interface shape during propellant transfer. Very little work has been done in this area. Both analysis and experimentation are needed.

Work done to date on suction dip problems has indicated that changes in flowrate will be desirable towards the end of the transfer. These may include gradual flow reductions. Methods are needed to describe the effects of step changes and gradual changes of flowrate.

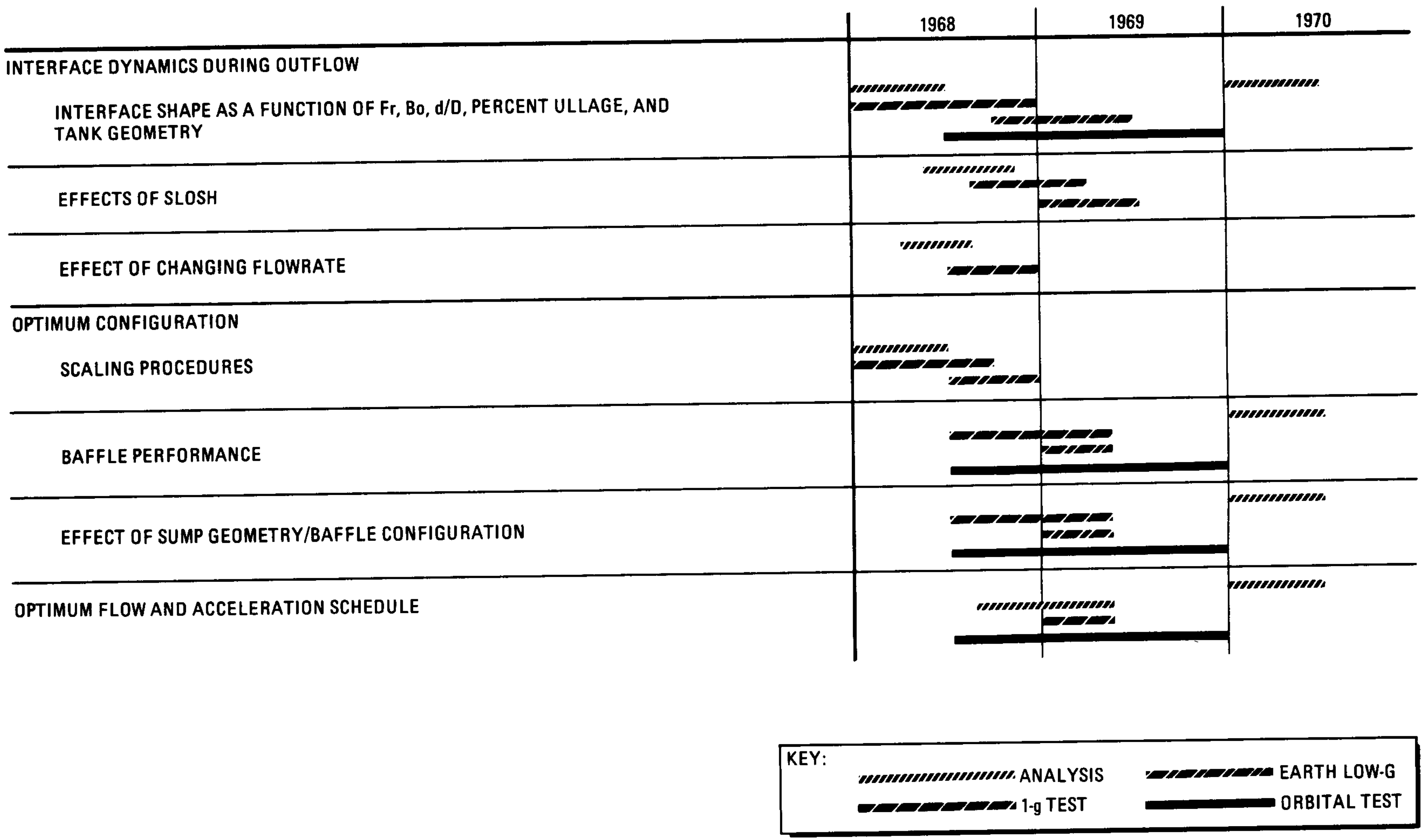

Figure 2-6. Schedule of Ullage Control During Propellant Outflow Technology

Baffles and modifications of sump geometry are expected to play a major role in control of suction dip. However, up to now, experimental attempts to use baffles for reduction of suction dip residual have had marginal success. An extensive program is needed to determine the best baffle configuration. Furthermore, the effect of baffles on surface distortion is expected to be quite different at low g than on the ground; therefore, scaling procedures must be established.

The first step in handling this problem should be to build workable analytical models to describe interface dynamics during outflow. To these models must be added methods for predicting the effectiveness of baffles and other unusual geometries. Finally, an optimum combination of flow schedule, vehicle acceleration, and configuration must be selected and verified. Figure 2-6 presents a schedule of analysis and testing for these tasks.

The existing experimental results in the area of interface dynamics must be extended to large tank sizes and low Bond numbers. Ground tests can be used to investigate large tanks as well as effects of sloshing and changing flow rates. Drop-tower testing will provide low Bond numbers and will also provide for low frequencies associated with low g sloshing. An orbital test is felt to be necessary in order to obtain low Bond numbers in combination with the large tank as a final step in verification of the analytical models. Such a test might be run in the KC-135 but it is felt that perturbations associated with aircraft low g tests could have a significant effect on the results.

In regard to outlet configuration, the first step should be an analysis to determine the best scaling parameters, particularly in regard to baffle dimension. Applicability of the designated parameters can then be verified by testing systems of different sizes in 1 g/g_e and in a drop tower. These results can then be applied to a ground test program to determine the best baffle configuration for the S-IIB (or the best combination of baffle and sump design if some modifications of the tanker are possible). Drop-tower tests will be useful in selecting the configuration, but because of difficulties in obtaining appropriate combinations of size and fluid velocity in a drop tower, a large-scale orbital test will be necessary for final verification.

An optimum procedure for minimization of suction dip residual can be determined from the information obtained as described in the preceding paragraphs. Because of scaling problems, it is felt that the final selection of procedure should be based on an orbital test run on as large a scale as possible. The timing of this test can coincide with that of the baffle verification test described above.

2.7 PROPELLANT TRANSFER RECEIVER TANK THERMODYNAMICS

The present S-IIB mission requires that transfer of LO_2 be made without venting of the receiving tank. Avoidance of venting is highly desirable since venting during low g transfer is at best a complex operation and could lead to excessive propellant losses. Assurance that venting can be avoided will, however, require an improvement of current technology in several areas of low g heat transfer and fluid mechanics. The most significant of these are convective heat transfer rates, liquid flow patterns and spray trajectories during inflow, heat transfer in condensation and boiling of LO_2, and line thermal transients. Furthermore, it will be desirable that such improvement be carried to the point where transfer time can be minimized. This will reduce requirements for ullaging propellant and will aid mission coordination.

It is unlikely that sufficient understanding of the processes involved in determining pressure history during propellant transfer can be obtained from analysis and model testing. It is, therefore, necessary to develop scaling procedures to be used in areas where physical understanding is limited. Scaling is necessary for heat transfer processes, tank pressurization, and liquid entrainment processes. The first two are already under investigation (NASA Contract NAS-20362). This study is to determine all parameters involved in analyses of cryogenic propellant transfer and to perform one g experiments to determine their significance. Since such significance may vary with gravity, it will be necessary to perform low g tests in order to use the results of this study in the S-IIB mission.

It will be desirable to design an inlet configuration to promote those processes which aid in avoiding venting. The S-IIB study designates use of a spray nozzle to promote condensation. If results of studies described here confirm the desirability of such a configuration, an investigation of spray configurations will be needed to select the best configuration. Also, it is desirable in the S-IIB to introduce the LO_2 to the receiver tank in such a way as to promote heat transfer between the liquid and the cold forward dome. Configurations for this purpose should be investigated.

If at some future date, it is decided that venting of the LO_2 tank during transfer on the S-IIB cannot be avoided, methods for control of inlet inertia will be necessary to provide for design of a combination of liquid inlet diffuser and tank baffle to control the liquid in order to avoid excessive loss during venting.

The overall technology schedule is shown in Figure 2-7. Based on current target dates for the S-IIB, all information necessary to feed into design of the S-IIB must be available by the end of 1970. Verification of the no-vent concept can then be available by the end of 1971.

Processes for which analytical models must be developed are shown in Figure 2-7. In nearly every case, it is felt that low g verification of the models is necessary. The KC 135 will be suitable for these verification tests.

Scaling procedures should be developed in areas where the effectiveness of analytical models is found to be limited. Low g verification of these procedures will be necessary by a relatively early date. Investigation of capabilities of existing drop towers and the KC 135 indicate that they will not be adequate to scale the combinations of flowrates and g levels anticipated for the S-IIB mission. Thus, an orbital test is required.

KC 135 tests (in conjunction with orbital LH_2 tests) will be appropriate for obtaining boiling and condensing data for LOX and for verifying effectiveness of inlet configurations which will be selected on the basis of ground test results.

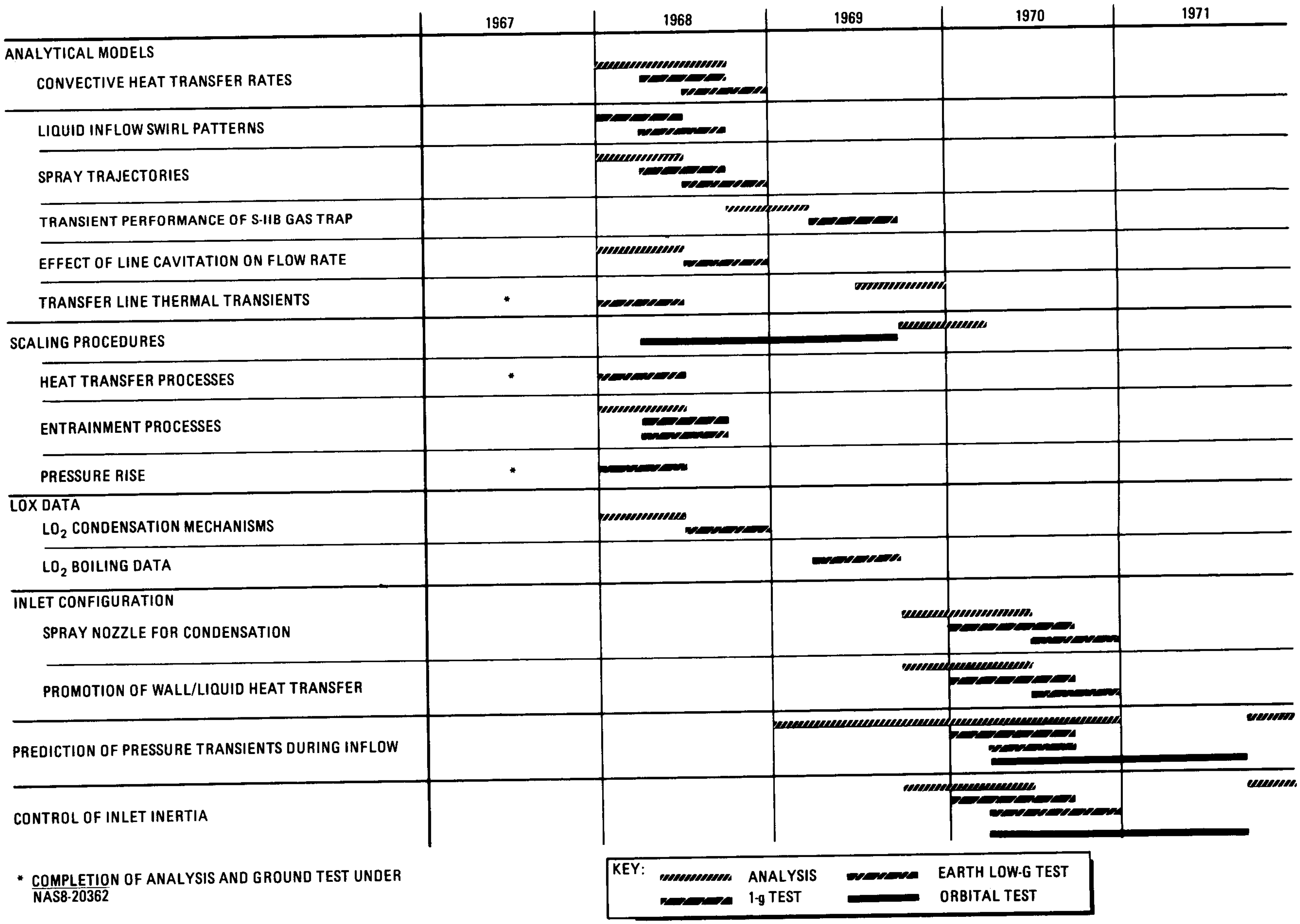

Figure 2-7. Schedule of Propellant Transfer Receiver Tank Thermodynamics Technology

In view of the complexity of the overall model for pressure transients, it is felt that the only valid test of the no-vent concept will be a large-scale orbital experiment. Coupled to this experiment can be an investigation of procedures for control of inlet inertia if the probability of a need for venting is felt to be high.

2.8 LIFE SUPPORT SYSTEMS

Many environmental control (ECS) components are part of some thermodynamic cycle used for the cooling or heating in low gravity. A brief survey was accomplished to identify systems requiring THERMO type technology. Discussions with personnel in the field were supplemented by a brief review of the literature. No comprehensive review of the effect of gravity on ECS equipment was found and the requirements prepared (Table 2-2) may not be typical, but technology requirements appear to revolve around boiling heat transfer and the two phase storage of cryogens.

2.9 ORBITAL RESTART OF ENGINES

Engine restart involves propellant settling. In addition, inlet gas flow momentum in low g may cause severe surface instability and liquid/gas mixing, resulting in pressure collapse factors much higher than observed in one g tests. Also, vapor bubbles in the liquid may sink, rather than rise, if the restart engine induces tank vibration.

The settling phenomena for orbital restart or venting are basically the same. Therefore, all of the information outlined and scheduled under Mechanics of Settling, Section 2.4.5, Low G Venting, is applicable. In addition, bubble removal and bubble sinking (a possible idle mode phenomena) must be understood (Figure 2-8).

Orbital restart and low g venting experiments are scheduled for two in-orbit tests in 1968-1970. In addition to the resettling phenomena, it is also necessary that proper diffuser designs and gas inflow conditions be employed in vehicle design so that propellant dynamic and thermodynamic disturbances are minimized. The dynamic disturbance may be studied with simulant liquid as a part of the resettling experiment. Thermodynamic effects must be studied with a cryogenic liquid and must, therefore, be performed in conjunction with a separate in-orbit experiment.

TABLE 2-2

INFORMATION REQUIREMENTS - LIFE SUPPORT EQUIPMENT

Subcritical Storage of Cryogenics	
1. Container Pressure Rise	
	Thermal Stratification and Boiling
	Artificial Heating Boiloff Rate
2. Liquid Ullage Control	
3. Thermodynamic Separator	
Boiling Heat Transfer	
1. Oxygen-Hydrogen Fuel Cells	
	Boiloff Rate Control to Supply Preheaters
2. Cryogenic Coolers for IR Detectors	
	Heat Transfer in Closed Cycle Cryogenic Refrigeration Unit
3. Lunar Surface Thermal Control System	
	Freon Heat Pump Refrigeration Unit
4. Reliquefaction	

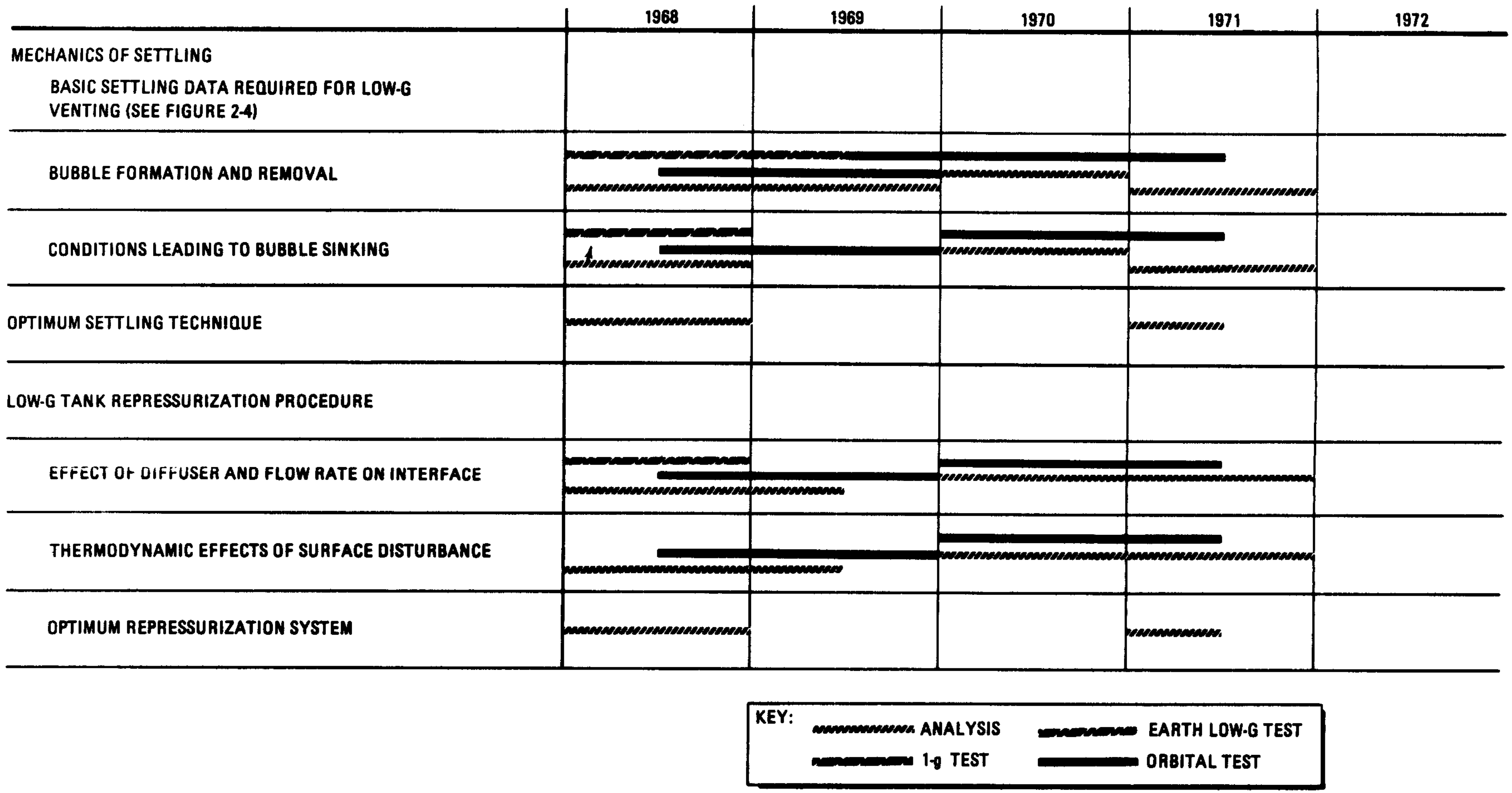

Figure 2-8. Orbital Engine Restart Technology Schedule

Section 3
CARRIER CAPABILITIES AND EXPERIMENT DEFINITION CONSTRAINTS

The objective of this effort was to determine the constraints on experiment conceptual design induced by the capabilities of the boosters, on board subsystems and ground tracking stations.

The payload weights and envelopes, costs, and applicability of available GSE, at KSC and PMR, were defined for several boosters systems ranging in payload from about 350 to 3,200 lb. Because payload capability and experiment feasibility is a strong function of attitude or drag, this parameter and its range of uncertainty was determined for the payload configuration and altitudes of interest. Equipment was evaluated and selected, as a study baseline, for telemetry, power, television, sequencer, guidance, and ACS. A significant constraint is provided by data acquisition considerations. Therefore, a survey of tracking station data handling capabilities as well as a mission time sequence of station acquisition for both a KSC and PMR launch was accomplished.

3.1 BOOSTER CAPABILITIES

The capabilities of Scout, Thor Delta, Atlas (OV-1, SLV-3A, and Atlas E&F series), Burner II and Thor Agena are presented. Also, the Saturn-IB Workshop is discussed. Cost data shown was obtained from the booster manufacturers. Official data must be obtained from the appropriate government agencies.

3.1.1 Scout

Scout data was obtained from Reference 3-1 and from conversations with LTV personnel. The vehicle is a four-stage solid propellant carrier capable of inserting 350 lbs in a 200 nmi inclined circular orbit. Launches are from WTR, Vandenberg, California, or Wallops Launch Site, Wallops Island, Virginia. Approximate cost for the carrier and launch support is $\$1.5 \times 10^6$. The payload envelope, shown in Figure 3-1, contains 17.72 ft^3.

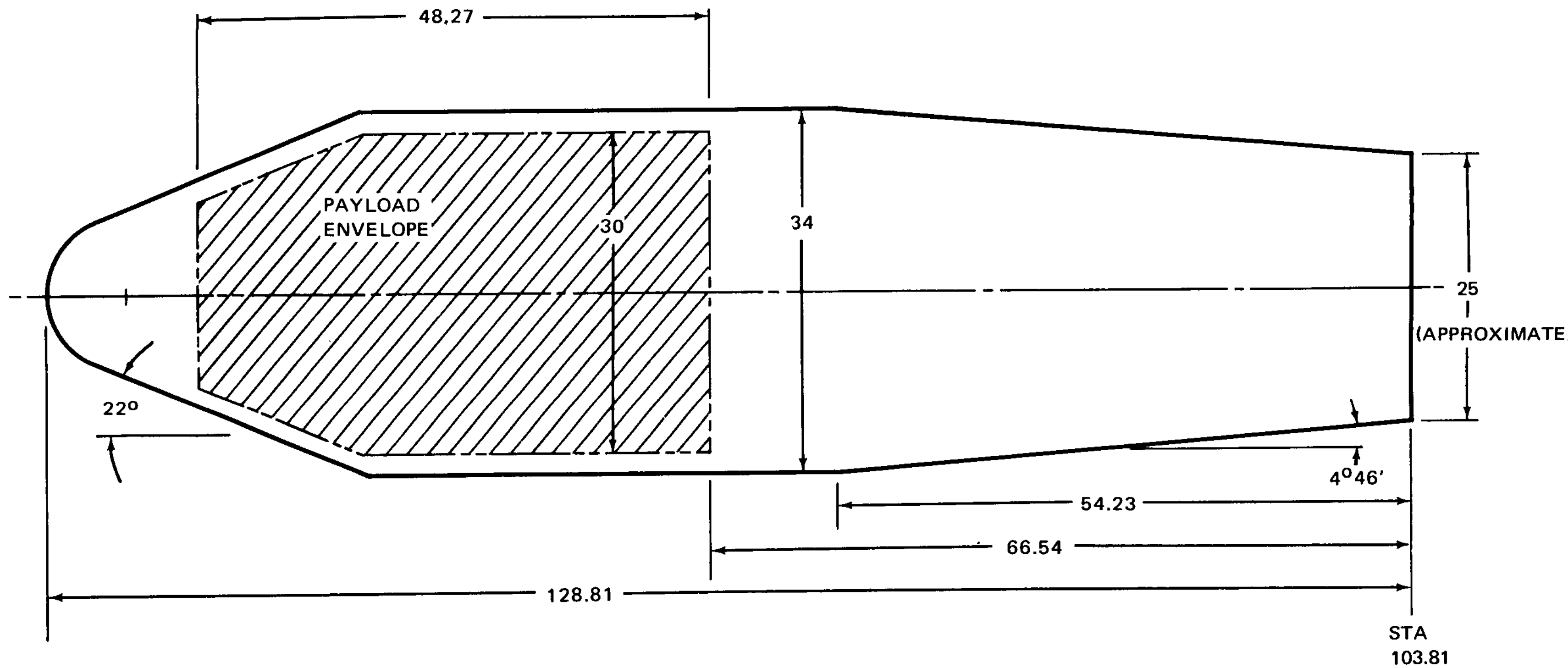

Figure 3-1. Scout

The fourth stage is spin-stabilized. Therefore, to avoid long residual propellant rotation after separation, a despin table between the fourth stage and the payload would be required. Also, a separate roll control system to maintain the payload in a static condition may be required in addition to the orbital roll control system.

3.1.2 Thor Delta

Considerable Delta information is available in Reference 3-2. Two versions of the Delta were examined: the DSV-3G and the uprated long tank DSV-3L. Since the third stage is spin-stabilized, a disadvantage for Project THERMO, only the two-stage versions were considered.

The long tank Thor has been launched from WTR, and will be launched from ETR this summer. Payload capabilities in a 200-nmi inclined circular orbit for the 3G are 1,200 lbs, and for the 3L are 1,600 lbs. Approximate costs are $\$3.4 \times 10^6$ and $\$3.7 \times 10^6$ for the 3G and 3L respectively. The payload envelope for one of the available fairings is shown in Figure 3-2.

3.1.3 Atlas

Three versions of the Atlas were considered: the OV-1, the Atlas E&F series, and the SLV-3A. These cover a wide range of payload capabilities and carrier costs.

3.1.3.1 OV-1

Presently, two OV-1 satellites, carrying different experiments, can be launched on one Atlas, while future versions may carry three or four OV-1 satellites. Therefore, Atlas boosters can be cost-shared between the experiments. OV-1 data was obtained from Reference 3-3.

The OV-1 satellite has a payload capability of 190 lbs in a cylindrical volume of 8.1 ft^3 (approximately 26 in. diameter and 26 in. long). In addition, a small telemetry system, electrical power system, and gravity gradient stabilization system are provided. Therefore, the OV-1 is comparable with the Scout in payload capability, and a payload similar to Figure 3-1 could be flown. Costs for the OV-1 are in excess of $600,000 plus booster costs.

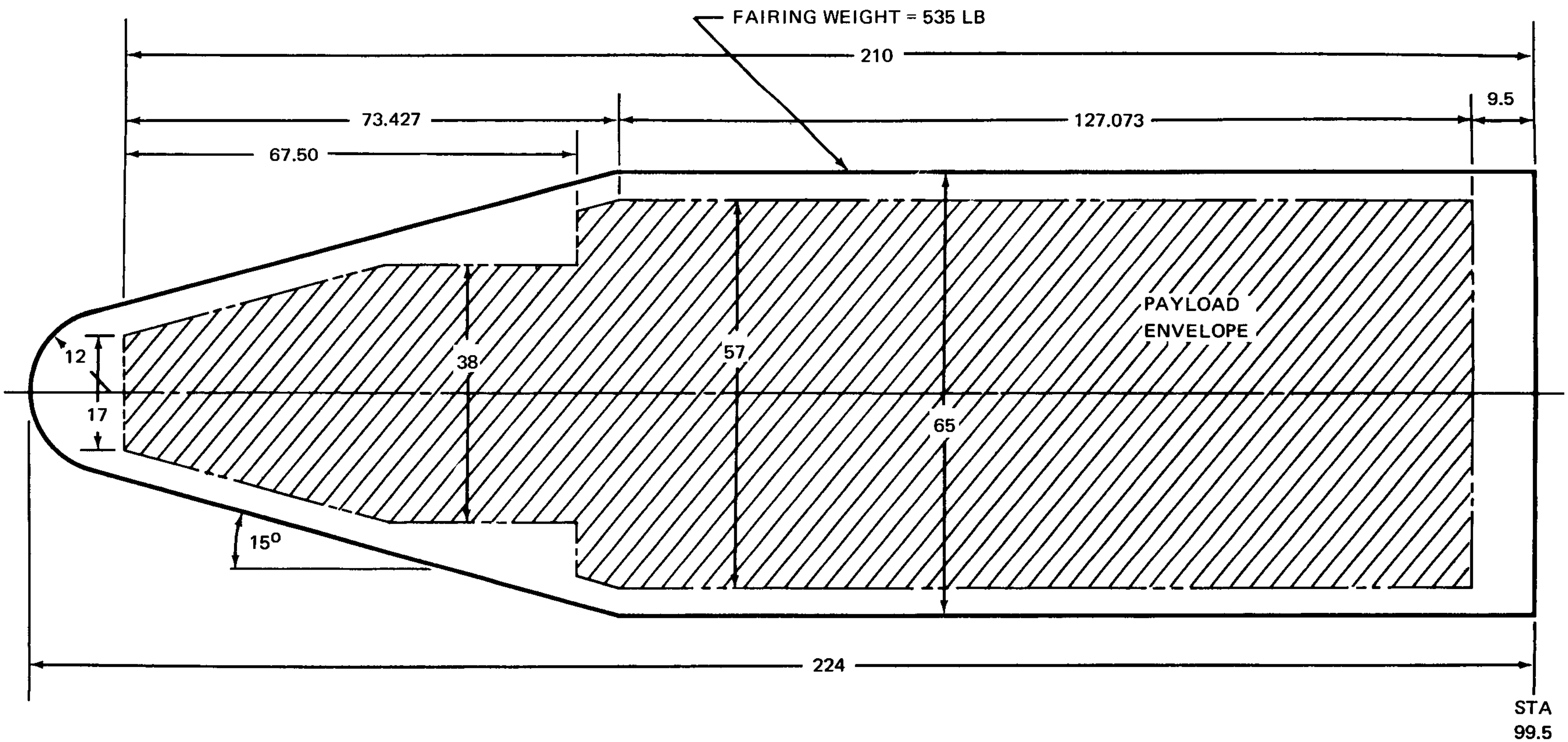

Figure 3-2. Thor Delta Fairing

3.1.3.2 SLV-3A

The SLV-3A is the extended version of the SLV-3 (References 3-4 and 3-5). To minimize costs, only a single-stage Atlas to orbit is considered.

The SLV-3A utilizes a number of standard fairings; however, to obtain maximum payload, the same fairing and payload envelope as shown in Figure 3-2 appears most attractive. Payload capability is quite dependent upon orbital altitude. For launches from ETR into inclined circular orbits, the payload, in excess of the fairing and a modified PRIME payload adaptor, is 1,265 lbs in 200 nmi, and 2,965 lbs in 150 nmi. Approximate costs in orbit are $\$3.7 \times 10^6$.

3.1.3.3 Atlas E&F

Atlas stages returned from weapon systems sites are being refurbished and flown from WTR, Vandenberg, California. Because of structural and guidance system differences between the E&F's and the SLV-3A, launches from ETR are not possible at this time. The payload in excess of the fairing and payload adaptor in a 100-nmi polar orbit is approximately 1,765 lbs. The cost of these carriers is approximately $\$1.7 \times 10^6$. The availability of these carriers can be established from Ballistic Systems Division, Norton Air Force Base.

3.1.4 Burner II

Burner II data was obtained from References 3-6, 3-7, and 3-8, and from conversations with Boeing personnel. Burner II is a solid propellant upper stage with integrated guidance and control systems, telemetry system, destruct system, and electrical system. Two successful launches have been made, as a second stage to Thor, from Vandenberg, California. The payload with a DSV-2L (uprated long tank Thor, first stage) is about 1,200 lb in a 200-nmi circular orbit, or about 1,900 lb in a 100-nmi circular orbit. This is about equivalent to a DSV-3G/Delta. The cost for this combination is about $\$2.6 \times 10^6$, plus about $200,000 for AGE if launched from ETR.

The Burner II can utilize a number of shrouds, including the Douglas shroud shown in Figure 3-2.

3.1.5 Thor Agena

The Thor Agena payload capability is larger than that of the Thor Delta, with some increase in cost. Data for the Agena and other booster combinations is given in Reference 3-9. The DSV-2L/Agena D payload is about 2,550 lb in a 200-nmi polar orbit, and 2,750 lb in a 100-nmi orbit. Cost is about $\$4.2 \times 10^6$. The stage is launched from WTR.

3.1.6 Saturn-IB Workshop

Since the Saturn IB is not now capable of boosting the workshop, and the modifications to uprate the booster have not been selected, the excess payload capability could not be determined.

3.1.7 Carrier Summary

Cost and performance data of the carriers studied are summarized in Table 3-1. The cost data includes (except for one case) all fairings and launch support, but does not include modifications to the GSE, if any, for experiment-peculiar requirements. The payloads are listed for three altitudes, 100 nmi, 150 nmi, and 200 nmi. Carrier costs range from $\$1.5 \times 10^6$ to $\$4.2 \times 10^6$, and payloads range from 190 lb to 4,465 lb.

In the small payload class carriers, Scout and OV-1, the OV-1 was eliminated from consideration due to its extremely small payload and high cost per pound in orbit. The next larger payload is provided by the Thor-Burner II and Atlas (E and F), both PMR launched. The former was eliminated due to high cost as compared to the relatively inexpensive military Atlas. The Thor Delta DSV-3L was selected as a third carrier class. It has a larger payload than the DSV-3G and will be the standard booster in the time period of interest, 1969. The Thor DSV-2L/Agena (PMR launched only) and Atlas SLV-3A provide a fourth and larger payload class. The Atlas was used for the study since it was lower in cost and KSC compatible.

Only two shroud envelopes need be considered to design experiments compatible with the selected carriers. The Scout requires a small fairing, Figure 3-1. All the other carriers use the standard Douglas Agena Clamshell Fairing, Figure 3-2, which was used as the second study payload envelope.

Table 3-1

CARRIER COMPARISONS

Carrier	Approx. Cost Includ. Fairings & Launch Support	Payload Circular Inclined Orbit (ETR Launch Unless Noted)		
		100 nmi	150 nmi	200 nmi
Scout, FW-4S, 4th stage	$\$1.5 \times 19^6$	405	380	350 lb
OV-1	0.6×10^6 + Booster	190	190	190
Thor Delta DSV-3G	3.4×10^6	1500	1300	1200
Thor Delta DSV-3L	3.7×10^6	2100	1850	1600
Thor Burner II (Polar Orbit)	2.6×10^6	660	610	530
Thor DSV-2L/Agena D (Polar Orbit)	4.2×10^6	2750	2650	2550
Atlas SLV-3A	$3.65 \times 10^{6*}$	4465	2965	1265
Atlas E&F, Polar Orbit	$1.7 \times 10^{6*}$	1765	765	Nil
Atlas SLV-3A Burner II (Polar Orbit) (Not Yet Developed)	4.24×10^6 + Develop. Cost	3900	3800	3700

*Excluding fairings, payload adaptors, separation system

Weights for a roll system and de-spin table on the Scout were not readily available. Hence, they were not included for conceptual design purposes, and would need to be included in any subsequent preliminary design effort.

3.2 DRAG CONSTRAINTS

The orbital drag used for definition of experiments is represented in Figure 3-3 and Table 3-2. The band of uncertainty shown is based on the maximum and minimum solar fluxes dependent upon the anticipated 1969 solar flare activity and a model atmosphere with the boundary condition such that it meets the 1962 Standard Atmosphere at and below 120 km. Above 120 km, the model atmosphere is the Jacchia (Reference 3-10) atmosphere modified by Walker (Reference 3-11) which is good up to a 45° latitude. At latitudes from 45° to 90°, caution should be used as very little data on atmospheric parameters was available for use in an unclassified form.

Drag computations are based on Sentman's (Reference 3-12) equations for free molecular flow and on a payload configuration compatible with Figure 3-2.

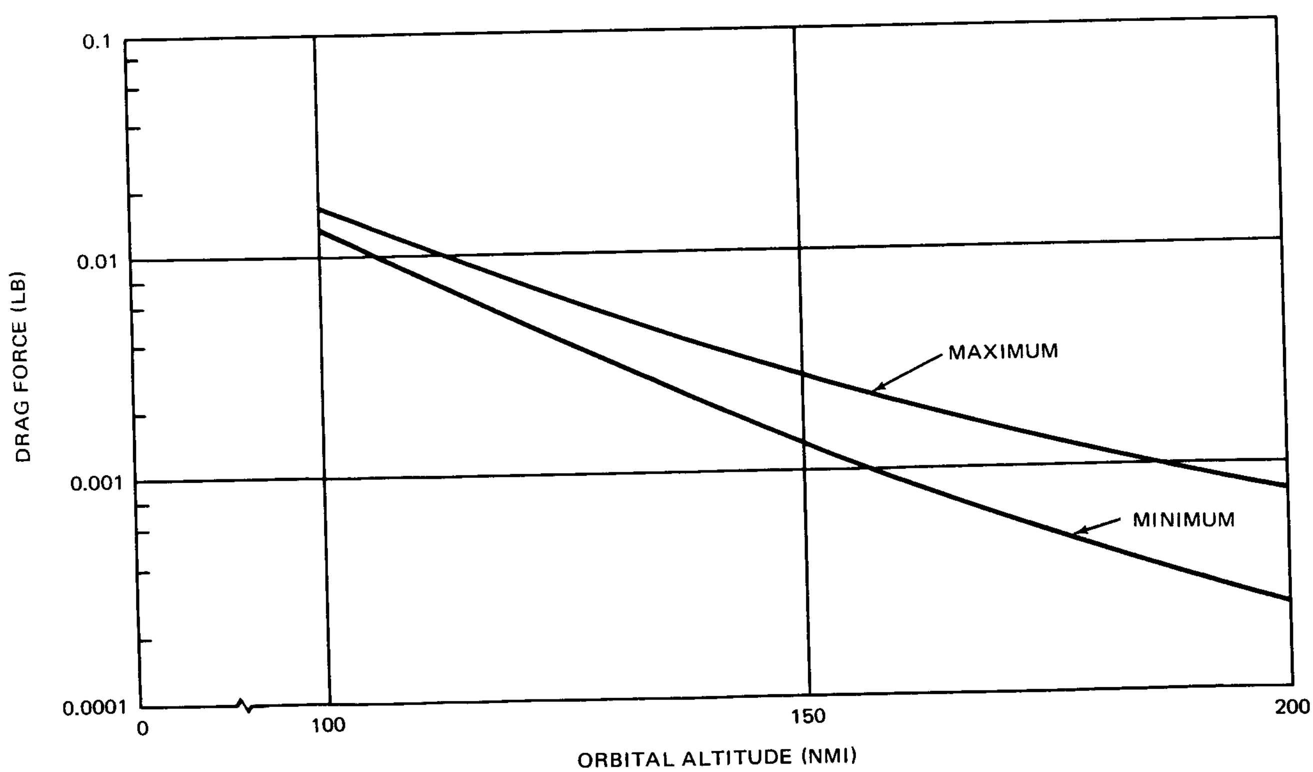

Figure 3-3. Drag Force Urbital Hydrogen Storage Experiment (Zero-Angle of Attack, $a = 0^0$)

Table 3-2
ORBITAL HYDROGEN STORAGE EXPERIMENT
90° ANGLE OF ATTACK

Altitude (nmi)	Min. Drag (lb)	Max. Drag (lb)
100	0.034	0.045
150	0.00325	0.006
200	0.00056	0.0015

3.3 TRACKING STATION DATA ACQUISITION CONSTRAINTS

The capabilities of the tracking station telemetry equipment and the time sequence of station acquisition impose significant constraints on experiment definition. To ensure experiment compatibility, data acquisition for a typical PMR launch (polar orbit, Atlas E and F) and a KSC launch was investigated along with a survey of tracking station network data handling capability.

3.3.1 Station Capabilities

Project THERMO experimentation requires combinations of television coverage, TM tape recorded data with high speed playback, real time TM data and experiment over-ride/command control from the ground.

Real time TM data acquisition and uplink experiment command capability is readily available. All of the numerous stations surveyed had AGAVE (Automatic Gimbal and Vector Equipment), the capability to receive transmissions in the range of 225 to 260 Mc and a command TM system. Experiment definition was, therefore, based on this capability being available whenever the payload was within the receiving cone of an actuated station of the Manned Space Flight Network.

Existing television recording equipment was not found at any station. It was assumed that Project THERMO TV data acquisition could be accomplished similarly to the Saturn 203 experiment at Carnarvon (CRO), Canaveral (CNV), Corpus Christi, Texas (TEX), and Bermuda (BDA).

Hawaii (HAW), Tananarive (TAN), Ascension Island (ASC), and Guaymas (GYM), the only stations found with high-speed TM-tape recording equipment, provide the recorder data dump capability for THERMO. These stations are compatible with the THERMO base line recorder, Section 3.4.

3.3.2 PMR Launch - Polar Orbit Mission

An 85° inclination, 150-nmi orbit (7-day duration) was considered as a typical case since it corresponds to about the practical upper altitude limit for the Atlas E and F vehicle.

Data transmission time over each station is relatively short with a maximum of about 6 minutes available. Based on the fly-over times for the four TV stations, transmissions of 4 minutes or less will be compatible with about 75% of the possible data acquisition opportunities. The 85% level is reached if transmissions are held to 3 minutes or less. Because the gain is small, 4-minute transmissions were selected for flight tape recorder and TV experiment sizing.

Table 3-3 presents a summary of acquisition times (over 4 minutes) for Hawaii, Canary Island, and the four TV stations. The Canary Island profile shown is about identical to what would be expected for Ascension Island (tape playback). Tananarive will be acquired in orbits between those shown for Canary Island and Carnarvon. Guaymas, the fourth tape-playback station, overlaps the Texas coverage.

Note that all TV and tape compatible stations occur in groups of orbits with gaps of several orbits in between. Hence, experiments requiring this capability must be designed around control of individual sequences from the ground with long periods of inactivity. It can also be concluded that many stations must be activated to provide much in the way of experiment coverage. Acquisition of the payload once per orbit is probably impossible.

3.3.3 KSC Launch

A 200-nmi, 28.5° inclination, circular orbit (7-day mission) was used as representative of THERMO launches from KSC.

Maximum transmission time over any given station is about 8 minutes. Based on the TV stations as typical, about 94%, 85%, and 64% of the transmission opportunities are greater than 4, 6, and 7 minutes each, respectively. Hence, any recorder with playback of less than about 6 minutes is

Table 3-3

TIME OVER STATION (MINUTES)
5° RISE ANGLE
PMR LAUNCH - 85° ORBIT, 150 nmi

Orbit	HAW	CYI	CNV	BDA	CRØ	TEX	Orbit	HAW	CYI	CNV	BDA	CRØ	TEX
1							57						
2							58	6.2					
3	5.8						59		6.4				
4		6.5					60						
5							61				5.7		
6				6.5			62			6.3		6.1	
7			6.1		5.1		63						5.8
8						4.0	64						
9							65						
10	5.5						66						
11		5.5					67						
12							68		5.3				
13				4.3			69						
14			6.2		6.5		70				6.3	4.6	
15						6.4	71			4.1(R)			5.7
16							72						
17							73						
18	5.3						74	6.4					
19							75		6.2				
20		6.3					76						
21							77				6.1		
22				6.3			78			6.4		6.0	
23			5.8		4.5		79						5.3
24							80						
25							81	4.0					
26	6.0						82						
27		5.8					83						
28							84		4.7				
29				5.0			85						
30			6.4		6.5		86				6.0	5.2	
31						6.3	87						5.8
32							88						
33							89						
34	4.8						90	6.5					
35							91		6.3				
36		5.9					92						
37							93				6.3		
38				6.2			94			6.3		5.7	
39			5.2			(R)4.6	95						4.8
40							96						
41							97	4.8					
42	5.9						98						
43		6.2					99						
44							100		4.0				
45				5.4			101						
46			6.2		6.1		102			4.6(R)	5.7	5.7	
47						6.1	103						6.1
48							104						
49							105						
50	4.0						106						
51							107		6.3				
52		5.6					108						
53							109				6.5		
54				6.6			110			6.1		5.3	
55			4.8(R)		2	5.2	111						4.1
56							112						

(R) Overlapping Stations

satisfactory. Note that complete taping of one orbit is impossible with standard 8:1 playback speed recorders.

The TV stations, TEX, CNV, and BDA, overlap providing for more extended experimentation than the polar orbit case. The time available for each opportunity varies from about 5 minutes to 15 minutes. Table 3-4 summarizes the TV opportunities available. All the TV and tape playback stations occur in groups of orbits with large gaps in between as shown by Table 3-5, a summary of the first 29 orbits. As was the case for polar orbits, experiments requiring TV or recorders must be designed to be compatible with this constraint. With stations HAW, GYM, and TAN, at least one tape playback transmission opportunity (sometimes three) occurs during the following orbits: 1-7, 14-22, 30-38, 45-53, 60-68, 76-84, 91-99, 106-112. Adding station ASC provides additional coverage in some of the above orbits and in orbits 8-9, 23-24, 39-40, 54-55, 69-70, 85-86, 100-101.

Satellite acquisition for each orbit throughout the seven days appears to be impossible. However, three stations, HAW, CYI, and ASC, as a group yield coverage for almost every orbit.

3.4 EQUIPMENT-IMPOSED EXPERIMENT DEFINITION CONSTRAINTS

The definition of an experiment and its conceptual design will depend very strongly on the equipment and subsystems selected for incorporation into the experiment package. To achieve truly cost effective experimentation, the experiments were defined around selected fully flight-qualified hardware as a base line. This yields a measure of the maximum that can be accomplished in each technological area for minimum cost.

It was recognized that the inclusion of development items may be necessary and where applicable they are indicated in each experiment (Sections 5 thru 10) along with the benefits to be accrued through their use. Three criteria were used as a test for development item justification: (1) is it required to fulfill experiment objectives; (2) would it provide significant improvement in the experiment; and (3) would it provide a cost-effective program, i.e., fewer flights.

The baseline equipment selected and the constraints used for the experiment definition work follow.

Table 3-4

AVAILABLE TELEVISION TIME (MIN)

(5° RISE ANGLE)

KSC Launch - 200 nmi, 28.5° Orbit

	STATIONS			STATIONS	
Orbit	TEX-CNV-BDA	CRO	Orbit	TEX-CNV-BDA	CRO
1	7.5	8.2	60	14.8	8.1
2	14.2	7.3	61	15.7	8.0
3	10.9	-	62	14.8	8.0
4	5.6	-	63		7.8
13	9.3	7.0	64	11.6	4.2
14	14.8	8.2	65	7.7	-
15	15.7	7.8	74	4.3	5.5
16		8.1	75	13.8	7.9
17	14.8	7.3	76	15.5	8.1
18	11.5	4.1	77	15.2	7.8
19	6.9	-	78		8.1
28	4.5	5.6	79	13.2	6.2
29	13.9	8.0	80	9.9	-
30	15.6	8.1	90	10.5	7.7
31	15.2	7.9	91	15.4	8.1
32	13.3	8.2	92	15.6	7.8
33		6.2	93		8.1
34	9.9	-	94	14.2	7.3
44	10.6	7.8	95	11.0	-
45	15.3	8.1	96	5.7	-
46	15.6	7.8	105	9.3	6.9
47		8.2	106	14.8	8.0
48	14.2	7.3	107	15.6	8.0
49	10.8	-	108		8.0
50	5.7	-	109	14.8	8.0
59	9.3	6.9	110	11.6	6.1
			111	7.2	-

Table 3-5

TIME OVER STATION (MINUTES)

(5° RISE ANGLE)

KSC Launch - 200 nmi, 28.5° Orbit

Orbit No.	CNV	CRO	HAW	CYI	ASC	TEX	BDA	GYM	TAN
1	4.0	8.2	7.3			8.17	7.5	8.2	7.9
2	8.1	7.3	8.0		7.8	7.87	5.8	8.1	6.6
3	6.5		7.4		7.1	5.64		8.1	6.2
4			7.6					7.4	7.5
5			8.1						8.0
6			6.4						3.5
7					3.0				
8					7.8				
9					6.8				
10				3.8					
11				7.8					
12				8.1					
13	4.8	7.0		8.0			6.0		
14	7.7	8.2		7.9		6.60	7.7		
15	8.2	7.8		4.9		8.13		7.6	5.7
16	8.1	8.1	6.1		6.6	8.09	7.8	8.2	7.9
17		7.8	8.0		7.8	7.92	6.9	8.0	7.1
18	7.3	4.1	7.6		3.3	6.92			6.1
19			7.4					7.9	7.0
20			7.9					5.0	8.0
21			7.5						6.2
22									
23					7.0				
24					7.7				
25									
26				7.1					
27				8.0					
28		5.6		8.2					
29	7.4	8.0		8.1		5.1	4.5		

3.4.1 Attitude Control System

Systems were investigated to provide experiment constraints and an ROM weight estimate for each of the four payload package sizes considered. A cold-gas nitrogen propellant system was selected over hydrazine, hydrogen peroxide, and resistojet systems. The selection criteria used were weight, availability of flight-qualified components, and cost. Bi-propellants were considered to be too complex for this particular application. A nitrogen system of this type and thrust level has been successfully flown on the Mariner program.

A fairly detailed system design was accomplished for an intermediate payload (1, 600 lb) and system weights for the other packages were estimated from this design. The attitude control system, Figure 3-4 provides experiment package attitude control in pitch, yaw, and roll. Pitch and yaw thrust are 2 to 3 millipounds (0.002-0.003 lb) per nozzle. Control in yaw and roll will utilize the same nozzles, but in different combinations. The thrusters are located at the base of the experiment package on the yaw axis.

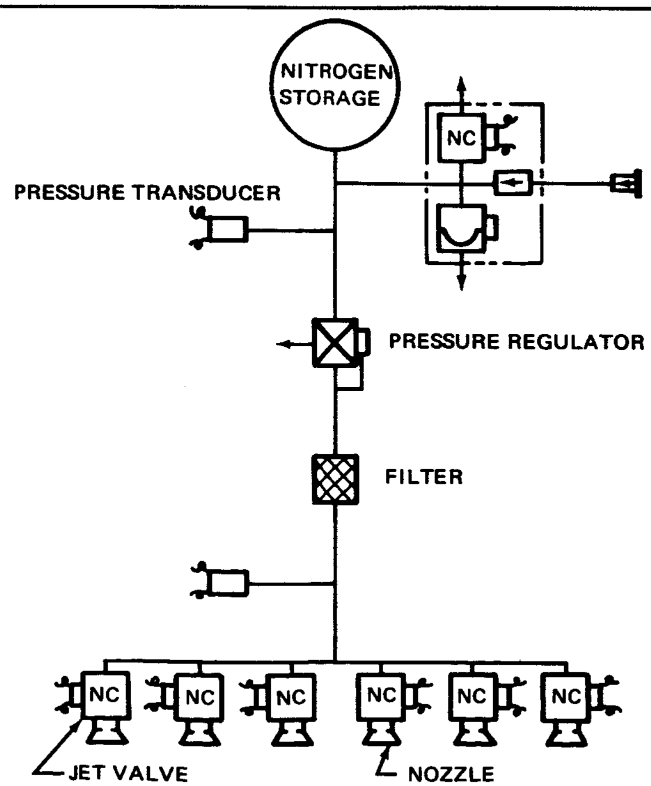

Figure 3-4. ACS Module Schematic (SK-201-PT)

The ACS weights used in experiment package definition were: 100 lb, 350 lb (Scout) payload; 130 lb, 765 lb (Atlas E and F) payload; 190 lb, 1,600 lb (Thor Delta) payload; and 370 lb, 3,200 lb (Atlas SLV-3A) payload. A constant hardware weight of 13 lb was used with the propellant and storage tank weights variable. Thruster sizes were 0.7 mlb, 1 mlb, 2 mlb, and 4 mlb for the four payloads, respectively.

3.4.2 Experiment Acceleration Thrust

Because of uncertainties and variations in drag, the experiments were defined to take primary data at acceleration levels at least one order of magnitude higher than the anticipated package drag. Positive acceleration levels are provided by an auxiliary propulsion system.

A mono-propellant hydrazine system was selected as being most appropriate for use on the experiment packages. Engines, in the thrust ranges of interest, for all the experiments are available, although not necessarily flight-qualified. Engine life is not indicated to be a problem for the seven-day missions planned.

A typical system, Figure 3-5, consists of three subsystems; a pressurization system including a nitrogen storage tank, fill and drain valve, nitrogen valve, filter, and pressure regulator; a propellant feed system including a propellant tank, and a fill and drain valve; and a thrust system including thrustor assemblies, made up of valves, filter, and thrust chamber. Engine weights used were: 0.5-1.0 lb weight for 0.01-0.1 lb thrust engines; 2-3 lb weight for 1-3 lb thrust engines; and, 5-10 lb weights for 5-15 lb thrust engines. A specific impulse of 230 sec was used for propellant weight and tank sizing.

3.4.3 Electric Power

Power requirements for the individual THERMO experiments vary considerably. A study was undertaken to define power sources from the "building block" standpoint in order to readily tailor source capability with the needs of each experiment package. Solar cells were rejected for experiment conceptual definition in favor of batteries due to cost and complexity. Costs of solar cell units were found to vary from about $50.00 to $200.00 per watt, comparing very unfavorably with the flight-type batteries used for the experiment definition study (Table 3-6).

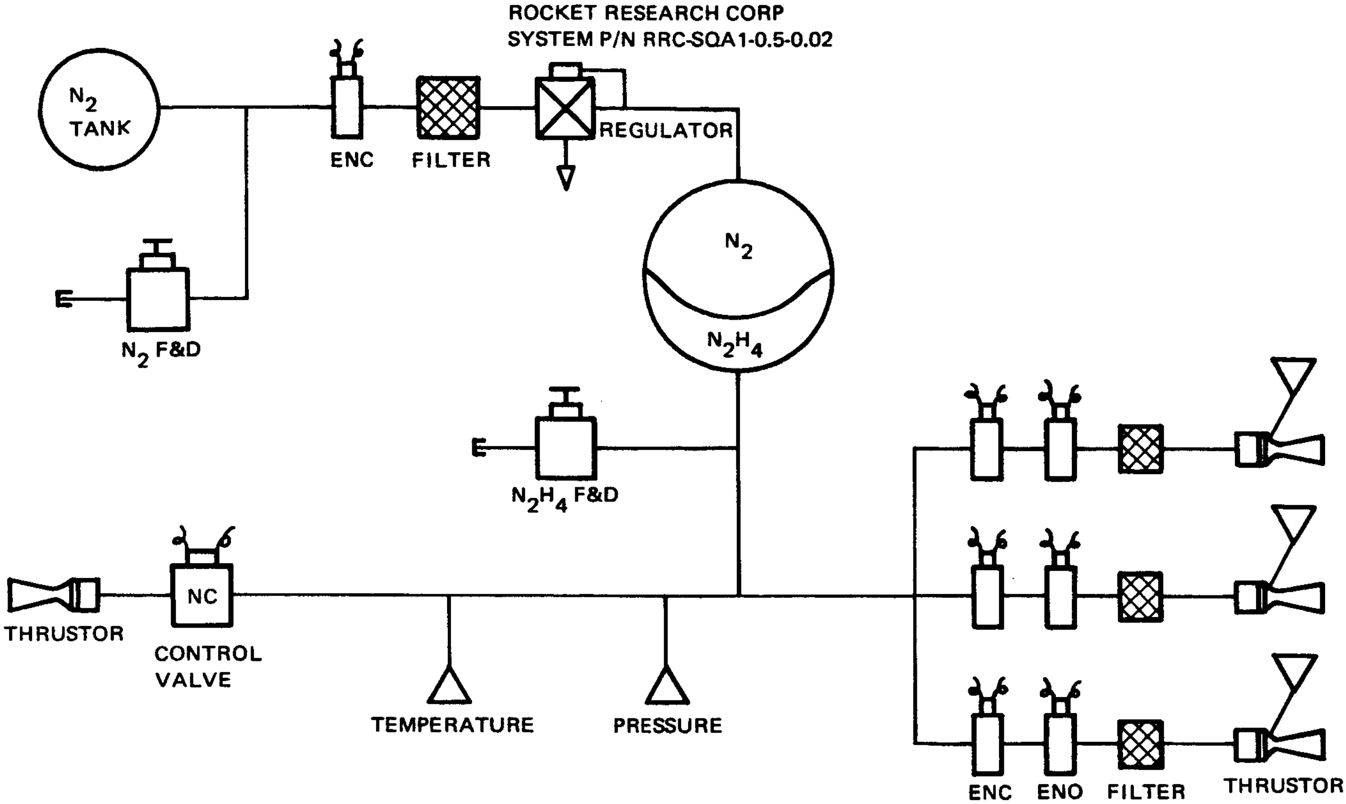

Figure 3-5. Ullage Control System (SK-202-PT)

3.4.4 Telemetry, Television, and Experiment Control Systems

The spacecraft data acquisition and transmitting system consists of two major subdivisions, telemetry and television. To maintain minimum cost, the systems selected for the study utilize existing flight qualified hardware, even to the point of selecting methods known to be somewhat overdesigned in relation to the requirements.

Table 3-6
BATTERIES

Designation	Volts	Amp. Hr.	Watt Hr.	Weight	Watt Hr. /Lb	Cost $	$/Watt Hr.
HR 05	6	0.5	3	0.5	6	200	66.70
HR 1	28	1	28	3.1	9	700	25.00
HR 3	28	3	84	5.3	15.8	1000	11.90
HR 5	28	5	140	8.4	16.7	970	6.93
HR 15	28	15	420	16.9	24.8	1040	2.48
HR 21	28	21	586	25.5	23	2050	3.50
Saturn Type Batteries	28		12,000	155	77.5	8000	0.67

3.4.4.1 Telemetry System

The basic building block telemetry system selected is shown in Figure 3-6. The system consists of three separate, parallel subsystems and a tape recorder. For smaller payloads, only one or two subsystems can be used with or without the recorder to reduce power and weight.

The capabilities of the complete system (max. error < 3%) are:

1. 120 channels of information, 20 samples per second. This is transmitted directly (no recorder) or taped and transmitted when over a receiving station.

2. 30 channels of continuous data. These are available upon command from the ground.

In selecting the system, 10 complete systems were analyzed and priced considering varying sampling rates, number of transmitters (one to three), and the use of PDM or slow-rate PCM. While others were adequate for the need, many were eliminated because low-cost, off-the-shelf, qualified equipment was not available. Noteworthy is the fact that a slow rate PCM (one transmitting link) system is more desirable from a system-electrical-load standpoint than the PDM system selected, but it requires development.

A time-sharing, sampling system is used for sampled data and a frequency-sharing system for the continuous data. Three independent radiating telemetry systems are required. The individual transmitter outputs are multiplexed on one VHF antenna system, radiating in the 225 MHz to 260 MHz telemetry band. Qualified components are available to use either the VHF or the UHF, "S" band. The three systems are modulated identically and consist of three identical sets of time-sharing and frequency-sharing components.

The tape recorder operates with a 1:8 record to playback ratio. With this arrangement, 30 minutes of orbital information can be "dumped" in 3.75 minutes while passing a receiving site. The received 30 KHz VCO frequency will, therefore, be 240 Kc. The receiver discriminator output is recorded directly and played back at one-eighth speed for reduction of data which appear at this playback as 30 KHz, Channel "B" VCO modulated by a 45 x 20 PDM system. Recorder capacity is 40 minutes of real-time data.

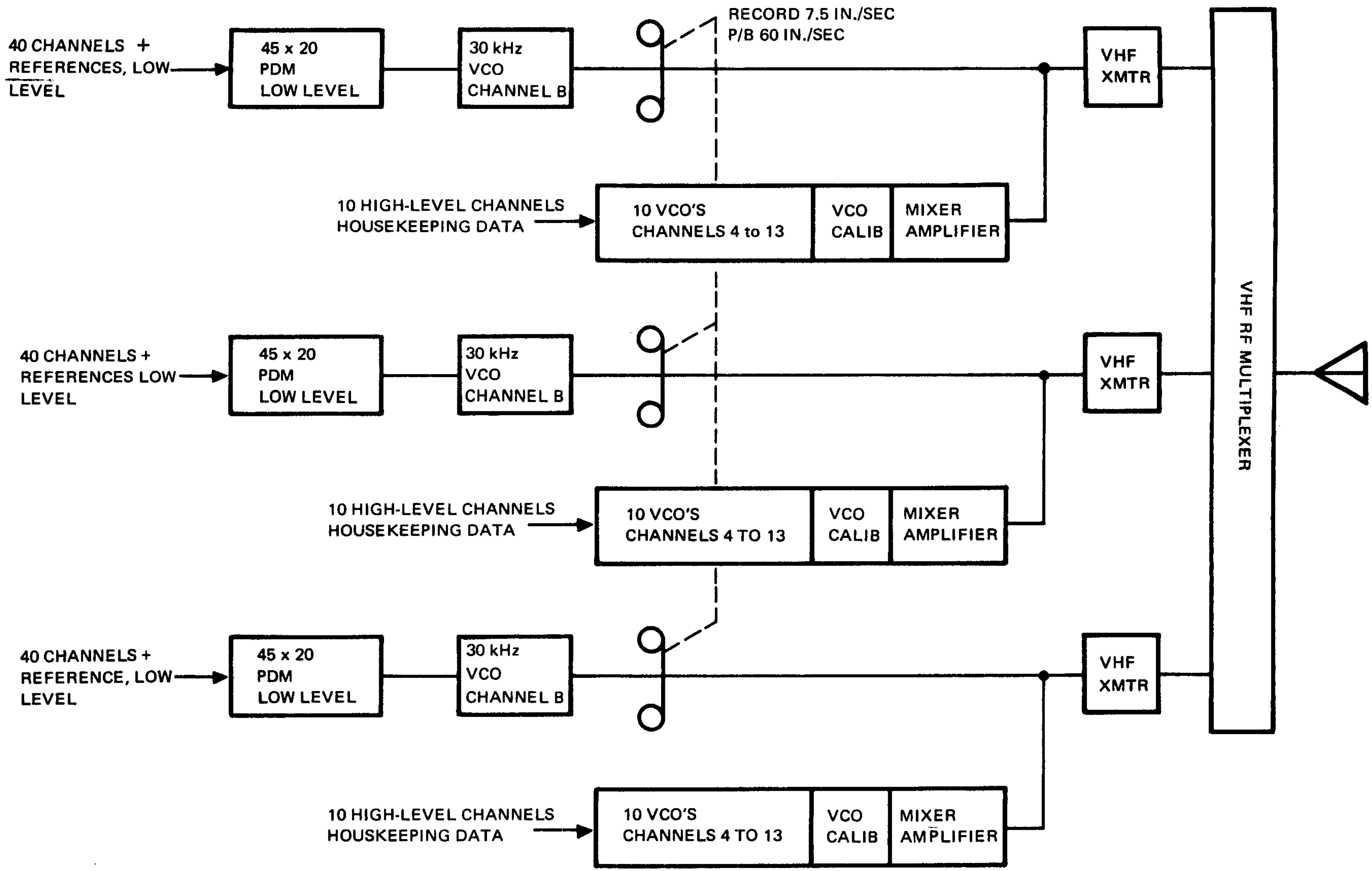

Figure 3-6. Telemetry System

Except for the interface stability experiment, the large bulk of measurements to be made will be temperature measurements in the cryogenic range. For this, a proven platinum resistance probe from the Saturn S-IVB system can be used. Other measurements such as liquid level, pressure, voltages, and currents can also utilize qualified hardware from other programs. The 0 - 40 millivolt input range PDM system makes signal amplification unnecessary in nearly all cases, if not all cases. An ROM weight of 0.5 lb per transducer was used.

3.4.4.2 Television System

Single camera TV systems as well as a dual camera system transmitting over a single RF link, attractive from the experiment definition standpoint, were investigated. Both were found to be feasible with existing qualified hardware.

A television system similar to that used on Saturn AS-203 can be used. The system will be activated periodically to conserve battery power. The transmitter can be FM-modulated with video signals up to 8 MHz. Minimum power would depend upon ground station capability, but may be as much as 20 watts which was used for the study.

Where required, two cameras and camera control units can be used in conjunction with a multiplexer and transmitter on the orbiting payload. No additional receivers or antennas are necessary over and above single camera system requirements. This appears to be compatible to existing tracking station equipment.

A typical in-flight multiplexer is the Lear Siegler Model 0792 Video Register, which requires a space envelope of about 9 x 6 x 4 inches and weighs about 6 lb. The unit transmits 100% of the signals from two cameras (30 frames per second, equivalent) with one transmitter. It is indicated that units have been flown on Gemini.

3.4.4.3 Experiment Control

TM System Duty Cycle

The telemetry system is commanded from the ground to radiate only when desired. This experiment constraint stemmed from the limited on-board battery capacity, the lack of need for continuous data, and a desire to minimize tracking station activation. The system can be arranged so that portions or all of the system can be directly actuated from the ground by way of the command receiver or indirectly by the experiment sequence.

Command Receiver

The experiments are designed to be directly controlled by the airborne sequencer which, in turn, will be commanded from the ground by RF means. For this purpose and other command functions, a standard Range Safety receiver can be utilized. The command receiver remains energized during the entire flight.

Payload Acquisition and Tracking

To avoid tracking a silent payload, a 1 watt continuous wave beacon transmitter, operating continuously, is included in the experiments. It radiates in the 225 MHz to 260 MHz band and can share the antenna system by means of a coax switch. Thus, when the telemetry is commanded to transmit data, the beacon, though still energized, will radiate into a dummy load. It might also be accommodated by a fourth input to the VHF multiplexer.

Programmer

The experiments were defined so that the sequence of operations during experimentation can be controlled by a programmer and switched by power distribution circuits. Basic sequences are ordered with the assumed capability to have some floating, i.e., sequences may be initiated at any time during an experiment.

A typical programmer consists of a timer and a matrix of logic circuits which provide outputs to sequence the controlled functions. The timer consists of a crystal-controlled clock driving binary countdown stages. A matrix array of "and" and "or" logic gates are provided to translate the outputs of the timer into commands to sequence the controlled functions. Experiment power distribution circuits take the low voltage, low power output of the programmer and switch in relays to operate the controlled functions.

Because these units are physically related to a given experiment sequence, ROM weight and power estimates were used for experiment definition. Unit weights of 5 lb and 10 lb were allotted for small and large experiment packages, respectively. Power usage was estimated at 75-watt hours for a seven-day mission.

3.4.4.4 Antennas

Depending upon experiment, three antenna systems, telemetry (VHF), video (L-band), and command receiver (UHF) are required. Due to a roll stabilized program, each antenna system should be designed to provide a broad beamwidth in the fore and aft direction of the vehicle. The antenna system was estimated at 4 lb.

3.4.4.5 System Components and Weights

The systems components, weights, and power draw used for the experiment definition study are tabulated in Table 3-7.

3.4.5 Autopilot

The experiments defined in the study are earth-oriented payloads, maintained within a stable limit cycle in all three axes by an attitude control system. This can be accomplished by sensing vehicle angular displacement using a horizon sensor for pitch and roll and periodically updated rate integrating gyro for yaw. Updating can be by a sun sensor or star tracker. The sensor outputs control an autopilot which subsequently activates the appropriate attitude thrust valves.

A weight estimate of 20 lb for this equipment was used in the study for all payload packages. A continuous power of 30 watts was assumed.

3.4.6 Data Acquisition During Launch

The TM/TV study indicated that both types of data can be readily transmitted from the package during launch to orbit. A shroud-mounted antenna or possibly direct transmission through the transparent shroud may be used. Problems, if any, would be associated with tracking station capability and the interrelated booster transmissions. This capability was assumed for experiment definition.

Table 3-7

TELEMETRY AND TELEVISION SYSTEMS

WEIGHT AND POWER REQUIREMENTS

		Wt, lb.	Power, watts	
Telemetry System				
150 Channels	No Tape Recorder	94	275	
	Tape Recorder	103	300	Record
			150	Playback
100 Channels	No Tape Recorder	64	185	
	Tape Recorder	73	210	Record
			105	Playback
50 Channels	No Tape Recorder	34	95	
	Tape Recorder	43	120	Record
			55	Playback
Beacon		0.5	3.9	
Command Receiver		3	6.15	
Multifrequency Antenna		4	0	
Television System				
Transmitter		18	50	
Power Amplified		2	140	
Camera & Control		10	12	
Light		3	100	

3.5 ACCELERATION MEASUREMENTS

Accelerometers or engine thrust may be used to determine acceleration, the most significant experiment parameter. Although accelerometers for the range of interest appear to be available, their limitations and flight qualification status was found to be uncertain. The AS-203 had accelerometers to measure to $10^{-3} g/g_e$, but engine thrust was reportedly the only usable positive measurement. The IU had accelerometers measuring to $10^{-1} g/g_e$, much too high for THERMO.

In light of the above, the experiments were defined around engine thrust as the primary measurement of acceleration. Accelerometers, where indicated, are considered experiments themselves which, if successful, enhance the quality of the THERMO experiment data.

Section 4
EXPERIMENT PERTURBATIONS

Many types of perturbations can cause large uncertainties in the experiment results. Attitude control system, astronaut motion, variable drag, and equipment induced perturbations were investigated for each experiment area. Allowable limits on the magnitudes of the perturbations are defined below along with an indication of where these conditions occur in flight vehicles. These perturbations will not affect the High Performance Insulation experiments but constraints are introduced in the other areas.

Astronaut motion effects on the experiments could not be assessed. Astronaut motion results in three-dimensional accelerations of various magnitudes and varying frequency. It is difficult to analytically resolve their effect on the experiments and adequate data is unavailable. Should design proceed on the manned laboratory concept, it is recommended that experiments be performed which duplicate the ratio of astronaut induced to vehicle accelerations.

The perturbations investigated were not found to affect the feasibility of the experiments; preliminary design may proceed. However, the experiments and full scale vehicles will not be completely devoid of some of their effects, particularly those introduced by the ACS. Further work is recommended, either prior to or in parallel with experiment package design, to delineate the magnitude of the effects to be expected and to include those of importance as experiment objectives.

4.1 STRATIFICATION/DESTRATIFICATION

4.1.1 Attitude Control System (ACS)

Lateral, Coriolis, centrifugal accelerations and the engine pulsing frequency must be considered. Limits for the resulting effects were developed in Project THERMO Phase B (Reference 2-7). The Phase B Prime Study recast them in terms of the allowable rotational speeds, accelerations and distance between the experiment and the vehicle C. G. For analysis, all effects are assumed continuous, yielding possibly over-conservative constraints. The ACS acceleration will be impulsive.

Lateral accelerations must be limited to values ensuring a non-disrupted boundary layer:

$$a_{ACS} < \frac{586\eta}{{Ra_x^*}^{1/5}} \qquad (4-1)$$

where η is the acceleration (g_e). This is plotted in Figure 4-1 as a function of Modified Rayleigh number and g level. A typical lateral ACS acceleration is shown. Note that the very low g, high Rayleigh number experiments are affected.

Coriolis acceleration effects will be eliminated if the angular acceleration is

$$\dot{\theta} < \frac{12.82\ g}{1.34\ v/x\ {Ra^*_x}^{3/5}} \qquad (4-2)$$

where v is liquid viscosity, and x is the distance from the tank bottom. A further limit on $\dot{\theta}$ is that the centrifugal acceleration be less than 10 percent of the applied acceleration g. This results in

$$\dot{\theta} < \sqrt{\frac{0.1g}{r}} \qquad (4-3)$$

Figures 4-2 and 4-3 show $\dot{\theta}$ limits along with a typical ACS $\dot{\theta}$. None of the proposed experiments are affected by Coriolis accelerations. Experiments at 10^{-5} and 10^{-6} g_e will experience a variation in longitudinal g level that is greater than 10 percent, due to the centrifugal acceleration induced by the vehicle rotation.

A further ACS design constraint is that the impulse frequency must be less than one-tenth the liquid natural frequency or larger than twice the liquid natural frequency (Reference 2-7). Figure 4-4 presents the natural frequency of the liquid as a function of g level and tank diameter.

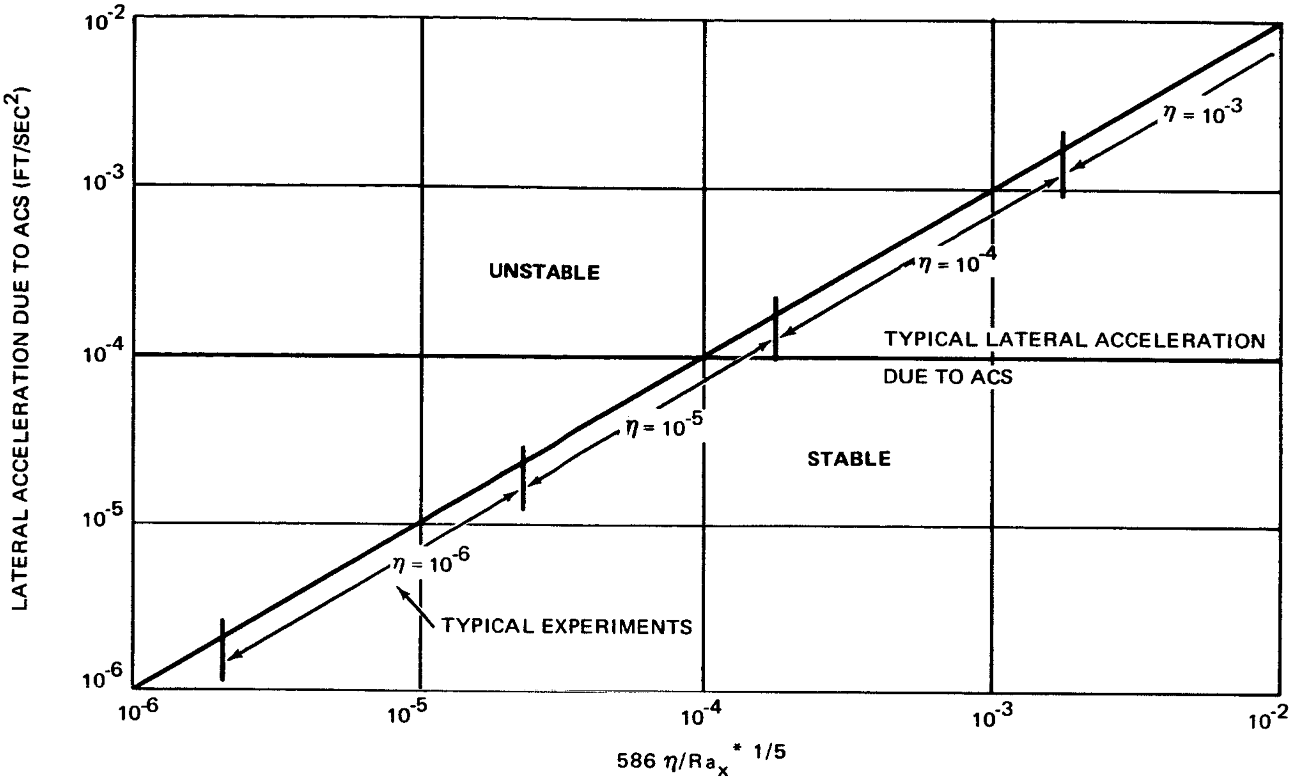

Figure 4-1. Allowable Lateral Acceleration

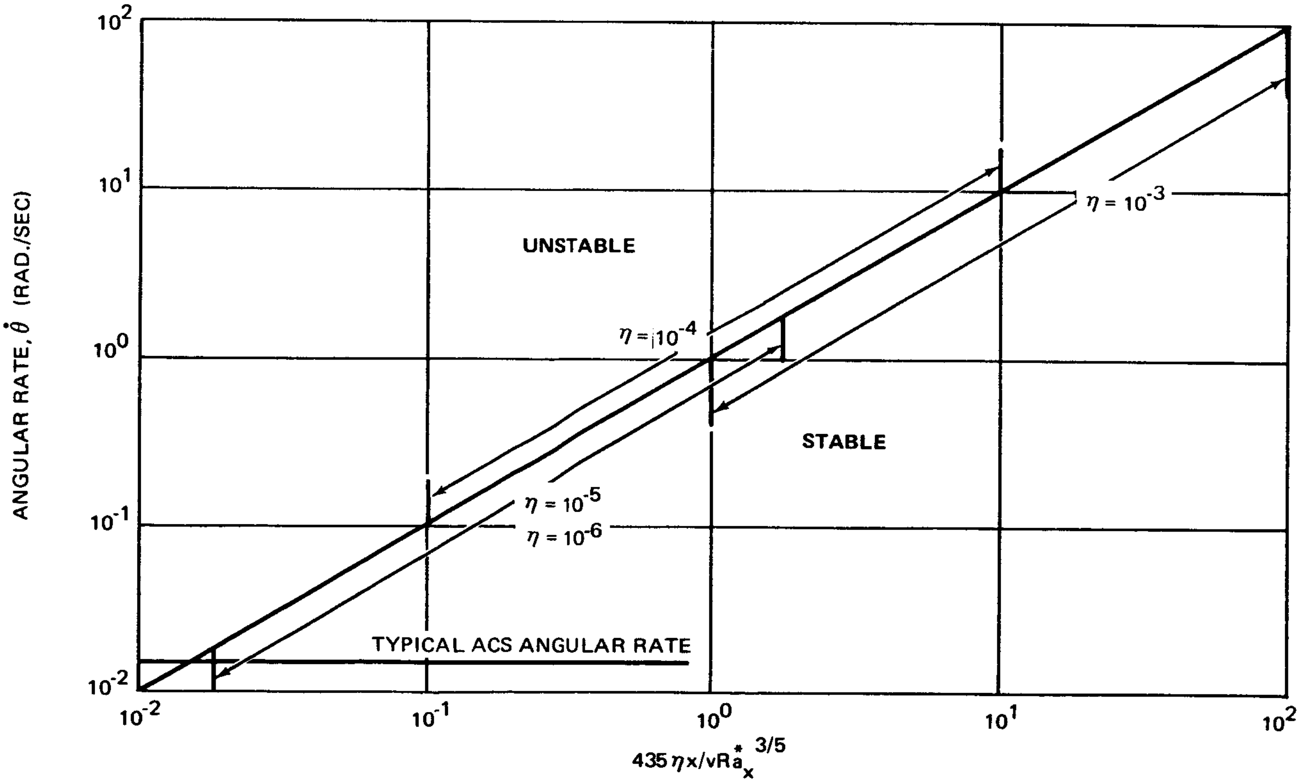

Figure 4-2. Allowable Angular Rate for Coriolis Accelerations

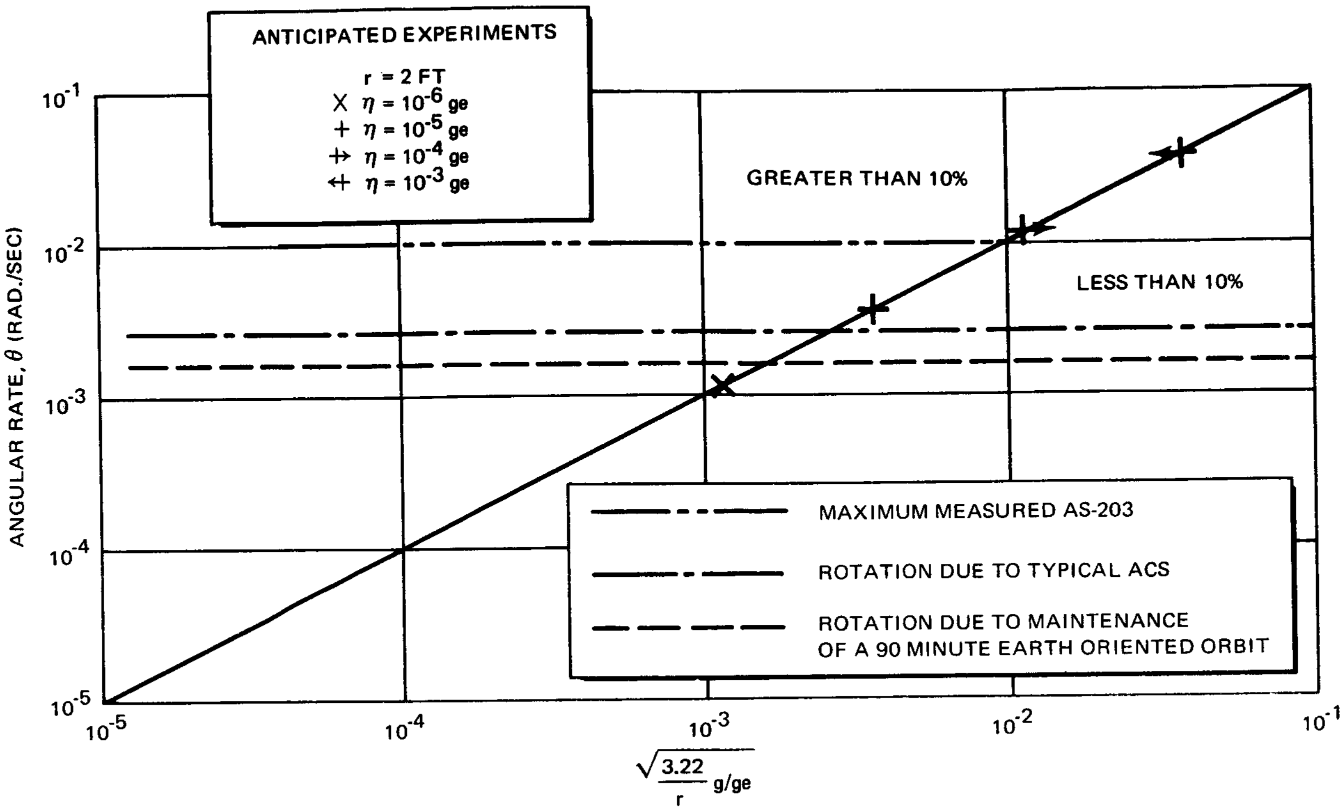

Figure 4-3. Variation in Longitudinal Acceleration Due to Angular Rate

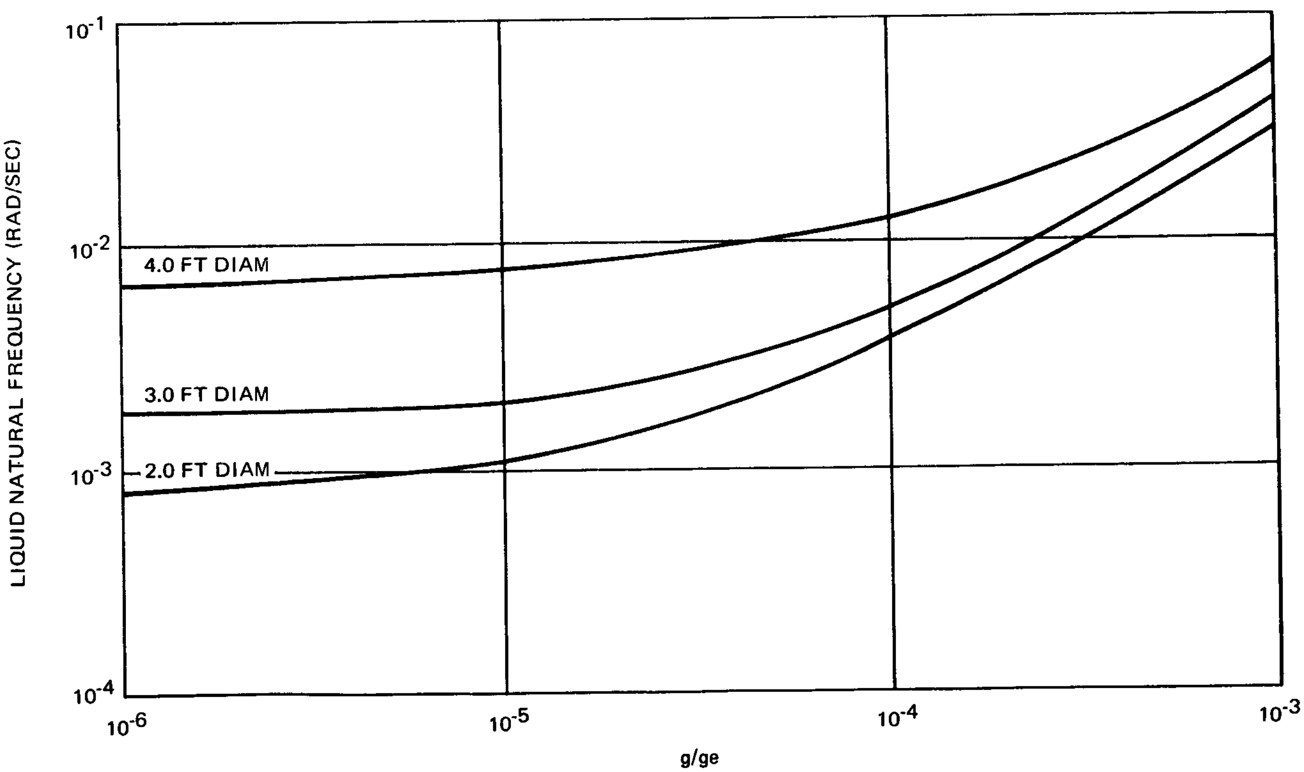

Figure 4-4. Liquid Hydrogen Slosh Frequency

It appears that the experiments can never be completely devoid of the effects of ACS induced rotation. Further, a typical orbiting vehicle will experience the same or greater rotation effects. Centrifugal accelerations are typically of the order of 10^{-6} g/g_e, and drag on an S-IVB (Figure 4-5) is typically less. Also, the c. g. is in the fluid so the centrifugal effect will be additive on one side and subtractive on the other causing acceleration gradients. In a full S-IVC (235-nmi orbit) this could cause flow above and below the c. g. with the warmer fluid collecting near the c. g. If a continuous vent is used, the g level will be about 10^{-5} g/g_e and this effect will be minimal. It is suggested that ground experiments be performed which duplicate the ratios of rotationally induced accelerations to longitudinal accelerations which are expected in the orbiting vehicles. If results show that these effects are important, the proposed orbital experiments should be refined to include rotation effects.

Vehicle roll can cause convection to occur in the horizontal plane due to centrifugal forces. The roll rate at which lateral convection is initiated is not known and experiments or theoretical work is necessary to delineate the significance of the effect. Simple experiments could be run using a centrifuge. If the effects are large, a re-definition of the orbital experiments must be made to include roll rate as a parameter.

4.1.2 Variable Drag

The maximum variations in drag, Figure 3-3, will be apparent only if the experiment is run with 10^{-6} g/g_e drag acceleration. There is a factor of two in the uncertainty when this is the case. The effect of angle of attack (10°) is small (see Section 3.2).

4.1.3 Equipment Effects

The destratification motor torque (0.003 ft-lbs) will be transmitted to the carrier vehicle. The ACS system must be designed to remove this torque. Cryogenic Valve operation does not appear to introduce significant perturbations.

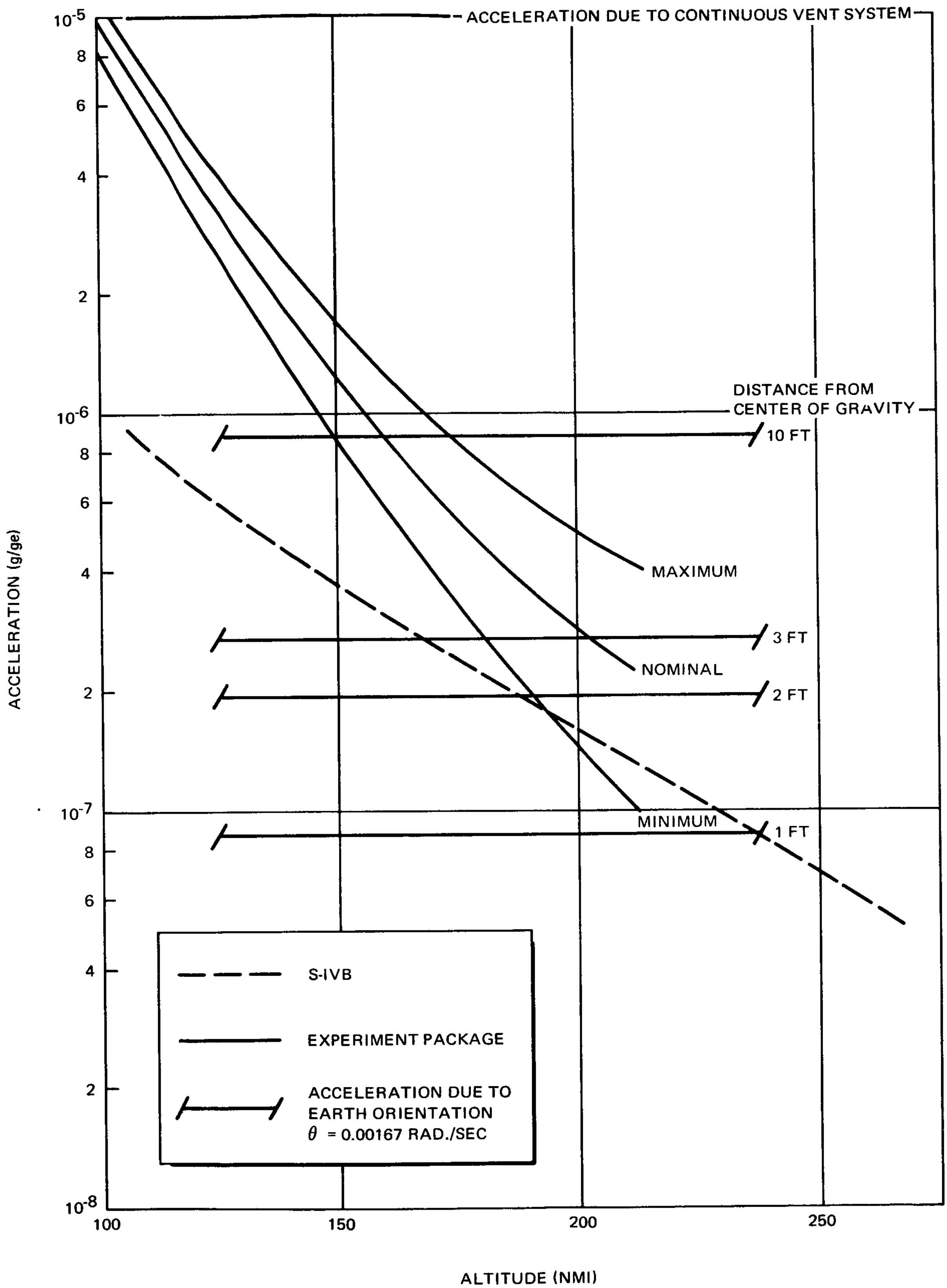

Figure 4-5. Acceleration Acting on the Vehicle Due to Drag (Nominal)

4.1.4 Conclusions

Pitch or yaw and roll are key parameters and some of their effects cannot be avoided. Because they will also be experienced on actual vehicles, it is recommended that the stratification experiments should include these effects. The rotationally generated g field in an S-IVC will be larger than the drag and could be of an oscillatory nature (no continuous vent). This should be considered. Gravity gradients, which could yield effective accelerations of the order of 10^{-7} g/g_e in actual vehicles are also important above 225 nmi.

4.2 INTERFACE STABILITY

4.2.1 Attitude Control System (ACS)

The ACS θ will generate a lateral acceleration of the order of 3×10^{-6} g/g_e (10^{-4} ft/sec^2) and will affect only the 10^{-5} g/g_e experiments. The effects of $\dot{\theta}$ are Coriolis accelerations and changes in the longitudinal g level (centrifugal forces). The latter will be less than 10 percent for all of the proposed interface stability experiments. Coriolis acceleration will increase the liquid natural frequency and decrease slosh wave amplitude. Figure 4-6 shows that the angular rate required to maintain a 90-minute orbit causes a 25-percent increase in frequency at 10^{-4} g/g_e. This effect is amplified to 30 percent at 10^{-5} g/g_e. The effect on a typical S-IVC will be less than about 30 percent. The S-IVB 203 data (Reference 4-1) indicates that $|\dot{\theta}|$ ranged from 0.0 to 0.5 degrees per second. The Coriolis effect can partially account for the decreased time per cycle observed. This should be included in experiment planning and all calculations of wave period should include it (approximate method given in Reference 2-7). Coriolis effect becomes extremely important at high Earth orbit, or during interplanetary flight.

A limit was set on the allowable roll rate by insuring that the elevation difference along the tank between center and end be no more than 10 percent of the tank radius. This yields the allowable roll rate

$$\Omega < (0.2\ g/r)^{1/2} \qquad (4\text{-}4)$$

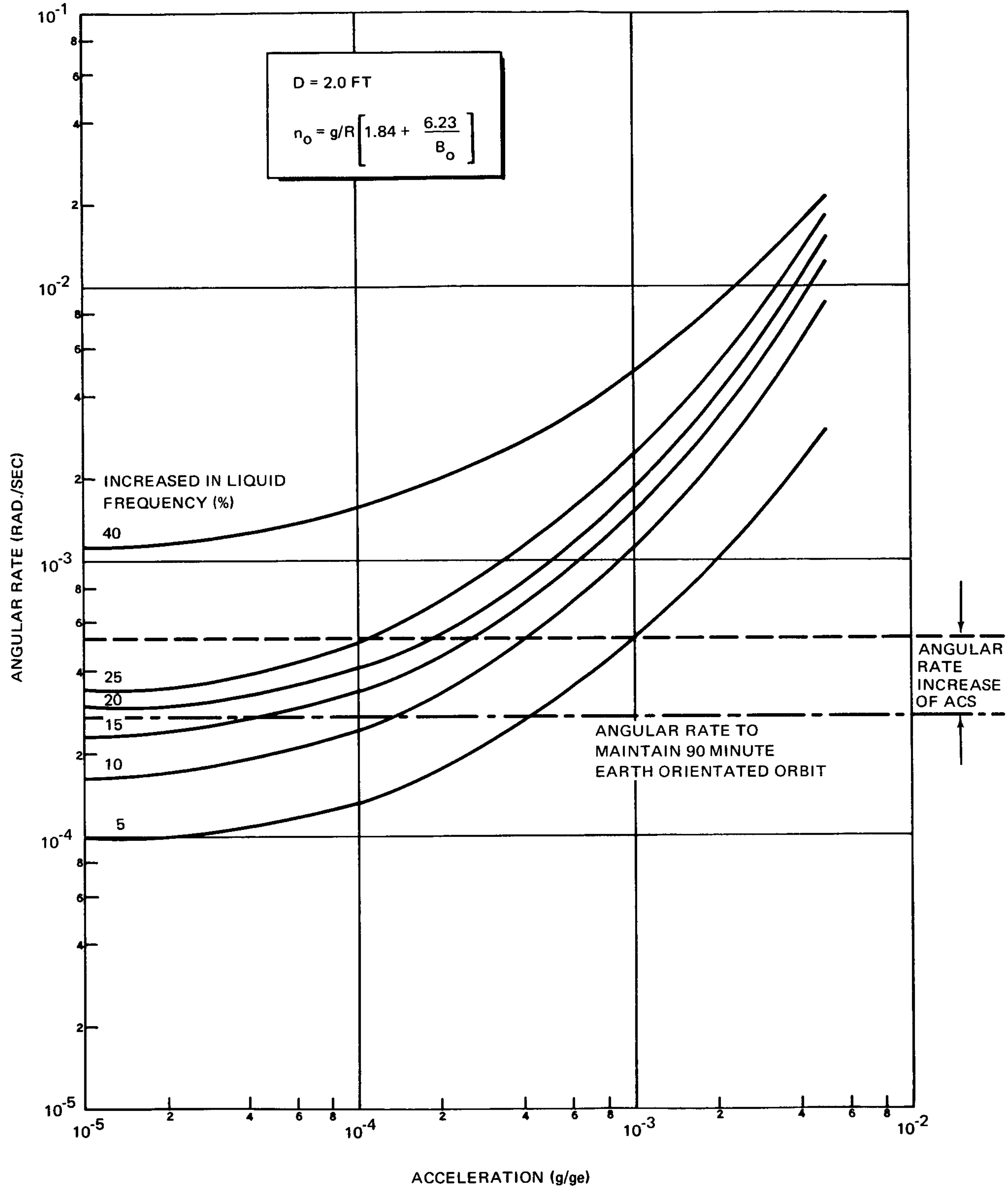

Figure 4-6. Allowable Angular Rate

where r is the tank radius. At the lowest anticipated experiment g level (10^{-4} g/g_e), and a radius of 1 ft, $\Omega < 4.5 \times 10^{-3}$ radians/sec or 0.26 deg/sec. This criteria can be readily met.

4.2.2 Variable Drag

Variable drag due to uncertainties in the atmospheric conditions or due to angle of attack will always be less than 10 percent of the applied g level and therefore are inconsequential.

4.2.3 Equipment Effects

The experiments require valving for fluid flow between tanks, such as a Sterer, DACo part number 1B66692, solenoid operated valve. The valve opens and closes in 150 ms. The pintel weighs 0.75 lb. The solenoid generates 35 lb.

The 0.75 lb pintel travels 0.13 in. in 150 ms and the average acceleration acting on the pintel will be 3×10^{-2} g/g_e. The acceleration acting on the vehicle will be 3×10^{-5} g/g_e. The average acceleration acting on the vehicle is low enough and for such a short duration that no problems are anticipated.

4.2.4 Slosh Coupling

Coupling between the ACS and the liquid in the tank must be considered. To minimize coupling, with one tank the ACS frequency must be

$$N_{ACS} < 0.1 \left[\frac{g}{r}\left(1.84 + \frac{6.23}{B_o}\right)\right]^{1/2} \qquad (4\text{-}5)$$

$$N_{ACS} > 2 \left[\frac{g}{r}\left(1.84 + \frac{6.23}{B_o}\right)\right]^{1/2} \qquad (4\text{-}6)$$

A second type of coupling could exist between the two tanks and the ACS system (see Figure 4-7, a schematic of the problem). The coupling between Tank 1 and Tank 2 is through the structure and the ACS input is into the structure. It is necessary to parameterize the system for a particular ACS system to obtain the optimum fluid masses and structure mass.

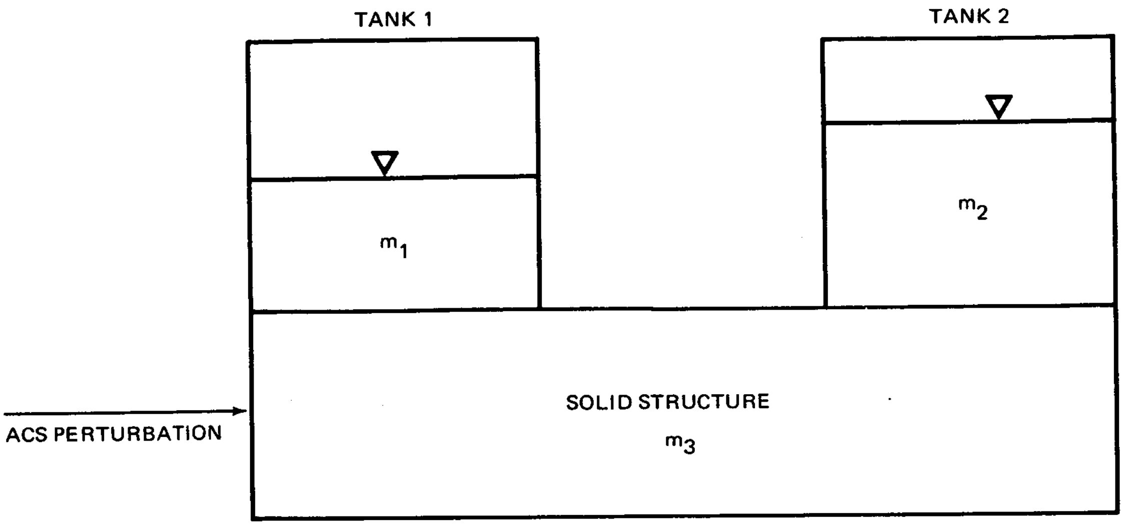

Figure 4-7. Slosh Coupling

The method of obtaining the solution is (1) set up solution for a single tank yielding slosh mass, forces and moments as a function of three dimensional translational and rotational perturbations; (2) couple the solution to the structure and through the structure to the other tank; (3) add a forcing function (ACS) and couple the ACS response to the system perturbations; and (4) solve for a range of m_1, m_2, and m_3. The experiments can be flown and the above utilized for detailed data reduction and correlations.

4.2.5 Conclusions

None of the perturbations were found to be incompatible with the experiment concept. The study showed that adequate knowledge to predict some slosh phenomena occurring in vehicles and in the experiment package is unavailable. Further effort is warranted to ascertain their importance and possible inclusion as experiment objectives.

Three areas require further analytical and experimental study. The first is to evaluate the importance of the effect of rotation on frequency changes. If it does, then ground experiments should be run to establish the degree of change with rotational rate. The second area is the importance of impulsive ACS perturbations. The third area requiring investigation is slosh coupling.

4.3 PROPELLANT TRANSFER

4.3.1 Attitude Control System (ACS)

The lateral accelerations due to the ACS $\dot{\theta}$ will affect propellant transfer experiments run at drag at any vehicle angle of attack. At a zero angle of attack, the lateral acceleration will be greater than the drag induced g level and the fluid will move to the side of the container. During the time the fluid moves from the tank inlet to the top of the tank, the tank should not move more than one-tenth of its radius. This criteria may be stated

$$\dot{\theta} < \frac{RV_i}{10\ HL} \qquad (4\text{-}7)$$

where R is the tank radius, H the tank height, L the distance from the vehicle c. g. to the tank top and V_i the lowest characteristic velocity. It should be noted that this is a simple way of accounting for Coriolis effects. Substituting into the above equation yields an upper limit on $\dot{\theta}$ of 0.25 deg/sec. The limit on roll rate will be the same as Section 4.2.1 (Equation 4-4), and is 0.26 deg/sec. This criterion can be readily met.

The ACS accelerations are higher for experiments requiring flight at a 90° angle of attack. Drag is also higher. Further effort is required to define the ACS characteristics for this flight mode and the magnitude of the effect on the experiment (See Section 9).

4.3.2 Equipment Effects

Valves will be required to control the flow. The valves will be the same type as that discussed in Section 4.2.3, and their effect will be small.

4.3.3 Slosh Coupling

Coupling between the liquid in the two tanks and the ACS must be considered. The problem is the same as for the Interface Stability experiment (Section 4.2.4). An analysis, in parallel with the preliminary design effort, is required.

4.3.4 Conclusions

The experiments appear to be feasible in light of the perturbations investigated. Further effort is suggested, particularly the slosh coupling with the ACS, such as experimentation using a shake table.

4.4 BOILING HEAT TRANSFER AND BOILOVER

4.4.1 Attitude Control System (ACS)

Pitch and yaw or lateral accelerations cause the dynamics of the bubbles to change. Lateral accelerations will change the effective direction of the applied acceleration. Pitch and yaw, however, manifest themselves in the form of Coriolis accelerations and as a result the bubbles will follow a curved trajectory.

The lateral acceleration developed by the ACS is 3×10^{-6} g/g_e and will affect only the experiments to be run at 10^{-5} and 10^{-6} g/g_e. It is intermittent, however, and should not have too great an effect on the results. This should be verified with ground tests where 0.3 g/g_e is applied in the lateral direction with the same frequency as the expected ACS.

The effect of sloshing will be minimal if the heater is submerged more than one tank radius beneath the liquid surface. The effect on boilover is not known but it is felt that sloshing will not affect the bubble velocities.

The Coriolis accelerations cause the bubbles to travel in some direction other than normal. This should not affect boiling from a horizontal surface but could affect a vertical surface experiment. The latter will require experimental investigation. Test of this type could be carried out using a centrifuge and existing Douglas equipment. The effects on boilover are more easily determined. The very small bubbles, less than 0.05 ft in diameter, will not be affected at any of the anticipated g levels. At g levels greater than 10^{-4} g/g_e, the upward component of the velocity of all the bubbles will be decreased by less than 5 percent. At 10^{-5} g/g_e, the velocity will be decreased 10 percent at 10^{-6} g/g_e by 30 percent. The bubbles whose diameters are greater than 0.05 ft will rise in a direction that is from 25 to 40 degrees from the vertical for all g levels. This is to be expected in all earth oriented vehicles and should not place a limitation on the ACS. Further ground tests (centrifuge) should be carried out to corroborate these results.

The allowable roll rate should be limited to keep the centrifugal acceleration less than 10 percent of the applied axial g level. This sets an upper limit of 0.25 deg/sec on the allowable roll rate; compatible with the systems investigated.

4.4.2 Variable Drag

Drag variations will have a negligible effect except when experiments are run at drag g levels. There is an acceleration level uncertainty of a factor of two when this is the case (see Figure 3-3).

4.4.3 Conclusions

The various vehicle perturbations should not affect the boiling experiments. However, experimental corroboration should be carried out using a centrifuge. The bubble dynamics will be effected and ground tests should be run to determine the dynamics due to the effects of rotation.

4.5 SUMMARY OF RECOMMENDED WORK

There are many types of accelerations acting on the Mars vehicles that in many cases will be larger or equal to the axial g level, Table 4-1. In the case of past propellant management analyse only the axial acceleration has been considered and an oversight may have occurred. In each experiment area, above, further work has been delineated to define the importance of these effects and incorporate them, where required, into the detailed experiment definition and data correlation. Also, verification of some of the conclusions presented was recommended. Table 4-2 presents a summary listing of these investigations.

Table 4-1

TYPES OF ACCELERATION ACTING ON FLUID IN SPACE

Type of Acceleration	Acceleration	Typical Value	
Self-induced	$a = -\frac{4}{3}\pi Gr$ (Sphere)	$a \approx 5x10^{-8} g_e$ at r = 10' in LH_2	r = distance from vehicle c. g.
Earth's Gravitational Field	$a = \omega^2 R\left(1-\frac{Ro^3}{R^3}\right)$ $\approx \pm \frac{3r}{R_o\, g_e}$	$a \approx \pm 10^{-6}\ g_e$ at r = 10' from orbit trajectory	R = Earth Radius; R_o = distance from center of Earth to vehicle orbit; r = distance from vehicle orbit
Centrifugal Acceleration due to Fixed Earth Orientation	$a = r\omega^2$	$a \approx 3x10^{-7} g_e$ at r = 10'	r = distance from vehicle c. g.
Atmospheric Drag S-IVB	$5x10^{-7}\ g_e$ at 130 n. m. $1.55 \times 10^{-7}\ g_e$ at 200 n. m. $1.2^{-7}\ g_e$ at 300 n. m.		
Effect of large Mass Nearby	$a = MG/r^2$	$a = 10^{-7}\ g_e$ Saturn S-IVB loaded at r = 10'	r = separation distance

Table 4-2

RECOMMENDED 1-g EXPERIMENTS AND ANALYSIS

Experiment Area		Experiment and Analysis Required
STRATIFICATION	1.	Effects of rotation caused by pitch and yaw on natural convection and stability of boundary layer.
	2.	Oscillatory g level due to On-Off characteristics of ACS.
	3.	Effects of sloshing.
INTERFACE STABILITY	1.	Effect of rotation due to pitch and yaw on slosh frequency.
	2.	Effect of impulsive lateral accelerations.
	3.	Slosh coupling when the disturbances are impulsive.
	4.	Effect of roll rate on slosh characteristics, particularly startup transients.
PROPELLANT TRANSFER	1.	Surface instabilities due to impulsive ACS during fill or drain.
	2.	Slosh coupling during drain.
BOILING - BOILOVER	1.	The effects of intermittent impulsive lateral accelerations.
	2.	The effects of sloshing on boiling heater submergence requirements.
	3.	The effects of rotation on bubble trajectory and velocities.

Section 5
INTERFACE STABILITY EXPERIMENTS

5.1 ORBITAL EXPERIMENT INFORMATION REQUIREMENTS

The Technology Survey (Section 2) showed the necessary information for the design and optimization of the S-IVC, S-IIB and Nuclear Stages. Most of this information must be obtained from properly scaled, long term low g experiments which simulate the vehicle geometry, supported by analyses and ground or aircraft tests. In-orbit investigations of propellant settling, orientation, maneuver and MECO induced slosh, and engine restart technology were found to be necessary and/or desirable.

New resettling technology was shown to be desirable for both venting and engine restart operations. In orbit tests provide an evaluation of the adequacy of current design time computations and the foundation for optimum resettling sequences.

Control of maneuver induced slosh involves two areas: ACS sloshing and the effects of corrective forces applied to the vehicle during docking. The information of concern in the design of ACS systems is the wave motion effects on the vehicle motion (slosh wave forces and moments), the effect of ACS impulses on the wave motion (wave mode and frequency), and determination of appropriate ACS impulse magnitudes, durations, and frequencies. Problem areas which exist in docking maneuvers include the motion of the vehicle induced by movement of the liquid and the subsequent possible increased vehicle motion induced by improperly applied correcting forces. Proper experimentation of these liquid/vehicle dynamic coupling effects can only be performed in orbit.

It was shown that the effect of the various static initial liquid configurations on resettling, docking, ACS sloshing, propellant transfer, etc. should be assessed to provide limits for design predictions. Long term low g liquid configurations, resulting from various dynamic initial conditions, should also be determined, since it plays an important role in the determination of propellant thermal energy distribution during space storage. The long-term effects of liquid motion resulting from main-engine cutoff must also be studied in orbit.

Optimum ullage thrust sequences for engine restart are obtained as a result of the resettling information required for low g venting. Other engine restart problems requiring in-orbit investigation include diffusion and control of the inflowing pressurization gas, and possible vibration induced bubble sinking and coalescence.

Since three liquid levels are required for most of the interface stability experiments, draining of the liquid is required. These draining sequences can provide data on propellant transfer dynamic phenomena.

Various types of control techniques such as baffles, screen tension devices or dielectrophoretic systems can also be evaluated in orbit. However, experiment definition was limited to those control devices (baffles) presently considered a part of the study vehicles.

5.2 DATA ACQUISITION PROGRAM AND EXPERIMENT REQUIREMENTS

5.2.1 Objectives

The program has two objectives: (1) evaluate specific vehicle design techniques or constraints, and (2) obtain scaled data on the basic interface stability phenomena which are important to vehicle operation and efficiency. The first is met by resettling, docking, ACS slosh, and low g liquid configuration experiments, which simulate as closely as possible the conditions expected on the S-IVC, S-IIB, and Nuclear Stage vehicles. The data can then be directly extrapolated. Geometric similarity is assured within limits by using proper vehicle configurations, length to diameter ratios and scaled internal hardware sizes and locations. The broader objective of obtaining phenomenalogical data is met by assuring that sufficient information will be obtained from the experiments to verify and refine existing analyses or provide a range of data for future work.

No basic distinction has been made between data for each vehicle since all experiment areas and general requirements are essentially identical at this stage in the program definition. However, at least two separate in-orbit tests will probably be required: one with the S-IVC/S-IIB inverted dome configuration, and one with a Nuclear Stage hemispherical dome configuration.

Two experiment configurations appear to be most suitable for the experiments and compatible with the weight and volume constraints imposed by the carrier vehicle. In both cases, transparent tanks are used with hexane. The first configuration consists of three tanks: one large, about 2 by 4 ft. and two small, about 1 by 2 ft. This system, Figure 5-1, is similar to that recommended in Project THERMO Phase B (Reference 2-7). Also shown is a second configuration consisting of two equally sized tanks, approximately 1. 5 by 3 ft. Details are presented in Section 5. 3.

5. 2. 2 Propellant Settling

This experiment's objective is to provide sufficient data to define an optimum settling acceleration sequence for baffled and unbaffled tanks, geometrically similar to the Mars vehicles. To determine total settling time, the separate settling phenomena, such as effects of liquid initial configuration and motion, Taylor instability, movement of the liquid from one end of the tank to the other, liquid impact, turbulent dissipation, laminar wave dissipation in low g, and bubble motion should be considered. The analyses of Reference 2-7 provide a possible means of determining and relating the characteristic times for each so that resettling times and propellant consumption can be calculated. The orbital experiments provide data to evaluate and refine these analyses.

Figure 5-2 illustrates typical curves of total resettling time as a function of initial and final accelerations. The circles depict the areas in which data could be taken and are included for illustration only; detailed sequences for inorbit experimentation can be determined only after supporting low g aircraft tests have been performed.

The initial acceleration is applied for the time period required to move the liquid from one end of the tank to the other. The final acceleration is applied for the time required to dissipate the wave energy or displace the bubbles

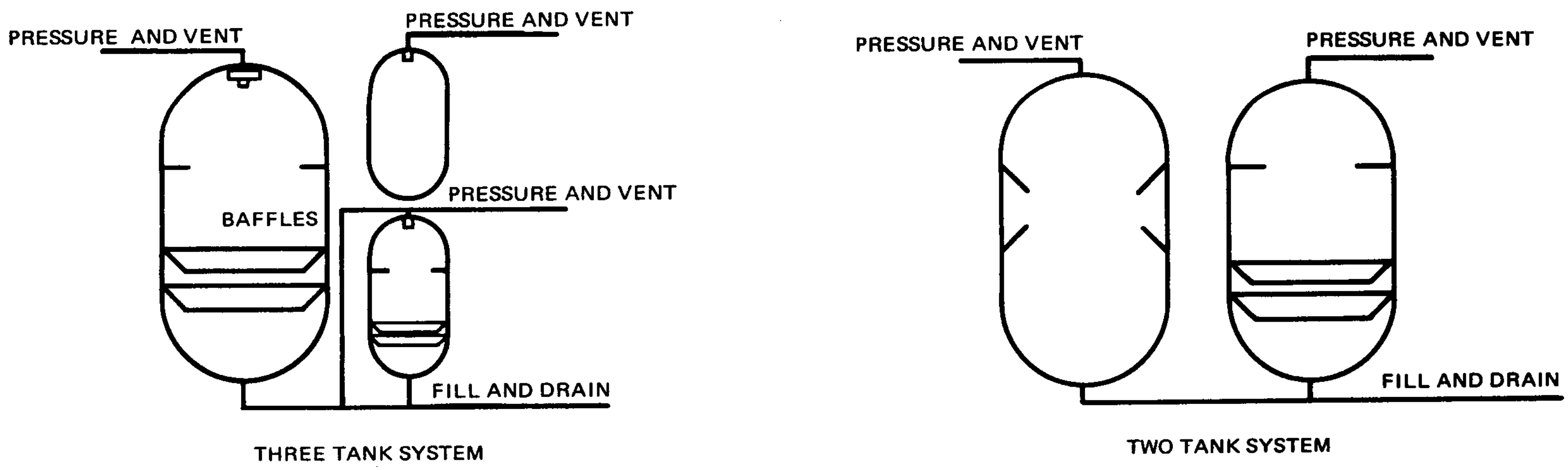

EXPERIMENT AREAS

1. PROPELLANT SETTLING
2. PROPELLANT SLOSH CONTROL DURING VEHICLE MANEUVERS
   (a) DOCKING
   (b) ACS SLOSH
3. ENGINE CUTOFF INDUCED SLOSH
4. PROPELLANT DRAINING AND TRANSFER DYNAMICS
5. PRESSURIZATION GAS FLOW DYNAMIC EFFECTS
6. VIBRATION EFFECTS
7. SURFACE TENSION PHENOMENA

Figure 5-1. Interface Stability Experiment

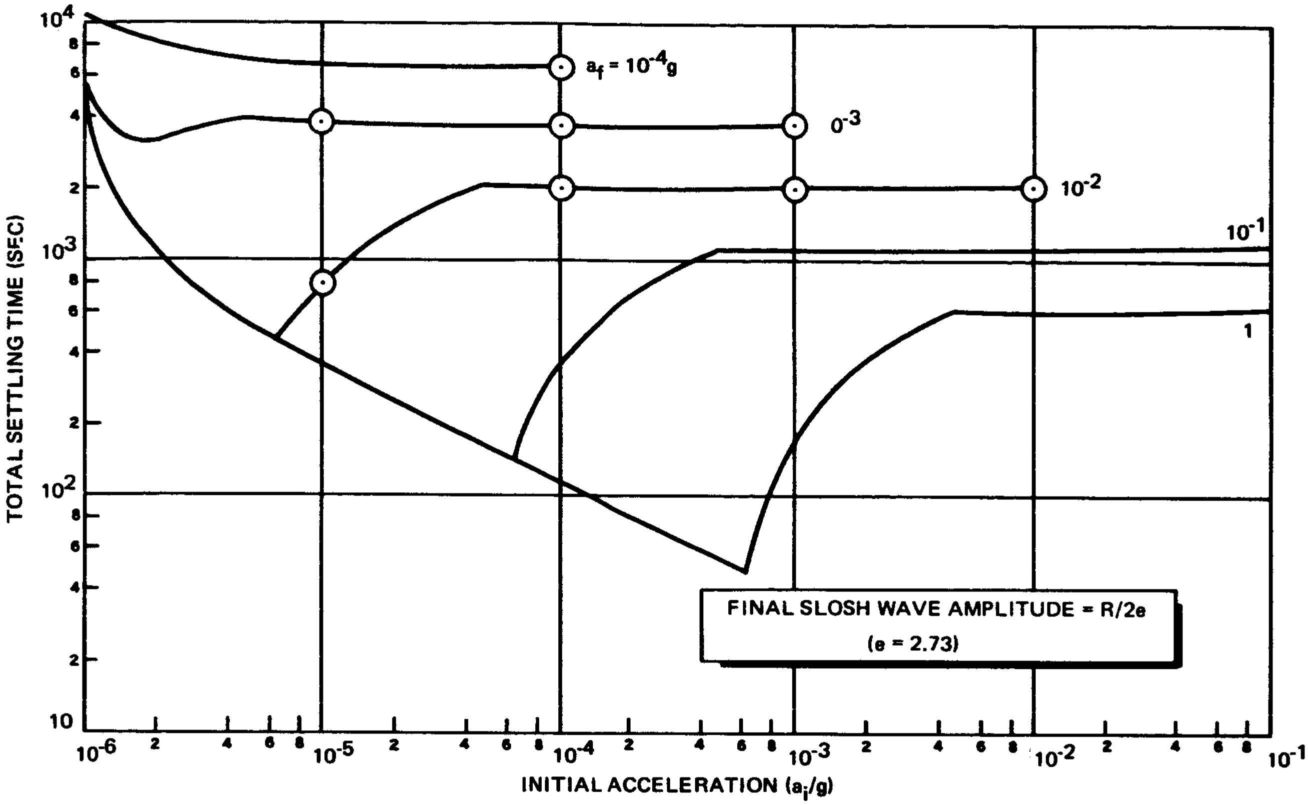

Figure 5-2. Settling Time vs Initial Acceleration for 15-ft Diameter Tank

entrained at impact, whichever is greater. Results are also shown for a constant applied acceleration. The minimum resettling time is obtained by applying low initial accelerations, thus limiting the liquid kinetic energy at impact, and then applying higher final accelerations to increase the wave energy dissipation rates. Application of a constant thrust level does not yield either minimum resettling time or minimum propellant consumption. These curves were obtained from a Douglas numerical resettling program (Section 5. 5).

Estimates of the minimum number of resettling experiments required and the approximate total experiment duration were estimated as follows: three resettling thrusts are used (10^{-2}, 10^{-3}, and 10^{-4} g) and the liquid is assumed to be accelerated from one end of the tank to the other and accelerated back to its initial position under two separate initial conditions (maximum initial wave kinetic energy and maximum initial wave potential energy). Three liquid levels should be included since the study vehicles resettle with tanks 40 to 95% full. The above accelerations are required to achieve approximate similarity with the study vehicles (Section 5.5). In addition, drag deceleration on the experiment package will provide lower acceleration levels which are required to investigate initial liquid motion and equilibrium configuration effects in resettling for vehicles operating in the extremely low acceleration environment of interplanetary space.

A minimum experiment sequence, one liquid level, is shown in Table 5-1. This sequence would be repeated at two other liquid levels for a total of 24 experiments. This sequence appears to be a minimum in terms of experiment time and APS propellant requirements. The number of experiments required to provide all possible combinations of the delineated experiment parameters (thrust level, liquid volume, initial conditions, and flow direction) is 108. However, the resettling analyses showed that applying high thrust levels first and then switching to low thrust levels is inefficient. Hence, it is not considered. It is also not considered necessary to obtain data on all possible combinations of initial conditions, since design constraints on the resettling system would be based on worst-case conditions.

The experiment definition effort delineated approximate experiment durations, propellant consumption requirements, and thrust level requirements. Further study of the experiment conditions, number of experiments and sequencing is required and should be supported by aircraft tests of resettling in tanks of approximately the same size and configuration as the recommended in-orbit experiment tanks.

5.2.3 Propellant Slosh Control During Vehicle Maneuvers

These experiments provide correlated low g data on propellant motion influenced by various applied perturbing forces which simulate expected vehicle conditions during docking and ACS maneuvers. The data is required to define APS/ACS design constraints (vehicle acceleration magnitudes and durations), and assess the effects of control baffles.

5.2.3.1 Docking Slosh

A major problem of vehicle docking is that relatively high accelerations (10^{-2} g/g_e longitudinal and 10^{-3} g/g_e lateral) are presently planned to effect changes in the vehicle orientation and position. These accelerations

Table 5-1. Experiment Conditions For Minimum Resettling Sequence

Acceleration Sequence	Liquid Level	Flow Direction	Initial Wave KE
Low Acceleration $\approx 10^{-4}$g	90% - 95%	Bottom → Top	Minimum
Medium Acceleration $\approx 10^{-3}$g	90% - 95%	Top → Bottom	Minimum
High $\approx 10^{-2}$g	90% - 95%	Bottom → Top	Maximum
Low Acceleration $\approx 10^{-4}$g	90% - 95%	Top → Bottom	Maximum
High 10^{-2}	90% - 95%	Bottom → Top	Minimum
Low → High $10^{-4} \rightarrow 10^{-2}$	90% - 95%	Top → Bottom	Maximum
Low → Medium $10^{-4} \rightarrow 10^{-3}$	90% - 95%	Bottom → Top	Maximum
Medium → High $10^{-3} \rightarrow 10^{-2}$	90% - 95%	Top → Bottom	Minimum

Sequence repeated for 70-80% level and 40-50% ⇒ 24 total experiments.

correspond to Bond numbers of about 4,000-80,000 for the study vehicles. Extreme surface deformations, dynamic responses, and ullage gas/liquid mixing and dispersion are expected. Acceleration duration is important since the total liquid kinetic energy gain is a function of acceleration time. The liquid response to a complex series of correcting accelerations is virtually impossible to predict by classical analytical means without resorting to use of numerical programs, such as the Los Alamos Scientific Laboratory Marker and Cell (MAC) Program which, however, is limited to two-dimensional or axisymmetric motion. Since there is virtually no supporting analytical work available on liquid motion in a low g field with relatively high perturbing accelerations, only a preliminary definition of the docking experiment can be given.

The experiment must be designed to simulate expected vehicle docking maneuvers. Hence, perturbing accelerations should be in the high Bond number regime. The liquid kinetic energy gained should be simulated; the Froude number, (kinetic to potential energy ratio) is a natural choice as a similarity parameter, in addition to Bond number. The Weber number (kinetic to free surface potential energy ratio) also appears significant, especially in correlating bubble entrainment and formation, and gas/liquid dispersion and mixing. However, additional analytical and experimental studies of liquid response to high Bond number perturbing accelerations in a low Bond number environment are required before specific experiments can be defined to simulate docking. Moreover, ranges of acceleration magnitudes and directions which are expected during actual docking maneuvers on the specific vehicles must be determined.

Some of the less complex liquid motions occurring during docking maneuvers have been analyzed. For example, during rendezvous the pursuit vehicle will be accelerated towards the target vehicle, and then the thrust will be decreased or terminated. At that time, wave amplification will occur which can be understood from MECO wave amplification studies. The wave amplitude, frequency and mode can be predicted with some success for linear waves from previous ACS slosh work. If thrust reversal is required to decelerate the pursuit vehicle, information on resettling phenomena is applicable. However, the extremely complex motion resulting from a series of high acceleration, long-duration correcting maneuvers probably defies complete analysis. It will be necessary to simulate the acceleration conditions experimentally and extrapolate the results.

During rendezvous and docking, the pursuit vehicles will be subject to orbital drag and the corresponding Bond number, directed fore or aft--depending on vehicle orientation--will be of the order of 0.1 to 10. During the docking experiments, a low acceleration ($10^{-4} g/g_e$) will be applied continuously to simulate the orbital drag acceleration acting on an actual vehicle. Different combinations of medium and high experiment accelerations ($10^{-3} g/g_e$ and $10^{-2} g/g_e$) will be applied with various durations to simulate docking maneuvers. Positive axial accelerations will be applied and then reversed or terminated and liquid motion observed. Lateral accelerations will be applied with frequencies and phases designed to induce high amplitude sloshing and even dispersion and mixing of the liquid and gas. Experiments will be performed at liquid levels corresponding to the design levels for the vehicles under consideration. Baffle effects will be assessed.

Slosh forces and moments must be measured in order to determine effective slosh masses, moments of inertia, impact forces, and baffle drag coefficients. Total wave forces and moments can only be measured with a strain gauge dynamometer system, a concept which is complex and not clearly feasible. With tanks having external plumbing connections and supports, the forces can not be measured because of the rigidity of the system. A sealed tank with no external plumbing, equipped with removable supports is required. Without this system wave forces and moments must be deduced from observation of slosh decay rates and estimates of wave momentum changes.

Accelerometers appear to be available although not flight qualified in the range of 10^{-2} to 10^{-4} g/g_e. These will significantly enhance the accuracy of the data. A constant thrust will result in experiment acceleration variations due to liquid initially in free fall, internal motion, and impact. Engine thrust provides an accurate determination of acceleration to be made only if the liquid mass is low compared to the experiment package mass or if there is little liquid movement.

Observation of liquid positions allows determination of c. g. locations to be made; then, estimates of vehicle movement can be made. Vehicle movement induced by sloshing liquid will exist after perturbing forces are removed; the movement of the pursuit vehicle relative to the target vehicle may be severe depending upon tank ullage volume. A constant thrust on the docking vehicle will produce a varying acceleration and after impact of the liquid against tank walls the acceleration will suddenly change. These effects further complicate the problem of understanding the liquid motion, since the acceleration rates on actual vehicles will be nonconstant.

During rendezvous and docking it may be necessary to rotate the vehicle(s) to present the proper orientation. The propellant will be perturbed, tending to rotate in the opposite direction to that of the vehicle (conservation of system angular momentum). This phenomena should be explored as a part of the in-orbit experiment.

Preliminary estimates of docking experiment durations and the corresponding acceleration levels are included in Table 5-3, Section 5. 4. These estimates were made to determine the approximate experiment time and weight and do not reflect a detailed docking experiment sequence. Further effort, based on Phase B' experiment conceptual design, is recommended.

5. 2. 3. 2 Attitude Control Induced Slosh

The ACS slosh experiments provide data on the effect of lateral accelerations on liquid motion in low-g. Impulsive lateral accelerations are applied to simulate ACS thrust. Series of lateral accelerations are applied at frequencies of 0. 7, 1. 0, and 1. 4 times the natural slosh frequency of the liquid. Approximately 10 cycles are observed at the applied impulsive forcing frequency and wave motion dissipation is observed with no lateral accelerations. Data is obtained on wave amplitudes as a function of lateral acceleration magnitude, duration and frequency for baffled and unbaffled tanks.

With the three tank system recommended (Section 5. 4), the wave amplitudes resulting from a given acceleration impulse will be different for each tank because of the size differences. A direct comparison between baffled and unbaffled tanks will also be obtained. Three liquid levels are recommended, covering the range of vehicle propellant loadings expected. The ACS-induced slosh experiments require of the order of 500 - 2,000 sec for each test and tests are performed at $\pm 10^{-4}$g, 10^{-3}g, and 10^{-2}g for each liquid level. Because of rigid constraints on APS propellant, experiment times were based on 10 impulsive cycles per test. Also, most of the experiment time is allotted to the $10^{-4} g/g_e$ acceleration which corresponds to Bond numbers of the order of 1 - 10. Additional data would be desirable at the higher Bond numbers. Table 5-3, Section 5.4, summarizes these experiments. Figure 5-3 illustrates the regions of sloshing for which data will be obtained with one tank.

Wave force and moment data is also desirable, as discussed above for the docking experiments. Small spherical tanks could be used.

5.2.4 Secondary Experiments

5.2.4.1 Engine Cutoff Induced Sloshing

This experiment will provide data on control of wave motion after main or auxiliary engine cutoff, and the degree and type of sloshing induced by acceleration level changes. Engine cutoff induced sloshing must be controlled to minimize liquid collection at the forward end of the tank, thus precluding venting, and to minimize dynamic reactions of the vehicle affecting the ACS. Data is required on amplification heights, wave energy dissipation rates, equilibrium configurations of the liquid, baffle effectiveness and wave circulation and breakup. Main Engine Cutoff (MECO) induced slosh transients are minimized by using properly designed baffles and deflectors and a proper thrust termination sequence (S-IVB-203). The MECO induced motion due to boundary layer kinetic energy and tank wall and thrust structure relaxation cannot be studied in the recommended Interface Stability Experiment. However, boundary layer kinetic energy data could be obtained from the recommended LH_2 experiments (Sections 7 to 10). This approach is discussed in Reference 2-7.

Liquid motion was observed at termination of the S-IVB 203 propulsive vent system which was significantly more rapid than predicted by analysis. The positive acceleration was decreased from approximately $5 \times 10^{-4} g/g_e$ to

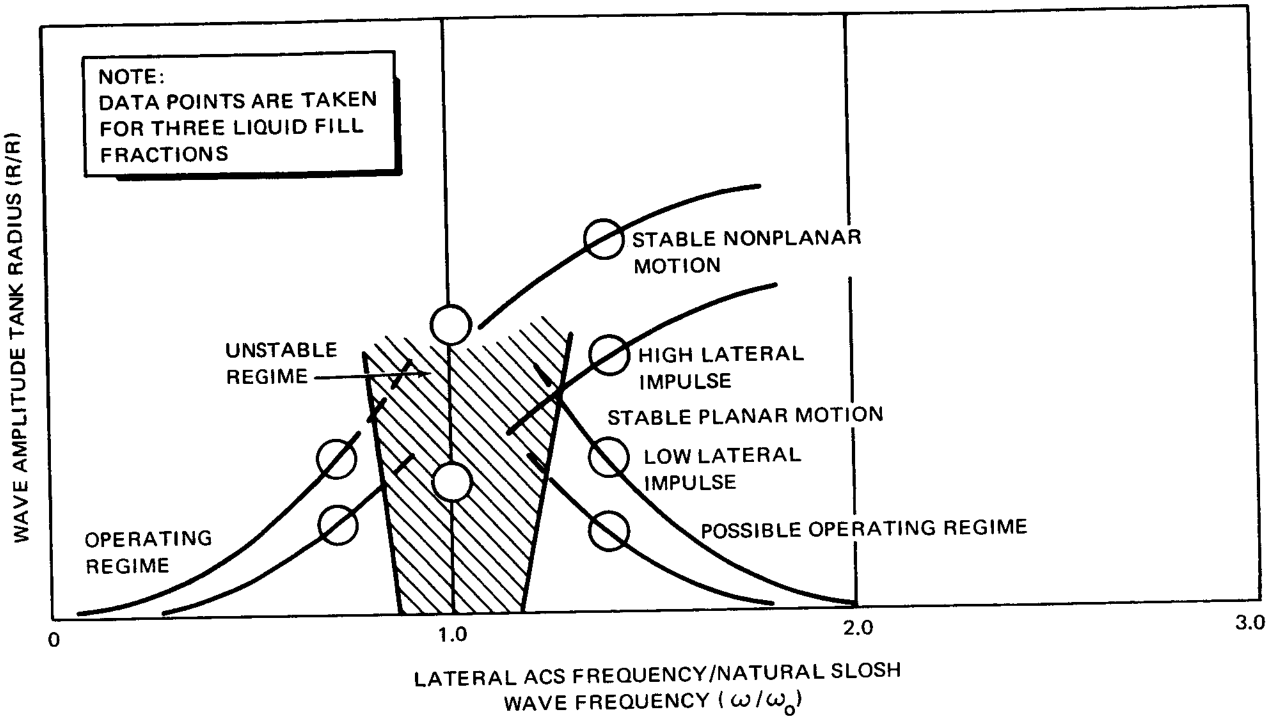

Figure 5-3. Slosh Amplitude Dependence on Lateral Forcing Frequency

approximately $3 \times 10^{-6} g/g_e$ in the opposite (negative) direction due to vehicle drag. The drag tended to collect liquid at the forward end of the tank. The problem of acceleration reversal will be studied as part of propellant settling experimentation.

Data on sloshing phenomena due to engine cutoff is gained as a natural consequence of the recommended experiment. During each pass of the satellite over a tracking station, it will be necessary to apply the proper experiment acceleration, perform the appropriate experiment, and then decrease acceleration to conserve propellant. Useful data on wave amplification and reduction will be gained both at the beginning and end of each experiment. Additional wave energy dissipation rate data will also be obtained as part of the resettling, docking, and ACS slosh experiments.

With live TV, there is some freedom on the part of ground control in selecting the proper wave phase at which to decrease or terminate thrust. Thus, for maximum wave amplification data, the thrust would be decreased at the instant the wave appears to have maximum kinetic energy. Similarly, if minimum sloshing is desired to start the next experiment with minimum perturbation, thrust could be terminated at maximum wave potential energy. The settled liquid must be at the proper end of the tank with respect to the orbital drag between station acquisition points, so that the drag will tend to keep the liquid settled. The reverse situation is desirable only for those experiments which simulate changing from a positive vehicle APS acceleration to a negative drag acceleration, as is presently envisioned with intermittant venting schemes.

Figure 5. 4 illustrates the type of wave amplification data desired. Wave amplification will be achieved over a range of initial and final tank Bond numbers of approximately 4 to 400 and initial to final g level ratios of 10^{-1} to 10^{-5}. Wave circulation about the top of the tank will be observed at the high wave amplification values. Baffle effectiveness will be seen and comparisons can be made between two different types of baffles by having liquid initially settled at the foreward end of the tank and observing wave movement towards the aft end of the tank, or vice versa. In the recommended three tank system, comparisons with an unbaffled tank can be also made.

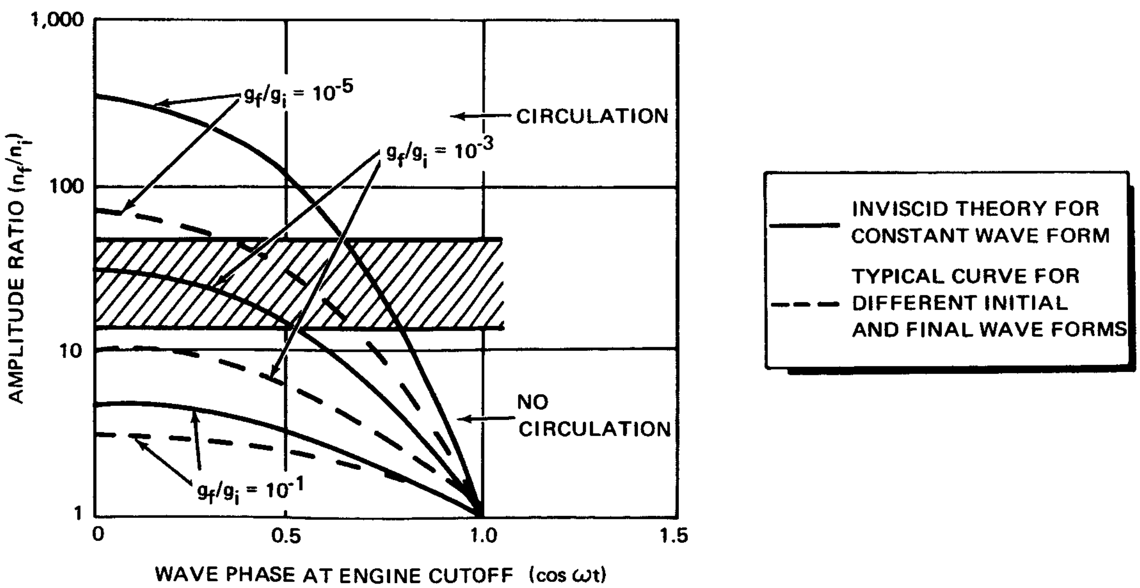

Figure 5-4. Slosh Wave Amplification

5.2.4.2 Propellant Draining and Transfer Dynamics

Propellant transfer can be studied as a natural consequence of the requirement for three liquid levels; liquid expulsion is necessary to change liquid levels. Since a noncryogenic (hexane) is used, visual data on the dynamics of transfer can be obtained. Various flow control baffles and diffusers will be incorporated to determine the effectiveness of these devices for actual vehicles. In addition, data will be gained on the liquid spike formation induced by valve closure. The transparent tanks with hexane eliminate the visability problem caused by fog formation obscuring the field of view as present with LH_2 in metal tanks. Table 5-3, Section 5.4 outlines the requirements for propellant draining.

5.2.4.3 Pressurization Gas Flow Dynamic Effects

Pressurization of the experiment tanks is necessary to change liquid levels. TV observation of the tank during low g pressurization will yield valuable data on effects of the inflow gas on cavity formation, globule stripping, bubble ingestion, and liquid circulation and disorientation. Low g data is necessary to verify extrapolations of one g model data, since the liquid dynamics is a function of g level.

A multiflow diffuser, (Reference 2-7) would be in one tank and bag diffusers in the others. The multiflow diffuser would consist of a bag diffuser and radial flow diffuser, which appear to be most promising for low g applications, and a louvered-tube diffuser, similar to that used on the S-IVB LO_2 tank. A straight inflow or axial jet diffuser could be tested as the worst case to demonstrate the maximum effects of gas inflow on the liquid dynamics.

Ground tests are needed to establish the approximate flow rates required to produce surface instability with each diffuser; these flow rates would be preset for the experiment orifices. Higher flow rates would be used to obtain data on cavity formation and liquid dynamics. Approximately three flow rates would be required. The effects of the gas inflow on the liquid would vary depending on the liquid height and the g level. Experiments are recommended at moderate and low Bond numbers in the two-ft. diam. tank corresponding to 10^{-3} and $10^{-4} g/g_e$.

The curves of Figure 5-5 illustrate data on the globule stripping or Kelvin-Helmholtz instability. This effect determines the principal design criteria for a diffuser: to minimize liquid motion and adverse thermodynamic effects, such as pressure collapse due to ullage gas/liquid mixing, the diffuser inflow rate must be below the critical value which induces the Kelvin-Helmholtz instability. If this design criteria is met, liquid motion, cavity formation, and liquid/gas mixing will be minimized.

Tanks will normally be pressurized for draining near the end of a pass over a TV station. Liquid motion will be damped out by the time TV is acquired at the next station. It is estimated that 20 pressurization inflow tests of 200 seconds each at 10^{-3} and 10^{-4} g/g_e should be accomplished (Table 5-3, Section 5. 4).

5. 2. 4. 4 Vibration Effects

The objective here is to obtain data on sinking bubble and surface spray phenomena to allow extrapolation of 1 g/g_e data to the full-size vehicle. Vibrations may be present due to idle mode engine operation, nuclear engine start-up, and operation of on-board machinery. If vibration accelerations are sufficiently high, surface spray will occur and bubbles ingested into the liquid will sink, rather than rise. Entrained gas could be maintained near the bottom of the tank and subsequent full thrust operation could lead to bubble ingestion.

To fully justify a vibration experiment, a system analysis of vibration magnitudes and durations must be made. If the problems appear significant, the recommended vibration experiment would be similar to that in Reference 2-7. It involves vibrating one of the tanks over a range of the dimensionless vibration acceleration, $\omega^2 x/g_e$, for various g levels. Observations of sinking bubble velocities, bubble formation, and coalescence would be made, as well as surface spray phenomena. Table 5-3 Section 5. 4 outlines the number of experiments and approximate durations.

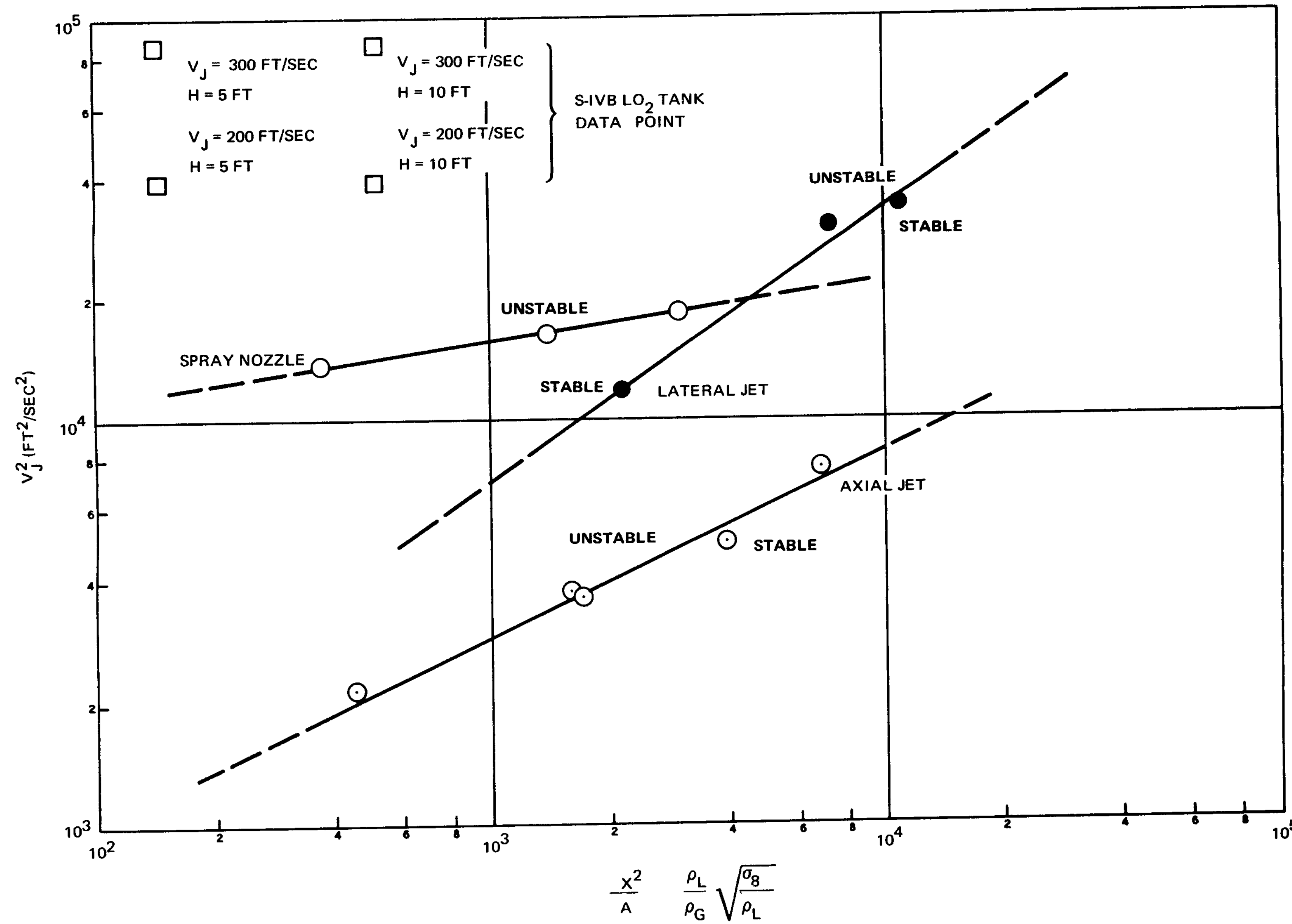

Figure 5-5. Dimensional Correlation of Kelvin-Helmholtz Instability

5.2.4.5 Surface Tension Phenomena

Data on isothermal, long-term, low Bond number surface tension phenomena will be gained automatically during many of the periods as the experiment satellite approaches each TV station. Primary data will be observation of the liquid configuration resulting from various initial conditions and acceleration perturbations. Data on the effects of baffles and internal hardware on the equilibirum configuration will also be obtained. No additional experiment requirements in terms of weight or power are required to obtain this data.

5.3 EXPERIMENT CONCEPTUAL DESIGNS

5.3.1 Experiment/Carrier Integration

Experiment definition constraints are imposed by (1) the requirements for scalable data, and (2) the available carrier vehicle weight and volume restrictions. These constraints necessitate compromises in the number and size of tanks, acceleration environment, and experiment duration. Based on the analyses presented in Section 5.5, it was concluded that tanks of about 2 by 4 ft. and accelerations of $10^{-4} g/g_e$ - $10^{-2} g/g_e$ are necessary to obtain similarity between experimental results and the actual vehicle propellant phenomena.

Weight estimates based on these approximate requirements preclude flying properly scaled experiments on vehicles having allowable payload weights of the order of 350 lb - 800 lb. The approximate total experiment weight is about 1,600 lb - 2,000 lb (Section 5.3.2). Therefore, experiments were defined to be compatible with the large fairing (Thor-Delta, Thor Agena, or Atlas).

Various fairing tank relationships were considered to optimize TV observation, structural integrity, and tank size, and to minimize APS-induced perturbations. Tanks placed with their longitudinal axes perpendicular to the longitudinal axes of the fairing appear to be the best approach. The APS thrust is applied along a line passing through the cg of the package, which is adjusted to lie at the midpoint of the tank in the longitudinal direction of the fairing. Then, as the tanks are drained, the package cg does not change, and the attitude control system will not be required to offset APS-induced moments. Also, because the system cg lies near the tank center, a close similarity between rotational effects on the experiment liquid and propellant in an actual vehicle can be achieved. Coriolis and centripetal force effects are minimized by having the cg close to the liquid surface. Having the longitudinal axis of the fairing perpendicular to the Earth's surface may have the additional advantage of being a stable equilibrium orientation. Thus, ACS corrections, which normally perturb the experiment, will be minimized.

Maximum observation of the transparent tanks is achieved with this approach (see Section 5.4 for recommended design). Another possibility is to have the tank axes parallel to the fairing axis; mirrors would then be required or the TV cameras would have to be mounted on a boom which would have to be swung out to the side of the experiment package after orbital injection; larger tanks could be used, but in keeping with the ground rules of minimum cost and complexity, this alternative was rejected.

5.3.2 Experiment Configurations and Weights

Five tank configurations, Figure 5-6, were investigated which would provide scalable data for the S-II, S-IVC, and the Nuclear Stage LH_2 tanks. Geometric similarity between experiment and vehicle tanks is employed. Due to the fairing envelope constraint on maximum experiment tank size, dynamic similarity is more closely achieved between the experiment and the S-IVC than for the S-IIB or Nuclear Stage (Section 5.5). Weight estimates are presented in Table 5-2.

Figure 5-6, Configuration I, shows a three-tank experiment designed to simulate the S-IIB and S-IVC LH_2 tanks. Two sizes of inverted dome tanks are used, 3 by 2 ft and 1.5 by 1 ft. Comparisons between the small and large tank data will aid in determining the extent to which data can be scaled and extrapolated. One of the small tanks is geometrically identical to the large tank; the other small tank is not equipped with baffles or internal hardware and serves as a control tank. A more efficient utilization of available space allowing larger tanks (3.5 by 2 ft and 1 by 2 ft) to be used is shown as Configuration II. This configuration is heavier; however, the larger tanks result in closer similarity between experiment and vehicle.

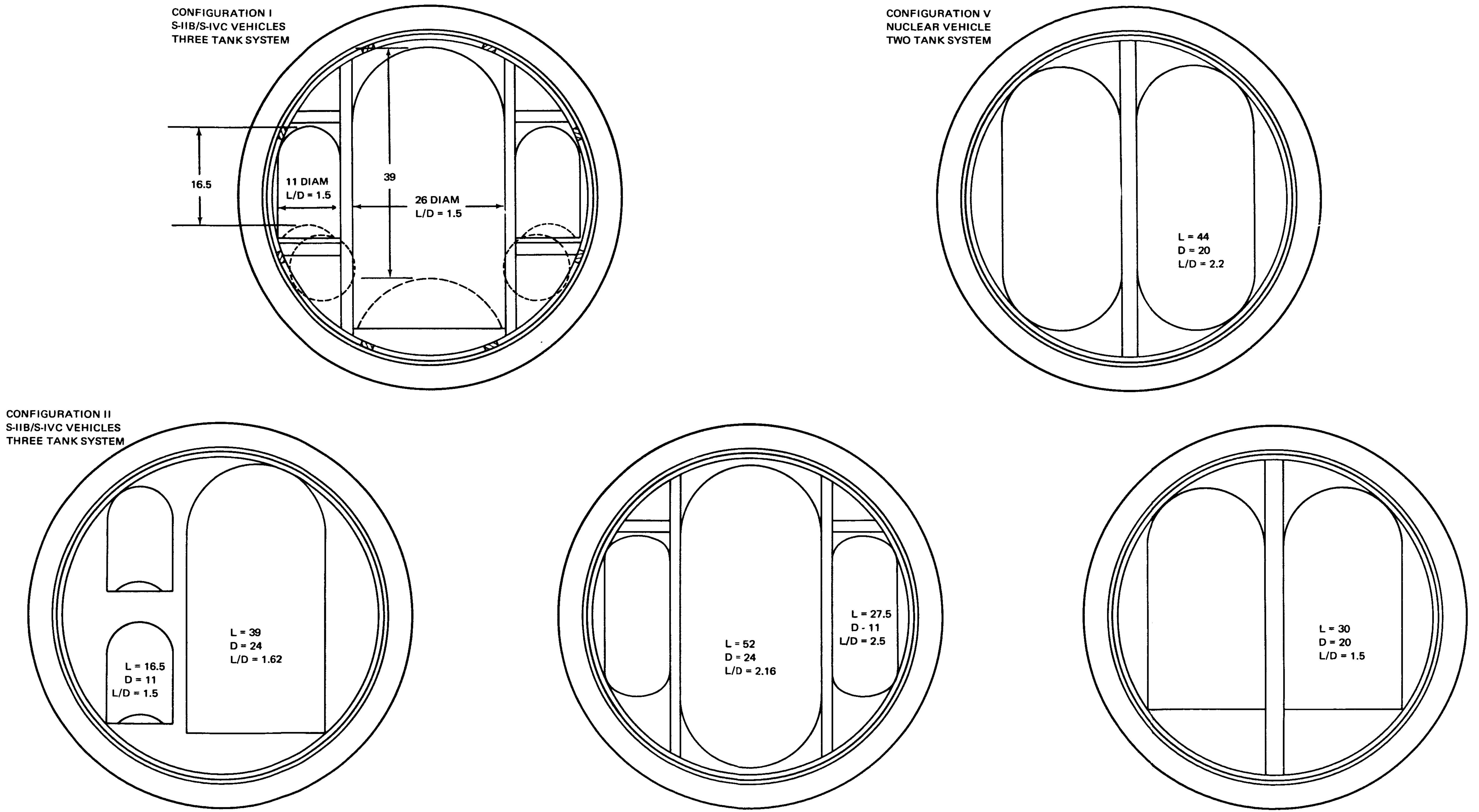

Figure 5-6. Interface Stability Experiment Confiugrations

Table 5-2

SUBSYSTEM AND COMPONENT WEIGHTS INTERFACE
STABILITY EXPERIMENT CONFIGURATIONS

	Config. I	Config. II	Config. III	Config. IV	Config. V
Simulant Liquid	283 lbs.	488 lbs.	450 lbs.	454 lbs.	460 lbs.
Transparent Tanks	255	280	255	350	350
Tank Vibrator (optional)	15	15	15	40	40
Internal Tank Test Equipment	15	15	15	25	25
Tank Supports	25	25	25	35	25
External Structure	100	100	100	100	100
APS Propellant	240	310	240	240	240
APS System	74	74	74	74	74
ACS System (7 days)	190	190	190	190	190
Battery System (2 batteries required)	310	310	310	310	310
TM System (94 channels with recorder)	35	35	35	35	35
TV System	36	36	36	36	36
Transducers (70 at 1/2 lb/transducer)	35	35	35	35	35
TM Command Receiver and Antennas	5	5	5	5	5
Guidance Sensor and Computer	20	20	20	20	20
Total	1, 638 lbs.	1, 933 lbs.	1, 805 lbs.	1, 949 lbs.	1, 945 lbs.

Configuration III depicts a three-tank (domed cylinder) system simulating the Nuclear Stage. The large tank (2 by 4 ft) is placed in the center with the two small tanks (1 by 2 ft) on the side. It is important that the experiment tank size be maximized.

Configuration IV illustrates a two-tank (inverted dome) system simulating the S-IIB and S-IVC. The two tanks (3 by 2 ft) are smaller than the large tank of Configuration II. Also, the c. g. of the system does not lie near the axis of either of the tanks.

Configuration V depicts two domed cylinders, 2 by 4 ft, simulating the Nuclear Stage. The cg of this system does not lie near the tank axis of either tank.

5. 3. 3 Subsystem Requirements

The total APS weight was estimated by first determining the total impulse required for the experiments (Section 5. 2) and then the propellant weight for two specific impulses, monomethyl hydrazine and hydrogen peroxide. Estimates of tank and pressurization system weights were based on weights of similar systems.

The hydrazine system was used in the weight estimates since the system weight was less and flight-qualified engines are available. However, a propulsion system should be selected only after performing a detailed system study of available engines considering cost, level of qualification, weight, reliability, and engine life. Table 5-3 presents a compilation of appropriate engines which are currently available and meet the requirements for the various experiment g levels and duration. It demonstrates that off-the-shelf hardware is available.

Tank weights were estimated from weights presented in the Project THERMO Phase B report (Reference 2-7). Plexiglass 55 tanks with an aluminum ring seal are recommended. For the inverted dome, an aluminum hemisphere could be used for greater structural integrity.

Table 5-3

AVAILABLE ENGINES FOR 1600-2200 LB INTERFACE STABILITY EXPERIMENT

Exp. Acceleration Level	Thrust Required	Available Engine Type & Part Number	Thrust	Specific Impulse	Engine Weight	Life	Qualification Level	Remarks
10^{-2} g	16-22 lbs	Rocket Research Corp. Monomethyl Hydrazine RRC-Q1900-23.0	23 lbs	232	3.5 lbs	6400 sec	Fully qualified to Minuteman missile specifications	Engine can be derated to less than 20 lb thrust
10^{-3} g	1.6-2.2 lbs	Rocket Research Corp. Monomethyl Hydrazine RRC-TB 1.5-002.50	2.5 lbs	228	-	16,920 sec	Fully qualified	Engine can be derated to 1.6-2.2 lbs thrust
10^{-4} g	0.16-0.22 lb	Rocket Research Corp. Monomethyl Hydrazine RRC-Q-2000-0.5	0.5 lbs	227	1.2 lbs	30,500 sec	Qualified for Airforce Classified System	Engine can be derated to 0.16-0.22 lbs thrust
10^{-3} g	1.6-2.2 lbs	Walter Kidde & Co., Inc. NASA-Huntsville Long Life Thrustor Hydrazine	1-5 lbs	-	-	7 hrs design life	Prototype test completed	
10^{-3} g	1.6-2.2 lbs	Walter Kidde & Co., Inc. Thrustor for Hughes Aircraft Corp. Aeronautical Satellite	2 lbs	-	-	15,000 pulses & 1 hr steady state demonstrated	Qualified to meet satellite specifications	
10^{-2} g	16-22 lbs	Walter Kidde & Co., Inc. Thrustor for AVCO Exhaust Plume Signature Study	10 lbs	-	-	-	Thrustors passed acceptance testing	
10^{-2} g	16-22 lbs	Walter Kidde & Co., Inc. Thrustor for Scout Vehicle Part No. 873819 and 873820. 90% H_2O_2	14 lbs	-	-	-	Qualified	
10^{-3} g	1.6-2.2 lbs	Walter Kidde & Co., Inc. Thrustor for Scout Vehicle Part No. 873798. 90% H_2O_2	2.2 lbs	-	-	-	Qualified	

Details of pressurization and flow lines, internal tank hardware and baffles, etc., will be similar to the Phase B Interface Stability Experiment (Reference 2-7).

5.4 RECOMMENDED EXPERIMENT DESIGN AND PROCEDURE

5.4.1 Configuration Selection

The three-tank systems, Figure 5-6, are recommended for the in-orbit experiments because in both the S-IIB/S-IVC and Nuclear stage configurations, the center tank is significantly larger than in the two-tank systems. Therefore, closer similarity can be obtained between the experiment conditions and actual propellant dynamics in the vehicles. Also, the center of mass of the experiment package will lie near the center of the large tank, along the longitudinal axis of the tank. It also appears practical to adjust the position of batteries, pressure bottles, etc., so that the c.g. lies close to the predicted c.g. of the S-IIB/S-IVC, or Nuclear Stage. Therefore, very close similarity can be obtained for phenomena involving pitch, yaw, or roll perturbations. Figure 5-7 presents a conceptual design.

The internal tank hardware, such as baffles and deflectors, are not shown. Detailed definition requires further testing and analyses. Typical baffle configurations are shown in Project THERMO, Reference 2-7.

With the three-tank systems, there is space to include one or two small sealed spherical tanks which could be equipped and supported with a strain gage dynameter system to measure slosh wave forces and movements. This data would be of great value in verifying and refining the results of low g slosh wave numerical programs.

5.4.2 Experiment Sequence

Experiment times have been compared with the TV observation times available per ground station and the total TV observation times for the satellite in a 200-nmi, 28.5° inclination orbit and a 150-nmi polar orbit. These comparisons showed that the polar orbit does not provide sufficient TV time (7-day mission) for the entire interface stability experiment. However, the other orbit provides approximately 17 hours of TV. Two TV ground stations

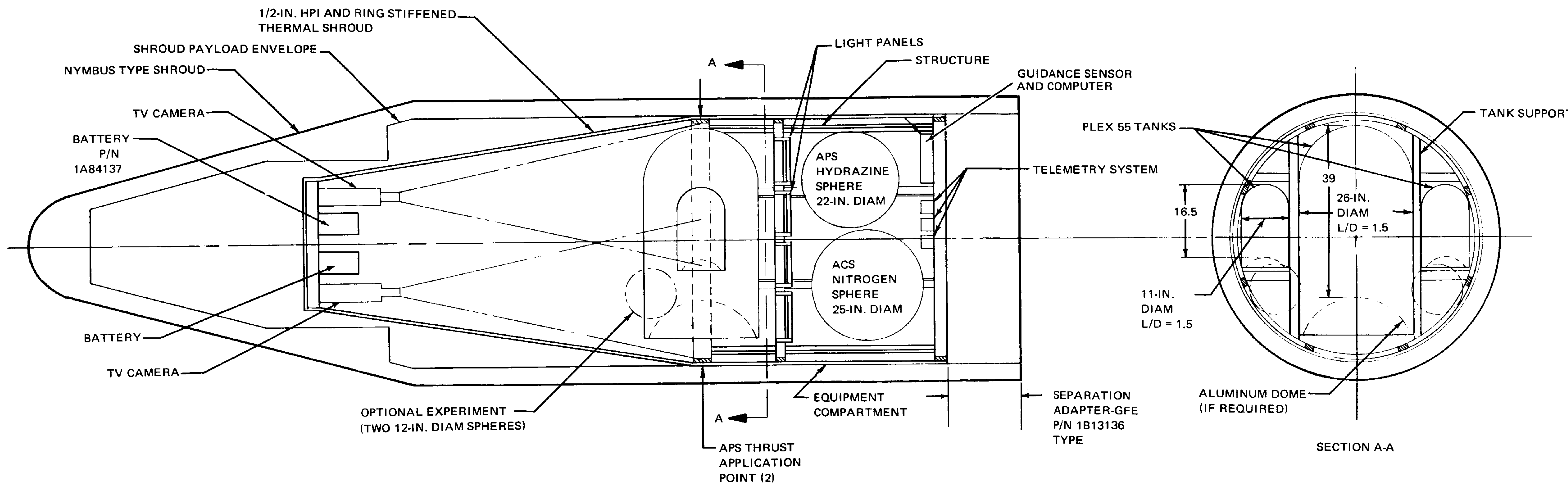

Figure 5-7. Interface Stability Experiment

5-24-2

provide a minimum of 7.5 hours of TV coverage for the satellite in orbit for one week. The average TV time for each station per fly-over is approximately six to seven minutes, which is sufficient for most of the experiments. The ACS-induced slosh and docking experiments may require longer time periods (about 600 sec to 800 sec for ten wave cycles at 10^{-4} g/g_e) and, therefore, two ground stations with overlapping TV coverage would be required.

Activating a third ground station would provide more efficient data retrieval. Overlapping TV coverage significantly improves the long-term experiment data, but a short time is available for perturbations to damp out between completion of an experiment at the first station and initiation of the next experiment at the second station. If a third station were available, separated from the two overlapping stations by 30-45 minutes of orbital time, then liquid motion would be damped out between experiments. With three stations, at least two experiments could be performed per orbit; if only two overlapping stations were used, it would not be feasible to perform two experiments within the maximum 12-14 minutes available, except in isolated cases.

The total orbit time available to perform the entire interface stability experiment would be approximately 12 hours with two overlapping TV stations and a third station. With only two overlapping stations, the total orbital TV time would be of the order of 6-7 hours. As an example, the two overlapping stations could be Texas and Canaveral and the third station could be Carnarvon.

The comparison of experiment and available TV showed that a detailed sequence compatible with the available tracking station capabilities can be readily defined.

The basic criteria for defining this sequence are:

1. Experiments must be run in an order which minimizes the effects of perturbations on the next experiment. For example, an ACS slosh experiment should be performed immediately prior to a resettling or sloshing experiment, but not vice-versa.
2. APS accelerations should be terminated over a station (wave amplification data would then be obtained).

3. Experiments should be ordered such that initial conditions of the next experiment are met. For example, a resettling experiment which placed liquid at the top of the tank should be performed prior to an ACS slosh experiment which required the tank in an "inverted" position.

4. ACS operation must be constrained for certain experiments to prevent perturbations and data degradation.

Estimates of individual experiment durations and required propellant weights are presented in Table 5-4. Estimates of individual experiment durations were based on Project THERMO (Reference 2-7) and on more current analyses. A DAC numerical resettling program was used to estimate maximum resettling times. Experiment durations for the docking experiments are ROM estimates, since little is known of propellant motion during docking. Total durations for the ACS slosh experiment were approximated by considering both the maximum TV observation time available from the overlapping ground stations (approximately 15 minutes) and the time required for ten wave cycles to occur. The Engine Cutoff Slosh experiments are performed, at the end of each pass over a ground station, by reducing the g level and observing the wave amplification. No additional time is required; it is included in the other experiment time estimates. The time required for liquid draining and vibration experiments are based on those in Reference 2-7. Equilibrium liquid configurations at very low Bond numbers are observed at the beginning of each pass over the ground station; no additional time is required.

Table 5-4 shows a comparison of primary and secondary experiment times. The total time required for the primary experiments is about 20,500 seconds of the total 27,880 seconds. However, approximately half of the draining and pressurization experiment time must be included for required operations and, therefore, the total primary experiment duration is approximately 22,750 seconds and the secondary experiments, 5,130 seconds. Approximately 80% of the total experiment time is devoted to the four primary experiments. Less than 30 lb of propellant is required for the secondary experiments. No additional hardware is required except for the vibration experiment. The vibrator weight is estimated at 15 lb. Less than 150 lb of the approximately 1,600 lb is required for secondary experiments.

Table 5-4

PRELIMINARY INTERFACE STABILITY EXPERIMENT REQUIREMENTS FOR 1600 LB PAYLOAD

Experiment Area	Total Number of Experiments	EXPERIMENT TIME, IMPULSE, AND PROPELLANT WEIGHT ASSOCIATED WITH G LEVEL: 10^{-2} g Time (sec)	10^{-2} g No. Exp.	10^{-2} g Impulse (lb sec)	10^{-2} g Propellant Weight-lbs	10^{-3} g Time (sec)	10^{-3} g No. Exp.	10^{-3} g Impulse (lb sec)	10^{-3} g Propellant Weight-lbs	10^{-4} g Time (sec)	10^{-4} g No. Exp.	10^{-4} g Impulse (lb sec)	10^{-4} g Propellant Weight-lbs
1. Resettling	24	1,600		25,600	111.0	2,000		3,200	14.0	3,500		560	2.5
2. Propel. slosh control during maneuvers													
a. Docking	TBD	300	TBD	4,800	20.8	2,000	TBD	3,200	14.0	4,000	TBD	480	2.08
b. ACS induced slosh	18	480	6	7,670	33.4	1,800	6	2,880	12.5	4,800	6	767	3.34
3. Engine cutoff induced slosh*	24-36	---	8-12	---	---	---	8-12	---	---	---			
4. Liquid draining & transfer	6	200	2	3,200	13.9	800	2	1,280	5.55	1,600	2	128	1.11
5. Press. gas inflow	16	---	-	---	---	1,600	8	2,560	11.1	1,600	8	256	1.11
6. Vibration effects (surface spray)	8	---	-	---	---	800	4	1,280	5.55	800	4	128	0.55
7. Surface tension (Equilibrium low g liquid configurations)	Passive observation prior to initiating Exp's.	---	-	---	---	---	-	---	---	---	-	---	---
	TOTAL	2,580		41,270	179.1	9,000		14,400	62.70	16,300		2,319	10.69

Total time = 27,880 secs or 7.75 hrs.

Total impulse = 54,989 lb sec.

Total propellant weight consumed = 252.5 (I_{sp} = 230 sec).

*MECO experiments are integrated into resettling, docking, and ACS induced slosh experiment sequences and are performed as a consequence of required g level changes; no additional experiment preparation time or acceleration environment is considered necessary.

5.4.3 TV Requirements

A two-camera system (Section 3) is required to view the liquid throughout the tanks. The 30 fps (equivalent) of the TV cameras is considered to be sufficient. The entire experiment in a 28.5° orbit between 100-200 nmi can be performed with live TV coverage over the TV ground stations. Two or three ground stations would be required if the experiments were performed during a 7-day period.

5.5 EXPERIMENT ANALYSIS

5.5.1 Similarity Criteria

Important similarity parameters, results of theoretical analyses, and empirical data correlations are compiled in Reference 2-7. These expressions are valid for the experiments recommended herein.

Additional analyses were made to ascertain required experiment tank size and g level. The similarity parameters which appear to be most important are Bond number, $g\rho R^2/\sigma$ and the viscogravitational number, gD^3/V^2. Table 5-5 shows comparisons for the S-IIB, S-IVC, Nuclear Stage, and model tanks. Note that the larger the model diameter, the better the similarity, and that better similarity is achieved between the model tank and S-IVC than for the Nuclear Stage or S-IIB, because these stages have a larger diameter.

Selection of experiment g levels was based on a compromise between obtaining perfect similarity with respect to Bond number and viscogravitational number and meeting the weight restriction of the 1,600 lb payload booster. Three g levels are recommended: 10^{-2} g/g_e, 10^{-3} g/g_e, and 10^{-4} g/g_e. If available payload capabilities can be increased, better similarity and more data could be obtained. Drag acceleration is also recommended for certain experiments.

Other parameters must be defined to ensure similarity. The ACS slosh phenomena will be a function of the internal acceleration Bond number and duration which determine the resulting change in liquid kinetic energy. Required ACS lateral acceleration will be of the order of 10^{-3} g/g_e for one second to five seconds (analyses of Reference 2-7). The inlet gas flow rates, vent flow

Table 5-5 (Page 1 of 2)

SIMILARITY CRITERIA

Acceleration	Bond Number ($g\rho R^2/\sigma$)	Visco-Gravitational Number gD^3/ν^2
S-IVC Vehicle:		
200-300 nautical mile orbital drag 10^{-7} - 10^{-6} g/g_e	.4 - 4	8.1×10^9 - 8.1×10^{10}
Auxiliary Propulsion 2×10^{-5} g/g_e	80	1.65×10^{12}
Auxiliary Propulsion 10^{-4} g/g_e	400	8.1×10^{12}
S-IIB or Nuclear Stage:		
200-300 nautical mile orbital drag 10^{-7} - 10^{-6} g/g_e	.8 - 8	2.75×10^{10} - 2.5×10^{11}
Auxiliary Propulsion 2×10^{-5} g/g_e	160	5.4×10^{12}
Auxiliary Propulsion 10^{-4} g/g_e	800	2.5×10^{13}
Model Tank (Radius = 0.5 ft)		
10^{-4} g/g_e	.8	10^8
10^{-3} g/g_e	8	10^9
10^{-2}	80	10^{10}
Model Tank (Radius = 1.0 ft)		
10^{-4} g/g_e	3.2	8.1×10^8
10^{-3}	32	8.1×10^9
10^{-2}	320	8.1×10^{10}

Table 5-5 (Page 2 of 2)

SIMILARITY CRITERIA

Acceleration	Bond Number ($g \rho R^2/\sigma$)	Visco-Gravitational Number gD^3/ν^2
Model Tank (Radius = 1.5 ft)		
10^{-4} g/g_e	7.2	2.5×10^9
10^{-3}	72	2.5×10^{10}
10^{-2}	720	2.5×10^{11}
2×10^{-2}	1440	5.0×10^{11}

Critical Bond number (axisymmetric) $\rho g R^2/\sigma$ = 0.842 (0° contact angle)

Critical Bond number (asymmetric) $\rho g R^2/\sigma$ = 3.39 (90° contact angle)

Critical Bond number (axisymmetric) $\rho g R^2/\sigma$ = 14.67 (90° contact angle)

Approximate Bond number range for resetting flow with partial dome formation*: $2 \leq B_o \leq 20$

Approximate Bond number range for resettling flow with dome or cylinder formation*: $10 \leq B_o \leq 400$

*Reference: Cryogenic Liquid Experiments in Orbit Volume I, July 1966 prepared for NASA-MSFC by Martin Co. under contract NAS 8-11328.

rates, vibration frequencies and amplitudes, liquid transfer rates, and g level changes required for wave amplification, are approximately the same as reported in Reference 2-7.

5.5.2 Error Analysis

The Project THERMO error analyses are also valid for this experiment. The accuracies of off-the-shelf, qualified instrumentation are adequate to achieve an experimental data correlation accuracy of better than 15%; in most cases, an instrument accuracy of 10% is sufficient.

If accelerometers are not available for the experiments, there will be a significant loss in data accuracy. Although engines are available which provide constant thrust within an accuracy of a few percent or less, movement of the liquid in the tank will cause significant changes in the acceleration. For example, with a liquid mass of 400 lb and a total satellite mass of 1,600 lb, the actual mass being accelerated will vary between 1,600 lb (liquid not moving with respect to container) to 1,200 lb (liquid freely falling). These differences correspond to a 25% change in acceleration. Liquid impact on the tank walls will also perturb the steady-state acceleration level. Therefore, acceleraometers should be used, especially with the high acceleration levels (10^{-2} g/g_e to 10^{-3} g/g_e).

5.6 INSTRUMENTATION LIST

The instrumentation list of Table 5-6 is based on the instrumentation list obtained as part of the Project THERMO Phase B study. The primary instrumentation is necessary for determination of experiment conditions. Twenty-five measurements are taken of events such as the opening and closing of valves. A minimum number of temperature transducers are used. Liquid flow measurements are made between tanks. Redundant pressure measurements are taken of the high-pressure bottle and the plastic tanks.

The most important instrumentation is the dual TV camera system. In order to ensure TV coverage in the event one TV camera fails, it would be worthwhile to use controllable TV lenses which could be switched to a larger field of view, encompassing all of the transparent tanks. Accelerometers should be included, on an experiment basis. They are important because the ratio of liquid mass to experiment package mass is high and, therefore, large variations in acceleration occur even with constant applied thrust, due to movement of the liquid. Accelerometers appear to be available, but their flight qualification status is questionable (Section 3).

Secondary instrumentation is included which corresponds to the secondary experiments or to additional data requirements of primary experiments. The strain gage dynamometer system is highly desirable, but can be obtained

Table 5-6 (page 1 of 2)

INSTRUMENTATION REQUIREMENTS FOR INTERFACE STABILITY EXPERIMENT

Measurement Title	No. Req'd	System Range/ Accuracy		Frequency Response	Environment Point of Measurement	
					Media	Temp
Events	25	On-Off		2.4 cps (12 sps)		
Temperature He Storage Sphere	1	340-540 ± 6°R	(±3%)	1 cps (4 sps)	He	340-620°R
Temperature He Reg Outlet	1	340-540 ± 6°R	(±3%)	1 cps (4 sps)	He	340-620°R
Temperature He Pres Orifice Inlet	3	340-540 ± 6°R	(±3%)	1 cps (4 sps)	He	340-620°R
Temperature Intf Stab Tk Inlet	3	300-600 ± 9°R	(±3%)	1 cps (4 sps)	Hexane	300-620°R
Temperature Intf Stab Tk Ull	2	300-600 ± 9°R	(±3%)	1 cps (4 sps)	Hexane	300-620°R
Temperature Intf Stab Tk Vent	1	300-600 ± 9°R	(±3%)	1 cps (4 sps)	Hexane	300-620°R
Temperature Intf Stab Tk Liq	3	400-660 ± 9°R	(±3%)	1 cps (4 sps)	Hexane	300-660°R
Temperature Intf Stab Tk Outlet	1	400-660 ± 9°R	(±3%)	1 cps (4 sps)	Hexane	300-660°R
Pressure He Storage Sphere	1	3500 ± 105 psi	(±5%)	1 cps (4 sps)	He	340 to 620°R(1)
Pressure He Reg Outlet	1	0-300 ± 15 psia	(5%)	1 cps (4 sps)	He	340 to 620°R(1)
Pressure He Pres Orifice Inlet	3	0-300 ± 15 psia	(±5%)	1 cps (4 sps)	He	340 to 620°R(1)
Pressure Intf Stab Tk Ull (2 per tank)	6	0-50 ± 1.5 psia	(±3%) (±1/2%)	1 cps (4 sps)	Hexane	300 to 620°R(1)

Table 5-6 (page 2 of 2)

INSTRUMENTATION REQUIREMENTS FOR INTERFACE STABILITY EXPERIMENT

Measurement Title	No. Req'd	System Range/ Accuracy		Frequency Response	Environment at Point of Measurement: Media	Environment at Point of Measurement: Temp
Pressure Intf Stab Tk Inlet	3	0-100 ± 5 psia	(±5%)	1 cps (4 sps)	He	300 to 620°R
Flow Intf Stab Tk Outlet	3	0-100 ± 5 lb/min		1 cps (4 sps)	Hexane (Operating Range 10-100 lb/min)	300 to 660°R (Two-Phase) 0-50 psia

NOTE: (1) Sensing line must isolate transducer to provide -60 to + 165°F environment only if small sealed transparent plastic tanks are included. In lieu of a strain gage system, wave pressure transducers would supply data on wave pressures for liquid impact against tank walls or baffles. Neither are developed. Eight pressure measurements are taken of inlet and outlet gas flow to obtain mass flow rates for the pressurization experiment. Two level sensors could be included, although accurate measurements of liquid surface position may be obtained by TV observation alone. The satellite angular velocities in pitch, roll, or yaw are measured for comparison with accelerometer readings and to determine centrifugal forces. Vibration measurements are required for the vibration experiment.

Section 6
HIGH PERFORMANCE INSULATION

6.1 ORBITAL EXPERIMENTATION INFORMATION REQUIREMENTS

The survey of the high performance insulation (HPI) technology needed for designing the planetary fly-by vehicles revealed several areas which will require in-space testing. These are:

1. Evacuation ability of the HPI.
2. Effect of boost forces on tank leakage.
3. Ability to maintain HPI position and structural integrity during boost.
4. HPI thickness history during boost and orbit.
5. Effects of pressure gradients and aerodynamic forces on external insulation during boost.
6. Adequacy of HPI ground testing to simulate space and boost environments.
7. Detection, location, and repair of tank leaks in space.
8. Techniques for HPI repair in space.

6.2 DATA ACQUISITION AND EXPERIMENT REQUIREMENTS

6.2.1 Evacuation Ability

In the area of HPI evacuation ability, data is needed from liftoff until that time at which the HPI interstitial pressure has dropped to approximately 10^{-5} torr. This HPI pressure history data will include the time taken to reach the orbital steady-state heat flux (approximately 10^{-5} torr). This pressure history data is needed for predicting the thermal performance of the HPI, since the heating rate through the insulation is adversely affected by the interstitial pressures within the HPI (References 6-1, 6-2, 6-3). The evacuation ability of the HPI during the initial part of boost (rapid pressure decay period) is also important because of the structural problems which can occur during this period. If the rate of evacuation of the gases from the insulation is too rapid, excessive ballooning of the insulation sheets will occur. This will result in a rupture or tearing of the sheets.

The instrumentation required for obtaining this data includes pressure gages, temperature sensors, TV camera, and HPI thickness gages. It does not appear that flight qualified pressure gages, capable of measuring pressures lower than 10^{-2} or 10^{-3} torr, will be available for these experiments. Consequently, it will be necessary to rely on temperature sensors within the HPI to indicate the time to steady-state orbital heat flux. The pressure gages can be used to determine the evacuation ability during the initial part of boost. Also, a TV camera or an HPI thickness gage can be used to indicate any ballooning of the insulation during the initial boost period.

The in-space experiment time required for this data will depend on the HPI system but should be less than 75 hr. Another experiment requirement is the need for constructing the test sample such that the gas evacuation path length is comparable to that in an HPI system on a large tank.

6.2.2 Effect of Boost on Tank Leakage

Data on the effect of the boost environment on tank leakage is needed because of the effect which the propellant leakage from the tank can have on the HPI interstitial pressure and because of the effect which this pressure will have in degrading the thermal performance of the insulation. The major requirement for this experiment is a leak detector, such as an RF mass spectrometer, which can detect the presence of small amounts of gas. At the present time, it does not appear that such a gage, which is flight qualified, is available.

6.2.3 HPI Structural Performance

Information pertaining to the ability of the HPI to structurally withstand boost forces is of obvious interest. TV cameras will be needed to obtain this information. The thickness gages can also be used but they will only indicate a major structural failure such as a section of the HPI being torn from the tank. Inspection of the system by an astronaut in space would be desirable. This inspection could occur at any time after the flight.

6.2.4 HPI Thickness History

The data on the effect of boost forces and subsequent zero gravity on the HPI thickness is needed for non-rigid systems since a permanent compression of the HPI thickness would greatly increase the heat flux, Reference 6-1. This data can be obtained with the HPI thickness gages. These gages are a capacitance type device and are reported in Section 4.15.4 of Reference 2-7. A TV camera could also be used to give rough data. The time period of most interest for this data is during boost and the first orbit.

6.2.5 Effect of Aerodynamic Forces

In certain applications, the external surface of the insulation will need to withstand the boost aerodynamic heating, pressure, and shear forces. No simple way to obtain this information in an actual flight is apparent since the mounting of a TV camera would be difficult. Inspection of the system by an astronaut in space would be desirable and could take place at any time after the flight. It is possible that the thickness gages could be used to indicate the removal of major portions of the insulation. Temperature sensors would be needed to monitor the effect of aerodynamic heating.

6.2.6 Adequacy of Ground Testing

A successful prediction of the space performance of an HPI system by preflight ground tests would greatly reduce the need for future in-space HPI tests. The data required is in all areas of insulation performance. In addition to those discussed previously, this includes the thermal performance of a system. The thermal performance data will be of prime importance in designing an HPI system which will ensure an adequate propellant supply, yet not penalize the vehicle weight by an overdesigned system. Clearly, the amount of propellant boiloff due to the heat flux through the HPI is of major importance to the vehicle performance and mission success.

In addition to the instrumentation mentioned previously for the structural and evacuation ability tests, temperature, pressure, liquid mass, and liquid level instrumentation will be needed for the thermal performance experiments. Other requirements for an in-space thermal performance experiment are: (1) thrust capability to settle the liquid for accurate data readouts; there is no other acceleration level requirement except for these few short time thrust periods; (2) a destratification device to greatly decrease the uncertainty results; this decrease in uncertainty results from increased experiment time periods and increased accuracy of tank energy data because of uniform tank temperatures; (3) long time periods in space and (4) a tank and associated hardware.

In order to make a reliable comparison between ground and flight thermal performance tests, the experimental apparatus will need to include a thermal shroud which is capable of controlling the temperature environment. An adequate number of carefully controlled ground tests will also be required.

6.2.7 Detection, Location, and Repair of Tank Leaks in Space

The detection and location of a tank leak is mainly an instrumentation problem and was discussed in Section 6.2.2. Once this instrumentation and the repair techniques are available, the in-space experiment to test these techniques can be designed. The execution of this testing will require an astronaut. This experiment would be a good candidate for an orbital workshop experiment.

6.2.8 HPI System Repair

Similarly to the repair of tank leaks in space, the testing of techniques for repairing HPI in space will require an astronaut and could be done as an orbital workshop experiment.

6.3 EXPERIMENT CONCEPTUAL DESIGNS

The capabilities of the Scout, Thor Delta, and Atlas boosters were considered in determining conceptual designs for the HPI experiments. However, no experiments were designed using the Scout because of the small payload envelope. In order to get meaningful data, the test panels or blankets of HPI need to be larger than can be placed on the Scout.

Two conceptual designs are presented. Also presented are possible variations for each of these conceptual designs. Both designs presented are capable of using the Atlas E & F booster. Since the payload envelope can be the same for the Atlas and Thor Delta boosters, the Thor Delta could also be used. The large (115-in diameter) Atlas OAO fairing was also considered. However, because of the much greater weight of this fairing, no conceptual designs are presented using it.

6.3.1 Experiment Conceptual Design A

The HPI experiments in conceptual design A have been selected and designed to give the maximum amount of reliable data within the limitations set up by the availability of power, payload envelope, payload weight, mission time, and flight-qualified instrumentation. The data obtained would include:

1. Evacuation ability of 4 HPI systems
2. Structural integrity performance of 4 HPI systems
3. Thickness history of 4 HPI systems
4. Adequacy of HPI ground testing to simulate space and boost environments. Included is the thermal performance of the HPI system on the tank. Thermal performance data obtained (for the HPI systems) includes:
   a. time to steady-state heat flux through HPI
   b. transient (boost and early orbits) heat flux through HPI
   c. Orbital steady-state heat flux through HPI
5. Additional non-space data
   a. HPI application information
   b. purge system performance data
   c. data from all preflight testing
   d. ground-hold HPI thermal performance
6. Additional non-HPI data
   a. thermodynamic separator performance
   b. R.F. mass gage performance
   c. continuous liquid level/mass gage performance

As shown, in addition to data on the performance of the HPI, information will be obtained on the performance of a thermodynamic separator, rf mass gage, and continuous liquid level/mass gage. The inclusion of these devices will not only provide valuable information on their performance, but will ensure the feasibility and increase the accuracy of the HPI experiments.

6.3.1.1 Configuration and Apparatus

The configuration and overall size of the tank and associated hardware for conceptual design A is shown in Figure 6-1. The 36 by 80-in. tank is enclosed in a shroud (hereafter called the thermal shroud) which will provide a uniform controllable external thermal environment for the tank HPI. Heaters placed on the thermal shroud will control the temperature of the shroud. HPI placed on the exterior of the thermal shroud will dampen, if not eliminate, the transient aspects of the exterior heating rate.

The tank, thermal shroud, and other test apparatus are designed to accommodate the use of any of the well known HPI systems.

The insulation on the shroud is divided into three sections with each section being a different HPI system. These three systems plus the system on the tank result in the use of a total of four different HPI systems. For this conceptual design, the aluminized mylar/open cell foam system was chosen to be placed on the tank because of its selection in preliminary designs by the S-IVC and S-IIB design groups. The three HPI systems chosen for the thermal shroud were aluminized mylar/dexiglas, NRC-2, and Dimplar.

Two TV cameras are utilized and are positioned to view the structural performance.

A thermodynamic separator is located in the tank. In addition to being an experiment by itself, this separator enhances the HPI experiments by ensuring efficient venting. Also, the mixer used to destratify the energy within the tank is part of the separator unit. The tank is supported by fiberglass struts which are insulated and designed to reduce these heat shorts to a minimum.

The plumbing and wiring is also insulated and designed to reduce the magnitude of the heat short caused by these items. A fiberglass cone is used on top of the tank to provide a supporting surface for the HPI. This cone encloses the plumbing and wires and will greatly simplify the layup of the HPI in this area. The HPI layup on the tank is designed to provide access through the HPI to the valves and wires inside the cone and to the interior of the tank through the manhole located in the bottom of the tank.

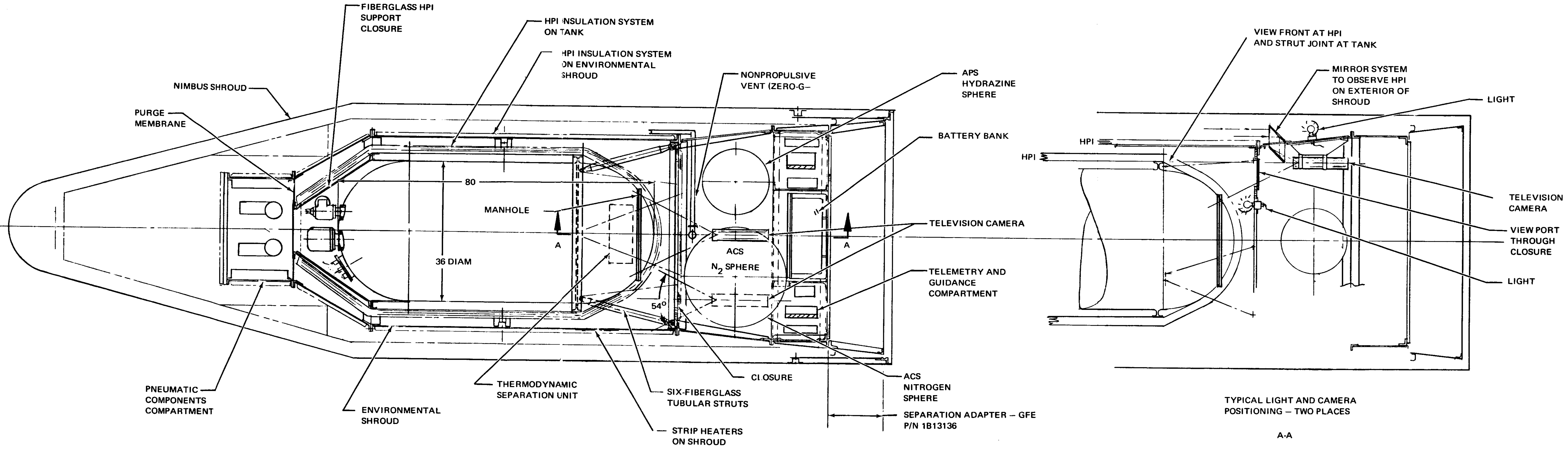

Figure 6-1. HPI Storage Tank Experiment

6-7-1 6-7-2 6-7-3

The thermal shroud will be used as the purge container with helium being used as the purge gas. The volume under the HPI support cone and closure directly above it will need to be purged independently from the HPI on the tank since a seal prevents transfer of gases between these areas. The purpose of the seal is to prevent any hydrogen leakage (from the valves, pipes, seals, etc.) from penetrating into the HPI and degrading the thermal performance. Further details on the HPI purge system are not shown because of the unavailability of any data or information on the design of a purge system for the aluminized mylar/open cell foam HPI system. The details of the purge system design would be determined during a detailed design of the experiments and apparatus.

6.3.1.2 Procedure

The experimental procedure for the evacuation ability, structural performance, and thickness history will simply involve taking data readouts at appropriate times. The time taken for the HPI system to reach the orbital steady-state heat flux will be indicated by the temperature data obtained from the sensors located within the HPI. The experimental procedure for the thermodynamic separator consists of taking pressure and temperature data, at critical points within the separator, during the venting periods. Data from the rf mass gage and continuous liquid level/mass sensors will be taken throughout the HPI experiments.

The procedure employed in obtaining the thermal performance of the HPI consists of determining the magnitude of the total heating rate to the tank and the portion of this which is due to the heat shorts. Temperature sensors placed on the heat shorts, in conjunction with preflight testing will give an indication of the magnitude of the heat shorts. The total heat input into the tank will be determined by measuring the increase in energy within the tank over a period during which there has been no venting. The primary reason for using a non-venting rather than a continuously venting system in this conceptual design is the uncertainty of the thermodynamic separator performance and the uncertainty of the accuracy of the venting period data. However, data from a continuously venting system would be desirable during the transient heat flux period (boost and early orbits) and should be considered in a detailed design of the experiments.

The energy within the tank will be determined by using data from pressure and temperature sensors, the rf mass gage, and liquid level sensors. The liquid level would be used with the temperature and pressure data to determine the hydrogen mass and provide a check of the rf mass gage data. Prior to high priority data readouts, the destratification device will be operated. This will result in a more accurate determination of the tank energy because of the uniform temperature throughout the tank skin, liquid, and ullage. Following these destratification periods, a thrust of 10^{-3} g/g_e will be applied to settle the liquid and flatten the liquid surface. These thrust periods will need to be approximately 6 min long. In addition to these high priority data readouts, less accurate data readouts, which do not utilize a destratification and settling operation, would be taken whenever possible. The transient heat flux experiment which occurs during the early part of the mission includes several of these high priority data readouts. These occur very early in the flight in an effort to determine the shape of the highly transient heat flux history curve. The energy leaving the tank during the venting periods through choked flow orifices will be measured by pressure and temperature sensors and will serve as a check on the nonvent period energy calculations.

Because of the inability to accurately predict the thermal performance of the system in space and because of the possibility for slight changes in the available data acquisition periods, an overall preprogrammed sequence for the mission will not be used. Instead, short subsequences will be used and will be initiated by command from the ground. These subsequences, which will be few in number, are short-time periods during which a unique series of events with a fixed time relationship will occur. An example of one of these subsequences is the series of events which occurs at the beginning of a venting period.

6.3.1.3 Feasibility

The sequence, analyses, and instrumentation details which show the feasibility of conceptual design A are reported in Sections 6-4, 6-5, and 6-6. In summary, the experiments appear to be feasible for use on an Atlas E & F booster. An estimation of the payload weight showed a total weight of 939 lb. This is 826 lb below the 1,765-lb payload capability of an Atlas E & F booster in a 100-nmi orbit. If a future detailed design should prove the unfeasibility of using an Atlas E & F booster, the Thor-Delta booster with a 1,600-lb payload capability (200-nmi orbit) or much greater payload capability at lower orbits could be used.

The payload weight and power requirements shown in Table 6-2 assume that no attitude control system (ACS) will be needed. It is felt that the use of additional antennas will eliminate the need of ACS for telemetry. The successful execution of the experiments do not require attitude control of the vehicle. If a future study indicates the need of an ACS system, it can be included as shown in Figure 6-1.

A 150-channel TM system should be more than adequate to handle the instrumentation needed. The instrumentation as shown in Section 6.6 requires 133 channels.

No problems should be encountered in matching a sequence to available data acquisition periods. The long periods needed for the thermal performance experiments make their length easily adjustable to correspond to the available data acquisition periods.

6.3.1.4 Possible Variations or Additions to Concept A

Variation I: Obtain data on the HPI thermal performance with the system exposed to an actual orbital environment

This will involve: (1) jettisoning the thermal shroud after 475 hr; (2) letting the heating rate through the insulation react to the new conditions (short time period) and then taking more data; (3) the addition of approximately 185 hr to the mission time; (4) the addition of at least three and preferably five high priority data readouts; (5) no additional instrumentation; (6) additional weight; (7) additional complexity because of the shroud jettisoning requirements.

Variation II: Obtain data on the ability of an HPI system to withstand the aerodynamic forces during boost. This will involve: (1) placing HPI on the exterior of the aerodynamic shroud; (2) placing thickness gages and temperature sensors on the HPI and relying on these to report any significant structural failure; (3) the addition of approximately three thickness gages; (4) the addition of approximately three temperature sensors; and (5) the addition of 20 to 40 lb of weight.

6.3.2 Experiment Conceptual Design B

The HPI experiments in conceptual design B have been selected and designed to give reliable data from a low cost and simple experimental apparatus and procedure. The data obtained would include:

1. Evacuation ability of several HPI systems
2. Structural performance of several HPI systems
3. Thickness history of several HPI systems.

6.3.2.1 Configuration and Apparatus

The configuration and overall sizes of the equipment necessary for experiment conceptual design B is shown in Figure 6-2. The simple test apparatus consists only of a framework which will support a total of six HPI systems. The framework supports each of the HPI systems in both a vertical and a horizontal position. The HPI systems could be completely different systems or could be different blanket joints or attachment methods for the same reflector and spacer materials. Two TV cameras are utilized and are positioned to view the HPI systems.

6.3.2.2 Procedure

The experimental procedure for this data simply involves taking data readouts during boost. Consequently, experiment time duration would probably be 1 hr or less. If pressure gages can be obtained to give pressures down to 10^{-5} torr, the experimental time period would be extended.

6.3.2.3 Feasibility

Because of the simplicity of the experiments, experimental procedure, and apparatus, no feasibility problems should be encountered. The low weight, power consumption, and number of instruments would not utilize the full capabilities of an Atlas E & F or Thor-Delta booster. Consequently, unless payload volume is inadequate, conceptual design B lends itself to being

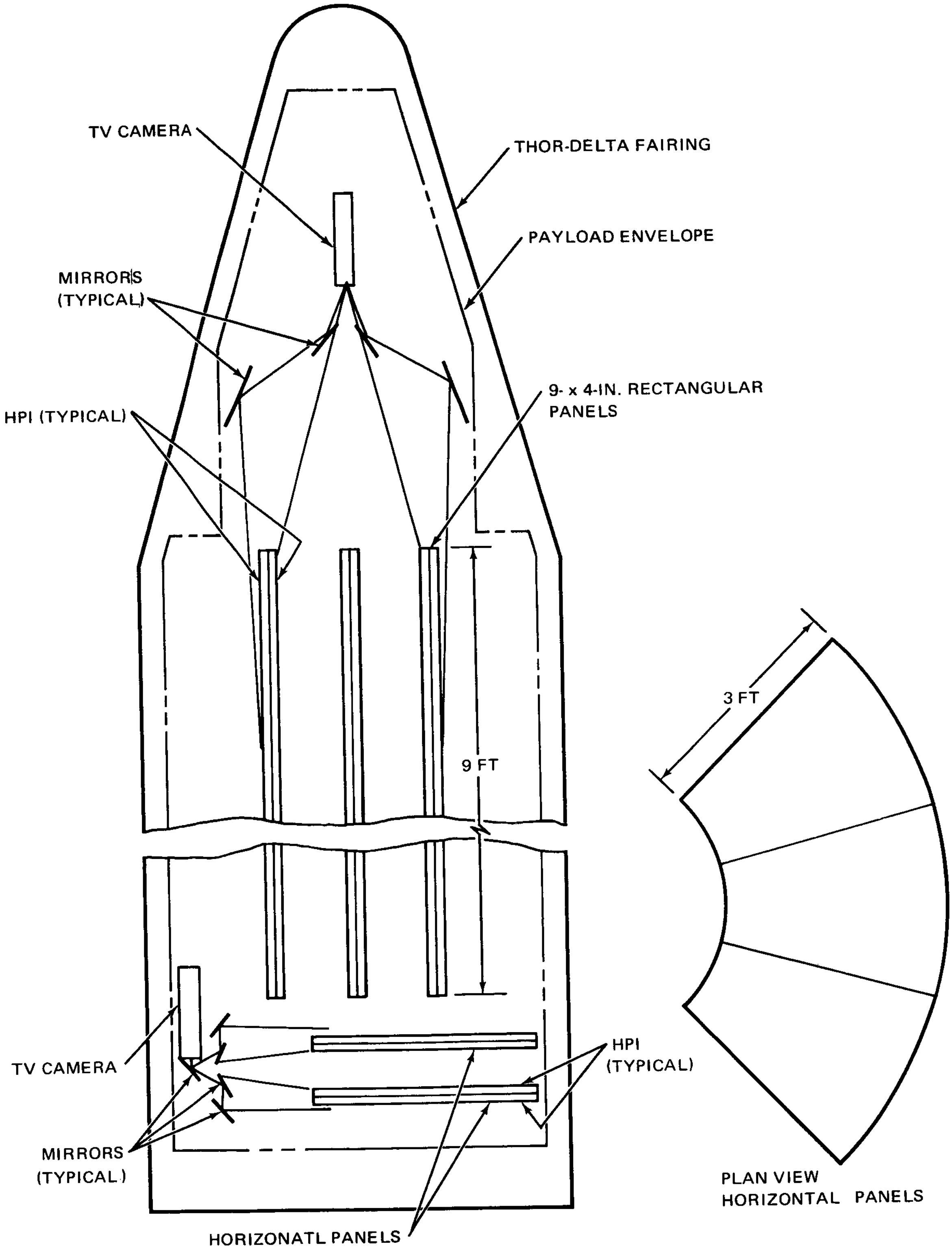

Figure 6-2. Concept B Configuration

combined with other small experiments. The inclusion of any or all of the possible variations or additions to concept B (Section 6.3.2.5) would greatly increase the value of the data. The feasibility of their inclusion should be seriously considered.

6.3.2.4 Possible Variations or Additions to Concept B

Variation I: Obtain data on the ability of an HPI system to withstand the aerodynamic forces during boost. This will involve the changes previously listed in an identical variation of concept A (see Section 6.3.1.4).

Variation II: Obtain the amount of time required for the heat flux through the insulation to reach the orbital steady-state value. This will involve: (1) the addition of cooling coils within the HPI support structure; (2) the tank, piping, valves, pumps, and ullage pressure sensors, necessary to supply the coolant for these coils; (3) the addition of at least 24 temperature sensors; (4) the addition of weight because of the tank and hardware; and (5) the extension of the experiment time duration to as much as 75 hr. The use of hydrogen as the cryogen would be desirable. However, this is not a necessity.

Variation III: In addition to variation I, variation III would include a determination of the HPI thermal performance by measuring the energy increase of the coolant due to heat flux through the HPI. In addition to those items listed for variation II, this will involve: (1) obtaining data on only three HPI systems instead of six; (2) the addition of temperature and pressure sensors to determine the enthalpy change of the coolant; (3) the extension of the experiment time to whatever length is feasible considering available power and propellant; and (4) the addition of temperature sensors on the HPI and surrounding structure. Heater blankets to control the thermal environment would be highly desirable.

6.4 PREFERRED EXPERIMENT DESIGN AND PROCEDURE

Because of the scope and extent of the data obtained and because it fully and efficiently utilizes the full capability of the booster, experiment concept design A is the preferred experiment design. The inclusion of both of the concept A variations is highly desirable and should receive serious consideration.

The procedure to be employed in executing the experiments was discussed previously in Section 6.3.1.2. The overall sequence of experiments is shown in Figure 6-3. A total of four, or possibly five, thermal performance experiments are shown.

The thermal performance experiment designated HT-1 gives data during the ground hold period and would be terminated just prior to liftoff. The transient heat flux period thermal performance experiment (HT-2) begins at liftoff and extends to approximately 50 hr after liftoff. Since data taken at the end of a venting period can be used to determine the energy which has left the tank and since this information can then be used as a check on the non-vent period energy calculations, the venting periods are considered part of the thermal experiments. Thermal performance experiment HT-3 is designed to determine the orbital steady-state heat flux through the HPI for an external environmental temperature of 530°R. Experiment HT-4 is designed to determine the orbital steady-state heat flux through the HPI for an external environmental temperature of 460°R. The short time period between HT-3 and HT-4 will allow the heat flux to reach a new steady-state value. The effect, on the sequence, of including design variation I (Experiment HT-5) is shown in Figure 6-3.

The evacuation ability, structural performance, and thickness history experiments all occur during the boost and early orbits period. A final check on the physical condition of the HPI occurs near the end of the mission. Data on the performance of the thermodynamic separator is taken during each vent.

6.5 EXPERIMENT ANALYSES

In designing the thermal experiments, an orbital steady-state heat flux of 0.2 Btu/hr-sq ft was assumed. A transient heat flux during the boost and early orbits was assumed with the heat flux reaching the orbital steady-state value at 50 hr after liftoff.

A total heat short in space of 7.5 Btu/hr was used in the design of the thermal experiments. Table 6-1 lists the heat short items and their contribution to the total heat short. Both the Fourier equation and a three dimensional heat transfer computer program were used to estimate the heat shorts.

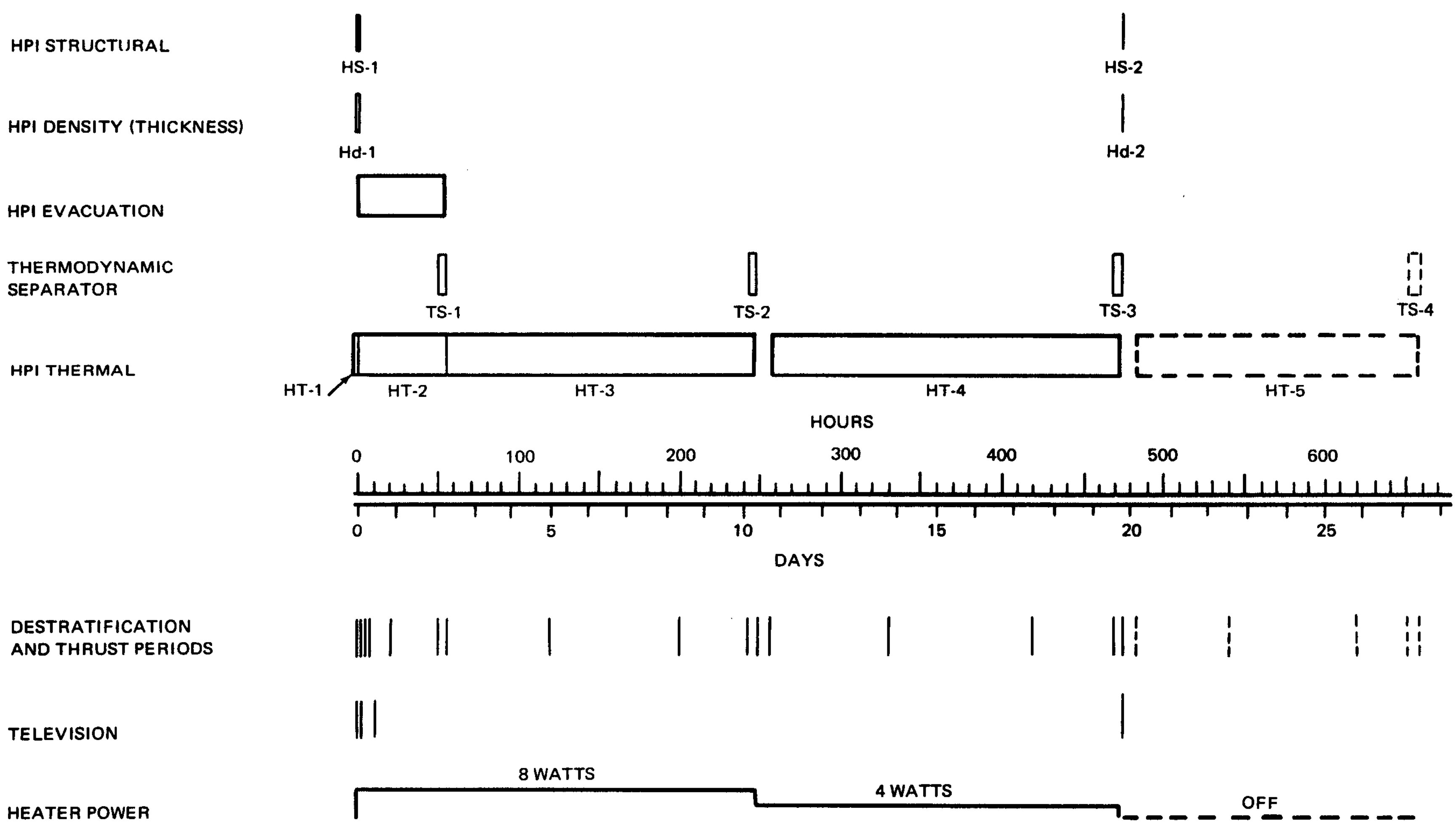

Figure 6-3. Sequence

Table 6-1

HEAT SHORTS

	$\dot{Q}$ (Btu/hr)
Tank supports	0.84
Pressure sensor tubes	0.20
Fill pipe	1.00
Vent pipe	1.00
Separator vent pipe	0.28
HPI support cone	0.82
Wire bundle	2.06
Miscellaneous (attachment apparatus, insulation penetration joints, etc.)	1.30
	7.50

In order to decrease the uncertainty of the calculated increase in tank energy during a non-vent period, it is necessary to pressurize the tank to the maximum permissible. Since the relief valve is designed to operate at a pressure of 50 psi, a maximum pressure of 47 psia was used in the determination of desirable experiment times. The desirable experiment time periods for the orbital steady-state heat flux experiments were calculated by assuming a propellant leak rate of 125 scim and the heating rates previously specified. Adequate propellant will be available to perform all of the experiments with 73 lb remaining at the end of experiment HT-4 and 51 lb remaining at the end of HT-5, see Figure 6-4.

An estimate of the payload weight has been made and is shown in Table 6-2. The total weight of 939 lb includes all of the payload necessary for the experiments through HT-4. The addition of experiment HT-5 would add an additional 78 lb.

One Saturn type battery (12,000 Whr) appears to be more than adequate to meet the power requirements. If experiment HT-5 is included, two additional batteries (HR21, 586 Whr per battery, see section 3) will need to be added. In determining the power requirements, the beacon and TM

Table 6-2
PAYLOAD WEIGHT

Table 6-2

PAYLOAD WEIGHT

	474 hours			659 hours (Includes experiment HT-5)		
	Weight (lb)	Power (watts)	Energy (watt hr)	Weight (lb)	Power (watts)	Energy (watt hr)
Batteries	155 (1 Saturn type)		-12,000	206 (1 Saturn + 2 HR21)		-13,172
Liquid hydrogen	150			150		
Tank, supports, plumbing, valves, and HPI support cone	137			137		
Thermal shroud structure	70			80		
HPI on tank	40			40		
HPI on thermal shroud	22			22		
Thermodynamic separator	11	7	119	11	7	151
Shroud heaters	35	8 4	1,975 908	35	8 4	1,975 908
APS engine	2			2		
APS plumbing and tank	25			30		
APS propellant	50			62		
TM system (150 channels)	90	275 (1.75 hr) 95 (15.2 hr)	1,921	90	275 (4 hr) 95 (19.3 hr)	2,930
Transducers	75			75		
TV transmitter	18	50	38	18	50	38
TV multiplexer	7	9	7	7	9	7
2 TV cameras and camera controls	20	24	18	20	24	18
2 TV lights	6	200	150	6	200	150
Power amplifier for TV	2	140	105	2	140	105
Sequencer	10	0.45	7	10	0.45	9
Antennas	8			8		
Beacon	3	3.9	1,850	3	3.9	2,570
TM command receiver	3	6.15	2,910	3	6.15	4,050
Total	939		-1,992	1017		-261

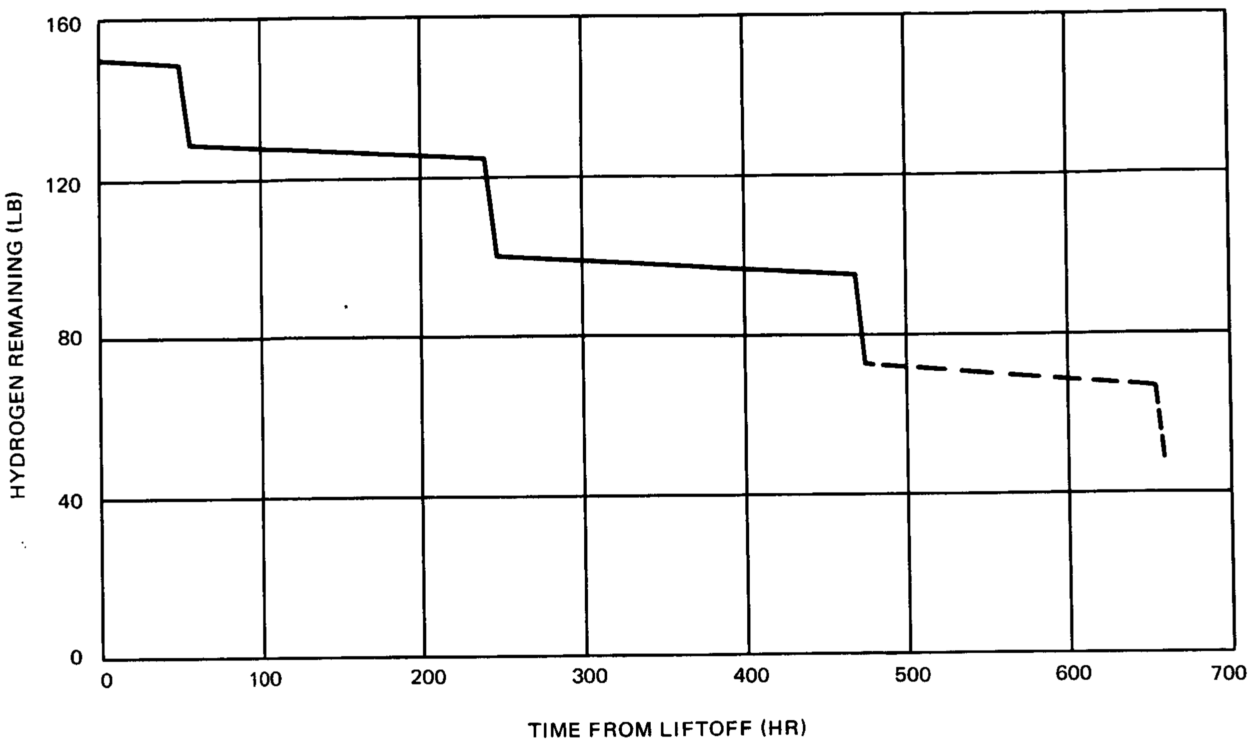

Figure 6-4. Propellant Utilization

command receiver were considered to be activated full time. However, since a sequencer can not be used for the overall sequence, the sequencer will be used only for the short-time-duration subsequence periods. In order to conserve power, only 50 channels (95 W) of the 150-channel TM system will be activated during the long venting periods. A total on-time of 45 min. was used for the TV cameras, lights, transmitter, multiplexer, and power amplifier.

6.5.1 Thermal Performance Experiments Error Analyses

The method developed by Kline and McClintock (Reference 3-9) for predicting the maximum expected error was used in all of the error analyses. This method states that the experimental uncertainty in single sample experiments is

$$W_F = \left[\Sigma_i \left(\frac{\partial F}{\partial V_i} w_i \right)^2 \right]^{1/2}$$

where F is the quantity whose uncertainty is being investigated, V_i is the measured parameter, and W_i is the respective uncertainty.

To determine the uncertainty in the calculated internal energy change, the Kline and McClintock method was applied to the following equation:

$$\Delta U = U_2 - U_1 = M_{g_2} H_{g_2} - M_{g_1} H_{g_1} + M_{f_2} H_{f_2} - M_{f_1} H_{f_1} - \frac{V_T P_2}{778 \times 12}$$

$$+ \frac{V_T P_1}{778 \times 12} + M_T C_{P_{T_2}} T_2 - M_T C_{P_{T_1}} T_1 + \dot{M}_V H_V \theta$$

Nomenclature

U	=	Internal energy	BTU
M	=	Mass	LB_M
H	=	Enthalpy	BTU/LB_M
V	=	Volume	$In.^3$
P	=	Pressure	$LB_f/in.^2$
C_P	=	Specific heat	BTU/LB_M °R
T	=	Temperature	°R
W_i	=	Magnitude of uncertainty in parameter i	
A	=	Area	Ft^2
Q	=	Heat	BTU
$\dot{Q}$	=	Heat rate	BTU/hr
q	=	Heat flux	$BTU/hr\text{-}ft^2$

k	=	Thermal conductivity	BTU/hr-ft°R
L	=	Length or thickness	Ft
θ	=	Time	Hr
$\dot{M}$	=	Mass flow rate	LB_m/hr

Subscripts

S	=	Shorts
g	=	Gas
f	=	Fluid
T	=	Tank
TOT	=	Total
t	=	Thickness
V	=	Vent
1	=	Data readout time #1
2	=	Data readout time #2

The internal energy uncertainty obtained was then divided by the time duration of the experiment to give the uncertainty in the total heating rate. This uncertainty in the total heating rate was used in the determination of the uncertainty in the heat flow rate through the insulation. The uncertainty in the experiment time duration was not considered since it will be negligible. In the analysis, the propellant lost through valve leakage was considered to be in the vapor phase.

The Kline and McClintock error analysis method was also applied to the simple equation which indicates the heat flow rate through the insulation, $\dot{Q}_{HPL} = \dot{Q}_{TOT} - \dot{Q}_S$. The uncertainty in the total heating rate ($\dot{Q}_{TOT}$) was obtained in previous calculations. Unless specified otherwise, a value of 10% was used for the uncertainty of the magnitude of the heat shorts ($\dot{Q}_S$). The resulting uncertainty in the heat flow rate through the insulation was used in the determination of the uncertainty in the apparent thermal conductivity. Because the uncertainty of the insulation surface area and the uncertainty of the temperature gradient across the insulation will be negligible, and since the uncertainty of the insulation thickness was neglected in these calculations, the uncertainty in the apparent thermal conductivity was equal to the uncertainty in the heat flow rate through the insulation.

The error analyses showed a maximum expected error, in the total heating rate, of 8.8% for experiment HT-2. The maximum expected error, in the total heating rate, for experiments HT-3, HT-4, and HT-5 is 7.5%, 7.9%, and 8.5% respectively. The maximum expected error, in the apparent thermal conductivity, for experiments HT-3 and HT-4 is 12% and 14.6% respectively. Additional results of the error analyses for experiment HT-3 are shown in Figures 6-5, 6-6, 6-7 and 6-8. These curves show the effect which a change in various parameters would have on the experimental error. Figure 6-5 shows, for various heating rates and experimental time durations, the maximum expected error in the total heating rates calculated from the experimental results. Figure 6-6 shows, for various heating rates and experimental time durations, the maximum expected error in the determination of the apparent thermal conductivity of the HPI. Figure 6-7 indicates

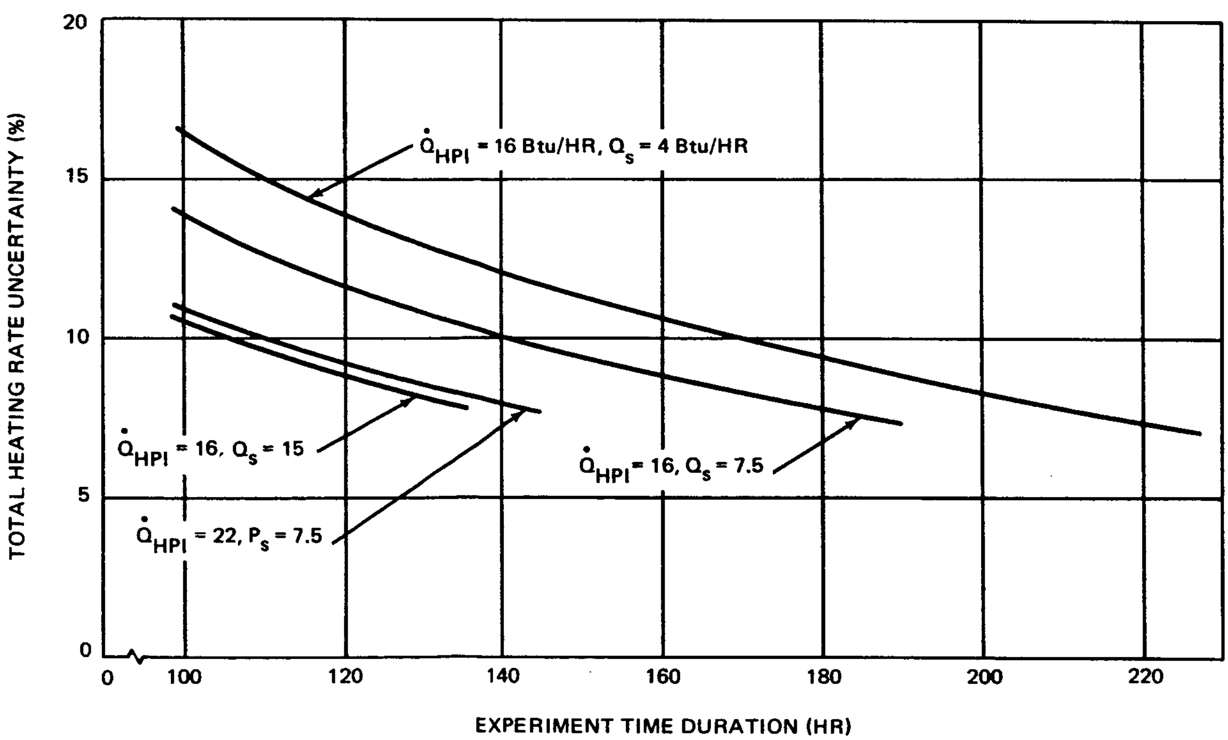

Figure 6-5. Maximum Expected Error in Tank Internal Energy Change (Experiment HT-3)

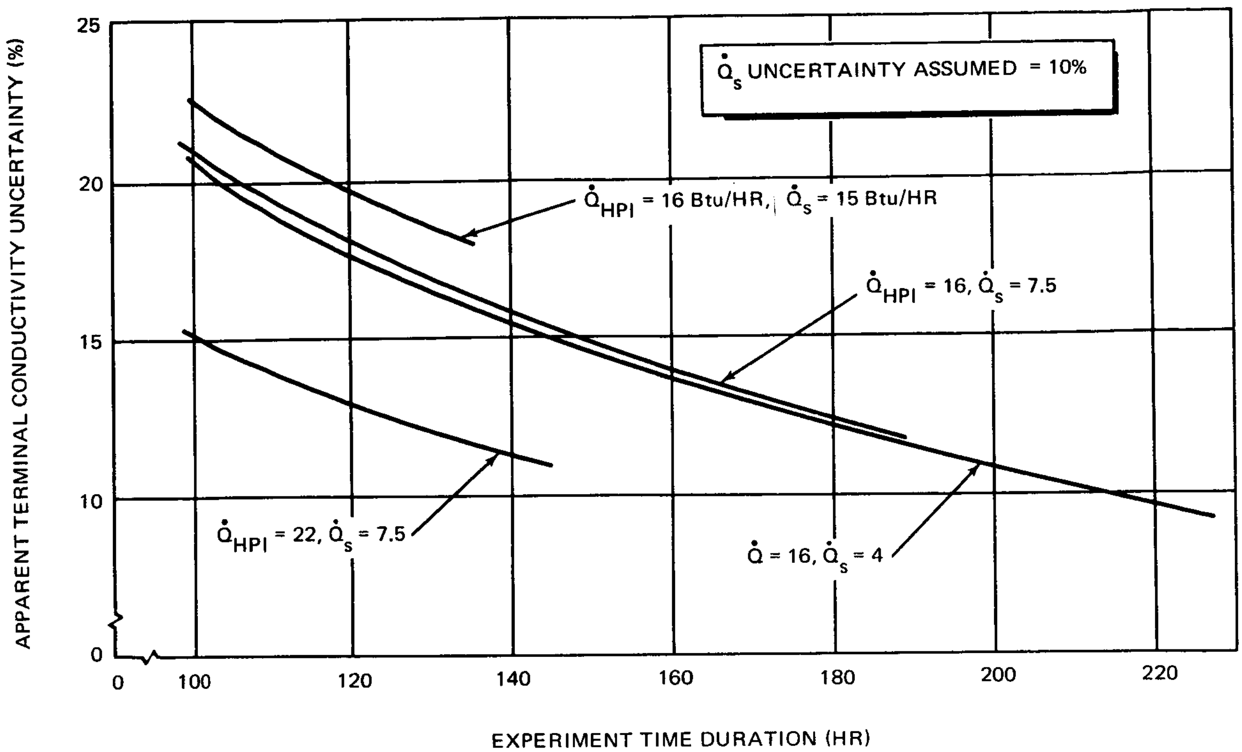

Figure 6-6. Maximum Expected Error in Apparent Thermal Conductivity (Experiment HT-3)

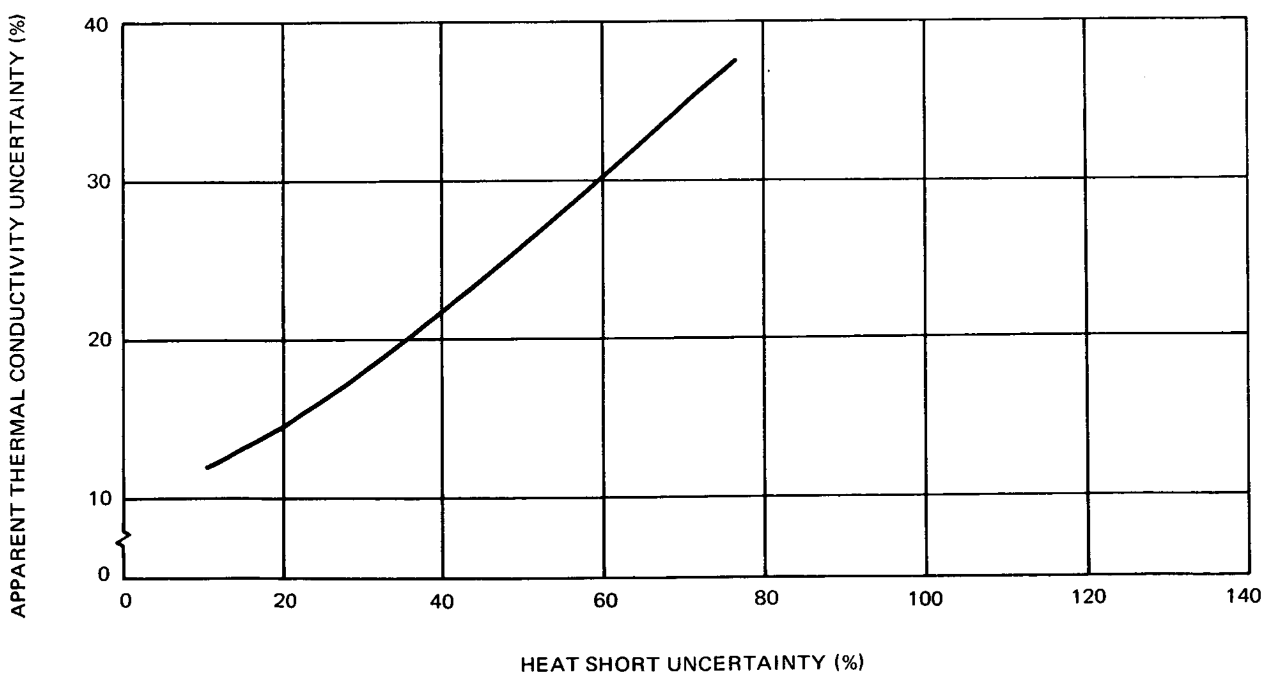

Figure 6-7. Effect of Heat Short Magnitude Uncertainty (Experiment HT-3)

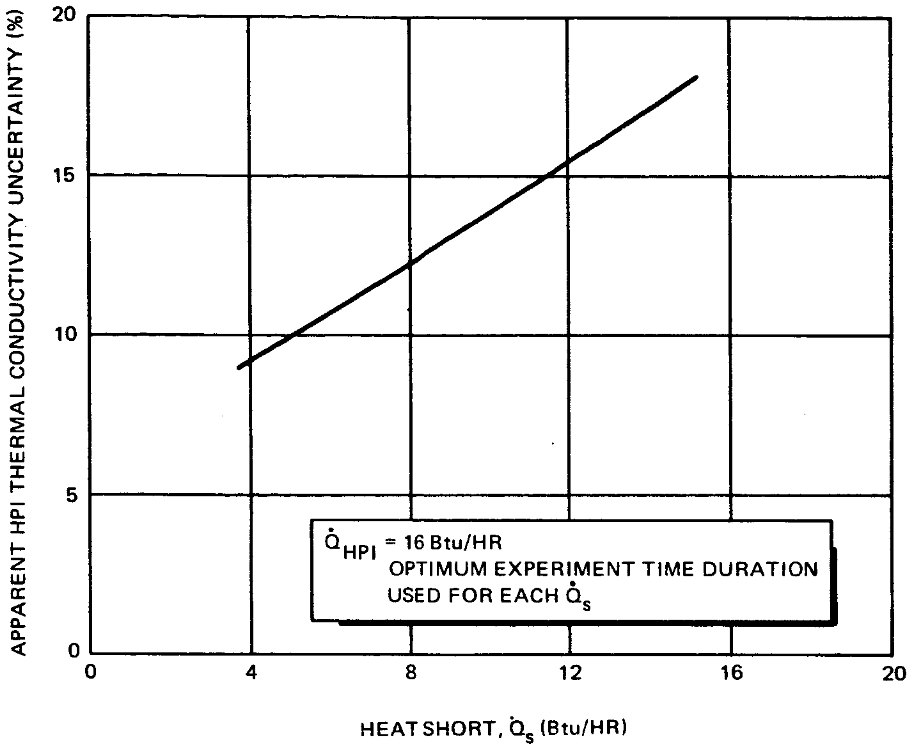

Figure 6-8. Effect of Heat Shorts (Experiment HT-3)

the effect which the uncertainty in the heat short magnitude has on the apparent thermal conductivity maximum expected error. Figure 6-8 shows the effect which a change in the magnitude of the heat shorts would have on the apparent thermal conductivity uncertainty.

6.5.2 Structural Performance and Evacuation Efficiency Experiments Error Analyses

The uncertainty of the insulation thickness readings will depend on the telemetry uncertainty and the accuracy of the calibration curve. Of these, the uncertainty caused by the telemetry is comparatively negligible. Since the development needed to obtain the optimum HPI thickness gage design has not yet been accomplished, the accuracy of the gage which would be used is not certain. However, the feasibility testing on this gage has shown that a thickness uncertainty of less than 20% should be possible. This is 20% of the thickness readout given by the gage and not 20% of the range of the gage.

The uncertainty of the HPI and shroud pressure gage data will be determined by the accuracy of the gages and telemetry system. This uncertainty should be 3% or less of the range of the gage.

6.6 INSTRUMENTATION

A detailed listing of the instrumentation needed is shown in Table 6-3. Figure 6-9 shows the location of the instrumentation.

6.6.1 Thermal Performance Instrumentation

The temperature sensors within the tank and on the tank surface, the pressure gage within the tank, the rf mass gage, and the liquid level indicators will be used to determine the energy within the tank. The rf mass gage will indicate the mass of hydrogen present. The liquid level can be used with the temperature and pressure readings to also give the hydrogen mass. The temperature sensors within the insulation blankets in conjunction with those on the tank surface and exterior HPI surface will indicate the temperature profile within the insulation. This temperature data in conjunction with HPI thickness data will be used to determine the apparent thermal conductivity of the HPI. This temperature data will also be used to determine the time taken for the HPI system to reach an orbital steady state heat flux.

The temperature sensors located on the surfaces of the heat shorts (pipes, tank supports, wire bundle, and HPI support cone) will be used to predict the amount of heat which has entered the tank through these insulation penetrations. In addition to their use in determining the apparent thermal conductivity, some of the temperature sensors located on the exterior surface of the HPI will be used to control the heaters on the thermal shroud. The temperature and pressure sensors placed in the vent line will be used to determine the energy leaving the tank during venting. The temperature sensors on the thermal shroud will indicate the temperature environment seen by the tank HPI.

The shroud heater power data will be used in calculations which will give a check on the amount of heat entering the tank through the HPI. The mixer power data will be subtracted from the total energy increase within the tank when determining the heat flux through the HPI.

Table 6-3
INSTRUMENTATION (HPI Experiments)

Measurement Title	Number Required	System Range/Accuracy	Frequency Response	Environment at Point of Measurement	
				Media	Temperature
Heater current (5 heaters, 1 mixer)	2	0 to 0.6 ± 0.018 amps (±3%)	1 cps (4 sps)		
Heater voltage	1	0 to 30 ± 0.9 vdc (±3%)	1 cps (4 sps)		
Insulation (thickness)	4	0.5 to 4 (±3% system)(2)	1 cps (4 sps)	He; vacuum	37 to 620°R
Insulation (thickness)	13	0.1 to 4 (±3% system)(2)		He; vacuum	37 to 620°R
Events	15	To be determined	2.4 cps (12 sps)		
Temperature He storage sphere	1	100 to 540 ± 14°R (±3%)	1 cps (4 sps)	GH_2	37 to 620°R
Temperature LH_2 storage tank liquid	2	36 to 40 ± 0.12°R (±3%)	1 cps (4 sps)	GH_2; LH_2	37 to 620°R
Temperature thermodynamic separator	1	40 to 100 ± 1.8°R (±3%)	1 cps (4 sps)	GH_2; LH_2	37 to 620°R
Temperature thermodynamic separator	1	35 to 47 ± 0.45°R (±3%)	1 cps (4 sps)	GH_2; LH_2	37 to 620°R
Temperature thermodynamic separator	1	28 to 46 ± 0.54°R (±3%)	1 cps (4 sps)	GH_2; LH_2	37 to 620°R
Temperature thermodynamic separator	1	28 to 40 ± 0.36°R (±3%)	1 cps (4 sps)	GH_2: LH_2	35 to 620°R
Temperature GH_2 vent	1	25 to 400 ± 10°R (±3%)	1 cps (4 sps)	GH_2; LH_2	25 to 620°R
Temperature GH_2 vent	1	25 to 125 ± 3°R (±3%)	1 cps (4 sps)	GH_2; LH_2	25 to 620°R
Temperature LH_2 storage tank liquid	5	36 to 46 ± 0.3°R (±3%)	1 cps (4 sps)	LH_2; GH_2	33 to 620°R
Temperature LH_2 storage tank surface	13	35 to 50 ± 0.45°R (±3%)	1 cps (4 sps)	LH_2; GH_2; He	33 to 620°R
Temperature differential, supports	15	33 ± 1°R (±3%)	1 cps (4 sps)	Air; vacuum, He	35 to 620°R
Temperature LH_2 storage tank gas	4	35 to 400 ± 10°R (±3%)	1 cps (4 sps)	LH_2; GH_2	33 to 620°R
Temperature shroud HPI	5	300 to 550 ± 4.5°R (±3%)	1 cps (4 sps)	Air; vacuum	300 to 620°R
Temperature LH_2 storage tank surface	2	35 to 400 ±10°R (±3%)	1 cps (4 sps)	LH_2; GH_2; He	37 to 620°R
Temperature HPI	4	330 to 530 ± 6°R (±3%)	1 cps (4 sps)	He; vacuum, air	37 to 620°R
Temperature HPI surface and shroud skin	9	400 to 550 ± 4.5°R (±3%)	1 cps (4 sps)	He; vacuum; air	400 to 620°R
Temperature, support bracket	1	250 to 550 ± 9°R (±3%)	1 cps (4 sps)	He; vacuum, air	37 to 620°R
Temperature HPI	4	60 to 260 ± 6°R (±3%)	1 cps (4 sps)	He; vacuum; air	37 to 620°R
Temperature HPI	4	200 to 400 ± 6°R (±3%)	1 cps (4 sps)	He; vacuum, air	37 to 620°R
Pressure LH_2 storage tank Ull	2	0 to 50 ± 1.5 psia (±3%)	1 cps (4 sps)	GH_2; LH_2	37 to 620°R(1)
Pressure He storage sphere	1	0 to 3500 ± 150 psia (±5%)	1 cps (4 sps)	GH_2	37 to 620°R(1)
Pressure GH_2 vent	1	0 to 50 ± 1.5 psia (±3%)	1 cps (4 sps)	GH_2; LH_2	37 to 620°R(1)
Pressure environment HPI	6	1 mm Hg - 1 Atm (±3%)	1 cps (4 sps)	He; vacuum; air	400 to 620°R
Pressure environment HPI	6	0 to 1 mm Hg (±3%)	1 cps (4 sps)	He; vacuum; air	400 to 620°R
Pressure thermodynamic separator	1	0 to 50 ± 1.5 psia (±3%)	1 cps (4 sps)	GH_2; LH_2	37 to 620°R(1)
Pressure thermodynamic separator	1	0 to 10 psia			
Pressure thermodynamic separator	2	0 to 25 psia (±3%)	1 cps (4 sps)	GH_2; LH_2	37 to 620°R(1)
Pressure differential (T/D S.)	1	±1 psia (±3%)	1 cps (4 sps)	GH_2; LH_2	37 to 620°R(1)
Pressure differential (T/D S.)	1	±20 psia			
Level/mass LH_2 continuous (propellant storage tank)	3	To be determined (±3%)	1 cps (4 sps)	LH_2; GH_2	37 to 620°R
Liquid/vapor indicator (2 GDA)	5	Liquid/vapor indicator	1 cps (4 sps)	LH_2; GH_2	37 to 620°R
TV camera	2				
Mass (RF)(3)	1	To be determined (±3%)	1 cps (4 sps)	LH_2; GH_2	37 to 620°R

Notes:
(1) Sensing line must isolate transducer to provide -60 to +165°F environment.
(2) Experimental measurement--gage reads approximately 20% of reading.
(3) Experimental measurement.

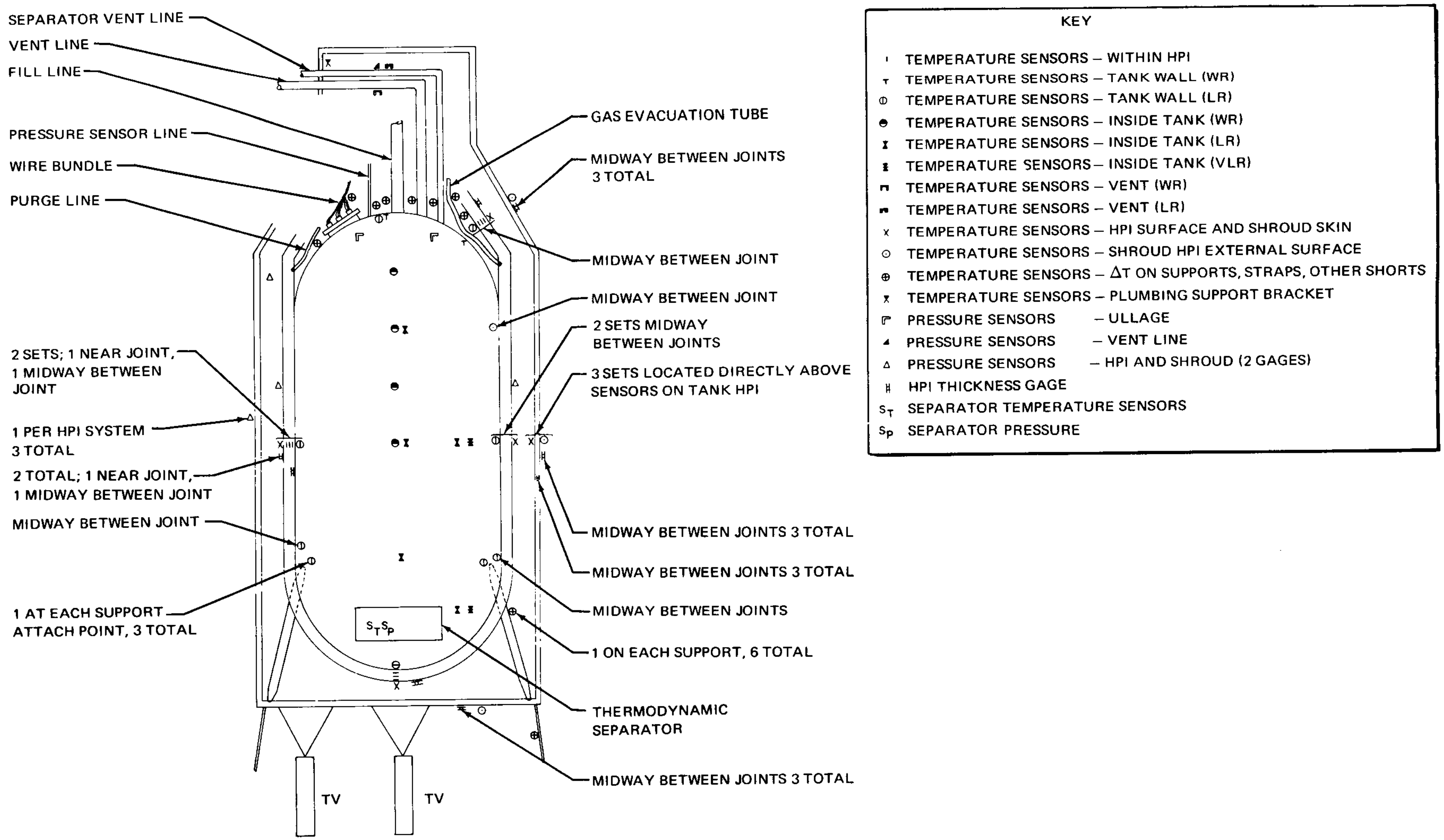

Figure 6-9. Instrumentation

6.6.2 Structural Performance and Evacuation Efficiency Instrumentation

The capacitance-type HPI thickness gages will be used to determine the thickness history of the insulation systems. These gages will also be used to indicate any major structural failure of the HPI system such as the removal of insulation in the gage area. The pressure gages, located within or under the HPI, will give the pressure history during boost. The shroud pressure data will be used with the HPI pressure data to determine the pressure differentials and evacuation efficiency of the system during boost.

Section 7
STRATIFICATION/DESTRATIFICATION

7.1 ORBITAL EXPERIMENTATION INFORMATION REQUIREMENTS

The technology survey of Section 2 indicated the analysis, 1.0 g/g_e tests, low g ground tests, and orbital tests required to meet the design needs of the S-IIB, S-IVC and nuclear stages. Within the areas of stratification and destratification, the primary concern is the prediction of the tank pressure history during the mission. To analytically predict the thermal energy distribution (i.e., the tank pressure history) will require knowledge of the heat transfer mode and the convective current patterns for a two-phase, confined system, with and without mixing.

A definition of the separation of the various heat transfer modes was found to be the most urgent requirement from the standpoint of the anticipated design need time schedule. The primary concern is to define the separation of the natural convection and boiling regimes as well as to establish the influence of bubble dynamics and latent heat transport on the energy distribution under low gravity conditions.

Once the heat transfer mode is defined, in order to determine the energy distribution, one must be able to describe the convective currents within the tankage. The reduced acceleration levels associated with the orbital environment causes the surface tension forces to become similar in magnitude to the gravity forces. This may cause severe surface distortion, resulting in significant changes in the flow patterns when compared to the flat liquid-vapor surface associated with a 1.0 g/g_e environment. Information is also required concerning the influence of the coupled effects of the heating pattern, tank geometry, boiling and liquid sloshing on these convection patterns and energy distributions.

Another information requirement is the effect of step changes and gradual fluctuations of the acceleration level on the energy distribution. The step acceleration changes are associated with docking maneuvers, personnel motion, and auxiliary propulsion system operation. Gradual fluctuations of the acceleration level will be the result of drag variations for elliptical orbits, orbital decay and attitude control operation. These acceleration variations will create transients in the convective patterns and the free surface shape, that will influence the thermal energy distribution. The variation in acceleration level in a manner corresponding to the drag acceleration fluctuation can only be performed in orbit.

The definition of scaling laws is required in order to directly utilize small-scale test data as design data. To ensure that scaling can be achieved, two areas must be included, nonboiling scaling and boiling scaling. Present analyses indicate that scaling of systems at a low-gravity environment with 1.0 g/g_e experiments cannot be achieved exactly. Additionally, miniature testing systems at 1.0 g/g_e that provide Bond numbers similar to those experienced by orbiting vehicles become too small to instrument. Therefore, orbital tests are required to establish and/or verify stratification/destratification scaling techniques.

Overcoming portions of the stratification problem by mechanically mixing the propellant will require an understanding of the effect of momentum added by the mixer on the propellant location and pressure response. The influence of both continuous and transient mixing on the propellant thermal energy distribution is desirable.

7.2 DATA ACQUISITION AND EXPERIMENT REQUIREMENTS

The objectives of the stratification/destratification orbital experimental program are: (1) to obtain specific design data applicable to the S-IIB, S-IVC and nuclear stages and (2) to provide a better phenomenological understanding of the thermal energy distribution processes. The first objective is met by applying the best scaling techniques available in defining the requirements for small-scale orbital experiments. This requires maintaining reasonable geometric similarity between the particular stage of interest and the small-scale experiment. The second objective can be met by properly selecting data points so that correlations may be developed, and also verify and/or correct existing analytical tools.

The requirement of geometric similarity necessitates the consideration of a minimum of two orbital experimental packages; one corresponding to the inverted dome geometry of the S-IIB and S-IVC and another corresponding to the hemispherical lower dome configuration of the nuclear stage. Since design requirements of the S-IIB and S-IVC occur earlier than the nuclear stage, the inverted dome geometry should be considered first. Therefore, only the inverted dome configurations are presented as conceptual designs. Additionally, data obtained from the initial orbital experiment certainly will be incorporated into future experiment designs. There also is the possibility that a second experiment may not be required because a sufficient fundamental understanding of stratification and mixing was obtained by the first experiment. The possibility of this occurrence appears remote at this time, due to the poor gross understanding of the problem.

7.2.1 Stratification Data Acquisition

There are two basic periods during which stratification data can be obtained; the boost and insulation transient period and the orbital coast period. The boost and insulation transient period is controllable only within certain limits and occurs only once for each orbital test. The orbital coast period will allow for the variation of parameters in an orderly fashion in order to develop a fundamental understanding of the problem.

Because of the nature of the orbital environment, it does not appear advisable to isolate each of the individual phenomena noted in the experimental requirements. That is, to try to hold all variables constant while one is varied to determine its individual influence on the energy distribution is not recommended. The feasibility of such an approach is questionable because of the large number of variables associated with stratification and destratification and the undue requirements that would be imposed on the carrier vehicle. For example, to maintain the liquid to ullage volume constant for an orbital experiment would require additional storage and low-g transfer capability. Consequently, the experimental procedure adopted is one that allows a relaxation of the experimental requirements by focusing attention on the apparent important parameters based on analyses and earth tests.

During the boost and insulation transient period the important items that should be observed are: (1) the sloshing due to the coupling of natural convection and rapid changes in the acceleration level (MECO slosh, etc.), (2) the transition of the heat transfer modes from boiling to natural convection as the insulation outgasses and improves in thermal performance, and (3) the thermal energy distribution during this period with the coupled effects of acceleration level transients, insulation performance transients, and propellant sloshing. Since this environment will establish the initial conditions for any long-term storage mission, it is an important portion of the data acquisition program.

During the orbital coast period the acceleration level and insulation performance will be stabilized, so that variation in the stratification parameters can be made. The only two basic parameters that can be reasonably controlled are the acceleration level and the wall heating rate. Fortunately, changing these two independent parameters will allow a variation of both the Bond number and the Modified Rayleigh number and will allow investigations well into the boiling regime. Holding the acceleration level constant and varying the heating rate for several experiments will allow examination of the effect of the modified Rayleigh number on the stratification at a constant Bond number. Similarly, holding the heating rate constant and varying the acceleration level for several experiments will allow examination of the effect of the Bond number on the energy distribution at constant modified Rayleigh number. Obtaining data points in this manner can result in data coverage illustrated in Figure 7-1. This permits a fundamental understanding of stratification to be obtained more readily.

To obtain design data, the scaling parameters for the experiment must be chosen to match the parameters associated with the S-IIB, S-IVC and nuclear stage. Although exact scaling may be impossible (see Section 7. 5), the important parameters to scale approximately for non-boiling conditions when the test and actual fluid are the same appear to be the Bond number, the Modified Rayleigh number, and the Fourier number. By utilizing the

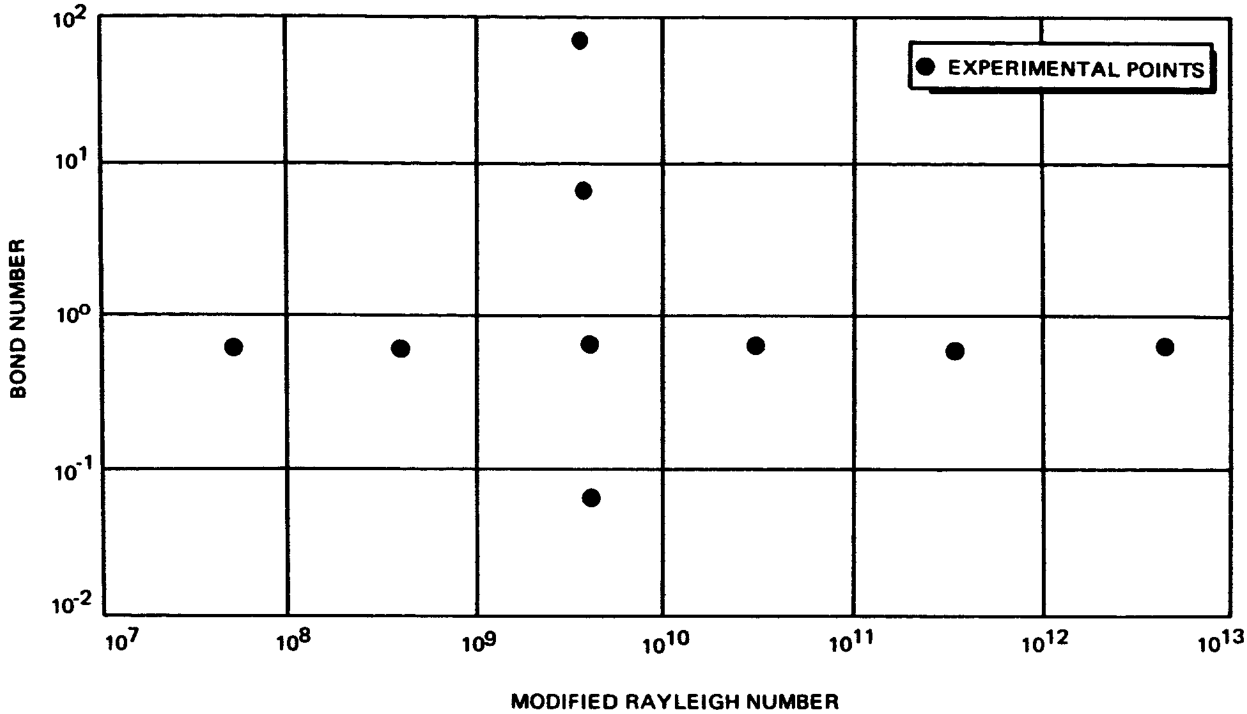

Figure 7-1. Typical Stratification Data Coverage

modified Rayleigh number, the Bond number and the Fourier number as scaling parameters, experiments performed at a given acceleration level and having a given tank radius will create a scale line that can be used for tankage in addition to the S-IIB, S-IVC and nuclear stage. Scale lines for a 3-ft diameter tank at 10^{-3}, 10^{-5} and 10^{-6} g/g_e are shown in Figure 7-2.

The stratification experiment time should be chosen so that the quasi-steady state stratification profiles have developed. This is important, since the entire storage system can be treated as a lumped mass after the establishment of the quasi-steady period and will enable the formulation of a conservative stratification model considerably better than the present all heat-to-vapor model (Reference 7-1). In actual practice, under some conditions, the tank pressure at the time quasi-steady state conditions are reached may be well above normal tank operating pressures. For these cases, the experimental time will be limited to that time required to reach tank operating pressure.

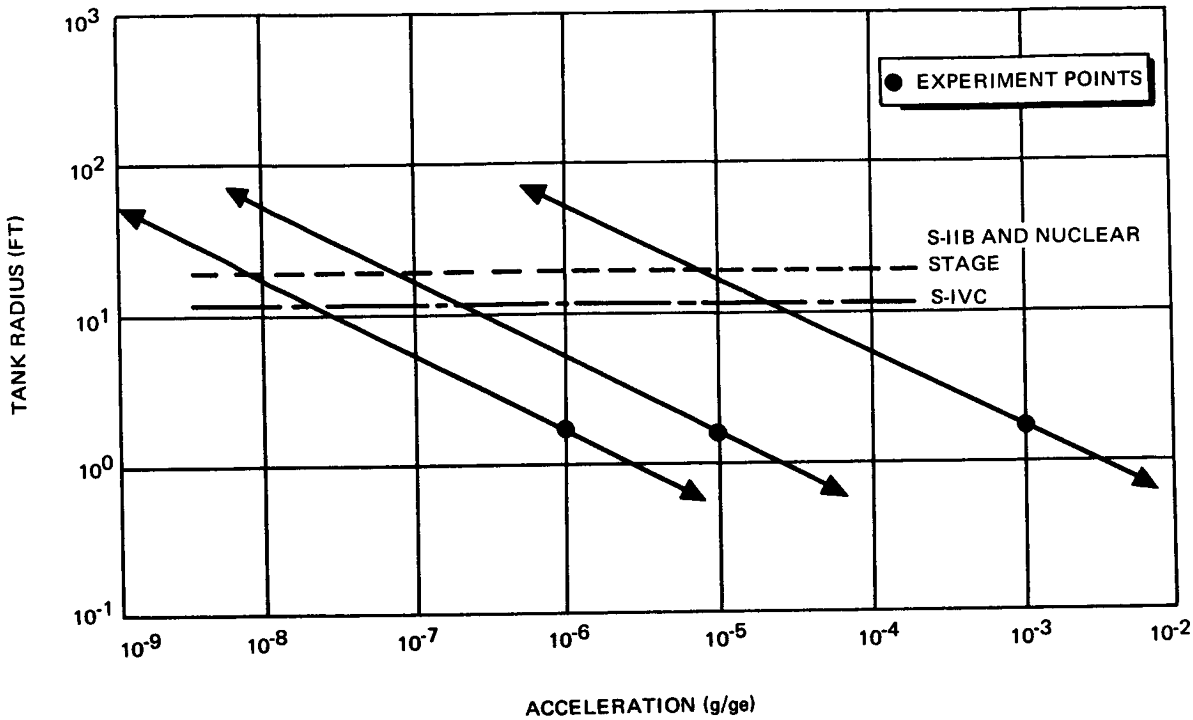

Figure 7-2. Stratification Scaling Provided by a 3.0-ft Diam Tank at 10^{-3}, 10^{-5}, and 10^{-6}g/ge

7.2.2 Destratification Data Acquisition

Bubble pumps, baffles, mechanical mixers and dielectrophrosis, to mention a few, have been considered for thermal stratification reduction. Each (or several combined) of these techniques could be tested in orbit; however, at the present time mechanical pumps as mixers appear to be the most attractive and were the only devices considered in this study.

Mechanical pumps can be utilized so that the outlet forms a radially directed jet, an axially directed jet, pumps liquid into the ullage, or pumps vapor into the liquid. Earth-based tests have centered attention on the axial and radial jets. The results of these analyses and tests have shown that axial jets require approximately an order of magnitude less power than radial jets to provide mixing in a stratified tank (Reference 7-2, 2-7). Axial jets, however, are more likely to cause ullage disruption that may result in settling problems prior to engine start. Therefore, both axial and radial jets have been considered in this study.

Data for stratification reduction should be obtained for both continuous and intermittent mixer operation. The intermittent operation should be performed for varying degrees of stratification in order to evaluate the influence of the stratification on the pressure response. An example of the results obtained from these tests is shown in Figure 7-3. For both the axial and radial jet configurations, the minimum amount of pump energy required to disrupt the ullage as a function of the liquid to ullage volume ratio for settled propellant conditions should be determined. This most likely will result in an ullage disruption map similar to Figure 7-4.

7.2.3 Stratification Requirements

In order to provide the proper scaling relationships for stratification, the Bond number must first be matched by selecting an acceleration level. The smaller the experimental tank the larger the acceleration level required to match the design vehicle. Once the acceleration level is chosen, the modified Rayleigh number is matched by adjusting the auxiliary heating rate. For the S-IIB and S-IVC the Bond number may range from 0.04 to 10^2; and

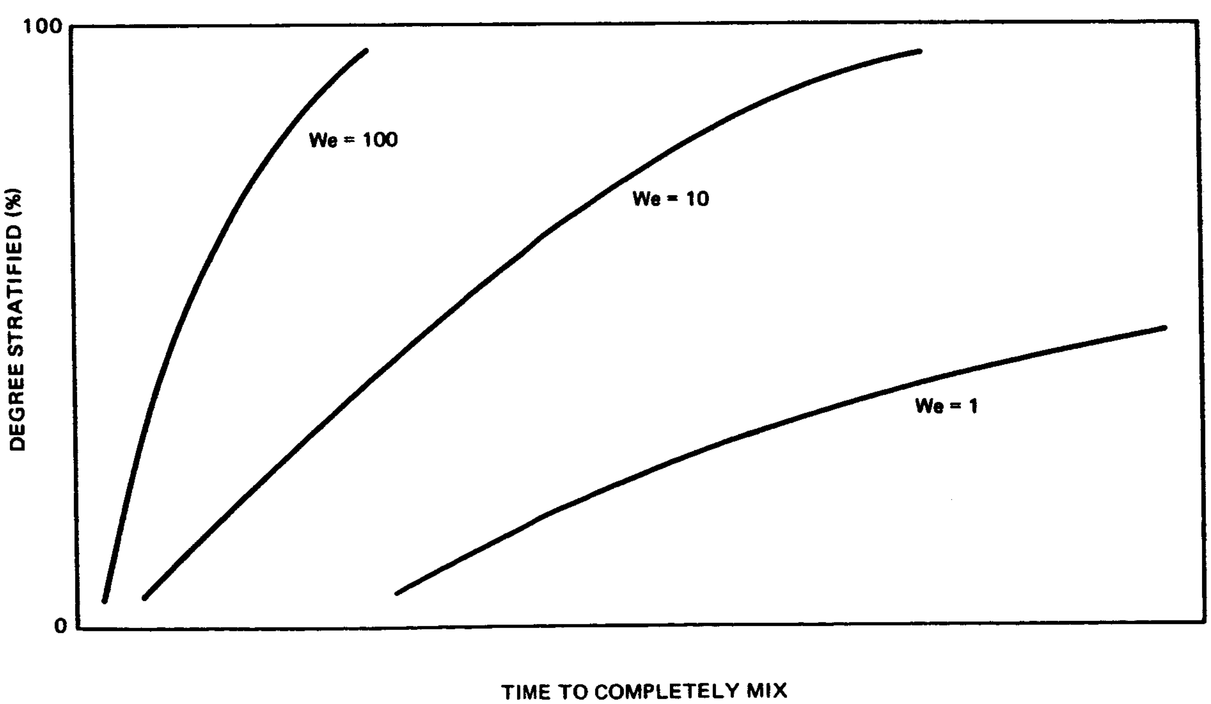

Figure 7-3. Typical Destratification Data-Time to Completely Mix as a Function of Stratification and Weber Number

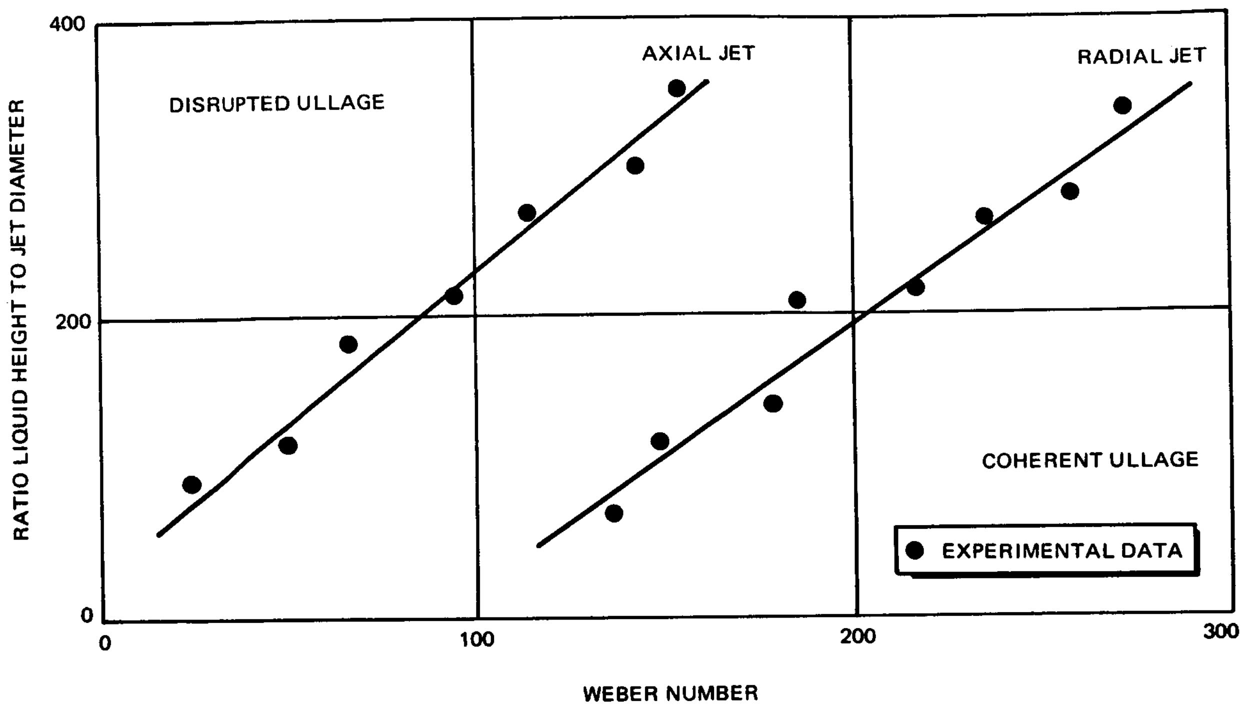

Figure 7-4. Typical Destratification Data-Definition of Critical Weber Number Required to Disrupt Ullage

the modified Rayleigh number from 3 x 10^7 to 10^{14}. For the nuclear stage the expected Bond number range is 0.01 to 80, and the modified Rayleigh number ranges from 9 x 10^7 to 10^{15}. Table 7-1 shows the acceleration level ranges and heating ranges needed to match the S-IIB, S-IVC and nuclear stages for a 1.5 by 3-ft, a 2.5 by 5-ft, and a 3 by 6-ft tank. The liquid height used to calculate the modified Rayleigh numbers was the straight wall length.

Table 7-1 indicates that acceleration levels from approximately 10^{-3} to 10^{-7} g/g_e are required. The higher acceleration, 10^{-3} g/g_e, can be provided by the auxiliary propulsion system. Drag accelerations for a 200 nmi orbit will be between 10^{-6} and 10^{-7} g/g_e and can be used to provide the lower acceleration levels. It is desirable to have an intermediate acceleration; 10^{-5} g/g_e was chosen since it does not require excess auxiliary propulsion propellant and qualified hardware appears to be available.

Table 7-1

EXPERIMENTAL PARAMETERS REQUIRED FOR S-IIB, S-IVC AND NUCLEAR STAGES

Tank	Bond No. Range	Acceleration Level Range (g/g_e)	Modified Rayleigh Range	Heat Transfer Rate Range ($Btu/hr\text{-}ft^2$)
1.5' x 3.0'	10^{-2} to 10^2	5.7×10^{-7} to 5.7×10^{-3}	3×10^7 to 10^{15}	1.66 to 5.5×10^3
2.5' x 5.0'	10^{-2} to 10^2	2×10^{-7} to 2×10^{-3}	3×10^7 to 10^{15}	0.59 to 1.97×10^3
3' x 6'	10^{-2} to 10^2	1.5×10^{-7} to 1.4×10^{15}	3×10^7 to 10^{15}	0.413 to 1.38×10^3

The lower limit of the heat transfer rate, approximately 0.4 $Btu/hr\text{-}ft^2$, can be easily provided by HPI insulation. Since the scaling parameters used in generating Table 7-1 are for nonboiling conditions, the upper limit for experimental heating rate is bounded by the incipient boiling point. This limit appears to be between 10 and 50 $btu/hr\text{-}ft^2$ for typical hydrogen tankage.

To obtain a fundamental understanding of stratification at low acceleration levels for analytical model development, the primary requirements are to have a Bond number on the order of 1.0 or less and to allow the thermal stratification profiles to reach quasi-steady state. Both of these requirements are compatible with the scaling requirements above.

The stratification experiment time required to reach quasi-steady state is

$$t = 1.57 \frac{HD}{\alpha} \frac{Ra_H^{*\,-1/5}}{Pr^{0.812}} \qquad (7\text{-}1)$$

for $Ra_H^* < 10^{11}$ and

$$t = \frac{5.75\, HD}{\alpha} \frac{(1 + 0.4 Pr^{2/3})^{2/7}}{Pr^{1/21}} Ra_H^{*\,-2/7} \qquad (7\text{-}2)$$

for $Ra_H^* > 10^{11}$ (see Section 7.5).

7.2.4 Destratification Requirements

The primary requirement for the destratification experiment is to provide a jet flow range that will traverse the critical Weber number to cause ullage disruption. A conservative estimate of the lower limit on the Weber number was derived for both an axial and a radial jet. The analyses considered zero gravity conditions with surface tension the only restoring force.

For an axially directed jet, the minimum Weber number (based on jet exit conditions) is given as (Reference 7-3)

$$We_{j_{crit}} = 4 \left(1 - \frac{H}{d_j} \tan \theta\right) \qquad (7\text{-}3)$$

where H is the liquid height, θ is the jet angle, and d_j the jet diameter. For a radial jet, the critical Weber number is

$$We_{j_{crit}} = \frac{D - H \tan \theta}{B} \qquad (7\text{-}4)$$

where D is the tank diameter, H is the liquid height, θ is the jet angle, and B is the jet perimeter.

The above critical Weber numbers should be considered in sizing the mixer flow rate and the jet area.

7.3 EXPERIMENT CONCEPTUAL DESIGNS

7.3.1 Experiment/Carrier Integration

Stratification/destratification experiments were considered for vehicles with payload capabilities of 350, 765, 1,600 and 3,200 lb. The experimental size envelope was limited on the lower end by the Scout booster and on the upper end by the Agena Clamshell Fairing. Consideration of larger fairings was precluded by their associated weight penalties. As was noted previously in Section 7.2, if the tank size is decreased, the auxiliary propulsion system acceleration level must be increased to maintain the proper scaling relationships.

Since the primary difference between the experimental concepts for the S-IIB and S-IVC experiments and the nuclear stage experiments was the geometry of the lower dome, only the designs for the S-IIB and S-IVC are presented here. The nuclear stage experiment conceptual designs can be considered identical to those presented except the hemispherical lower dome will replace the inverted dome.

For vehicles that are spin-stabilized a despin table is required so that the experimental package can be earth oriented. The spin stabilization limits the value of the boost and orbit injection data acquisition period. The centrifugal forces associated with spinning will most likely alter the convection pattern when compared to the non-spinning vehicle.

For each of the conceptual designs it is recommended that at orbit insertion the experiment be oriented in a manner so that the APS and drag accelerations are in the same direction. Although this will result in orbit degradation by the APS, it will enable the utilization of drag as an additional acceleration level for the stratification and destratification experiments. It is also suggested that the batteries and other equipment be placed at the forward end of the experimental apparatus in order to provide the proper relationship between the center of gravity and center of pressure for the attitude control system stability.

7.3.2 Experiment Configurations and Weights

Three tank configurations were defined for the stratification/destratification experiments; one compatible with the 350-lb payload, one compatible with a 765-lb payload and one compatible with a 1,600-lb payload. A conceptual design for the 3,200-lb Agena payload was not defined since the additional weight available was not required.

Experimental Concept I, Figure 7-5, is a single, superinsulated 18 by 36-in. tank designed for the 350-lb payload. As defined Concept I will consist of a 76-hr experiment having a 50-channel TM system without TV. Table 7-2 shows the weight estimates for this system. These estimates were based on

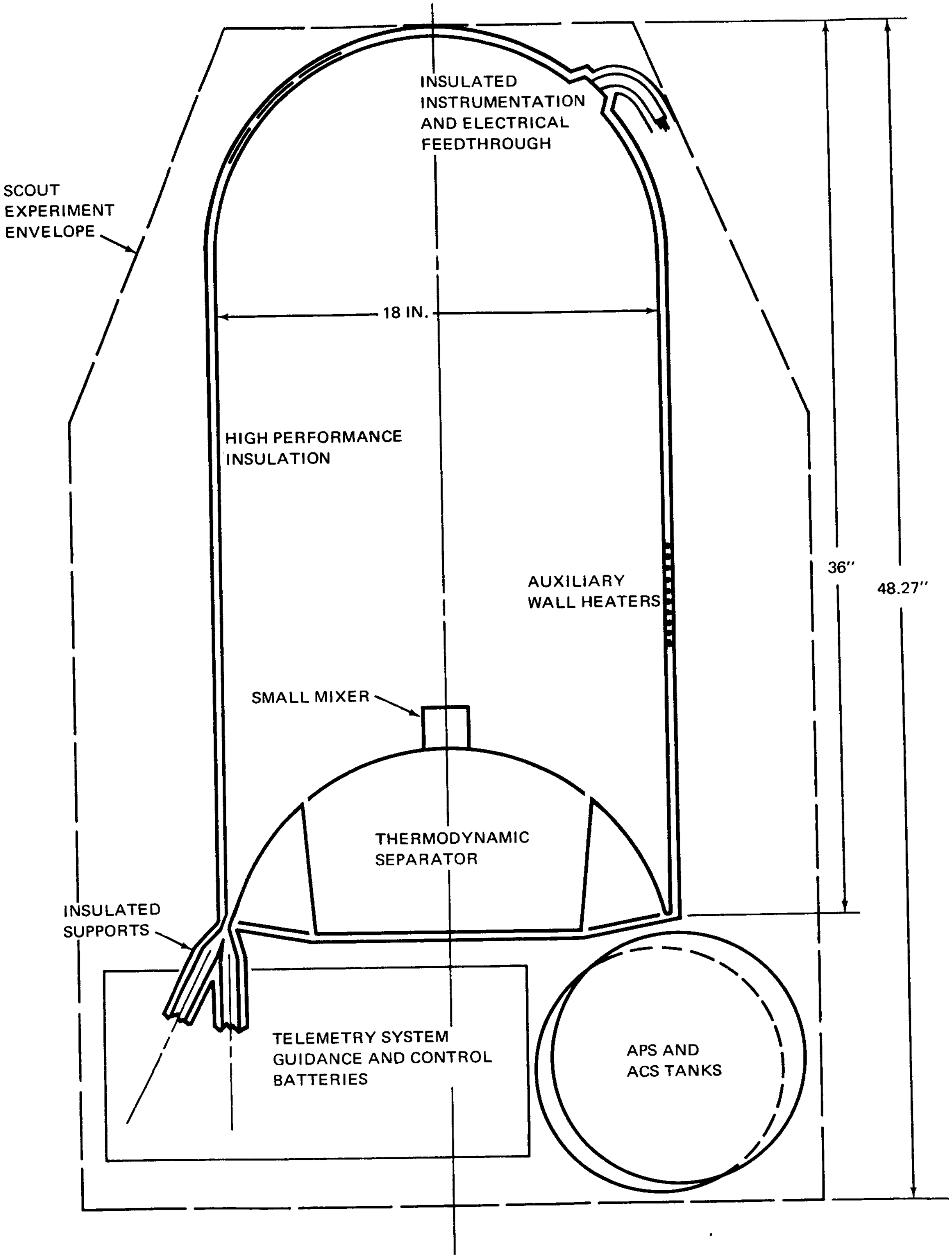

Figure 7-5. Stratification/Destratification Experimental Concept I (350 lb Payload)

Table 7-2

STRATIFICATION/DESTRATIFICATION CONCEPTUAL DESIGN I
(350 pound Payload*)

	Item	Weight (lb)	Power (watts)	Energy (watt-hours)
1.0	Guidance Sensor and Computer	20	30 (76 hours)	2,280
2.0	Sequencer	5	0.45	342
3.0	Antenna	4		
4.0	Beacon	0.5	3.91	296
5.0	TM Command Receiver	3	6.0	420
6.0	Attitude Control System	60		
7.0	TM System (50 channel w/o recorder)	34	95	285
8.0	Transducers	25		
9.0	Auxiliary Propulsion System (10^{-5} g/g_e 38 hours) (10^{-3} g/g_e 50 min)	45		
10.0	Tank (18 in. x 36 in.)**	70		
11.0	Auxiliary Heaters	10	3.2	67.2
12.0	Mixer	3	4.0	16
13.0	Vent System	11	7.0	70
14.0	Power Inverter	3	7.0	70
15.0	Miscellaneous Structure	30		
16.0	Batteries (1-Saturn type)	155		-12,000
	Total	478.5		-8,154

*Total experiment time--76 hours.
**HPI insulated, $\dot{Q} \cong 0.3$ Btu/hr-ft^2.

weight information described in Section 3. Although the total weight is 128.5 lb over the experimental limit this payload was not discarded since the overweight is due to the lack of appropriate batteries. To supply the required power, 3,846 watt-hours, one can either use 10 HR15 batteries weighing 169 lb or 1 Saturn type battery weighing 155 lb. The Saturn battery is capable of delivering an excess of 8,154 watt-hours. Thus, if more efficient batteries than the HR15 batteries can be obtained the total experiment weight may then approach the 350-lb limit and thereby produce an appealing, inexpensive experiment.

The 765-lb payload design, Concept II, is shown in Figure 7-6. This system consists of a 30 by 60-in. superinsulated tank with a 100-channel TM system with a recorder. A recorder was included so that a polar orbit mission, with its fewer tracking stations, could be considered. A single TV camera is included in this experiment. Table 7-3 is the weight statement for this experiment. The weight is within the prescribed limit but the energy required is slightly over that supplied by a single Saturn type battery. The discrepancy is within the limits of this study and does not preclude consideration of this concept for a more refined investigation.

Figure 7-7 is the conceptual design for the 1,600-lb payload. This design consists of a 36 by 72-in. superinsulated tank protected by a thermal shroud. A 150-channel TM system with a recorder and two TV cameras are utilized. The experiment time for this concept is 168 hours. The weight estimate for this system is included in Table 7-4. The total weight and the power consumed are both below those available for the system.

7.3.3 Subsystem Requirements

A number of the subsystems are common to all three experimental concepts. The common subsystems that are not associated with normal housekeeping, guidance and telemetry are:

1. Auxiliary propulsion system.
2. Zero g vent system.
3. Auxiliary heaters on the tank wall.
4. Destratification mixer.

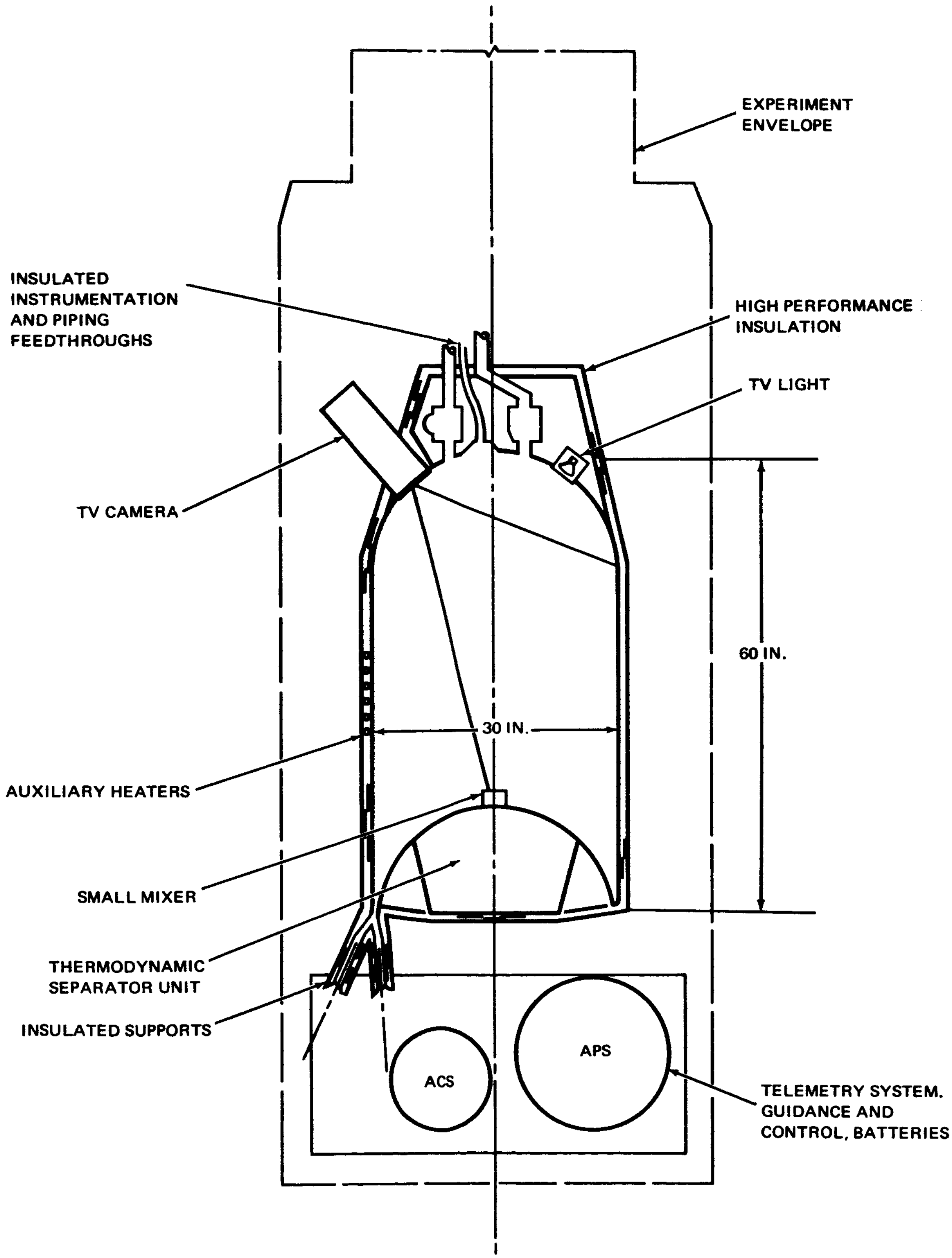

Figure 7-6. Stratification/Destratification Experimental Concept II (765 lb Payload)

Table 7-3

STRATIFICATION/DESTRATIFICATION CONCEPTUAL DESIGN II
(765 pound payload*)

	Item	Weight (lb)	Power (watts)	Energy (watt-hours)
1.0	Guidance Sensor and Computer	20	30	4,800
2.0	Sequencer	10	0.45	75
3.0	Antenna	4		
4.0	Beacon	0.5	3.91	626
5.0	TM Command Receiver	3	6.15	984
6.0	Attitude Control System	130		
7.0	TM System (100 channel with recorder)	73	210 (record) 105 (playback)	3,780 237
8.0	Transducers	47		
9.0	TV Transmitter	18	50	438
10.0	TV Power Amplifier	2	140	1,225
11.0	TV Camera and Control	10	12	105
12.0	TV Light	3.0	100	875
13.0	Auxiliary Propulsion System (10^{-5} g/g_e 45 hours) (10^{-3} g/g_e 30 min)	48		
14.0	Tank (30 in. x 60 in.)**	147		
15.0	Auxiliary Heaters	20	8.8	300
16.0	Mixer	3	4.0	25
17.0	Vent System	11	7	280
18.0	Power Inverter	3	7	280
19.0	Miscellaneous Structure	45		
20.0	Battery (1-Saturn type)	155		-12,000
	Total	749.5		2,030

*Total experiment time--160 hours.

**HPI insulated, $\mathring{q} \cong 0.3$ Btu/hr-ft^2.

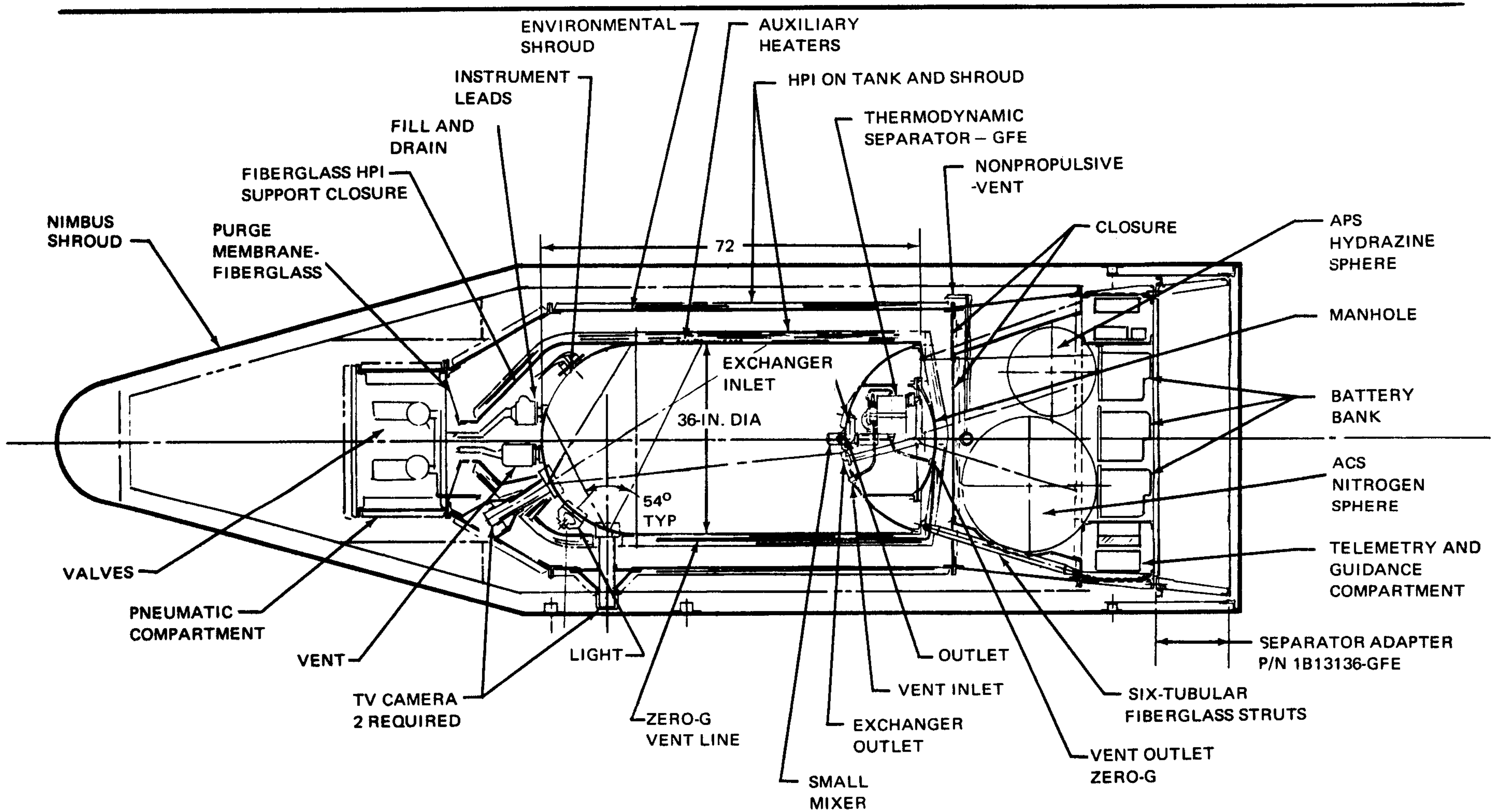

Figure 7-7. Stratification/Destratification Experiment

Table 7-4

STRATIFICATION/DESTRATIFICATION CONCEPTUAL DESIGN III
(1,600 pound payload*)

	Item	Weight (lb)	Power (watts)	Energy (watt-hours)
1.0	Guidance Sensor and Computer	20	30	5,040
2.0	Sequencer	10	0.45	75
3.0	Antenna	4		
4.0	Beacon	0.5	3.91	656
5.0	TM Command Receiver	3	6.15	1,030
6.0	Attitude Control System	190		
7.0	TM System (150 channel with recorder)	103	300 (record) 150 (playback)	15,150
8.0	Transducers	72		
9.0	TV Transmitter	18	50 (15.75)	675
10.0	Power Amplifier	2	140	1,890
11.0	TV Cameras and Controls (2)	20	24	324
12.0	TV Lights (2)	6.0	200	2,700
13.0	TV Multiplexer	6.25	9	122
14.0	Auxiliary Propulsion System (10^{-5} g/g_e 54.5 hours) (10^{-3} g/g_e 170 min)	150		
15.0	Tank Total (36 in. x 72 in.)**	260		
16.0	Auxiliary Heaters	25.0	130 (maximum)	482
17.0	Mixer	3	4	60
18.0	Vent System	11	7	420
19.0	Power Inverter	3	7	420
20.0	Miscellaneous Structure	60		
21.0	Thermal Shroud	75	8	1,344
22.0	Batteries (3-Saturn type)	465		-36,000
	Total	1,498.75		-4,667

*Total experiment time--168 hours.
**HPI insulated $\mathring{q} \cong 0.3$ Btu/hr-ft^2.

The auxiliary propulsion system is required to provide the acceleration level necessary for scaling and to settle the propellant. The APS weight estimates used in generating tables 7-2, 7-3, and 7-4 were based on a monomethyl hydrazine system.

A "zero g" vent system is required to relieve the tank pressure. For the stratification/destratification experiments a bulk heat exchanger, thermodynamic separator corresponding to that used in Project THERMO Phase B was selected. To power the separator, a power inverter will be required to provide a 17-volt, 60-cycle source. Due to the size of the system it is necessary to provide a cylindrical housing beneath the inverted domes so that the stratification/destratification flow patterns will not be altered.

The auxiliary wall heaters are required in order to provide scaling of the modified Rayleigh number. These heaters should be placed uniformly on the exterior of the tankage. These elements can either be resistive elements embedded in rubber and bonded to the tankage or a spray-on resistive element. Both heater types were successfully tested in LH_2 during Project THERMO Phase B.

To provide the necessary mixing a small mixer will be required. The mixer associated with the thermodynamic separator is too large to provide the required mixing rates.

7.4 RECOMMENDED EXPERIMENT DESIGN AND PROCEDURE

7.4.1 Configuration Selection

The 1,600-lb experiment module, Concept III, is recommended as the preferred stratification/destratification experiment design. The selection of this design was made on the basis of technical criteria and applicability of data to vehicle design. The arguments for this concept are presented below.

The 1,600-lb design has as advantages over the 350-lb and 765-lb designs of additional experiment time, an environmental shroud that will enable control and easy definition of the experimental boundary conditions, and additional TV camera that will allow an increased viewing range and depth perception.

Additionally, the larger tank of the 1,600-lb design will provide data that is of more value as design data and will allow easier experiment instrumentation. Recent analytical studies have indicated that scaling for stratification and destratification is inexact. Consequently, in order to obtain the best design data by maintaining close similarity, the experiment module size and the actual vehicle size should be as close as possible. The instrumentation for the experiment should be as small as possible so that it does not interfere with the phenomena under investigation. Due to the relatively large size of qualified temperature probes, it is advisable to select the largest tank in order to prevent experiment contamination by the instrumentation.

7.4.2 Experiment Procedure

The basic experiment procedure for the stratification/destratification experiments consists of monitoring the energy distribution during boost, orbit injection and the insulation transient period, and sequentially performing periods of stratification, stratification reduction, and venting during the steady orbital coast period. Table 7-5 illustrates an experimental sequence that might be selected for stratification/destratification experimentation.

As noted in the results of Project THERMO Phase B, a number of criteria must be considered prior to starting a settled stratification experiment with auxiliary heating. Residual mixing velocities and sloshing of the propellant should be small and the propellant should be free of bubbles entrained during mixing.

Sequencing constraints are imposed by the TV tracking stations. Prior to each experiment, a mass reading should be taken in order to make an energy balance. This can be best accomplished by observing the liquid vapor interface during a high thrust period when the free surface is flat. TV is also required both to determine the shape of the free surface during stratification and to observe when the free surface is disrupted by mixing. For a 200-nmi orbit at a 28.5-degree inclination, stratification experiments can be sequenced to have appropriate TV data acquisition periods with little difficulty. For polar orbit experiments, the TV sequencing appears to be difficult and will present a significant constraint on the experimental procedure.

Table 7-5

TYPICAL STRATIFICATION/DESTRATIFICATION EXPERIMENT LIST (168-HOUR MISSION)

Experiment	Designation	Acceleration Level g/g_e	Sidewall Heating Rate (Btu/hr-ft^2)	Modified Rayleigh Number	Bond No.	Weber No.
Boost and Orbit Injection Energy Distribution	S-1	Variable (-10 to 10^{-5})	Variable (100 to 0.5)	---	0.71	100 50 10
Energy Distribution During HPI Transient Performance Period	S-2	10^{-5} with 10^{-3} settling thrust	0.5 to 0.3	1.7×10^9 and 9.0×10^8	0.71	10 100
Settled Stratification Period at High Heating Rate	S-3	10^{-5}	10.0	2.9×10^{10}	0.71	10
Unsettled Stratification at HPI Heating Rate & 10^{-5} g/g_e	S-4	10^{-5}	0.3	---	0.71	10
Settled Stratification at HPI Heating Rate & 10^{-5} g/g_e	S-5	10^{-5}	0.3	3.9×10^8	0.71	50
Settled Stratification at HPI Heating Rate & Drag Acceleration	S-6	Drag (-10^{-6})	0.3	-3.9×10^6	0.071	50
Unsettled Stratification at HPI Heating Rate & Drag Acceleration	S-7	Drag (-10^{-6})	0.3	---	0.071	100

7.5 EXPERIMENT ANALYSIS

7.5.1 Experimental Time

A number of investigators have attempted experimentally to predict the time it takes to reach the quasi-steady state. Neff (Reference 7-4) has suggested that this time is the same as the time for the stratified layer to reach the container bottom based on the boundary layer model correlations. For laminar flow, this condition is given as

$$FoRa_H^{1/5} = \frac{1.59}{P_r\ 0.812} \qquad \text{where} \qquad F_o = \frac{\alpha t}{HD} \tag{7-5}$$

For turbulent flow, it is

$$FoRa_H^{*\,2/7} = \frac{5.75\left(1 + 0.4\,P_r^{2/3}\right)^{2/7}}{P_r^{1/21}} \tag{7-6}$$

Recent experimental work by Evans, et al. (Reference 7-5), using a wide range of liquid height to tank diameter ratios, indicates that the quasi-steady-state period is achieved when

$$FoRa^{*\,1/5} \cong 4.0 \tag{7-7}$$

for glycerine and glycerine and water solutions, and when

$$FoRa^{*\,1/5} \cong 10 \tag{7-8}$$

for water solutions. These experiments, however, were conducted with subcooled fluids. Results from the pilot test program of Project THERMO Phase B using saturated Freon 113 indicate that the quasi-steady-state period is reached when

$$FoRa_H^{*\,1/5} = 0.2 \text{ to } 1.5 \tag{7-9}$$

and

$$\mathrm{FoRa}_H^{*\,2/7} \cong 1.86 \text{ to } 5.83 \qquad (7\text{-}10)$$

The data points are shown in Figures 7-8 and 7-9.

It is felt that minimum experimental times taken from Equations (7-5) and (7-6) are reasonable in light of both the experimental data and boundary layer model analysis. Of course, the maximum tank pressure must be also considered in determining the maximum experimental time available. To determine the tank pressure rise rate, an energy integral value (I), reference 7-4, for the boundary layer models was taken as 0.2. This value was chosen since it was the lower limit of the experimental values reported by Neff.

7.5.2 Scaling Relationships

A further examination of the scaling parameters (reference 7-1) has shown that the parameters indicated in Project THERMO Phase B were in error. The scaling parameters for a two-phase, single component system without boiling or surface tension gradients are presented below

$$\mathrm{Fo}^* = \frac{\alpha}{\sqrt{L^3 g}} = \text{Modified Fourier Number}$$

$$\mathrm{Ra}_L^* = \frac{g\beta\dot{q}L^4}{k\nu^2} \cdot P_r = \text{Modified Rayleigh Number}$$

$$G = \frac{\beta\alpha^2}{C_p L^2 g} = \text{a Number associated with ullage compressibility}$$

$$\mathrm{Bo} = \frac{\rho g L^2}{\sigma} = \text{Bond Number}$$

$$K = \frac{k_\nu}{k_\ell} = \text{Ratio of the vapor thermal conductivity to liquid thermal conductivity}$$

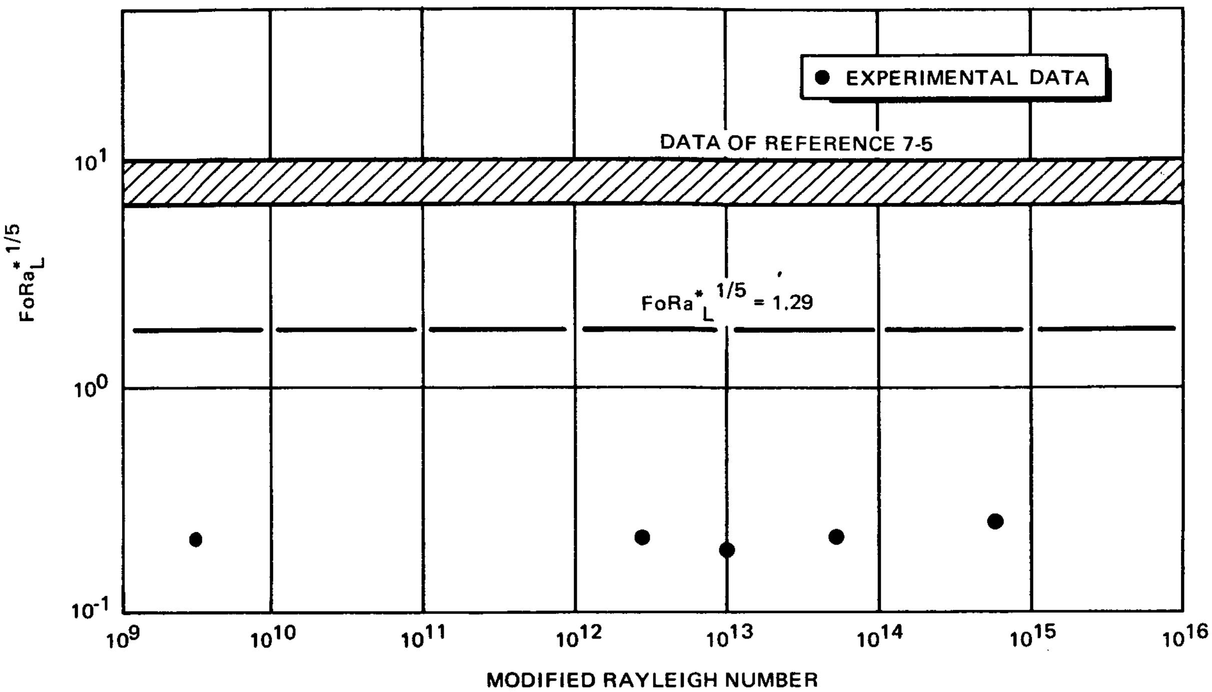

Figure 7-8. Time to Reach Quasi-Steady State (Laminar)

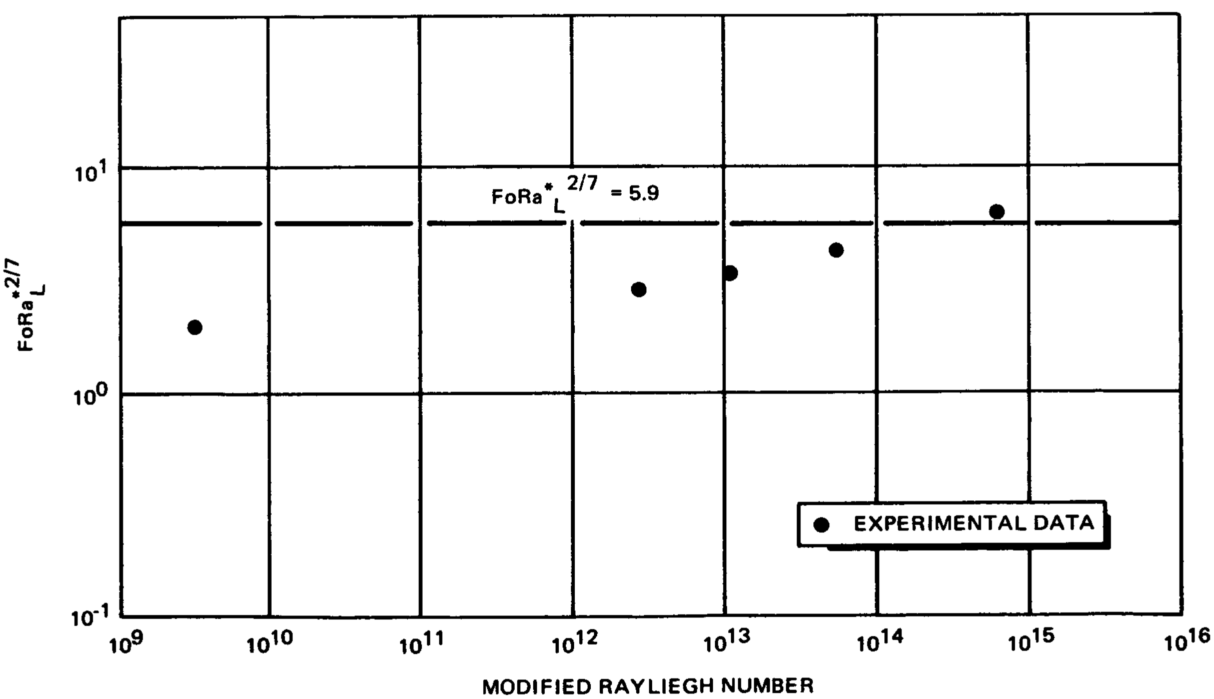

Figure 7-9. Time to Reach Quasi-Steady State (Turbulent)

$$Z = \frac{h_{fg}\ k_\ell}{C_{p\ell}\ qL}$$ Number associated with the Latent Heat at the interface

To scale, the Pr, Fo*, Ra^*_L, and G must be matched for the vapor, the Pr, Fo*, and Ra^*_L must be matched for the liquid and the Bo, K, and Z must be matched across the liquid vapor interface. Boundary conditions are conserved by maintaining geometric similarity between the systems.

7.5.3 Surface Contamination by Instrument Rake

An analysis was performed to define the maximum size permissible for the instrumentation rake so that severe surface distortion does not occur. A worst case condition of zero gravity was examined with the criteria that the meniscus height on the probe should not be greater than 20% of the meniscus height at the walls. A numerical solution of the Young and Laplace equation indicates that to provide this condition the probe diameter to tank diameter ratio should be 0.125 or less.

7.5.4 Error Analysis

The error analysis presented in Project THERMO Phase B was extended to include the destratification scaling correlations. These results along with those previously developed are contained in Table 7-6.

7.6 INSTRUMENTATION LIST

An instrumentation list was prepared for the preferred experiment design, Concept III, and is presented as Table 7-7. Instrumentation is required to determine both the experimental boundary conditions and the experiment parameters. Because of the large sensor size and limitation of the number of sensors available, redundant measurements are taken only for the tank pressure.

A number of channels are required for normal housekeeping duties; 19 channels are allocated for event functions and system monitoring.

Table 7-6

ERROR ANALYSIS UNCERTAINTY PARAMETERS

Parameter	Uncertainty Relationship	Comments
Prandtl number $(\frac{\nu}{\alpha})$	$\frac{\omega}{F} = \left\{\left(\frac{\omega_{11}}{v_{11}}\right)^2\right\}^{1/2}$	Property Dependent only
Fourier number $(\frac{\alpha t}{H^2})$	$\frac{\omega}{F} = \left\{\left(\frac{2\omega_2}{v_2}\right)^2 + \left(\frac{\omega_{11}}{v_{11}}\right)^2\right\}^{1/2}$	
Modified Rayleigh number $(\frac{g\beta \dot{q} H^4}{k\nu^2} \cdot \frac{\nu}{\alpha})$	$\frac{\omega}{F} = \left\{\left(\frac{\omega_1}{v_1}\right)^2 + \left(\frac{4\omega_2}{v_2}\right)^2 + \left(\frac{\omega_3}{v_3}\right)^2 + \left(\frac{\omega_8}{v_8}\right)^2 + \left(\frac{\omega_{11}}{v_{11}}\right)^2\right\}^{1/2}$	
Bond number $(\frac{\rho g R^2}{\sigma})$	$\frac{\omega}{F} = \left\{\left(\frac{\omega_3}{v_3}\right) + \left(\frac{\omega_{12}}{v_{12}}\right)^2\right\}^{1/2}$	
Total heat input $\left(\pi R^2 m C p \int_0^H \frac{T(x_1, t) - T(x_1, o)}{H} dx\right)$	$\frac{\omega}{F} = \left\{\left(\frac{\omega_2}{v_2}\right)^2 + \left(\frac{\omega_9}{v_9}\right)^2 + \left(\frac{\omega_{10}}{v_{10}}\right)^2 + E^2\right\}^{1/2}$	E is error associated with changing from an integral to a difference summation.
Laminar stratified layer depth $\left(1 - \frac{\Delta(t)}{H} = \left[1 - 0.63 \frac{\nu t}{HR} \frac{Gr_H^{*\,1/5}}{Pr^{0.388}}\right]^5\right)$	$\frac{\omega}{F} = v_1^{1/5} v_2^{-1/5} v_3^{1/5} v_4 \left[1 - v_1^{1/5} v_2^{-1/5} v_3^{1/5} v_4\right]^{-1} \left\{\left(\frac{\omega_1}{v_1}\right)^2 + \left(\frac{\omega_2}{v_2}\right)^2 + \left(\frac{\omega_3}{v_3}\right)^2 + \left(\frac{5\omega_4}{v_4}\right)^2\right\}^{1/2}$	$0 \le v_1^{1/5} v_2^{-1/5} v_3^{1/5} v_4 \le 1.0$
Turbulent stratified layer depth $\left(1 - \frac{\Delta(t)}{H} = \left[1 - 0.924 \frac{\nu t}{HR} Pr^{-2/3} \left(\frac{Gr_H^*}{1 + 0.433 Pr^{2/3}}\right)^{2/7}\right]^{7}\right)$	$\frac{\omega}{F} = v_1^{2/7} v_2^{1/7} v_3^{2/7} v_5 \left[1 - v_1^{2/7} v_2^{1/7} v_3^{2/7} v_5\right] \left\{\left(\frac{2\omega_1}{v_1}\right)^2 + \left(\frac{\omega_2}{v_2}\right)^2 + \left(\frac{2\omega_3}{v_3}\right)^2 + \left(\frac{7\omega_5}{v_5}\right)^2\right\}^{1/2}$	$0 \le v_1^{2/7} v_2^{1/7} v_3^{2/7} v_5 \le 1.0$
Laminar time for stratified layer to reach bottom $\left(t = 1.59 \frac{HR}{\nu} \frac{Pr^{0.388}}{Gr_H^{*}} v_5\right)$	$\frac{\omega}{F} = \left\{\left(\frac{\omega_1}{5v_1}\right)^2 + \left(\frac{\omega_2}{5v_2}\right)^2 + \left(\frac{\omega_3}{5v_3}\right)^2 + \left(\frac{\omega_6}{v_6}\right)^2\right\}^{1/2}$	
Turbulent time for stratified layer to reach bottom $\left(t = 5.75 \frac{HR}{\nu} Pr^{2/3} \left(\frac{1 + 0.443 Pr^{2/3}}{Gr_H^*}\right)^{2/7}\right)$	$\frac{\omega}{F} = \left\{\left(\frac{2\omega_1}{7v_1}\right)^2 + \left(\frac{\omega_2}{7v_2}\right)^2 + \left(\frac{2\omega_3}{v_3}\right)^2 + \left(\frac{\omega_7}{v_7}\right)^2\right\}^{1/2}$	
Residual stratification parameter $\lambda = (\frac{Q}{\Delta T C p \dot{m}})$	$\frac{\omega}{F} = \left\{\left(\frac{\omega_2}{v_2}\right)^2 + \left(\frac{\omega_9}{v_9}\right)^2 + 2\left(\frac{\omega_{10}}{v_{10}}\right)^2 + \left(\frac{\omega_{13}}{v_{13}}\right)^2 + E^2\right\}^{1/2}$	For conditions without auxiliary tank heaters
	$\frac{\omega}{F} = \left\{\left(\frac{\omega_1}{v_1}\right)^2 + \left(\frac{\omega_9}{v_9}\right)^2 + \left(\frac{\omega_{13}}{v_{13}}\right)^2\right\}^{1/2}$	For conditions with auxiliary heating
Critical Weber number $(\frac{\rho U_j D_j}{\sigma})$	$\frac{\omega}{F} = \left\{\left(\frac{\omega_{12}}{v_{12}}\right)^2 + \left(\frac{\omega_{14}}{v_{14}}\right)^2\right\}^{1/2}$	

Nomenclature:

- F = parameter under investigation
- ω = error in parameter
- ω_i = error in respective variables
- v_1 = $\dot{q}$
- v_2 = H
- v_3 = g
- v_4 = $0.630 \frac{\nu t}{R} P_r^{-0.388} (\beta / k\nu^2)^{1/5}$
- v_5 = $0.924 \frac{\nu t}{R} P_r^{-2/3} \left(\beta / k\nu^2 (1 + 0.443 P_r^{2/3})\right)^{2/7}$
- v_6 = $1.59 P_r^{0.388} \frac{R}{\nu} (\beta / k\nu)^{1/5}$
- v_7 = $5.75 P_r^{2/3} R (\beta / k\nu)^{2/7} (1 + 0.443 Pr)^{2/3}$
- v_8 = $\beta / k\nu^2$
- v_9 = m
- v_{10} = $\left|T(x, t) - T(x, o)\right|$
- v_{11} = ν / α
- v_{12} = $\rho R^2 / \sigma$
- v_{13} = $\dot{m}$
- v_{14} = $U_j D_j$
- E = Error in changing from integral to summation

Table 7-7

STRATIFICATION/DESTRATIFICATION INSTRUMENT LIST (page 1 of 4)

Measurement Title	No. Req'd	System Range/Accuracy	Frequency Response	Transducer Environment	
				Media	Temperature
Voltage, Battery	1	0-28 ± 0.84 Vdc (±3%)	1 cps		
Current, Heater					
(Tank Wall)	8		1 cps		
(Shroud)	1		1 cps		
Current, Separator	1		1 cps		
Current, Light	1		1 cps		
Events	45	TBD	TBD		
TV Camera On	(3/channel)				
TV Lights On					
NPV Open T/B					
NPV Closed T/B					
NPV Open CMD					
NPV Closed CMD					
Pressure Switch 1 P/4					
Pressure Switch 2 P/4					
Pressure Switch 3 P/4					
Thermodynamic/Separation Vent 1 On					
Thermodynamic/Separation Vent 2 On					
Thermodynamic/Separation Mixer On					
Attitude Continued CMD	6				
Ullage Settling CMD	1				
Ullage Continued CMD	3				
Switching Amplifier Outputs	6				
Programmer Sequence Output	7				
Programmer Countdown Output	3				
Attitude Positions	3	TBD			

Table 7-7 (page 2 of 4)

Measurements Title	No. Req'd	System Range/Accuracy	Frequency Response	Transducer Environment	
				Media	Temperature
Pressure LH_2 Tank Ullage	2	0-50 ± 1.5 psia (±3%)	1 cps	GH_2, LH_2	400 to 620° R(1)
Pressure ACS GN_2 Sphere	1	0-3500 ± 105 psia (±3%)	1 cps	GN_2	400 to 620° R
Pressure ACS Regulator Outlet	1	0-25 ± 0.75 psia (±3%)	1 cps	GN_2	400 to 620° R
Pressure Ullaging P_c	1	0-50 ± 1.5 psia (±3%)	1 cps	N_2H_4	400 to 1,950° R(2)
Pressure N_2H_4 Storage TK	1	0-300 ± 9 psia (±3%)	1 cps	N_2H_4	400 to 620° R
Pressure T.D. Separation Vent	1	0-50 ± 1.5 psia (±3%)	1 cps	GH_2, LH_2	400 to 620° R(2)
Pressure T.D. Separation 1	2	0-25 ± 0.75 psia (±3%)	1 cps	GH_2, LH_2	400 to 620° R(2)
Pressure T.D. Separation 2	1	0-10 ± 0.3 psia (±3%)	1 cps	GH_2, LH_2	400 to 620° R(2)
Pressure T.D. Separation Diff 1	1	±1 psia	1 cps	GH_2, LH_2	400 to 620° R(2)
Pressure T.D. Separation Diff 2	1	±20 psia	1 cps	GH_2, LH_2	400 to 620° R(2)
Pressure, NPV	1	0-50 ± 1.5 psia (±3%)	1 cps	GH_2, LH_2	400 to 620° R(2)
Pressure, Shroud	1	1 mm H_2 - 1 atm (±3%)	1 cps		
Pressure, Shroud	1	10^{-3} mm H_g - 1 mm H_g (±3%)	1 cps		
Pressure HPI	1	1 mm Hg - 1 atm (±3%)	1 cps	He	200 to 620° R
Pressure HPI	12	1 mm Hg - 1 atm (±3%)	1 cps	Air	400 to 620° R
Pressure HPI	1	0-1 mm Hg (±3%)	1 cps	He	200 to 620° R
Pressure HPI	12	0-1 mm Hg (±3%)	1 cps	Air	400 to 620° R

Note:

(1) Sensing line must isolate transducer to provide -60 to +165° F environment

Table 7-7 (page 3 of 4)

Measurement Title	No. Req'd	System Range/Accuracy	Frequency Response	Transducer Environment: Media	Transducer Environment: Temperature
Level, Liquid/Vapor Point					
Loading (GSE)	3			GH_2, LH_2 at 1 x 10^{-5}g	37 to 620° R
T/D Separation	3				
Temperature LH_2 Tank Liquid	19	35-47 ± 0.45° R (±3%)	1 cps	GH_2, LH_2	35 to 620° R
Temperature LH_2 Tank Liquid (VLR)	2	36-40 ± 0.12° R (±3%)	1 cps	GH_2, LH_2	35 to 620°R
Temperature LH_2 Tank Liquid (VLR)	2	40-46 ± 0.18° R (±3%)	1 cps	GH_2, LH_2	35 to 620°R
Temperature LH_2 Tank Ullage Gas	9	35-300 ± 8° R (±3%)	1 cps	GH_2, LH_2	35 to 620°R
Temperature LH_2 Tank Surface	22	35-47 ± 0.45° R (±3%)	1 cps	GH_2, LH_2	35 to 620°R
Temperature LH_2 Tank Surface	10	35-300 ± 8° R (±3%)	1 cps	GH_2, LH_2	35 to 620°R
Temperature, Camera Window Surface	4	115-450 ± 10° R (±3%)	1 cps	GH_2, LH_2	35 to 620°R
Temperature HPI Inner Surface	2	35-100 ± 2° R (±3%)	1 cps	GHe, Vacuum	35 to 620°R
ΔT Struts Surface	6	33 ± 1° R (±3%)	1 cps	GHe, Vacuum	35 to 620°R
Temperature Shroud Surface	1	400-600 ± 6° R (±3%)	1 cps	GHe; Vacuum	400 to 620° R
Temperature HPI Outside Surface	7	400-600 ± 6° R (±3%)	1 cps	GHe; Vacuum	400 to 620° R
Temperature HPI in Layers Surface	2	60-260 ± 6° R (±3%)	1 cps	GHe; Vacuum	60 to 620° R
	2	200-400 ± 6° R (±3%)	1 cps	GHe; Vacuum	200 to 620° R
	2	330-530 ± 6° R (±3%)	1 cps	GHe; Vacuum	330 to 620° R
ΔT Heat Shorts Surface	8	33 ± 1° R (±3%)	1 cps	GHe; Vacuum	400 to 620° R
Temperature NPV Vent Gas	1	25-125 ± 3° R (±3%)	1 cps	GH_2, LH_2	25 to 620° R
Temperature Thermodynamic/ Separator	1	40-100 ± 1.8° R (±3%)		GH_2, LH_2 at 1 x 10^{-5}g	25 to 620° R

Table 7-7 (page 4 of 4)

Measurement Title	No. Req'd	System Range/Accuracy	Frequency Response	Transducer Environment: Media	Transducer Environment: Temperature
Temperature Thermodynamic/ Separator	1	28-46 ± 0.54° R (±3%)		GH_2, LH_2 at 1 x 10^{-5}g	25 to 620° R
Temperature Thermodynamic/ Separator	1	28-40 ± 0.36° R (±3%)		GH_2, LH_2 at 1 x 10^{-5}g	25 to 620° R
Temperature, Thermodynamic/ Separator Vent	1	25-125 ± 3° R (±3%)		GHe and Vacuum	35 to 620° R
Temperature Pipe Support Bracket	1	115-450 ± 10° R (±3%)		GH_2, LH_2	25 to 620° R

Temperature and pressure sensors have been allocated to determine the insulation performance, the heat transfer through the heat shorts, the energy supplied by the heaters, and the performance of the thermodynamic separator. This instrumentation is required to properly define the tank boundary conditions and 63 channels have been utilized for this function.

The remaining 78 channels are utilized to define the thermal energy distribution in the propellant and the tank wall temperatures. Liquid sensors can be positioned to provide both axial and radial temperature profiles within the liquid and the ullage. Four low-range sensors are included to provide in-flight correction of temperature data. Surface patches on the tank surface can be utilized to determine the wall thermal map. The temperature distribution in an axial direction along the wall, circumferentially around the wall, and at each heat short will be measured.

Section 8
BOILOVER/ENTRAINMENT

8.1 ORBITAL EXPERIMENTATION INFORMATION REQUIREMENTS

Low-g venting of nearly full propellant tanks has been identified as a required operation for interplanetary vehicles (Section 2). Cyclic direct venting is one technique being considered. Associated with direct venting are the problems of liquid loss by excessive level rise (boilover), and entrainment of liquid in the vented vapor. There are presently no satisfactory techniques available for predicting liquid level rise and entrainment under conditions of reduced gravity. A strictly analytical approach to the problem would be quite formidable. Correlation of data by the method of dimensionless parameters appears promising. Orbital experimentation is necessary to evaluate the coefficients of such correlations.

In the following sections an experiment is proposed to establish design criteria for cyclic direct venting. Correlation techniques are derived to correlate the liquid level rise and entrainment in terms of tank configuration, parameters of operation, and fluid properties. An orbital experiment is outlined to evaluate the experimental constants of the correlations. In the orbital experiment the liquid level rise and entrainment will be measured during cyclic direct venting of a LH_2 tank at a number of conditions of operation applicable to future space vehicles. Television coverage is provided to observe the nature of the process.

8.2 DATA ACQUISITION AND EXPERIMENT REQUIREMENTS

Cyclic direct venting is accomplished in the following manner:

> Prior to opening the vent valve, a thrust is applied with the A. P. S. engines to settle the propellant at the end of the tank opposite the vent. Once venting is initiated, thrust from the vented vapor is used to keep the liquid settled. Consider the tank of saturated propellant shown in

Figure 8-1(a). Prior to venting, the liquid level is h_{LO} and the ullage height is H_{VO}. When the vent is opened, boiling is initiated by the pressure decrease. The presence of the bubbles rising in the liquid causes the level to rise as shown in Figure 8-1(b). Interface disturbances caused by rising bubbles eject droplets into the ullage space, some of which are entrained by the vented vapor and carried out of the vent. If the level rises sufficiently, severe propellant loss can result by splashing or actual boilover of liquid out the vent. Both the level rise and entrainment become more severe with reductions in the gravity level and ullage height.

8.2.1 Analytical Methods

A purely analytical study of the boilover and entrainment problem is quite complicated because it involves integrating into a single description the effects of bubble formation, growth, and rise, and droplet formation and entrainment. Each of these basic mechanisms by itself constitutes a rather

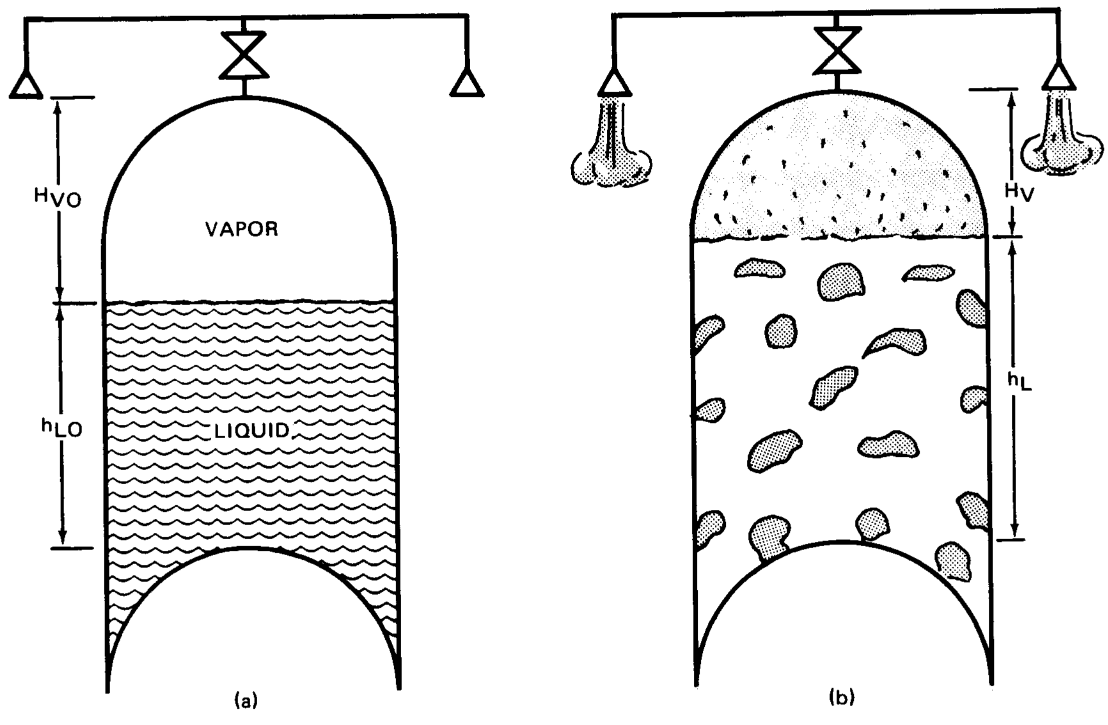

Figure 8-1. Level Rise and Entrainment in a Vented Tank

complicated problem and continues to be a subject of investigation. Formulation of analytical models for boilover and entrainment is complicated by the possibility for each of the basic mechanisms to occur in several ways depending upon the operating conditions. Bubbles can nucleate and grow either on the walls of the container or within the liquid bulk. The degree of bubble coalescence and breakup influences the velocity of rise of the bubbles by affecting the bubble size. The degree of induced liquid motion also affects the bubble velocity enabling larger bubbles to sweep smaller bubbles from the liquid that would otherwise be removed very slowly. Entrained liquid droplets can be formed in three different ways: from breakup of the shell of bursting bubbles, from breakup of the jet formed in the crater of bursting bubbles, and from splashing. The drag coefficient both for bubbles and liquid droplets varies according to considerably different laws for different regions of operation.

In order to formulate a successful analytical model of boilover and entrainment, the correct mode must be known for each of the basic mechanisms for the region of operation being considered, and the appropriate laws describing the mechanism must be introduced into the analytical description. A change in the mode of a mechanism constitutes a change in the flow regime of the boilover and entrainment process. The behavior of the process can change drastically with a change in the flow regime. Furthermore, results in the form of dimensionless correlations obtained at one condition of operation cannot be extrapolated to another condition unless the flow regime is the same for both conditions. For normal gravity, three flow regimes have been observed with liquid entrainment and two with liquid level rise. It is quite possible that gravity reductions cause the existence of additional flow regimes. It is very important, therefore, that data and observation of the boilover and entrainment process be obtained under the actual conditions of operation. Once the flow regime has been established it may be possible to obtain data from tests at normal gravity.

8.2.1.1 Proposed Correlation for Liquid Level Rise

Several equations have been proposed for correlating data on the level rise of a bubbly mixture at normal gravity where the bubbles are introduced from the bottom of the container (8-1). The most promising of these was derived by

Sterman (8-2) by applying the theory of similarity to the equations describing a two-phase flow. Although the equation was not derived with gravitational variations in mind, gravitational effects were accounted for in the derivation. The vapor fraction α is determined by a power law relation of three dimensionless groups, namely

$$\alpha = \frac{A_v}{A_v + A_l} = a\left[\frac{u_o^2}{g\left(\frac{g_e\sigma}{g(\rho_l - \rho_v)}\right)^{0.5}}\right]^b \left[\frac{\left(\frac{g_e\sigma}{g(\rho_l - \rho_v)}\right)^{0.5}}{D}\right]^c \left[\frac{\rho_v}{\rho_l - \rho_v}\right]^d \tag{8-1}$$

where A_l and A_v denote the cross sectional area occupied by liquid and vapor, respectively, u_o denotes the effective vapor velocity, which is equal to the volume flow rate of vapor divided by the cross sectional area of the container, g denotes the gravity level, g_e the standard gravitational constant, σ the surface tension, ρ_l and ρ_v the densities of the liquid and vapor, D the diameter of the container, and a, b, c, and d are experimentally determined parameters which have the values 1.07, 0.4, 0.25, and 0.17, respectively, for water-steam mixtures.

For sufficiently large diameters the level rise appears to be independent of the tank diameter. For water-steam mixtures with diameters larger than those determined according to the following equation, the second term in Equation (8-1), which accounts for the diameter effect, can be eliminated:

$$D = 260\left(\frac{\rho_v}{\rho_l - \rho_v}\right)^{0.2}\left(\frac{g_e\sigma}{g(\rho_l - \rho_v)}\right)^{0.5} \tag{8-2}$$

The vapor velocity u in the ullage space of a cylindrical container of fully saturated liquid being vented at a depressurization rate dp/dt can be determined by the following expression:

$$u = \frac{\rho_l c_s}{\rho_v h_{fg}} \left.\frac{dT}{dp}\right|_s h_{LO}\frac{dp}{dt} \tag{8-3}$$

where c_s is the specific heat under saturation conditions, h_{fg} the latent heat of vaporization, $dT/dp|_s$ the slope of the vapor pressure curve, h_{LO} the initial liquid level, and all other terms have been defined previously.

In the situation where a tank is being vented, u_o varies with the depth in the tank. If uniform vapor generation per unit volume and a constant bubble velocity are assumed in the liquid, it can be shown that the average effective vapor velocity in the liquid $\bar{u}_o$ is determined according to the following expression

$$\bar{u}_o = u/2 \tag{8-4}$$

It seems reasonable that Equation (8-1) will be applicable to venting of a saturated liquid if $\bar{u}_o$ is substituted into Equation (8-1) for u_o.

8.2.1.2 Proposed Correlation for Entrainment

As with liquid level rise, there have been several equations proposed for correlating data on liquid entrainment for a bubbly mixture at normal gravity where the bubbles are introduced from the bottom of the container (8-1). The most complete of these has been proposed by Sterman (8-3), and applies for intermediate flow rates of vapor where the droplets are formed by breakup of the jet formed in the crater of bursting bubbles. This equation was derived by an intuitive argument involving the theory of similarity and the equations of motion for a two-phase flow. The entrainment E is described by the following power law:

$$E = \frac{\dot{m}_e}{m_v} = i\left[\frac{u_o^{\,2}}{\alpha g H_v}\right]^j \left[\frac{g\left(\frac{g_e \sigma}{g(\rho_1 - \rho_v)}\right)^{1.5}}{v_1^{\,2}}\right]^k \left[\frac{\rho_v}{\rho_1 - \rho_v}\right]^1 \tag{8-5}$$

where $\dot{m}_e$ denotes the mass flow rate of entrained liquid, $\dot{m}_v$ the mass flow rate of vapor, H_v the ullage height, v_1 the kinematic viscosity, and i, j, k, and 1 are experimentally determined constants which have the values 2.75×10^8, 2.3, -1.1, and -0.25, respectively, for water-stream mixtures. The existing data indicates that for low vapor flow rates, E is directly proportional to u_o and for large vapor flow rates, E is proportional to $u_o^{\,7}$ to $u_o^{\,20}$. For these situations, values of j of 0.5 to 10.0 would be indicated.

Equation (8-5) was not derived with gravitational variations in mind, but gravitation effects were accounted for. It seems reasonable, then, that if the value of u_o is determined according to Equation (8-3), Equation (8-5) should be applicable to venting of propellant tanks.

8.2.1.3 Similarity Requirements

When propulsive venting is employed, a definite relation exists between the depressurization rate, the acceleration level, and the characteristics of the vehicle. It can be shown that for a tank of fully saturated propellant, these parameters are related by the following expression:

$$\frac{g}{g_e} = \frac{M_F}{M_s} \frac{c_s}{h_{fg}} \left.\frac{dT}{dp}\right|_s I_{sp} \frac{dp}{dt} \tag{8-6}$$

where g/g_e denotes the ratio of the settling acceleration to the standard gravitational constant, M_F the mass of propellant being in the tank vented, M_s the mass of the vehicle including propellant, I_{sp} the specific impulse for the propulsive vent nozzles, and other quantities have been defined previously.

For a cylindrical tank, this equation can be rearranged into the following form:

$$\frac{g}{g_e} = \frac{A_T}{M_s} \frac{\rho_l c_s}{h_{fg}} \left.\frac{dT}{dp}\right|_s I_{sp}\, h_{LO} \frac{dp}{dt} \tag{8-7}$$

where A_T denotes the cross-sectional area of the tank, and h_{LO} denotes the liquid height.

The similarity requirements for applying data on boilover and entrainment to different vehicle configurations can be obtained by examining Equations (8-1) through (8-7). Similarity requirements must be satisfied both for vehicle dynamics and internal fluid dynamics. For similarity between two systems containing fully saturated propellant at the same temperature and pressure and considering the influence of tank diameter to be small, it can be seen from Equations (8-1) and (8-5) that u_o, g, and H_v must be equal in both systems. Examination of Equation (8-3) shows that this requirement is identical to equivalence of $h_{LO}\frac{dp}{dt}$, g, and H_v between the systems.

Examination of Equation (8-7) indicates that equivalence of g between systems for a given $h_{LO} \frac{dp}{dt}$ prescribes equivalence of A_T/M_S. Thus, for similarity between two tanks being vented propulsively, the parameters $h_{LO} \frac{dp}{dt}$, A_T/M_S, and H_v must be equal in both systems.

8.2.2 Applicability to Future Missions

Data is necessary to evaluate the constants of the above correlation equations. It is necessary that at least some data be obtained under space vehicle operating conditions to establish the validity of the correlations. Therefore, it is necessary to establish the range of values the parameters in the correlation equations will have for future vehicle applications.

Pertinent characteristics of three potential stages for future missions are listed in Table 8-1. These values correspond to fully loaded stages except for the S-IIB where three LOX transfers are required in orbit. The symbols employed in Table 8-1 were defined previously in Section 8.2.1.3. The stages listed in Table 8-1 are designed to operate with tank pressure in the range 15 psia to 50 psia. Their mission characteristics require relatively rapid vent sequences. Therefore, a range of depressurization rates of 0.5 psi/min to 5.0 psi/min can be considered applicable for potential missions of these vehicles. The lower limit corresponds to a time of 70 min. to vent a tank between 50 psia and 15 psia. The upper limit is arbitrarily selected as a limit where level rise and entrainment might become serious. The range of settling accelerations that will be encountered employing propulsive venting with the vehicles listed in Table 8-1 for the range of tank pressures and depressurization rates considered applicable are shown in Figure 8-2. These values were calculated employing Equation (8-6) utilizing a value of 60 sec for I_{SP}. The lower limit corresponds to the S-IVC with a depressurization rate of 0.5 psi/min and the upper limit corresponds to the nuclear stage with a depressurization rate of 5.0 psi/min. Applications for the S-IIB fall between these limits. Likewise, the range of effective vapor velocities of interest are presented in Figure 8-3. These velocities were calculated employing Equation (8-3).

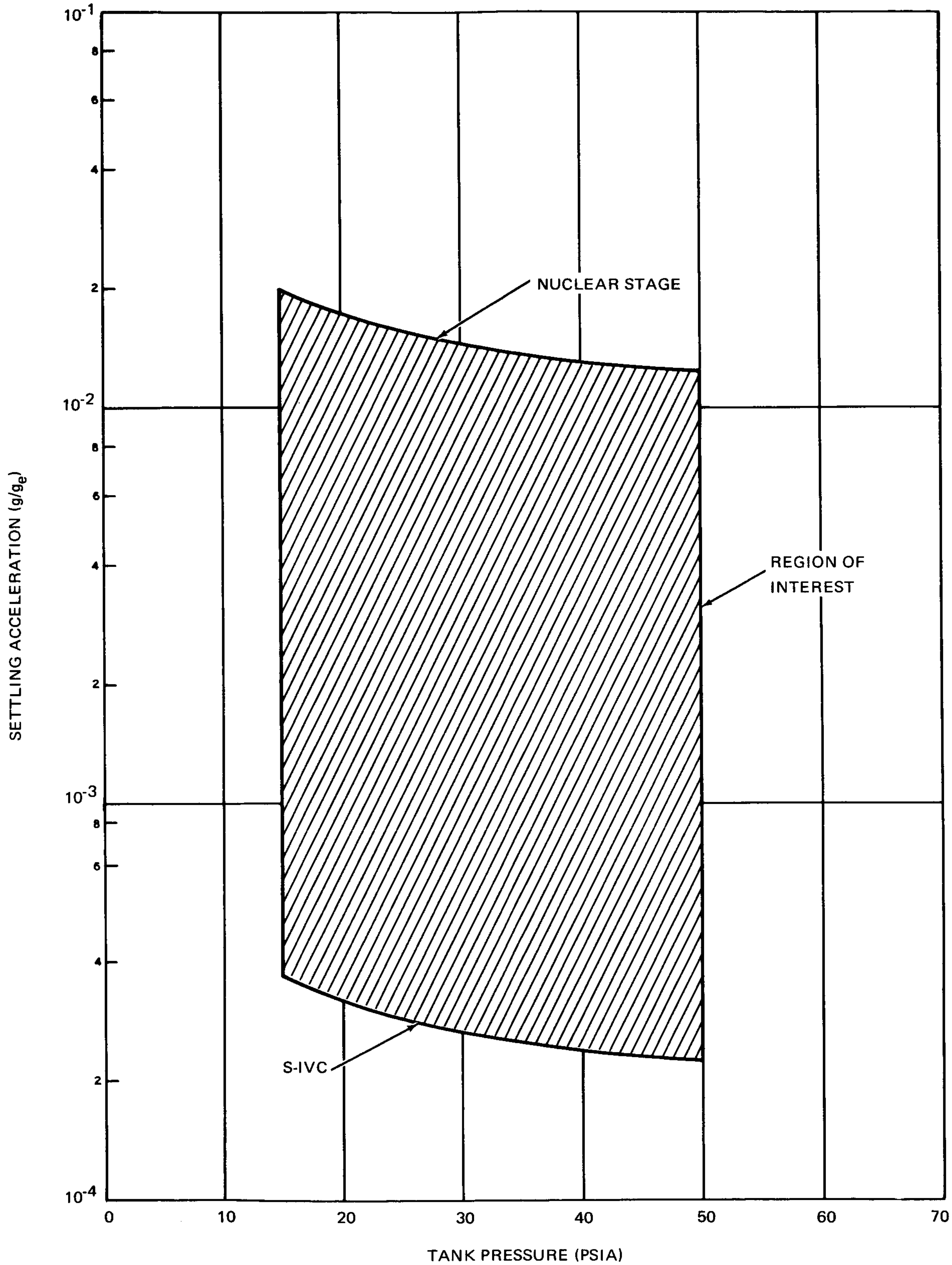

Figure 8-2. Range of Accelerations of Interest

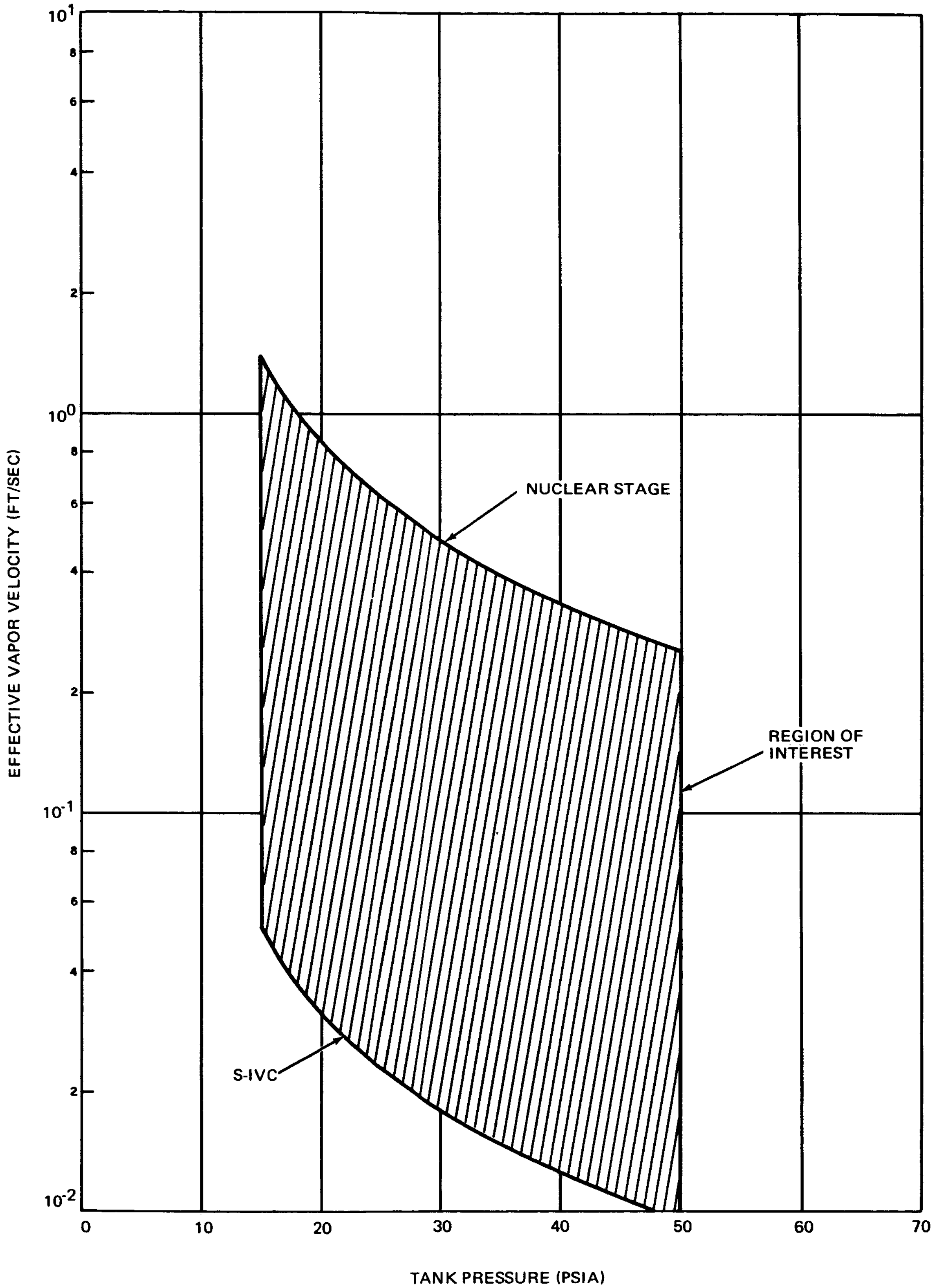

Figure 8-3. Range of Effective Vapor Velocities of Interest

Table 8-1

CHARACTERISTICS OF POTENTIAL FUTURE SPACE VEHICLES

Vehicle	M_F/M_s	$A_T(ft^2)$	$h_{LO}(ft)$	$A_T/M_s(ft^2/lb)$
Nuclear Stage	0.804	855	66.4	2.75×10^{-3}
S-IVC	0.148	368	24.7	1.36×10^{-3}
S-IIB (NO LOX)	0.638	855	39.9	3.64×10^{-3}
(1 LOX TRANS)	0.345	855	39.9	1.97×10^{-3}
(2 LOX TRANS)	0.236	855	39.9	1.35×10^{-3}
(3 LOX TRANS)	0.180	855	39.9	1.02×10^{-3}

Examination of Equations (8-1) and (8-5) reveals that for a given gravity level the effective vapor velocity u_o exerts the predominant influence on level rise and entrainment. Both level rise and entrainment increases as u_o is increased. Examination of Equation (8-3) reveals that u_o is influenced by the depressurization rate and the pressure level. The value of u_o increases as the depressurization rate is increased and as the operating pressure is decreased. Thus, level rise and entrainment will increase as the depressurization rate is increased or the pressure level is decreased. Likewise, as can be seen from Equations (8-1) and (8-5), level rise and entrainment increase as the gravity level is decreased.

8.3 EXPERIMENT CONCEPTUAL DESIGN

8.3.1 Experimental Module

Only one basic module concept is necessary to obtain the information required by orbital testing. A schematic representation of this concept is presented in Figure 8-4.

Subsystem requirements for the module; e.g., A.P.S. and A.C.S. systems, guidance, and electronic equipment, are essentially the same as for the boiling heat transfer module. Therefore, the integration of the tank for the boilover experiment into the carrier is essentially the same as that presented in Figure 10-9 for the boiling heat transfer experiment.

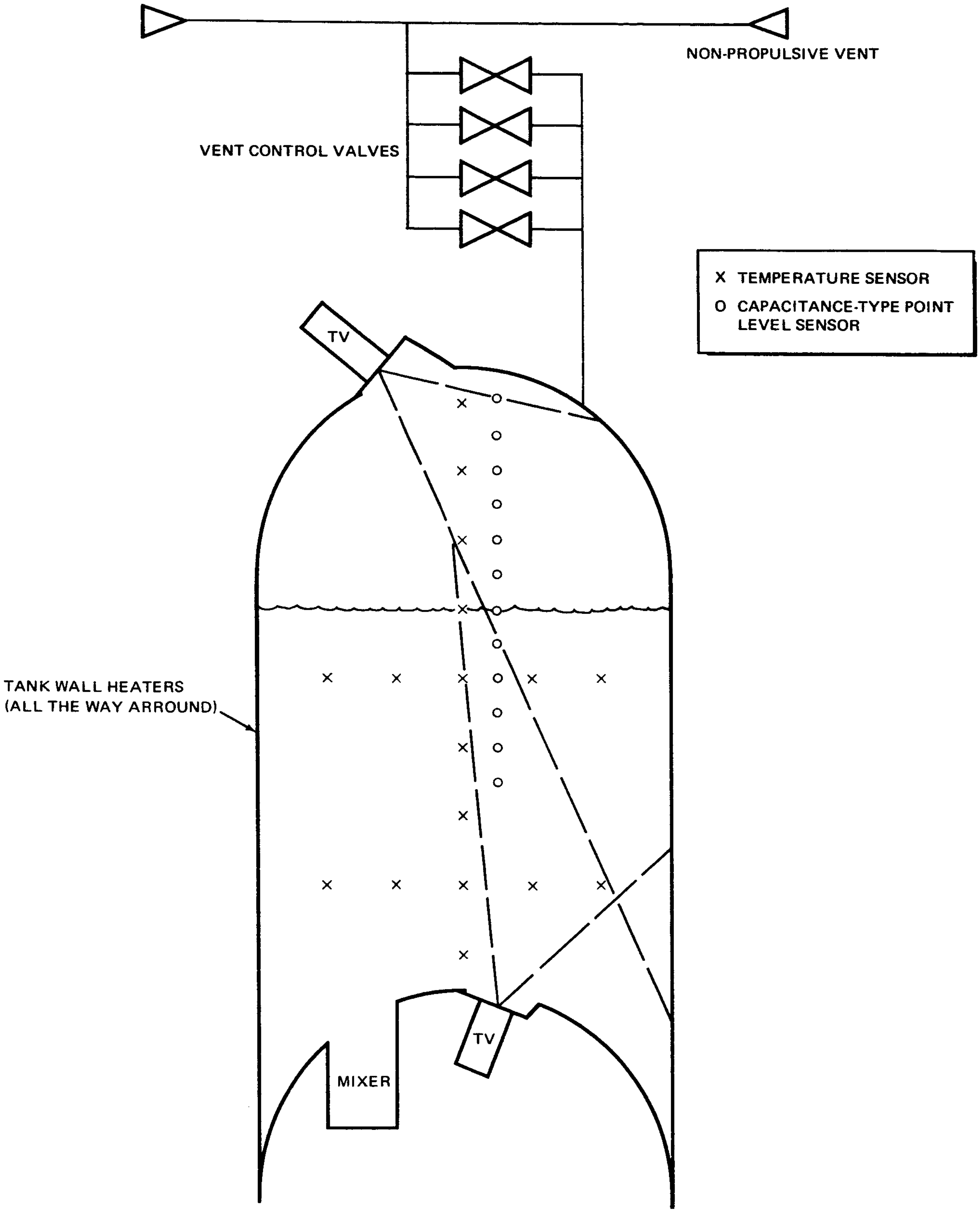

Figure 8-4. Schematic of Tank Configuration for the Boilover and Entrainment Experiment

A number of vent control systems are installed in parallel on the module to facilitate venting at prescribed depressurization rates (Figure 8-4). An orifice in series with an "on-off" valve is considered sufficient for flow control. Venting is performed nonpropulsively, with the settling acceleration being furnished by the A. P. S. engines. This method is preferable to propulsive venting for the tests to facilitate variation of the settling acceleration as an independent parameter. The settling acceleration can also be calculated considerably more accurately from the characteristics of A. P. S. engines than a propulsive vent, particularly when entrained liquid is discharged through the vent.

Two television cameras are installed on the module for observing the nature of the venting process. One camera provides a view of the boiling process within the liquid, and the other provides a view of the entrainment phenomena in the ullage. The cameras are also utilized to measure the liquid level before and after venting. It is questionable how effective the TV cameras will be in measuring the level rise. A fog appeared above the liquid-vapor interface during venting in the S-IVB-203 experiment and obscured the view of the camera. The fog was likely caused by condensation of ullage vapor and will probably be present to some degree during any venting experiment. An alternate system of sensing the level utilizing capacitance-type point-level-sensors can also be employed to sense the level rise. Testing of this system will be necessary, since the performance of such probes has not been established for two-phase systems. If this technique is not satisfactory, a technique based on the attenuation of gamma rays might be applicable (8-2).

Surface heaters are installed on the outside of the tank for heating the LH_2 to pressurize the tank after each vent. A mixer maintains conditions of saturation during pressurization. High performance insulation will be installed on the tank to make possible mission durations of several days without excessive boiloff losses.

8.3.2 Experimental Sequence

The sequence of events for a typical data point is presented in Figure 8-5. This sequence is as follows: The LH_2 is heated and mixed to ensure that it is uniformly saturated, and then settled. The initial liquid level is measured utilizing the television camera. An observation period sufficiently long to provide observation of two complete slosh waves is provided in case slosh has not completely damped. Next, the experimental depressurization is accomplished, followed by resettling to remove extrained vapor bubbles. Then the liquid level is remeasured. All experiments are scheduled to occur over the Texas-Kennedy-Bermuda tracking stations, because approximately 15 min of continuous TV coverage is necessary. The module is allowed to coast under drag conditions during times other than those shown in the sequence.

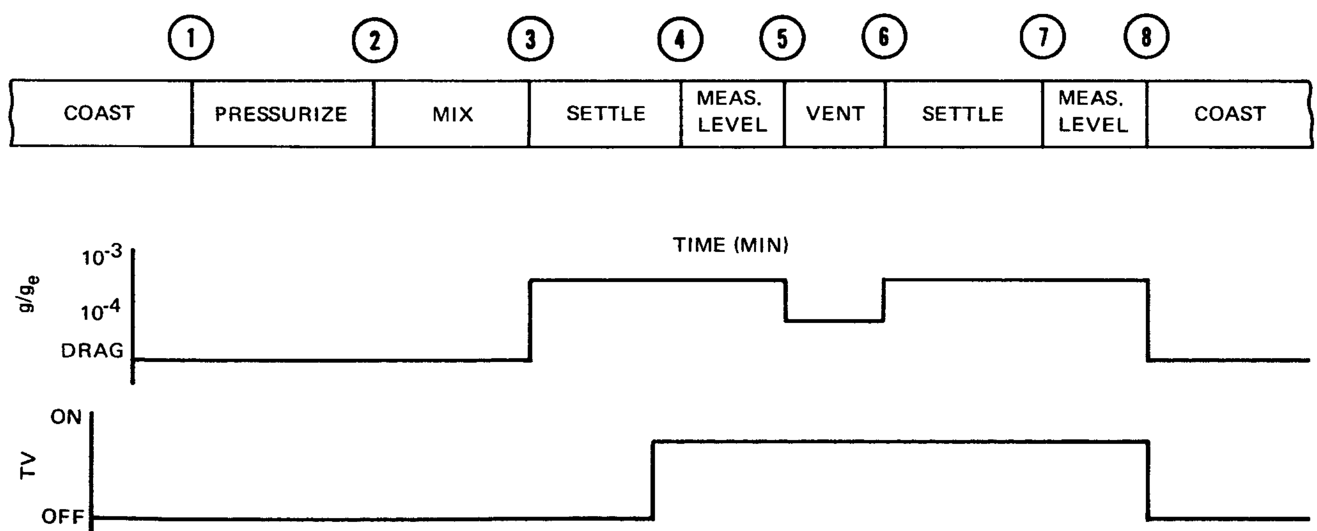

EVENTS
1. HEATER ON, MIXER ON, INSTRUMENTS ON
2. HEATER OFF
3. MIXER OFF, $10^{-3} g_e$ ON
4. TV ON
5. LIGHTS ON
6. VENT CONTROL VALVE OPEN, $10^{-3} g_e$ OFF, EXPERIMENTAL "g" ON
7. VENT CONTROL VALVE CLOSE, EXPERIMENTAL "g" OFF, $10^{-3} g_e$ ON
8. TV, LIGHTS, INSTRUMENTS, $10^{-3} g_e$ OFF; $10^{-5} g_e$ ON

Figure 8-5. Typical Sequence for Boilover Experiment

8.3.3 Carrier

Of the carriers under consideration for the orbital experiments, only the 1,600-lb class vehicles are considered applicable for the boilover and entrainment experiment.

Sufficient payload capability is not provided by the 350 lb class vehicles for installation of TV, which is basic to the experiment. The 765-lb class vehicle (Atlas E and F) is not applicable because this vehicle is launched from the PMR into a polar orbit. The longest duration of TV coverage in a polar orbit is approximately 6 min. Approximately 15 min of continuous coverage is necessary for the experiment. The 3,200-lb class vehicle provides more than adequate payload capability, but does not allow installation of a larger tank than the 1,600-lb class.

8.3.4 Prospective Experiments

Two consecutive orbital flights are necessary to obtain all the information concerning low-g venting technology outlined in Figure 2-4. The purpose of the first experiment is to measure the liquid level rise and entrainment during venting of fully saturated LH_2 for different combinations of settling acceleration, depressurization rate, pressure, initial liquid height, and initial ullage height. The performance of cyclic direct venting can be ascertained from the results of this experiment, and the validity of the proposed correlation equations can be established. Observations of the basic mechanisms of the process made during the experiment can be utilized to interpret data and modify the correlation equations, if necessary.

The purpose of the second experiment is to investigate the effect of tank diameter, thermal stratification, and initial interface disturbances on venting. Therefore, a different tank diameter will be employed in the second experiment than the first. Different degrees of thermal stratification of the LH_2 can be provided by heating the liquid hydrogen without operating the mixer. Different degrees of initial liquid-vapor interfacial disturbances can be provided by venting at different times after the initiation of settling before interface disturbances have completely damped.

8.4 PREFERRED EXPERIMENT DESIGN AND PROCEDURE

An outline of an orbital experiment proposed to obtain data on venting of fully saturated LH_2 is presented in Table 8-2. This experiment will be conducted in a 40-in. diameter by 72-in. long tank of the configuration presented in Figure 8-4. A detailed description of the experiment, the experimental sequence, and the equipment required will be presented in the following subsections.

The following notation is used in Table 8-2:

Symbol	Definition
Orbit number	Orbit number at the start of a data point
Mission time	Mission time at the start of a data point
g/g_e	Settling acceleration
$\overline{dp/dt}$	Average depressurization rate
$\overline{p}$	Average pressure
t	Duration of depressurization
u	Effective vapor velocity
M_{LH_2}	Mass of LH_2 remaining after depressurization
t_p	Duration of self-pressurization period
P_{M+H}	Electrical energy utilized in self-pressurization
I_T	Total impulse of A. P. S. system

Table 8-2

OUTLINE OF PROPOSED ORBITAL EXPERIMENT

Point No.	Orbit No.	Mission Time	g/g_e	$\overline{dp/dt}$	$\overline{p}$	t	u	M_{LH_2}	t_p	P_{M+H}	I_T
		Day:Hr:Min		Psi/Min	Psia	Min	ft/sec	lb	hr	Kw-Hr	lb-Sec
1	1	0:1:29.33	10^{-3}	1.0	47.5	5.0	0.0029	128.0	1.370	0.880	2016
2	14	0:21:10.83	10^{-3}	2.5	43.7	5.0	0.0071	122.4	0.177	0.113	2016
3	15	0:22:47.21	10^{-3}	4.0	40.0	5.0	0.0109	114.6	0.429	0.274	2016
4	16	1:00:24.62	10^{-3}	6.5	40.0	3.08	0.0166	107.2	0.640	0.410	1832
5	18	1:02:02.07	10^{-3}	10.0	40.0	2.0	0.0239	100.0	0.603	0.386	1728
6	30	1:21:42.68	10^{-3}	2.5	21.25	5.0	0.0271	94.8	0	0	2016
7	31	1:23:19.92	10^{-3}	1.0	17.5	5.0	0.0103	92.6	0.181	0.116	2016
8	45	2:20:38.17	10^{-3}	4.0	25.0	5.0	0.0402	85.3	0.637	0.408	2016
9	46	2:22:15.05	10^{-3}	6.5	25.0	3.08	0.0601	78.5	0.587	0.376	1832
10	47	2:23:52.53	10^{-4}	1.0	17.5	5.0	0.0085	76.8	0.150	0.096	1584
11	60	3:19:34.03	10^{-4}	2.5	21.25	5.0	0.0209	72.8	0.355	0.227	1584
12	61	3:21:10.40	10^{-4}	4.0	25.0	5.0	0.0315	67.0	0.501	0.321	1584
13	62	3:22:47.82	10^{-4}	6.5	25.0	3.08	0.0417	61.3	0.462	0.296	1566
14	76	4:20:05.88	10^{-2}	4.0	25.0	5.0	0.0266	56.5	0.422	0.270	6336
15	77	4:21:43.06	10^{-2}	6.5	25.0	3.08	0.0398	52.0	0.389	0.249	4493

8.4.1 Data Points

The venting process is investigated for three levels of settling acceleration, 10^{-2}, 10^{-3}, and 10^{-4} g/g_e, which span the range of interest for future space vehicles (Figure 8-2). In order to investigate the effect of pressure, experiments are conducted at two pressure levels with $g/g_e = 10^{-3}$. Five depressurization rates are indicated with $\bar{p}$ equal to approximately 40 psia and four depressurization rates with $\bar{p}$ equal to approximately 22 psia. Four depressurization rates are included at the lower pressure level with $g/g_e = 10^{-4}$ and two with $g/g_e = 10^{-2}$, to investigate the effect of gravity level.

The range of effective vapor velocity for the data points proposed is 0.0029 to 0.0601 ft/sec. These velocities are located either in the lower portion of the range of interest, or just below the range of interest (Figure 8-3). The range of u being investigated should be sufficient to establish the validity of the correlation equations, however. Unreasonably large values of depressurization rate are required to investigate values of u in the upper portion of the region of interest with the small tank being utilized in the experiment, since the magnitude of u is directly proportional to the quantity h_{LO} dp/dt (Equation 8-3). The value of h_{LO} for the nuclear stage is 66.4 ft, compared to 3.7 to 1.35 ft for the tank in the proposed experiment.

8.4.2 Experimental Sequence

The operational sequence for a typical data point was presented in Figure 8-5. The orbit number and mission time at the beginning of each experiment depressurization are presented in Table 8-2. Mission times correspond to the time from orbital insertion for a KSC launch into a 200-nmi orbit at 28.5° inclination. Data points are taken on each orbit that provides a sufficient length of experiment TV coverage. Continuous coverage of approximately 15 min. is required for each data point. Such a duration can be provided by the combined Texas-Kennedy-Bermuda tracking stations.

The time duration required for self-pressurization prior to each data point are also presented in Table 8-2. A heating rate of 10 watt/ft^2 and a heater surface area equal to 80% of the tank surface area was used.

8.4.3 Equipment

A list of the equipment required for the mission along with weight estimates is presented in Table 8-3. The power requirements of electronic equipment are also listed. Total system weight is 1,627 lb, with a 40-in. diameter by 72-in. long tank and an initial LH_2 loading of 130 lb. Propellant consumption during the experimental depressurizations is presented in Table 8-2. Electrical energy consumption for the mission is presented in Table 8-4. Total energy consumption is 13.07 kw-hr.

A mono-propellant hydrazine A. P. S. engine was considered for the mission. Propellant consumption was calculated on the basis of a specific impulse of 230 sec. The total propellant consumption for the mission is 151 lb.

8.5 EXPERIMENT ANALYSIS

8.5.1 Data Reduction

An instrumentation list for the experiment is presented in Section 8-6. The instruments listed below will be utilized for experimental measurements:

Thermometers	LH_2 tank (Liq)
	LH_2 tank ullage (Gas)
	Nonpropulsive vent (Gas)
	Boilover vent (Gas)
Pressure	LH_2 tank ullage
	Nonpropulsive vent
	Boilover vent
Level sensors	R. F. Gage
	Point sensors
Television	LH_2 and ullage.

Table 8-3

WEIGHT ESTIMATE FOR BOILOVER AND ENTRAINMENT EXPERIMENT

Equipment	Weight (lb)	Power Required (watts)
1. Structures		
Tank shell, fittings, and supports	150	
Tank shroud	60	
Insulation		
LH_2 tank	41	
Thermal shroud	25	
Miscellaneous structure	125	
	401	
2. Propulsion systems		
Pneumatic systems	20	
LH_2 fill and drain	20	
Vent System	70	
ACS system (includes 55 lb N_2)	185	
APS system	74	
APS propellant	151	
Purge system	7	
Mixer	2	7.0
Tank wall heater	20	
	549	
3. Telemetry system/instrumentation		
T/M system (50 channels)	34	95.0
Temperature probes (26)	3	
Pressure transducers (5)	1	
Level sensor (RF mass gage)	5	
Level sensor (point) (12)	36	
	79	

Table 8-3 (page 2 of 2)

Equipment	Weight (lb)	Power Required (watt)
4. TV system		
Camera and control (2)	20	12.0
Lights (2)	6	200.0
Power amplifier (2)	4	140.0
Transmitter	18	50.0
Multiplexer	6	9.0
	54	411.0
5. Command receiver system	5	10.05[c]
6. Antenna system	4	
7. Guidance and control		
Attitude sensors	22	30.0[c]
Autopilot	7	
3 phase, 400 cycle supply	10	
Programmer and power distribution	8	0.5
	47	
8. Power distribution system		
Battery (2)	310	
Electrical connectors	8	
Wire and attachments	40	
	358	
9. Propellant for experiment	130	
Total weight	1627	

[c]Operates continuously during the mission.

Table 8-4

CONSUMPTION OF ELECTRICAL ENERGY FOR THE BOILOVER AND ENTRAINMENT EXPERIMENT

Function	Total Time (hr)	Power (watt)	Energy (kw-hr)
Tank heater	6.91	640.0	4.42
Telemetry--(other than data points)		95.0	1.83
Telemetry--(prior to TV)	1.50	95.0	0.14
TV warm-up	0.75	211.0	0.16
Telemetry & TV--(data points)	3.57	506.0	1.81
Continuous equipment	117.72	40.05	4.71
		Total	13.07

The following parameters must be measured or evaluated to establish the validity of the correlation equations:

- LH_2 and GH_2 properties
- Effective vapor velocity
- Initial liquid height
- Settling acceleration
- Liquid entrainment
- Liquid level rise.

Temperature and pressure measurements will be utilized to evaluate fluid properties. It is anticipated that the temperature will be nearly constant in the tank. Depressurization rate and liquid superheat will also be obtained from the temperature and pressure measurements. Liquid superheat is an important parameter in calculating bubble growth rates.

The effective vapor velocity will be calculated from the measured mass flow rate of vapor vented, and by Equation 8-3 utilizing the depressurization rate. The mass flow rate of vented vapor will be calculated from the temperature, pressure, and orifice characteristics of both the vent control system and the nonpropulsive vent. Both systems will operate choked. Calculations based on the vent control system should be the more accurate of the two, because the orifices in the vent control system will be sized specifically for the flow rates experienced. Measured flow rates will not be valid if entrained liquid reaches the orifices. A heater will be installed on the vent line to evaporate entrained liquid if it appears that the thermal inertia of the vent line is not sufficient for this purpose.

The liquid height will be measured before and after each depressurization utilizing the TV camera by viewing a calibrated scale on the tank wall. An rf mass gage will also be available, but since the performance of this gage has not been proven for reduced gravity operation, it will not be relied upon exclusively.

The settling acceleration will be calculated from the mass of the system and the propulsive characteristics of the A. P. S. engine. A check on the validity of this calculation can be obtained from an analysis of trajectory data.

Liquid entrainment will be calculated as the difference between the mass flow rate of vapor vented and the mass flow rate of liquid evaporated. Liquid evaporation rate can be calculated by an energy balance on the liquid utilizing the pressure-temperature data. A secondary check on entrainment is provided by the liquid levels before and after a vent.

The liquid level rise will be observed with the TV camera. Twelve capacitance-type point-level-sensors will serve as a secondary system in case fog formation obscures the liquid-vapor interface from the camera as was experienced in the S-IVB-203 Experiment. A purge ring can be included to remove any entrained liquid that strikes the TV port.

8.5.2 Error Analysis

An error analysis was conducted by the method of Kline and McClintock (8-4). The uncertainties for measured quantities that were used in the calculations are presented in Table 8-5. The resulting uncertainty in the parameters of the correlation equations, Equations (8-1) and (8-5), as well

Table 8-5

UNCERTAINTIES IN MEASURED AND CALCULATED PARAMETERS

A. Measured Parameters

Quantity	Percent Uncertainty
All Fluid Properties	2.0
g/g_e	5.0
D	1.0
u_o	5.0
H_{VO}	2.0
h_{LO}	2.0
α	5.0

B. Calculated Parameters

Quantity	Percent Uncertainty
$\dfrac{u^2}{g\sqrt{\dfrac{g_e}{g}\dfrac{\sigma}{(\rho_l-\rho_v)}}}$	10.4
$\dfrac{\sqrt{\dfrac{g_e}{g}\dfrac{\sigma}{(\rho_l-\rho_v)}}}{D}$	3.05
$\dfrac{\rho_v}{\rho_l-\rho_v}$	2.83
$\dfrac{u^2}{\alpha g H_V}$	13.2
$\dfrac{\left[\dfrac{g_e}{g}\dfrac{\sigma}{(\rho_l-\rho_v)}\right]^{3/2}}{v^2}$	4.70
α	4.25
E	30.8

as in the level rise α and entrainment E calculated by these equations are also presented in Table 8-4. The experimental constants for water-steam mixtures at normal gravity were used in calculating the uncertainty of α and E. Therefore these uncertainties may not necessarily be correct for hydrogen.

The maximum uncertainty of the parameters in the correlation equations is 13.2% (Table 8-5). The resulting uncertainty in level rise is 4.25% and in entrainment is 30.8%. The uncertainty of the effective gas velocity u contributes most to the uncertainties of calculated quantities. A value of 5% was assumed for the uncertainty of u.

As was discussed in Section 8.5.1, an experimentally determined value of liquid entrainment will be calculated from the measured mass of vapor vented during each depressurization, and will be compared with a value calculated from the total liquid volume decrease during the same depressurization. Uncertainties in entrainment were determined for both calculation techniques and are presented in Table 8-6 as a function of the entrainment. The values presented apply for an acceleration level of 10^{-3} g/g_e, a depressurization rate of 4.0 psi/min, an average pressure level of 25 psia, and a liquid height of 2.56 ft. This point was selected as representative of an average data point for the experiment.

It can be seen from Table 8-6 that only the order of magnitude of the entrainment can be determined for values of entrainment less than 0.10. The large uncertainties for low entrainments are due exclusively to the uncertainty in measuring the quantity of vapor vented, and the change in liquid volume. An uncertainty of 5% was assumed for the volume of vapor vented. The uncertainty in liquid volume stems from an assumed error of 0.6 in. in sensing the liquid level and an uncertainty of 2% in the cross sectional area of the tank.

The consequence of the large uncertainties for low entrainments is not considered serious because entrainments less than 0.10 can be considered acceptable. Thus, data points can be classified as acceptable or unacceptable with respect to entrainment. This procedure is satisfactory for design purposes.

Table 8-6

UNCERTAINTY IN THE EXPERIMENTALLY DETERMINED ENTRAINMENT

E	Percent Uncertainty	
	From Vent Flow	From Volume Change
0.01	700	2460
0.10	76.1	244
1.00	13.8	25.4

8.6 INSTRUMENTATION LIST

An instrumentation list for the experiment is presented in Table 8-7.

Table 8-7

INSTRUMENTATION REQUIREMENTS FOR BOILOVER EXPERIMENTS

Measurement Title	No. Req'd	System Range/Accuracy		Frequency Response	Environment at Point of Measurement Media	Temp
Voltage, Heater	1	0-30 ±0.9 Vdc	(±3%)	1 cps (4 sps)		
Current, Heater(7)	1	0-1.5 ±0.045 amps	(±3%)	1 cps (4 sps)		
Current, Mixer	1	0-0.25 ±0.0075 amps	(±3%)	1 cps (4 sps)		
Events	15	On-Off		2.4 cps (12 sps)		
Temperature LH_2 Liquid	14	36-46 ±0.3°R	(±3%)	1 cps (4 sps)	LH_2, GH_2	37-630°R
Temperature LH_2 Ullage	4	35-85 ±1.5°R	(±3%)	1 cps (4 sps)	LH_2, GH_2	37-620°R
Temperature LH_2 Ullage	2	85-400 ±10°R	(±3%)	1 cps (4 sps)	LH_2, GH_2	37-620°R
Temperature NPV (Gas)	2	35-85 ±1.5°R	(±3%)	1 cps (4 sps)	LH_2, GH_2	37-620°R
Temperature B.O. Vent (Gas)	1	35-85 ±1.5°R	(±3%)	1 cps (4 sps)	LH_2, GH_2	37-620°R
Temperature NPV (Gas)	2	85-400 ±10°R	(±3%)	1 cps (4 sps)	LH_2, GH_2	37-620°R
Temperature B.O. Vent (Gas)	1	85-400 ±10°R	(±3%)	1 cps (4 sps)	LH_2, GH_2	37-620°R
Pressure LH_2 Boil Ht Trans Ullage	2	0-50 ±0.5 psia	(±1%)	1 cps (4 sps)	GH_2, LH_2	37-620°R
Pressure NPV	2	0-50 ±0.5 psia	(±1%)	1 cps (4 sps)	GH_2, LH_2	37-620°R
Pressure B.O. Vent	1	0-50 ±0.5 psia	(±1%)	1 cps (4 sps)	GH_2, LH_2	37-620°R
Level Liq (3-Loading)	12	Liq/Vapor Indicator	(±3%)	24 cps (120 sps)	LH_2, GH_2	37-620°R
Level Liq (RF)(2)	1	TBD	(±3%)	1 cps (4 sps)	LH_2, GH_2	37-620°R
TV-Boil Ht Tank	2	TBD				

(1) Sensing line must isolate transducer to provide -60 to +165°F environment.
(2) Experimental measurement.

Section 9
PROPELLANT TRANSFER

To provide for the design of an efficient propellant transfer system for the S-IIB Mars flyby mission, it is recommended that three orbital experiments be performed in accordance with schedules shown in the Technology Survey, Figures 2-6 and 2-7.

The objectives for ullage control during outflow (Figure 2-6) would be met by an experiment using plexiglass tanks to provide the best possible visual data. This experiment can be flown on an E or F type Atlas.

Two experiments are required to satisfy the objectives for receiver tank thermodynamics. The first would be used for development of analytical models and scaling procedures; the second would provide verification of the S-IIB no-vent concept and aid in optimizing S-IIB transfer procedures. Both experiments use LOX as the transfer fluid and require boosters in the Thor/ Agena class.

This Phase B Prime effort has developed experiment concepts applicable to the problems associated with transfer of LOX in the S-IIB mission. However, with little or no modification, these concepts could be used to provide general data on low-g propellant transfer of the type sought in Project THERMO, Phase B. This is particularly clear in regard to the outflow experiment which, as defined here, will provide data of nearly universal applicability.

9.1 ORBITAL EXPERIMENTATION INFORMATION REQUIREMENTS

In the area of ullage control during outflow, three problems are designated as requiring orbital testing (Section 2). The first is to obtain general data on interface dynamics in large tanks at low Bond number. This requires a program with tests at various flow rates and g levels with provision for determining qualitative liquid/vapor interface behavior as well as the quantity of of liquid residual at ullage pull-through. The second problem is to determine the effectiveness, in minimizing suction dip residual, of the most promising baffle configuration selected by ground test. The final problem is the selection of a flow and acceleration schedule for use in the S-IIB mission. While the solution to this problem is not needed as early in the program as the others it can be obtained in the same experiment.

The schedule for receiver tank thermodynamics was set up to provide for development of the S-IIB no-vent concept and to select an optimum inlet configuration for that mission. Development of analytical models and scaling procedures for the processes associated with pressure transients during inflow will require orbital verification at an early date. This verification should be obtained by performing a number of transfer runs in orbit with various combinations of flow rate, g level, and configuration. Later in the program, a scale model orbital test is called for to verify the no-vent concept. Testing is coupled with the scale model experiment to verify methods for control of inlet inertia if venting is required during the S-IIB transfer.

9.2 DATA ACQUISITION AND EXPERIMENT REQUIREMENTS

Data programs to satisfying the orbital testing objectives were delineated. Experiment requirements were established based on the present state-of-art for scaling of the processes involved. It may be necessary to modify these requirements as technology advances through analysis and ground testing.

9.2.1 Ullage Control During Outflow

The dimensional analysis of Reference 2-10 identifies the Froude, Bond, and Reynolds numbers as the parameters governing interface dynamics during outflow for a given configuration. The Reynolds number is not expected to be important where the boundary layer is small relative to the flow path.

The recommended program for orbital experimentation is presented in Table 9-1. It calls for a wide range of variations in Froude and Bond numbers in an unbaffled tank. Baffle effectiveness will also be investivated at various Froude and Bond numbers. Effects of changes of flow and acceleration schedules will be checked at a likely value of Froude number and Bond number. Anticipated correlations of the data are shown in graphical form in

Table 9-1

DATA PROGRAM FOR ULLAGE CONTROL DURING OUTFLOW

Program for General Data on Interface Dynamics during Outflow

Run	Froude No.	Bond No.
1	6.7×10^{-2}	100
2	6.7×10^{-2}	25
3	2.7×10^{-1}	25
4	6.7×10^{-4}	100
5	1.3	5
6	1.3×10^{-2}	5
7	2.7×10^{-3}	25
8	1.7×10^{-4}	100

Program for Baffle Effectiveness

Run	Froude No.	Bond No.
9	6.7×10^{-2}	100
10	6.7×10^{-2}	25
11	2.7×10^{-1}	25
12	2.7×10^{-3}	25
13	6.7×10^{-4}	100

Program for Flow and Acceleration Schedule

Run	Froude No.	Bond No.	Flow Schedule
14*	6.7×10^{-2}	100	#1
15	2.7×10^{-1}	25	#2
16	6.7×10^{-2}	100	#2
17	6.7×10^{-2}	100	#3
18	6.7×10^{-2}	100	#4

*Same as run 9 (steady flow and acceleration).

Figures 9-1 and 9-2. Also important in evaluation of the data for each of the three problem areas will be comparison of the interface behavior with that predicted by analytical models.

The basic data for each of the problem areas will be in the form of TV transmission which will yield both a quantitative estimate of the residual at ullage pull-through and qualitative interface behavior during the entire outflow process. A transfer line flow meter will also be useful in determining the precise instant of ullage pull-through and providing a means of checking the residual estimate.

The program for general data places the most stringent requirements on the experimental apparatus, calling for four different flow rates and three g levels. For a given experimental tank size the g levels are determined from the Bond number. The flow rates can then be determined by duplicating Froude numbers corresponding to flow rates called out for the S-IIB mission. Having selected g level and flow rate in this manner, the Reynold numbers for the S-IIB mission will be simulated if

$$\left(\mu_1/\mu_2\right)^2 = \sigma_1 d_1/\sigma_2 d_2$$

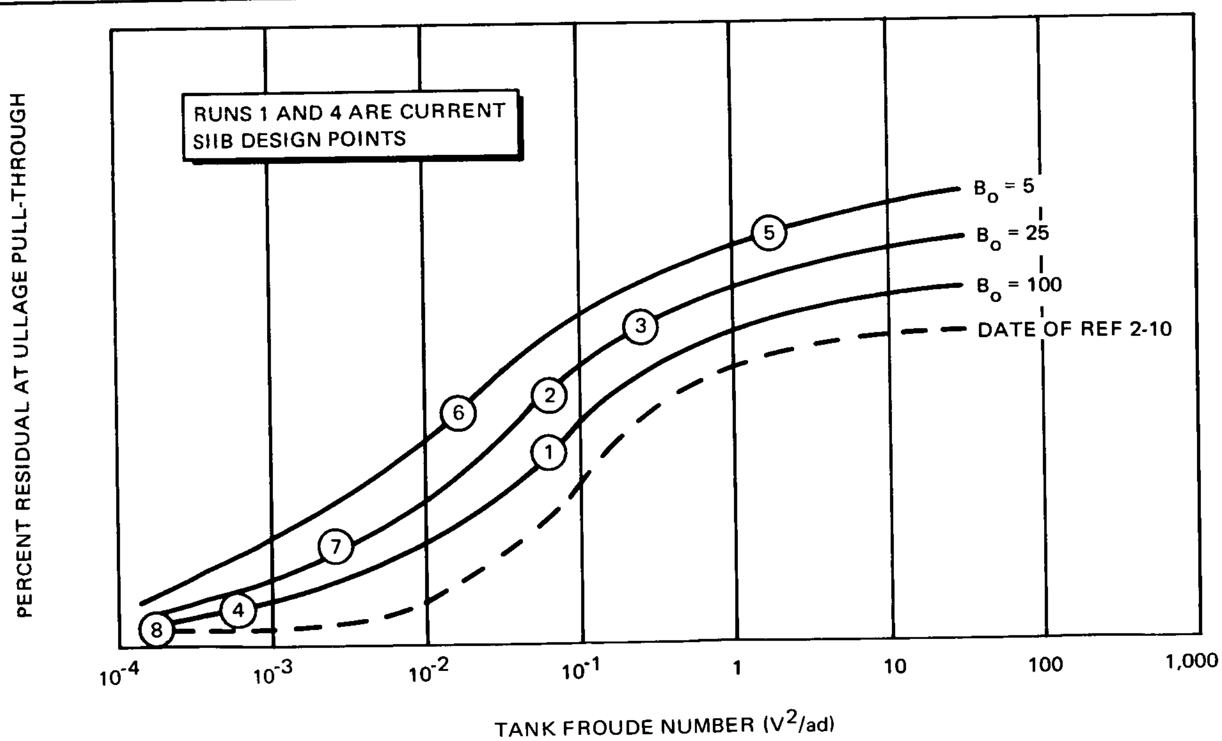

Figure 9-1. Sunction Dip Correlation for Unbaffled Tank

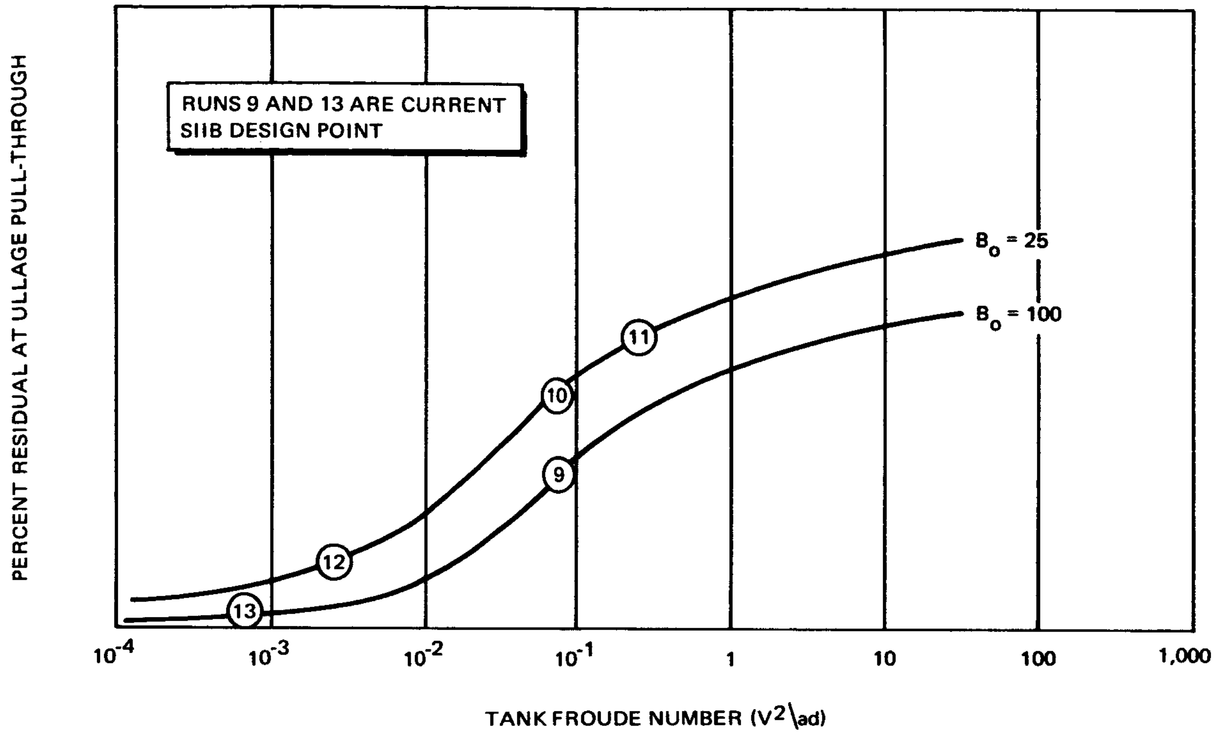

Figure 9-2. Suction Dip Correlation for Baffled Tank

where μ is the viscosity, σ is the surface tension, and d is the tank diameter. A preliminary survey indicates that fluids coming closest to meeting this criteria are hexane and ethyl ether. Since it is unlikely that a fluid will be found to meet the criteria for simulating Reynolds number exactly, it is recommended that the tank size be made as large as possible to minimize boundary layer effects.

9.2.2 Propellant Transfer Receiver Tank Thermodynamics

The problem of predicting pressure transients during inflow in a cryogenic system has been subjected to a thorough dimensional analysis in Reference 9-1. That analysis identifies only one gravity dependent parameter, the inlet Froude number. The situation for the S- IIB is complicated somewhat by the need for the selection of a characteristic dimension for the Froude number when using unusual inlet configurations (as is recommended by the S-IIB study).

The program for development of analytical models and scaling procedures is presented in Table 9-2 while that for verification of the no-vent concept is given in Table 9-3. The odd numbered runs in Table 9-2 involve flow into two different size tanks. Two Reynolds numbers are shown for these cases, since holding the Froude number constant leads to variation of Reynolds number in proportion with (dia.)$^{3/2}$. Also included in Table 9-3 are tests for optimizing the transfer procedure and investigating methods for control of inlet inertia for receiver tank venting. The anticipated approach to evaluation of the data for the scaling exerpiment is illustrated in Figures 9-3 and 9-4. These figures show how the effect of Froude number on a parameter such as the average heat transfer coefficient between the liquid and the ullage could be determined by providing runs at various Froude numbers while holding constant other significant quantities such as the inlet Reynolds number. For this example the heat transfer coefficient should be computed using measured pressure, ullage temperature, and inlet flow histories. The figures also illustrate how experimentation with different sized tanks will be useful in determining the validity of scaling procedures. Furthermore, analytical models to be developed prior to the flight can be verified by comparing their predictions with the results as given by plots of the form of

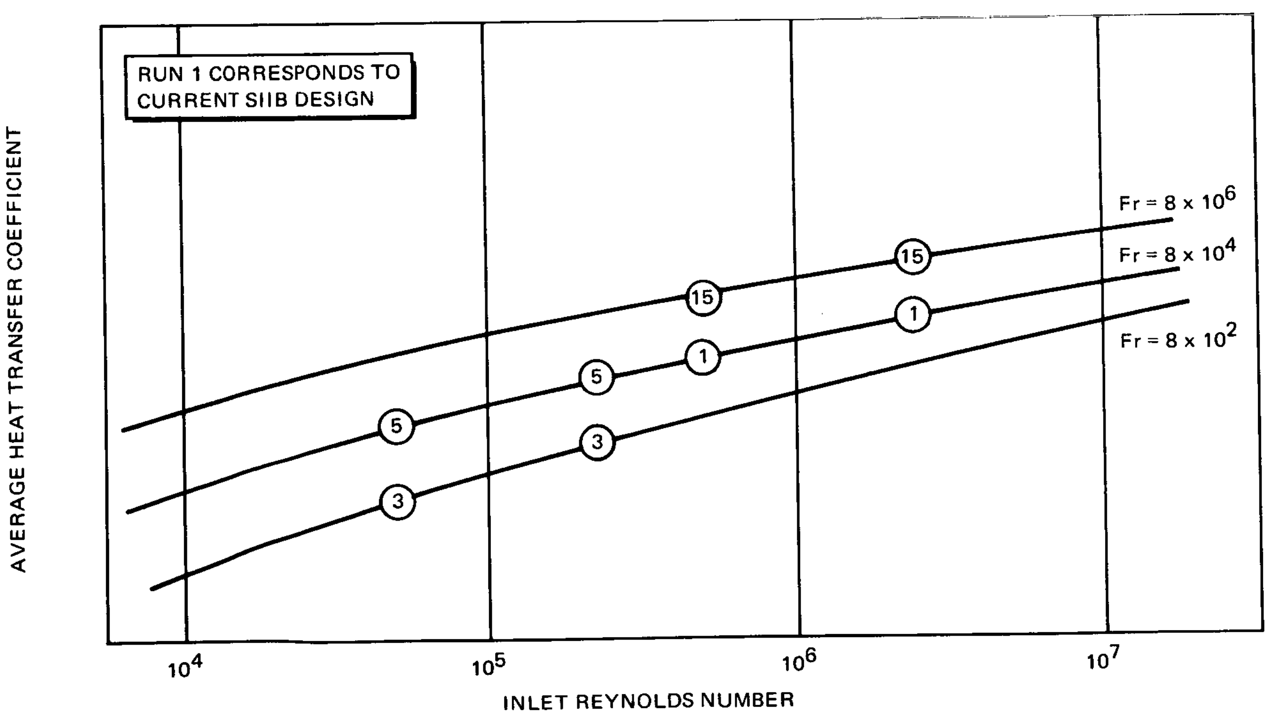

Figure 9-3. Scaling for Receiver Tank Thermodynamics

Table 9-2

DATA PROGRAM FOR SCALING OF RECEIVER TANK THERMODYNAMICS

Run	Inlet Froude No.	Inlet Reynolds No.	Inlet Configuration: Diffused	Spray	Swirled	Warm Line
1	8×10^4	2×10^6		X	X	
		7×10^5				
2	8×10^4	2×10^6	X			
3	8×10^2	2×10^5		X	X	
		7×10^4				
4	8×10^2	2×10^5	X			
5	8×10^4	2×10^5		X	X	
		7×10^4				
6	8×10^4	2×10^5	X			
7	8×10^4	2×10^6	X			
		7×10^5				
8	8×10^6	2×10^6	X			
9	8×10^4	2×10^6			X	
		7×10^5				
10	8×10^4	2×10^6	X			X
11	8×10^2	2×10^5			X	
		7×10^4				
12	8×10^2	2×10^5	X			X
13	8×10^4	2×10^5			X	
		7×10^4				
14	8×10^4	2×10^5	X			X
15	8×10^6	2×10^6		X	X	
		7×10^5				

Table 9-3

DATA PROGRAM FOR RECEIVER TANK THERMODYNAMICS VERIFICATION

Run	Inlet Froude No.	Inlet Configuration	Flow Schedule
1	8×10^4	#1	#1
2	8×10^4	#2	#1
3	1×10^4	#1	#1
4	1×10^4	#2	#1
5	8×10^4	#1	#2
6	8×10^4	#2	#2
7	8×10^4	#1	#3
8	1×10^4	#2	#4

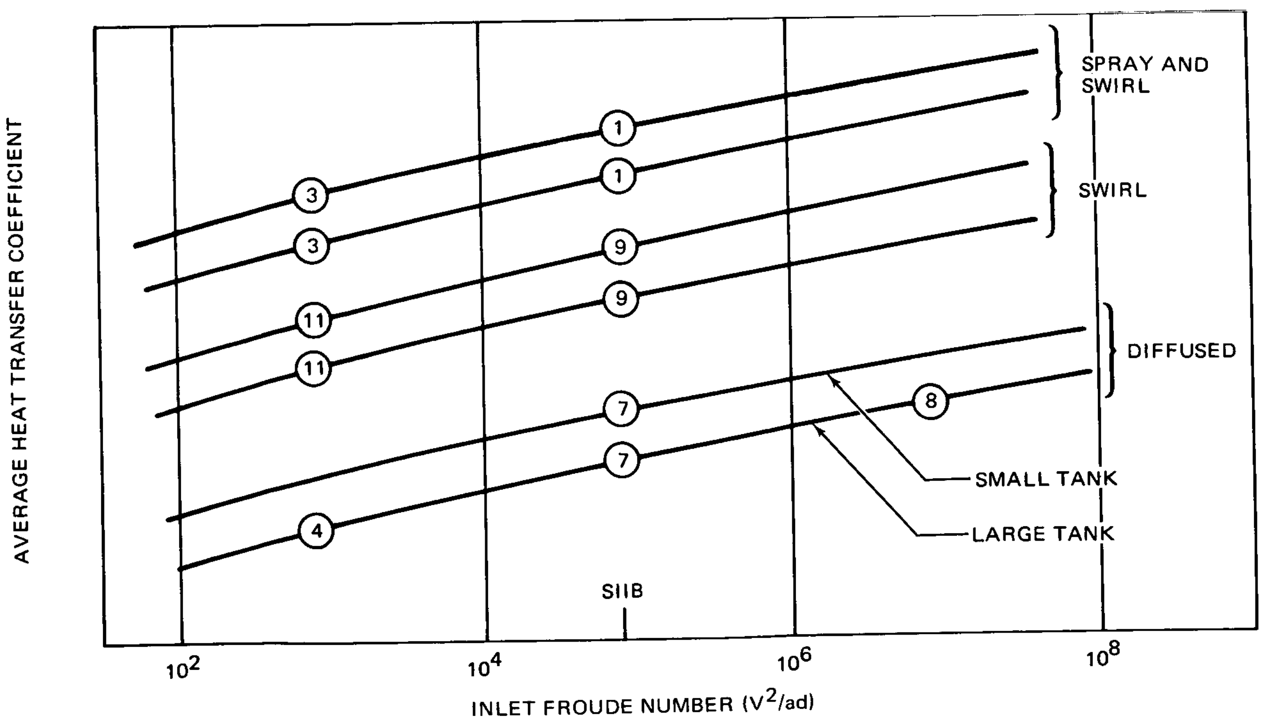

Figure 9-4. Scaling for Receiver Tank Thermodynamics

Figure 9-3. Evaluation procedures of this type can be applied to all of the transport processes affecting pressure transients during inflow. In regard to the verification program, the main interest will be in results of the form of Figure 9-5, which indicate the validity of the no-vent concept and provide for selection of optimum configuration and procedure.

The basic data to be obtained for both scaling experiment and the verification experiment will consist of flow rates, tank pressures, and various internal tank temperatures. Flow rate and inlet temperature will determine the experimental parameters such as Froude number and Reynolds number, while measurement of internal fluid temperatures will provide for estimates of such parameters as heat transfer coefficients. A relatively large number of temperature measurements will be needed since fluid conditions may vary quite drastically throughout the tank. As indicated above, the main interest in the verification experiment will be in tank pressure transients. However, temperature measurements will be required to provide information on the processes effecting the pressure. Investigation of control of inlet inertia during venting presents significant problems here in that it requires instrumentation quite different from that for the process involved in determining

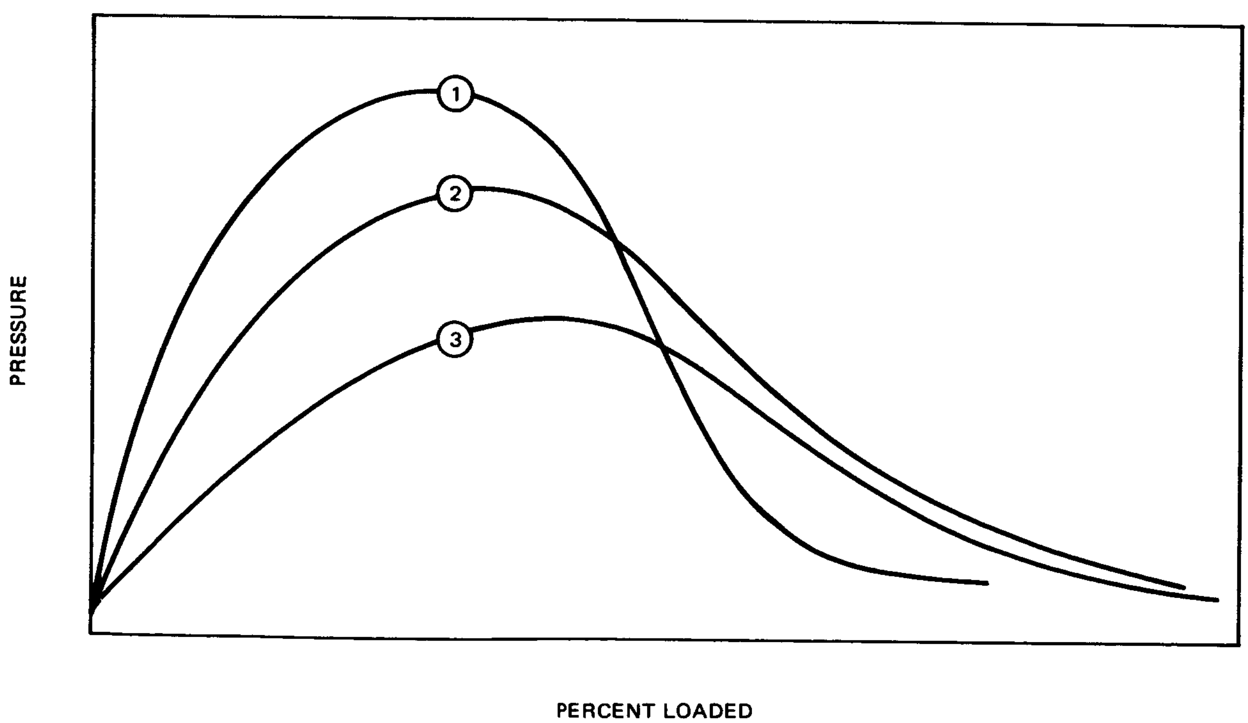

Figure 9-5. Verification Experiment for Receiver Tank Thermodynamics

pressure transients. The easiest approach to this problem will be to use vent line instrumentation to determine in a qualitative manner whether or not significant quantities of liquid are vented over board.

Reference 9-1 states that in situations where change of phase is involved, proper scaling can be obtained only by using the same fluid. The requirement for using the same fluid is reinforced by the many property ratios and other dimensionless parameters which are found to influence the inflow processes. Most of these can be eliminated from consideration if LOX is used as the experimental fluid. These advantages associated with the use of LOX are felt to justify the significant increase in experimental weight involved.

For a given tank size, the flow rates for the experiment are determined by simulating Reynolds numbers anticipated for the S-IIB experiment. G levels are then determined by simulation of Froude numbers. Table 9-2 calls for a variety of inlet configurations. This is particularly important because of the difficulty in scaling the effects of such configuration. Use of two different size tanks in the scaling experiment permits coverage of a wider range of Froude numbers and Reynolds numbers with two experimental flow rates and two g levels in addition to providing verification of scaling procedures.

9.3 EXPERIMENT CONCEPTUAL DESIGN

Conceptual designs were established for two sets of orbital experiments. One set would require three launches: an outflow experiment, incorporating all of the objectives of Section 9.2.1, to be flown in 1969; an experiment for scaling of receiver tank thermodynamics, also with a 1969 flight date; and an experiment to verify the no-vent concept to be flown as late as 1971. The second set reduces the number of launches to two by: combining the collection of general data on interface dynamics during outflow with the receiver tank thermodynamics scaling experiment, combining the selection of flow and acceleration schedules for outflow with the receiver tank verification experiment, and obtaining data on effectiveness of outflow baffles from both flights. Schedule considerations appear to preclude the use of only one launch to satisfy all of the orbital requirements, since development of scaling procedures is needed early for input to the S-IIB design and the design is to be verified after it is at a reasonable state of completion.

The three component experiments of the first set are described in Sections 9.3.1 through 9.3.3. The two experiments of the second set are described in 9.3.4 and 9.3.5. These conceptual designs are, in general, applicable to any size of experiment tank and any number of runs. Discussion of considerations which led to rejection of the second set is presented in Section 9.4. Also shown in 9.4 is the selection of boosters for the experiments.

9.3.1 Experiment for Ullage Control during Outflow

The basic objectives in this area are to identify the parameters which govern interface control during propellant transfer and to determine at what parameter value control is maintained during bulk transfer and suction dip residual is minimized. The most useful data for satisfaction of these objectives would be visual data showing the configuration of the liquid/vapor interface under various influences. Results obtained with plexiglass tanks during Phase B of Project THERMO indicate that these tanks will provide best visual data obtainable under present technology. Of the two potential simulant liquids, hexane is more compatible with the plexiglass tank. The desire to minimize boundary layer effects calls for use of as large an experiment tank as possible. Experience gained in handling plastic tanks during Phase B indicates that a 30 in. diameter is an upper limit, if sufficient pressurization capability is to be provided. The experiment uses two tanks, one with a plain outlet and the other with an optimum outlet as determined by ground testing. The tanks will be spherical or clam-shell shaped depending on tanker concepts.

In addition to the two tanks, systems are included for pressurization, venting, and transfer of liquid. A schematic is shown in Figure 9-6. Figure 9-7 shows a conceptual design of tanks, TV cameras, and lights within the Thor-Delta Shroud. Supporting subsystems include ullaging propulsion, attitude control, instrumentation and telemetry, a sequencer, and other electrical equipment.

Figure 9-7 represents the most convenient installation from a structural standpoint. However, it is questionable as to whether or not the attitude control system will be capable of handling the shift in center-of-gravity that will result from propellant transfer without imposing excessive perturbations on the vehicle. A preliminary investigation of this problem has indicated that the system described in Section 3 may be marginal. Further study is needed. If necessary, the tanks could be mounted side by side so that the center of gravity will remain at or near the axis and axial thrust could be used. This, however, will increase the complexity of the installation.

The tanks can be of the type built under the Project THERMO Phase B contract. Spherical tanks are recommended; however, other shapes could be used depending on the most promising tanker configuration at the time of initiation of experiment build-up. With the spherical tank, withdrawal can take place through a fitting in the center of the metal portion of the tank; but if geometry of the S-IVB tanker is simulated, an internal withdrawal line will have to be used. The motive force for transfer will be provided by pressurization with helium gas. It can be stored at high pressure and low temperature in a 3.5 ft^3 bottle of the type used on the S-IVB. Preliminary analysis indicates that if the bottle is loaded at near LH_2 temperature shortly before launch and is covered with high-performance insulation, the gas temperature will be maintained within the safe operating range of the bottle

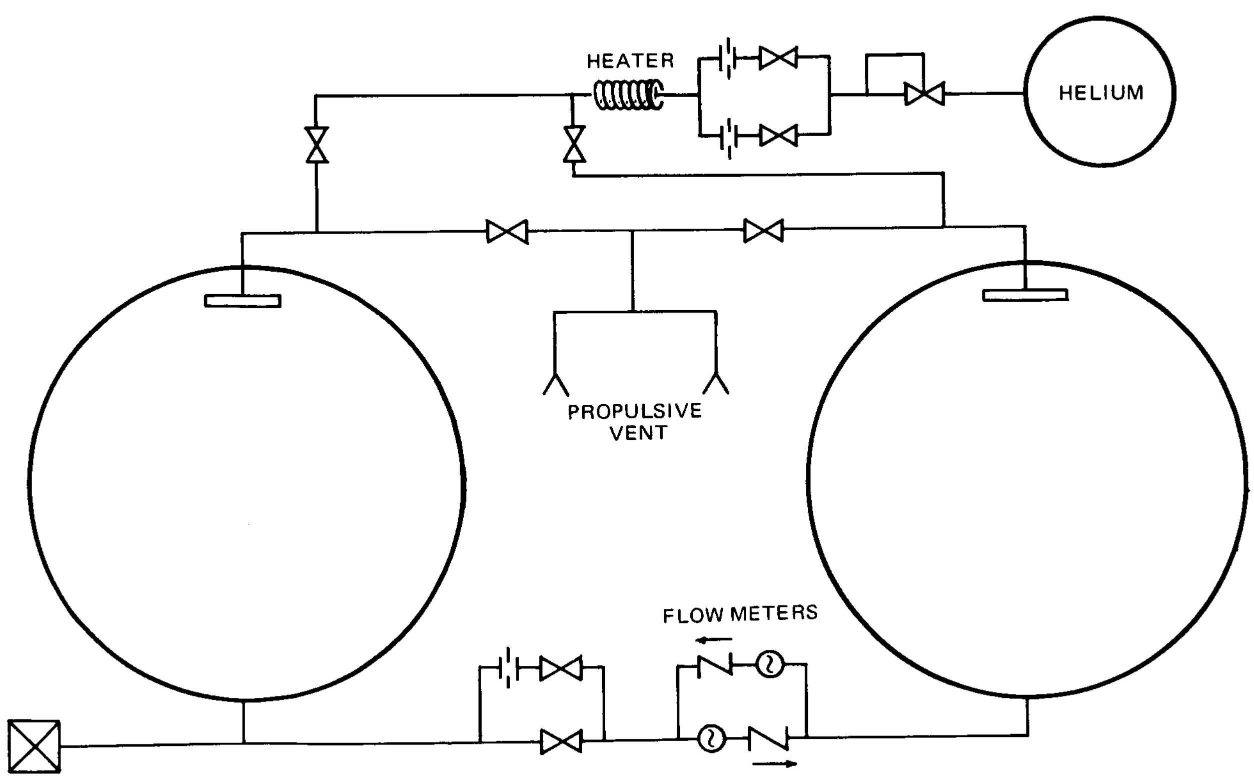

Figure 9-6. Experiment for Ullage Control During Outflow

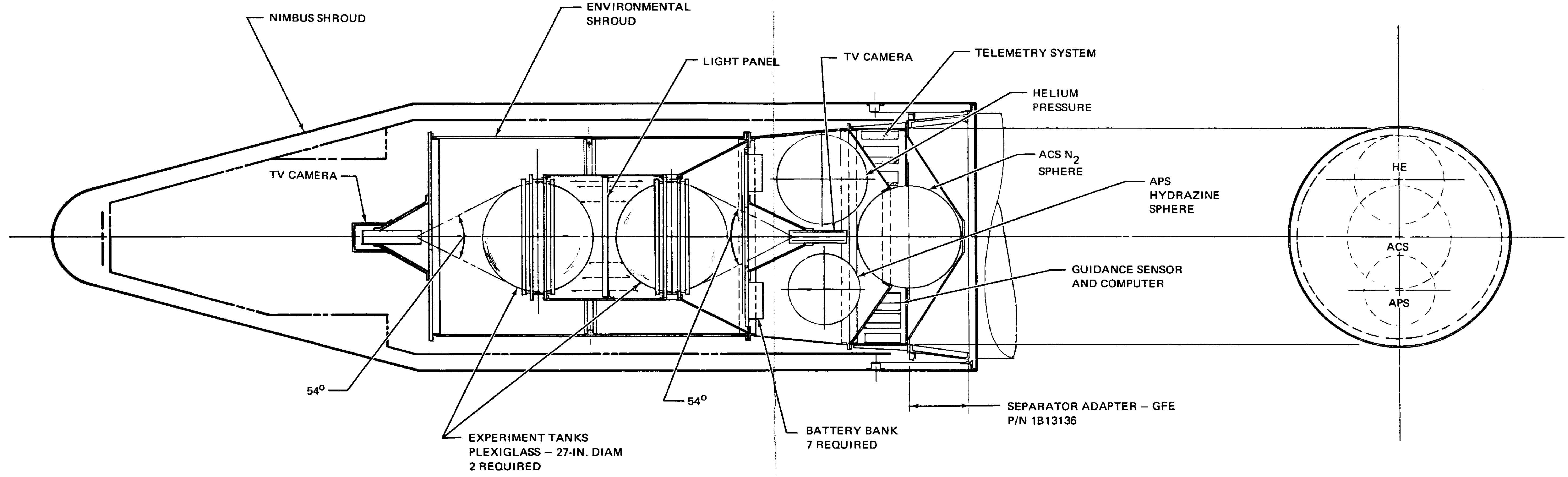

Figure 9-7. Propellant Transfer Outflow Experiment

9-13-1

9-13-2

throughout the experiment. The gas will be heated electrically to provide for a minimum of storage capacity. In order to provide uniform flow rates for the experiment, the pressurization flow can be controlled by pressure switches sensing the pressure differential between the two tanks. The research program in Section 9.2 calls for four different flow rates. These can be obtained using two different pressures and two flow paths between the two tanks. Inlet diffusers of the bag type should be used to minimize the influence of pressurizing gas on the interface dynamics. Between experiments, it will be necessary to vent one of the transfer tanks. Propulsive venting should be used so that the resulting thrust can be utilized in transferring residual resulting from ullage pull-through at the end of the experiment.

The program of Section 9.2 calls for three different g levels which can be provided by three pairs of hydrazine monopropellant engines, all fed from the same propellant supply system (Section 3.4).

If a polar orbit is used, all but the longest runs (about 10 min. maximum) can be completed in one pass of one of the TV equipped tracking stations. A KSC launch will provide for TV coverage for the longest runs. Thus, sequencing will not be a difficult problem in this experiment and data recording will not be needed. Runs, which cannot be completely covered by TV, can be started before reaching the station and run to completion over the station. If unexpected phenomena are observed upon initial pick-up of the signal, the run can be started over from the beginning at the next pass by ground command. This procedure provides four to seven runs per day.

9.3.2 Experiment for Scaling of Receiver Tank Thermodynamics

A schematic of the selected system for this experiment is shown in Figure 9-8 and a conceptual design of the experimental installation is given in Figure 9-9. Subsystems for pressurization, flow control, venting, and ullaging thrust are very similar to those described in Section 9.3.1.

Three aluminum tanks are used. Although the item of interest is an S-IIB LOX tank, it is felt that for the purposes of investigating scaling procedures, spherical tanks will provide sufficient simulation of the S-IIB geometry. This greatly simplifies tank construction. The tanks are enclosed in a shroud covered with high performance insulation to provide for experiment durations on the order of a few days. Strip-type heaters can be installed on the outside of the tank as well as in the transfer line for investigation of chilldown phenomena.

Analysis indicates that residual due to ullage pull-through will be a significant problem for the high flow rate runs (see Section 9.4). In addition to providing for propulsive venting at the end of the run, it will probably be necessary to continue operating the ullage engines for transferring the residual at a low flow rate.

Very little difficulty is expected in sequencing this experiment. Since no visual data is needed, it will be possible to carry out transfer runs until an on-board tape recorder is saturated and resume after the data has been played back to the ground. The longest single run will take about 20 minutes which is well within the capacity of the tape recorder. It is estimated that two to three days will be required to complete the program described above.

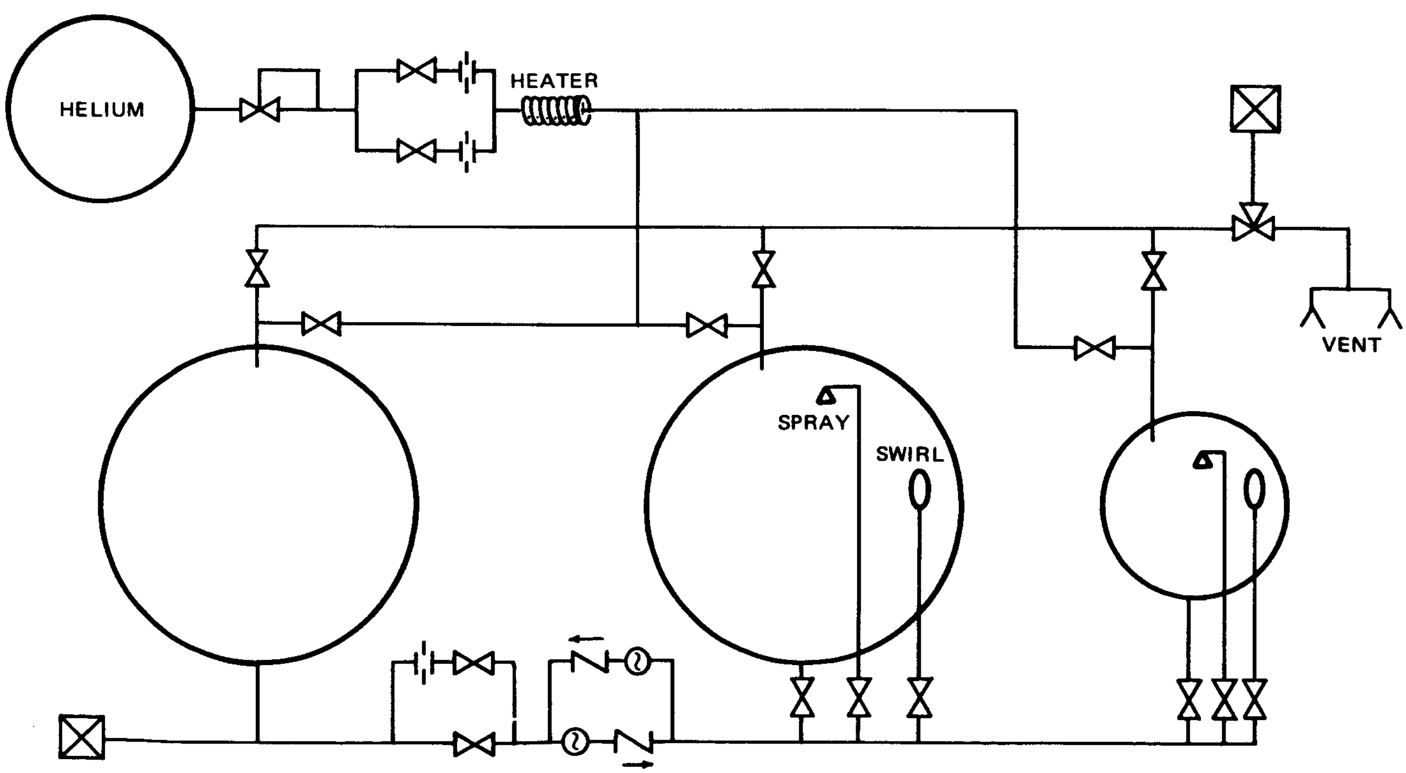

Figure 9-8. Experiment for Scaling of Receiver Tank Thermodynamics

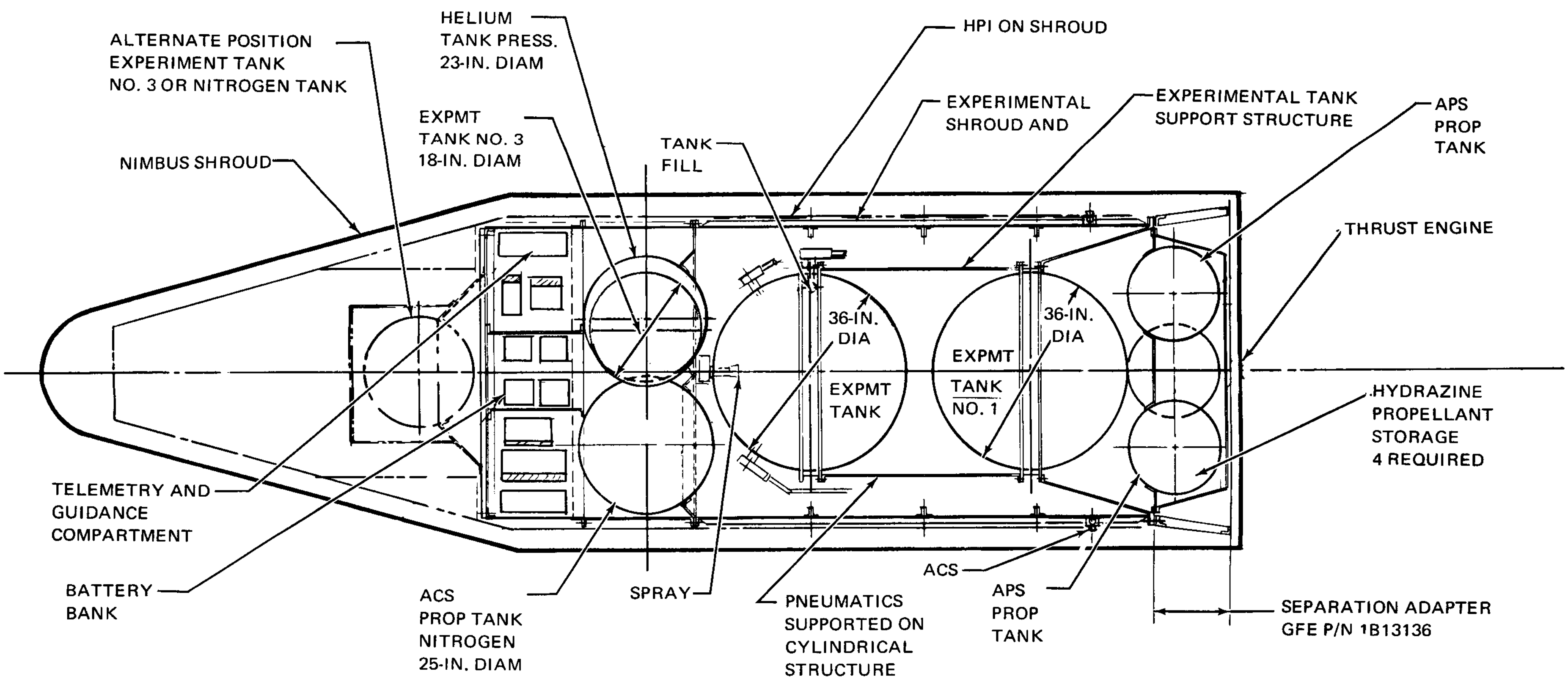

Figure 9-9. Propellant Transfer Receiver Tanks Thermodynamics Experiment

The tank size appears to be limited by the amount of space available within the Nimbus-type shroud. Figure 9-9 shows an installation of tanks, 36-in. in diameter, which appear to be a maximum. It would be possible to use larger tanks if the insulating shroud were eliminated and HPI were applied to the individual tanks. This, however, would greatly reduce the predictability of the thermal environment.

9.3.3 Verification Experiment for Receiver Tank Thermodynamics

Subsystem hardware and procedures for this experiment are essentially the same as that for the scaling experiment described above. The basic differences between the two is that only two tanks are used here, the tanks are designed to conform with S-IIB LOX tank geometry, and the experimental program is considerably shorter. As in the scaling experiment, the payload weight depends mainly on the size of the tanks used. Provision can be made for testing two or three inlet configurations to provide for S-IIB final design selection.

9.3.4 Experiment for Combination of Ullage Control During Outflow and Scaling of Receiver Tank Thermodynamics

The most important conflict of experimental requirements resulting from combining the two programs involves the need for visual data for outflow and the requirement for use of LOX for inflow. Since plastic tanks cannot be used with LOX, it will be necessary to use viewing ports of the type designed for the propellant transfer experiment in Phase B of Project THERMO. This significantly reduces the quality of the visual data. Furthermore, referring to Figure 9-9, it can be seen that the space inside the shroud is already crowded and the addition of TV cameras and lights may necessitate removal of the third experiment tank. Otherwise, the system could be essentially the same as that described in Section 9.3.2. However, the sequence will be somewhat more complicated since some of the transfer runs will take considerably longer than the time available over the tracking station and the visual data cannot be recorded onboard. Hence, this concept was rejected.

9.3.5 Experiment for Combination of Ullage Control During Outflow and Receiver Tank Thermodynamics Verification

Here, too, the significant hardware change is the addition of TV ports to the system of Section 9.3.3. Again, sequencing and telemetry will be more complicated and the number of runs may have to be increased. These factors lead to concept rejection.

9.4 PREFERRED EXPERIMENT DESIGN AND PROCEDURE

The set of experiments described in Sections 9.3.1, 9.3.2, and 9.3.3 are recommended. This selection was based in part on analyses of payload requirements and experimental fluid usage presented in 9.4.1 and 9.4.2; but the most significant consideration was the advantage of using plastic tanks to provide visual data on outflow.

The payload analysis was also used, in conjunction with the program requirements of Section 9.2, to select boosters for each of the experiments (the systems described in 9.3 are applicable to any booster). The analysis showed that reduction of the number of transfer runs would have little effect on the payload requirements, so that deletion of any portions of the data programs was rejected.

9.4.1 Experiment Payload Analysis

Payload requirements for the systems described above have been parameterized in terms of tank size and number of runs. The primary factors affecting payload requirements for the propellant transfer experiments are fluid weight, structural weight, electrical power requirements, pressurization system weight, propellant weight for ullaging, and for the guidance system. Primary assumptions used in the analysis were as follows:

1. A 5% ullage volume at full load was assumed.
2. Two battery levels were used: 400 watt hrs and 12 kilowatt hours.
3. Helium stored at cryogenic temperatures and heated electrically would be used as the pressurant. A rough trade-off analysis indicated that this would represent substantial weight saving over a warm helium system or a nitrogen system.

4. A hydrazine monopropellant system would be used for ullaging thrust (I_{sp} = 235)
5. The ACS propellant weights were reduced from those described in Section 3.4.1 because of the reduced experiment time.

The required flow rates and g levels were determined as a function of tank diameter by the scaling procedures discussed above. Electrical uses are telemetry and TV systems for the duration of the runs and the energy required for heating the helium which was based for each run on an estimate of required tank pressure to yield the designated flow rate. One 3.5-ft^3 bottle was found to be sufficient for pressurization in all cases investigated.

Significant results of the payload analysis are shown in Figures 9-10, 9-11 and 9-12. Figure 9-10 shows that, if tanks of about 27-in. in diameter are used, the entire outflow technology program can be carried out with a payload corresponding to the E&F type Atlas. Figures 9-11 and 9-12 show that, if the tank diameter is set at or near 36-in., a launch vehicle in the 1,600-lb plus payload class will be needed. It should be noted that little can be gained by reducing the number of runs in the experiment. The payload requirements for the combined experiments of 9.3.4 and 9.3.5 are similar to those shown in Figures 9-11 and 9-12.

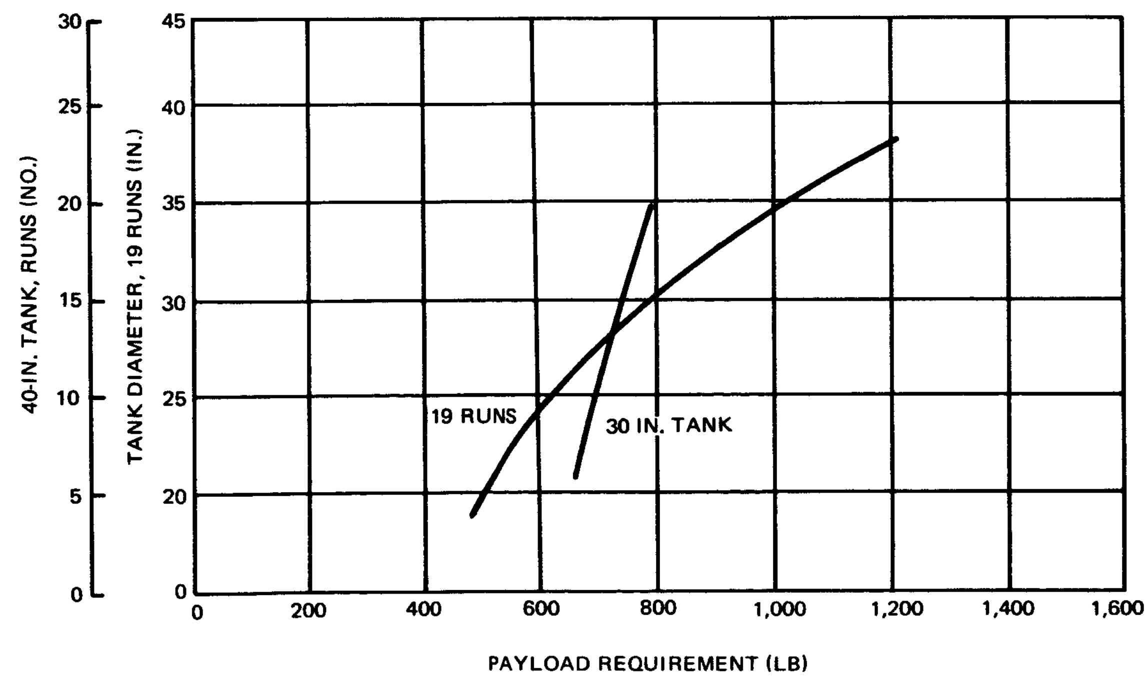

Figure 9-10. Experiment Payload for Ullage Control During Outflow

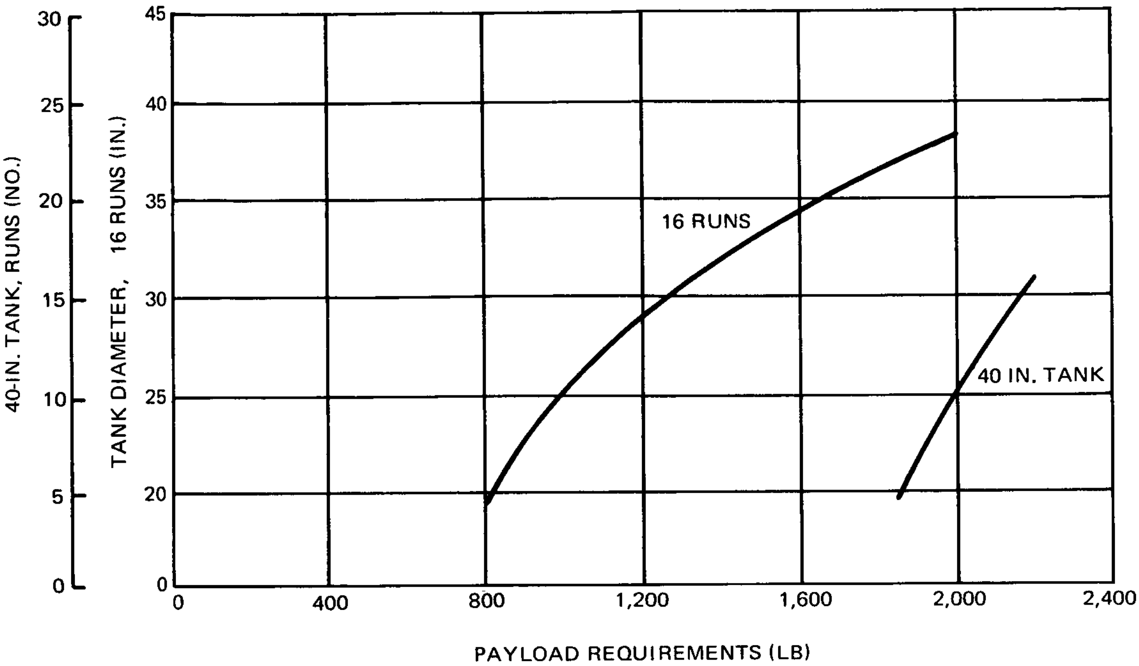

Figure 9-11. Experiment Payload for Scaling of Receiver Tank Thermodynamics

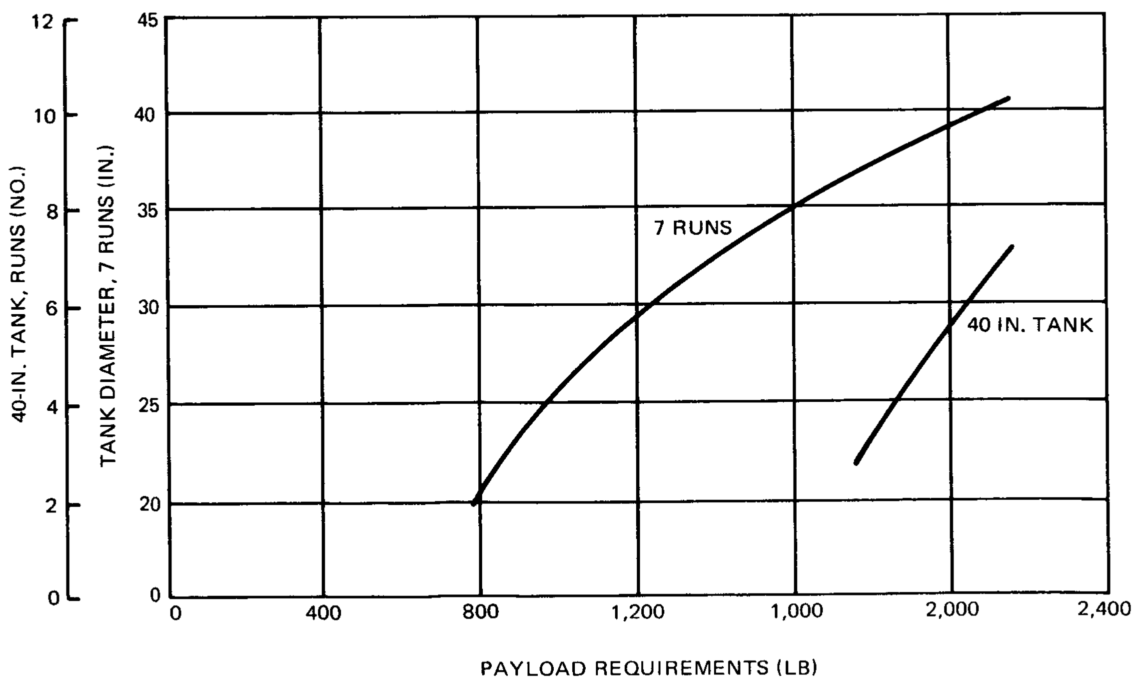

Figure 9-12. Experiment Payload for Receiver Tank Thermodynamics Verification

A weight breakdown by subsystems for each of the three experiments is presented in Table 9-4.

9.4.2 Experiment Fluid Usage Analysis

In both the outflow experiment and the receiver tank thermodynamics experiments untransferable residuals resulting from ullage pull-through will be the most significant source of depletion of experimental fluids. Since a cryogenic fluid will be used in the receiver tank experiments, additional losses will result from environmental heating, chilldown of experimental hardware, and evaporation during pressurized outflow.

Ullage pull-through losses were estimated using the correlation of Reference 2-10. At Froude numbers corresponding to the maximum S-IIB flow rate residuals at ullage pull-through would be on the order of 30%. For the case of the outflow experiment, the tank must be depressurized between runs, but not to a pressure lower than the vapor pressure of the hexane; so that the only losses of liquid overboard will result from entrainment of residual liquid

Table 9-4

EXPERIMENT SUBSYSTEM WEIGHTS

	Ullage Control 30-in. Tank--19 Runs	Receiver Tank Thermodynamics Scaling 40-in. Tank --16 Runs	Receiver Tank Thermodynamics Verification 40-in. Tank--7 Runs
Experiment liquid	305	1,250	1,250
Tanks, supports, plumbing	235	300	280
Pressurization	60	75	60
Ullage thrust	45	405	440
Attitude control	20	40	30
Electrical	120	120	70
Total	785 lb	2,190 lb	2,130 lb

during the blowdown. If venting is continuous with the transfer run and uses propulsive nozzles to keep the residual settled, it is felt that very little liquid will be lost overboard. For the case of outflow at high flowrate and high g level, it may be necessary to continue the transfer operation beyond pull-through at either the higher g level or the lower flow rate in order to ensure that sufficient propellant is contained in the other tank at the start of the next run.

For the inflow case using LOX, where most of the residual would be vaporized and lost overboard during the blowdown. It appears to be necessary to reduce the flow rate and increase the g level at the end of each run. Calculation indicates that the pull through residual can be limited to about 2% for a 30-in. tank and about 1% for a 40-in. tank if the highest experimental g level and lowest flow rate are used. A detailed study is needed to determine coordination of the procedure following the first inception of ullage pull-through, including the possibility of using thrust from the ullage blowdown for transferring part of the residual.

Methods developed during Phase B of Project THERMO for estimating environmental heating in an HPI system were applied to the inflow experiment configuration described above. Boiloff during ground hold, boost, and the insulation evacuation transient of about 10 hours was found to be negligible (less than 25 lb). The steady-state boiloff rate was found to be 1.2% per day for a 40-in. tank and 1.6% per day for a 30-in. tank.

The problem of boiloff resulting from chilldown of hardware is somewhat nebulous at this point because the requirements for hardware chilldown in the S-IIB mission are not well defined. At the start of transfer, the S-IIB LOX tank will have a cold forward dome and a relatively warm aft dome. For the receiver tank experiment, the hardware will be chilled to some extent by the blowdown in-between runs. Provisions for including heaters is recommended to provide for simulation of the warmer aft dome and the probability of a warm transfer line. Even if it is decided that these heaters need not be used for S-IIB simulation, some heat-up of the receiver tank hardware will be unavoidable. To provide an estimate of the impact of chilldown requirements on the experiment, a 200°R temperature change was assumed for the transfer line and 100°R for the tank and internal hardware. Calculations, assuming that all of the hardware sensible heat went into boiloff, indicated that the losses associated with the line chilldown would be negligible and that the losses for tank chilldown would be 0.8% per run for a 40-in. tank and 1.2% per run for a 30-in. tank.

Use of helium as the pressurant for transfer will result in loss of oxygen due to evaporation during pressurized outflow. This is a complicated process involving convective heat and mass transfer in the ullage as well as convective heat transfer in the liquid phase. It is assumed that, since the ratio of liquid surface area to mass is large, the liquid surface will be maintained at a rather low temperature and the evaporation rate will be controlled by the rate of heat transfer from the ullage to the liquid. This rate was estimated using standard natural convection correlations and was found to correspond to a propellant loss rate of 0.8% per hour for the 40-in. diameter and 1% per hour for the 30-in. diameter. This loss rate will apply both during the transfer and during the additional time required for reduction of ullage pull-through residuals.

An overall estimate of the rate of liquid usage is presented in Figure 9-13. For the purposes of preparing this estimate, the average experiment run time was taken to be 15 minutes and it is assumed that 8 runs would be made during each day. Since the receiver tank experiments involve attempts to complete the transfer operation without venting, it is important that the quantity of liquid transferred approach the 75% load value of the S-IIB. It is seen from Figure 9-13 that even with a 36-in. tank this will not be achieved for all runs. However, 36 in. is the largest diameter permitted by the Nimbus-type shroud. Use of a tank smaller than 36 in. in diameter would require that a large percentage of the runs not reach the 75% level.

9.4.3 Selection of Boosters

Since the E&F Atlas is considerably cheaper than the larger payload vehicles and since the 27-in. tank size is near the upper limit of existing plastic tank technology, the Atlas is recommended for the outflow technology experiment.

For the scaling and verification experiments for inflow thermodynamics, two factors require that the largest possible tank should be used. The first of these is the expected significance of the ratio of wall area to tank volume. It

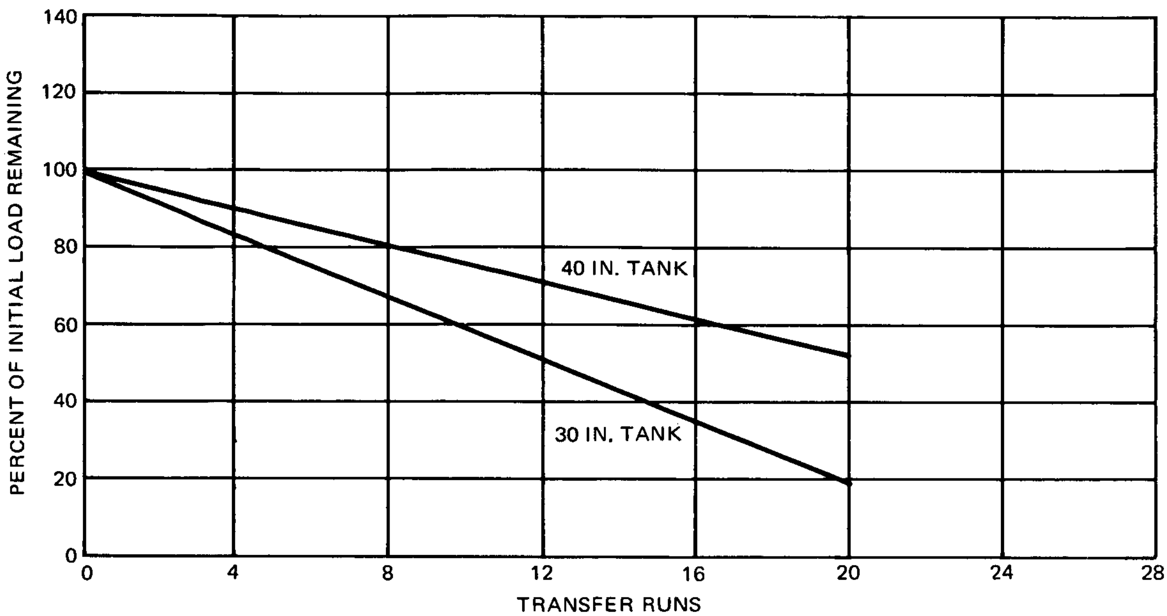

Figure 9-13. Rate of Liquid Oxygen Usage

is felt that the closest possible simulation of large tanks should be provided in this area. The second factor is the usage rate of the experimental fluid. It is seen from Figure 9-13 that the usage rate climbs sharply for diameters lower than the 36-in. diameter which is the maximum allowed by existing shrouds. To provide tanks of sufficient size, use of the Thor/Agena booster is recommended.

9.4.4 Selection of Preferred Experiment

The three experiments described in Sections 9.3.1, 9.3.2, and 9.3.3 were selected for recommendation because of the difficulties that would result from reduction to two launches.

The most significant result would be the reduction in the quantity of information obtained in each of the experiments. The outflow experiments would be most seriously effected since plastic tanks could not be used. It is felt that the plastic tanks represent a vast improvement in both scope and quality of experimental data obtained over the window mounted TV such as was used on AS203. Also, the results of the experimental liquid usage analysis indicate that the total number of runs will be limited to about 20 due to ullage pull-through losses and to evaporation losses during pressurized transfer. A program using 20 runs for the combined outflow and scaling experiment would eliminate several tests from Table 9-1 and 9-2.

Also, since the schedule in Figure 2-6 would have to be modified, the time for implementation of the results of the later outflow experiments would be shortened.

A further problem in regard to combination of experiments is that present scaling techniques for outflow yield different results from those for inflow thermodynamics. For example, the combination of flow rate and g level, which will simulate the Reynolds number and Froude number for the S-IIB, will not provide an appropriate combination of Bond number and outflow Froude number. Thus, particularly for the verification experiment, an individual run may not give usable data for both inflow and outflow.

9.5 INSTRUMENTATION LISTS

An instrumentation list for the outflow experiment is presented in Table 9-5. At the present time, it is felt that TV and flow rate data will be sufficient to satisfy the objectives of the experiment. Alternate methods of determining the liquid interface configuration such as temperature sensors and continuous or point liquid level sensors could easily be added at a later date if future work such as ground testing indicates them to be desirable. Pressurant inlet conditions will be measured for determination of their effect, if any, on the interface dynamics. Fluid temperature and pressurant storage conditions have been added to aid ground control of the experiment.

Table 9-6 presents an instrumentation list for the scaling experiment for receiver tank thermodynamics. The list for the verification experiment would be essentially the same with all measurements associated with the third tank in the scaling experiment deleted. The basic instrumentation for this experiment will be internal tank temperature sensors and tank wall skin patches. A small number of wide range temperature sensors will be provided to cover the initial phases of tank loading, but most of the internal temperature measurement will cover a narrow range of LOX temperatures, since it is felt that variations of liquid temperature throughout the tank will have a strong influence on the pressure transients. Other basic measurements are tank pressure, liquid flow rate, and tank inlet conditions.

Table 9-5

INSTRUMENTATION REQUIREMENTS FOR INTERFACE DYNAMICS DURING OUTFLOW EXPERIMENT OF PROJECT THERMO

Measurement Title	No. Req'd	System Range/Accuracy	Frequency Response	Environment at Point of Measurement	
				Media	Temp
Events	10	On-Off	2.4 cps (12 sps)		
Temperature He Storage Sphere	1	37 to 500 ± 14°R (±3%)	1 cps (4 sps)	He	37 to 620°R
Temperature Tk Inlet	1	37 to 500 ± 14°R (±3%)	1 cps (4 sps)	Hexane, He	37 to 620°R
Temperature Trans Line	2	260 to 560 ± 19°R (±3%)	1 cps (4 sps)	Hexane, He	260 to 620°R
Temperature Tk Vent	1	150 to 560±12.5°R(±3%)	1 cps (4 sps)	Hexane, He	150 to 620°R
Pressure He Storage Sphere	1	0-3500 ± 105 psi (±3%)	1 cps (4 sps)	He	37 to 620°R(1)
Pressure Vent	1	0-40 ± 1.2 psia (±3%)	1 cps (4 sps)	He, Hexane	37 to 620°R(1)
Pressure He Pres Orifice Inlet	3	0-500 ± 15 psia (±5%)	1 cps (4 sps)	He	37 to 620°R(1)
Pressure Tk Ull (2 per tank)	4	40 ± 1.2 psia (±3%)	1 cps (4 sps)	Hexane, He	150 to 620°R(1)
Pressure Tk Inlet	1	0-100 ± 3 psia (±3%)	1 cps (4 sps)	He, Hexane	37 to 620°R(1)
Flow Transfer	2(2)	0.5 ± 0.015 lb/min (Measure Liquid Only)	1 cps (4 sps)	Hexane (Operating Range 0.1 to 0.4 lb/sec)	300 to 660°R (Two-Phase) 0 to 50 psia
TV Cameras	2				

NOTES: (1) Sensing line must isolate transducer to provide -60 to +165°F environment
(2) Must measure flow in both directions--requiring two flowmeters

Table 9-6 (page 1 of 2)

INSTRUMENTATION REQUIREMENTS FOR RECEIVER TANK THERMODYNAMICS (PROPELLANT TRANSFER) EXPERIMENTS

Measurement Title	No. Req'd	System Range/Accuracy	Frequency Response	Environment at Point of Measurement	
				Media	Temp
Events	25	On-Off	2.4 cps (12 sps)		
Temperature LOX Prop Trans Tank Liq	45	155 to 170±0.45°R (±3%)	1 cps (4 sps)	GOX;LOX; He	100 to 620°R
Temperature LOX Prop Trans Tank Gas	15	100 to 400 ± 9°R (±3%)	1 cps (4 sps)	GOX, LOX; He	100 to 620°R
Temperature LOX Prop Trans Tank Surf	30	100 to 400 ± 9°R (±3%)	1 cps (4 sps)	GOX;LOX; He	100 to 620°R
Temperature LOX Prop Trans Line Liq	3	160 to 170±0.3°R (±3%)	1 cps (4 sps)	GOX; LOX; He	100 to 620°R
Temperature LOX Prop Trans Line Gas	5	100 to 250±4.5°R (±3%)	1 cps (4 sps)	GOX;LOX; He	100 to 620°R
Temperature He Storage Sphere	1	37 to 500±14°R (±3%)	1 cps (4 sps)	He	37 to 620°R
Temperature LOX Prop Trans Tank Inlet	2	37 to 500±14°R (±3%)	1 cps (4 sps)	He;GOX; LOX	100 to 620°R
Temperature LOX Tank Vent	1	150 to 560±12.3°R (±3%)	1 cps (4 sps)	GOX;LOX; He	37 to 620°R
Pressure LOX Prop Tank Ull	6	0 to 60 ± 1.8 psia (±3%)	1 cps (4 sps)	LOX;GOX; He	100 to 620°R[1]
Pressure LOX Tank Ull Diff	2	±10 psid ± 0.6 (±3%)	1 cps (4 sps)	LOX;GOX; He	100 to 620°R[1]
Pres He Storage Sphere	1	0 to 3500±105 psia (±5%)	1 cps (4 sps)	He	37 to 620°R
Pres He Pres Orifice Inlet	1	0 to 500 ± 15 psia (±3%)	1 cps (4 sps)	He	37 to 620°R

Table 9-6 (page 2 of 2)

Measurement Title	No. Req'd	System Range/Accuracy	Frequency Response	Environment at Point of Measurement	
				Media	Temp
Pres LOX Tk Inlet	2	0 to 100 ± 5 psia (±5%)	1 cps (4 sps)	He	37 to 620°R
Pres LOX Tank Vent	1	0 to 60 ± 1.8 psia(±3%)	1 cps (4 sps)	LOX;GOX; He	37 to 620°R
Flow LOX Transfer	2	0.5 to 12 lb/sec (±3%) (Measure liquid phase only)	4 cps (20 sps)	LOX;GOX; He (Two-Phase)	100 to 620°R
Flow LOX Tank Vent	1	TBD (±3%)	4 cps (20 sps)	LOX;GOX; He	37 to 620°R
Level Liq	6	Liq/Vapor Indicator	(Loading Only)	LOX;GOX; He	100 to 620°R

NOTES: (1) Sensing line must isolate transducer to provide -60 to + 165°F environment

Section 10
BOILING HEAT TRANSFER EXPERIMENTS

10.1 ORBITAL EXPERIMENT INFORMATION REQUIREMENTS

The technology survey showed that a better understanding of boiling is necessary to efficiently design the S-IVC and Nuclear Stage propellant storage systems. Boiling data is required for the development and proper use of present and future models which predict the propellant tank pressure time history. Specifically, the criteria predicting incipient boiling is needed to define under what conditions the existing non-boiling stratification models can be used. Also, the development of models which include boiling, should it occur in these vehicles, will require information on the mechanism of boiling, including the ranges of boiling regimes and bubble dynamic phenomena.

10.1.1 Incipient Boiling

Available analytical methods indicate that the transient periods involved in the low-gravity study of boiling exceed the capabilities of drop towers and aircraft. Consequently, orbital experiments are necessary.

To determine the heat flux at which boiling initiates on a vertical wall, it is necessary to measure a bracketing range of heat fluxes to locate the critical value with certainty. Because the transient period of boundary layer development at the heat fluxes below incipience is proportional to $g^{-1/2}$, the time to steady state increases considerably in a low gravity field. Figure 10-1, based on a simplified analysis (Reference 10-1), indicates that this period is of the order of hours in the low heat flux region where incipience is expected.

10.1.2 Boiling Regimes

It is also important to study the heat transfer mechanism in the nucleate boiling regime. Again, the transient period is an important consideration, but little analyses exist. The time it takes for a vapor bubble to grow to

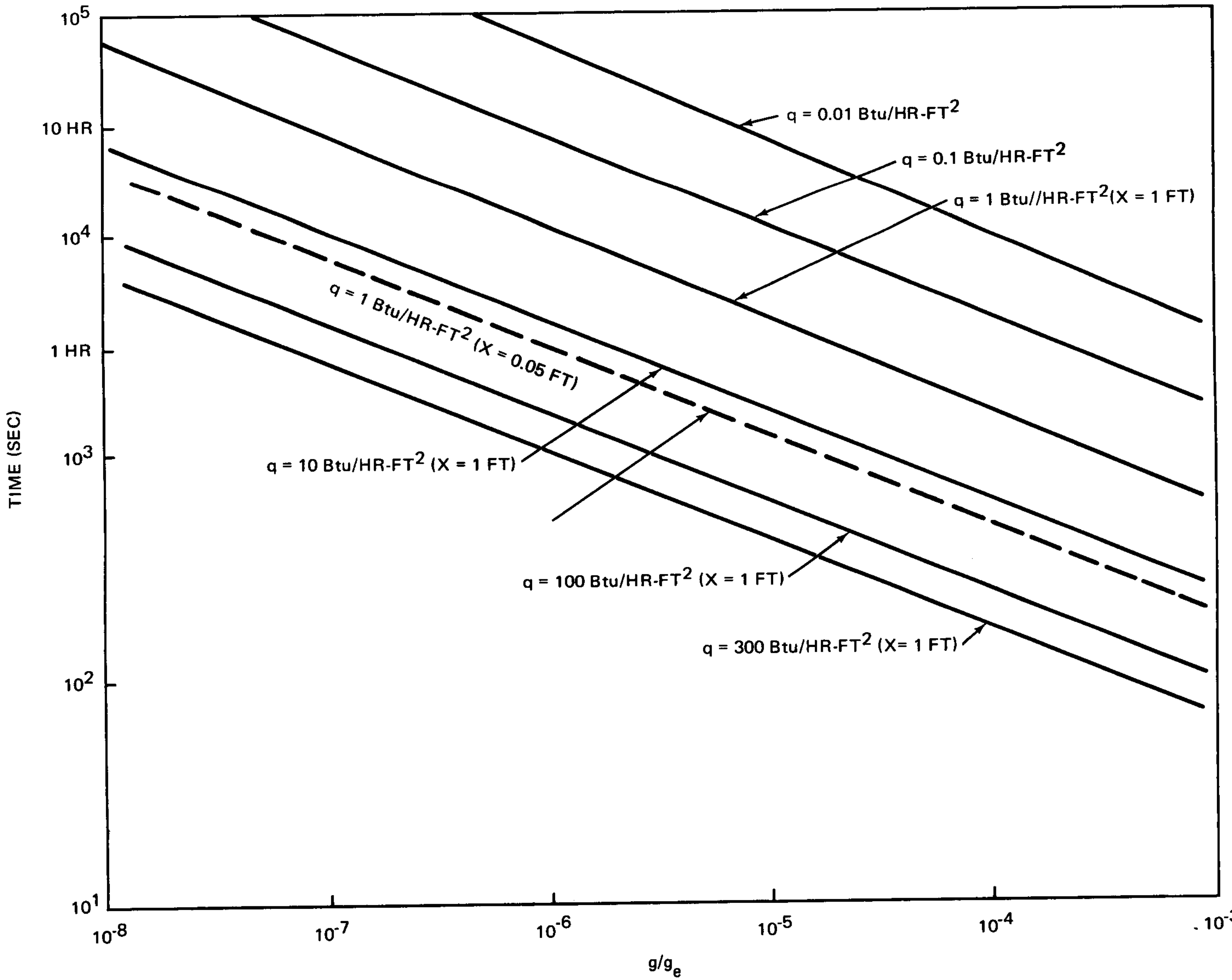

Figure 10-1. Non-Boiling Transient Time (LH_2)

some reasonable breakoff diameter was assessed, Figure 10-2. The time increases as heat flux and gravity are reduced (Reference 10-2) and is large for heat flux values of interest, about 1 $Btu/hr\text{-}ft^2$. Although this period is not necessarily the transient period, but only the time necessary for bubbles to grow to sufficient size to be removed, the results show time periods which are excessive for drop tower and aircraft experimentation. Also, the development of bubble flow over the heater is expected to require time periods which exceed simulated low gravity capabilities.

10.2 DATA ACQUISITION PROGRAM AND EXPERIMENT REQUIREMENTS

The basic objectives of the orbital boiling heat transfer study are obtaining the criteria for predicting the onset of nucleate boiling and establishing the domains of boiling. The heat flux-gravity incipient boiling relationship for different levels of subcooling is required to determine under which propellant tank boundary conditions boiling will occur. The various boiling regimes require definition so that the effect of boiling on thermal stratification and tank pressure rise can be assessed.

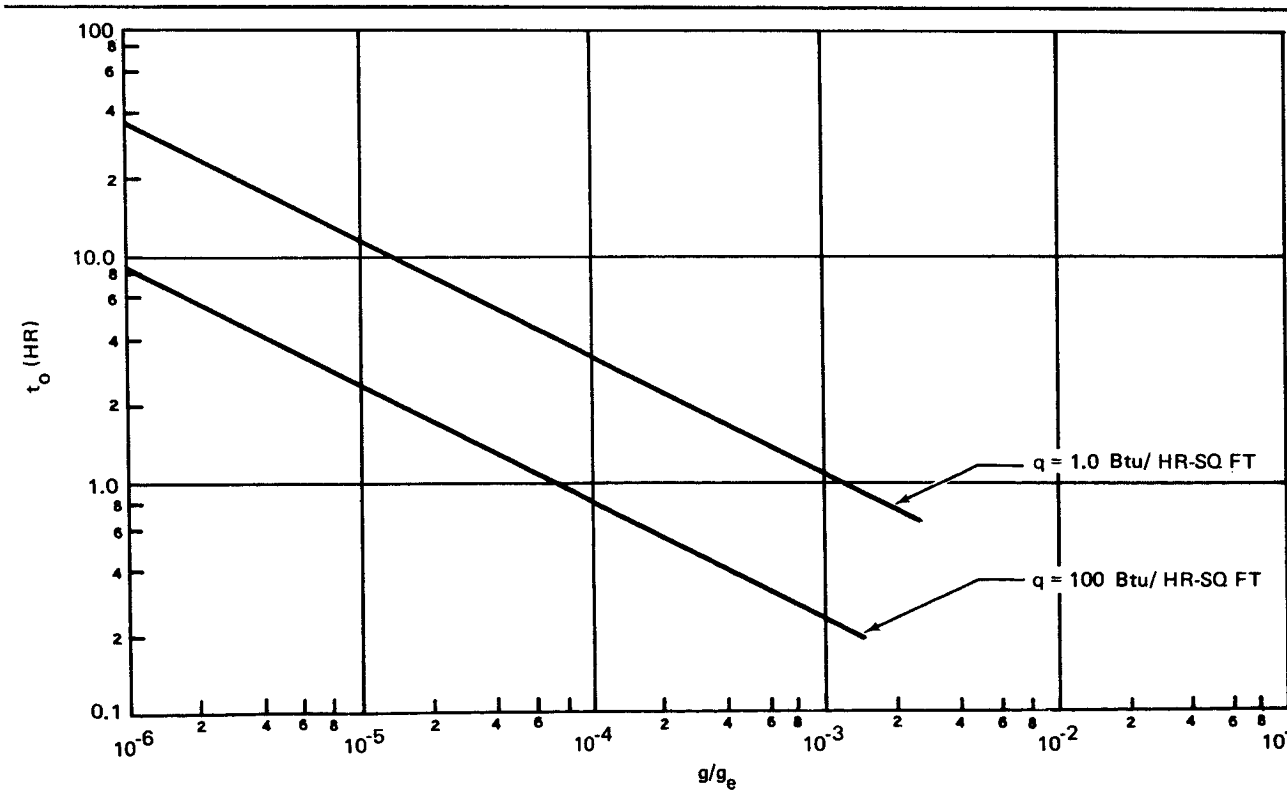

Figure 10-2. Time for Bubble to Grow to Breakoff Diameter

10.2.1 Incipient Boiling

Figure 10-3 shows an approximation of the heat flux-gravity relationship for incipient boiling. The intersection of the natural convection portion of the boiling curve with the nucleate boiling portion, assumed to remain invariant with gravity, was used to obtain the nucleate boiling threshold. A similar graph could also be constructed assuming that the temperature of the heater surface at the onset of boiling remained invariant with gravity. Results differ somewhat but both show the same trends with a lower incipient heat flux indicated for a reduced gravity environment. Since the heat flux values shown approximate a propellant tank of LH_2 insulated with HPI, it appears necessary to develop a more accurate prediction correlation.

Method of Obtaining

Two methods can be used to experimentally obtain incipient boiling criteria. The first is to plot the steady-state heater temperatures for each value of heat flux. By starting with values below the expected incipient point and proceeding to values above it, a curve which changes slope rather abruptly is

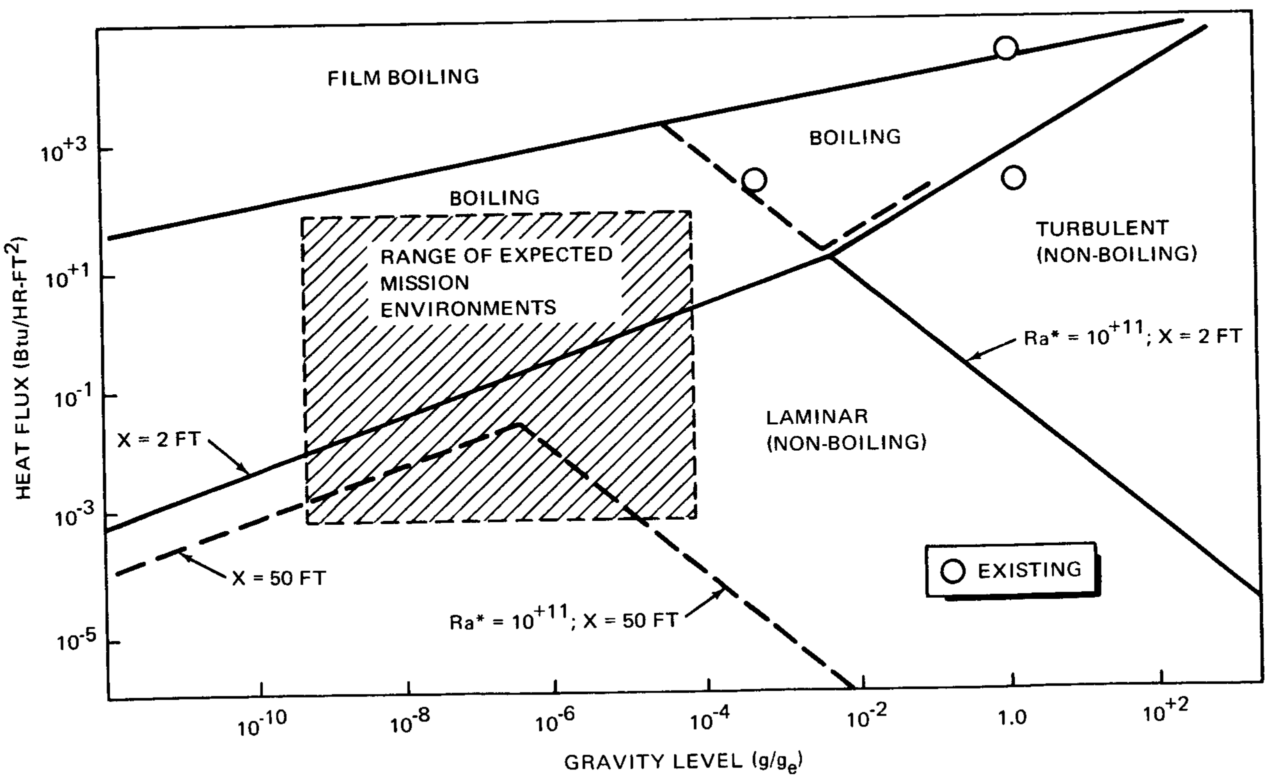

Figure 10-3. Heat Transfer Envelope

expected. The location of the change in slope should be in the vicinity of the incipient point since vapor bubbles enhance the heat removal mechanism and, hence, cause the slope of the boiling curve to increase. Figure 10-4 illustrates how this may be done using a 10^{-5} g/g_e model to locate the possible data points.

The second method is to visually observe the heater surface to ascertain the heat flux at which bubbles are first formed.

Development of Correlation

The development of a correlation will require a relationship between the incipient heat flux and the gravity level. The confidence level which canbe placed on such a relationship will depend both on the experimental accuracy and the number of gravity levels which are investigated. The 1 g/g_e value can be obtained with little difficulty since time and instrumentation problems are minimal. A second data point would provide the opportunity of drawing a straight line through the two points. This, of course, can be misleading,

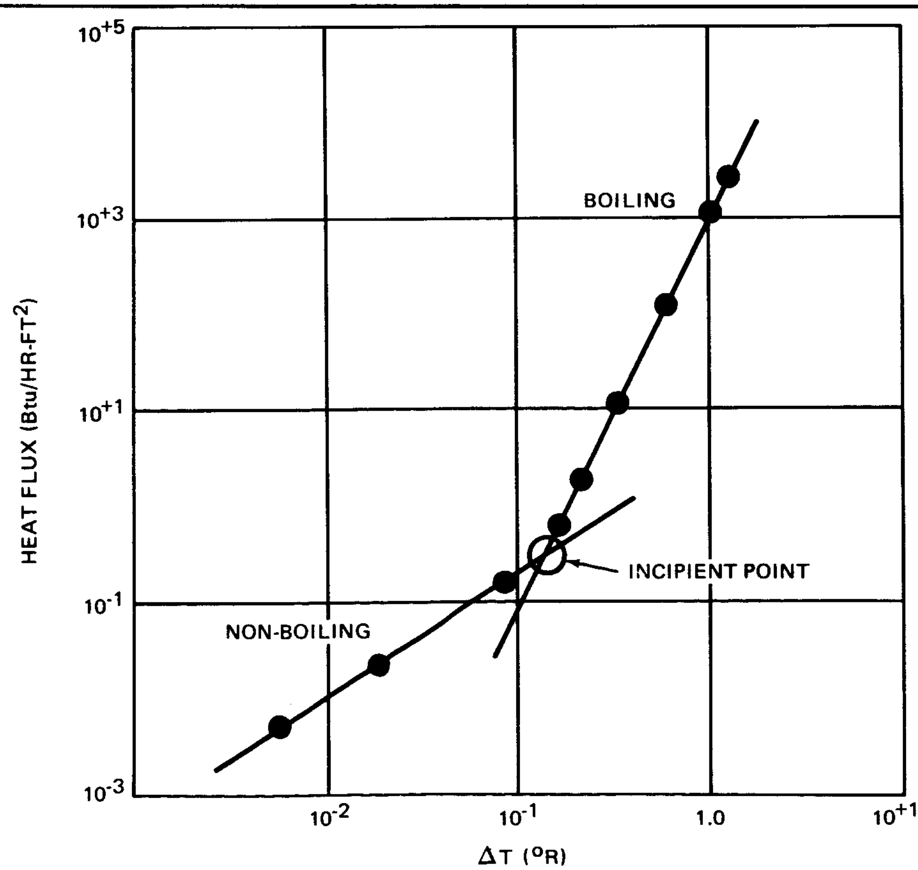

Figure 10-4. Location of Incipient Boiling Point

but would give some indication of the trend of the heat flux-gravity relationship as well as the magnitude of the trend. For a small experiment package, where more than one gravity level is not possible, it is suggested that 10^{-5} g/g_e be investigated since this covers the widest possible experimental range. However, for larger capacity experiment payloads, gravity levels of 10^{-3} and $10^{-4} g/g_e$ should also be studied. Figure 10-5 is a plot of the proposed data points and possible trend of the relationship on a logarithmic scale.

10. 2. 2 Boiling Regimes

The application of orbital boiling heat transfer experimental results to the thermal stratification problem can be made on two levels of complexity. A qualitative assessment of the effect of boiling on thermal stratification and pressure rise rate can be made from boiling movies. Here the overall characteristics of the boiling phenomenon for different heat flux-gravity domains can be obtained. The size, number and trajectories of the vapor bubbles yields insight into the potential effect these bubbles will have on the distribution of thermal energy within the propellant.

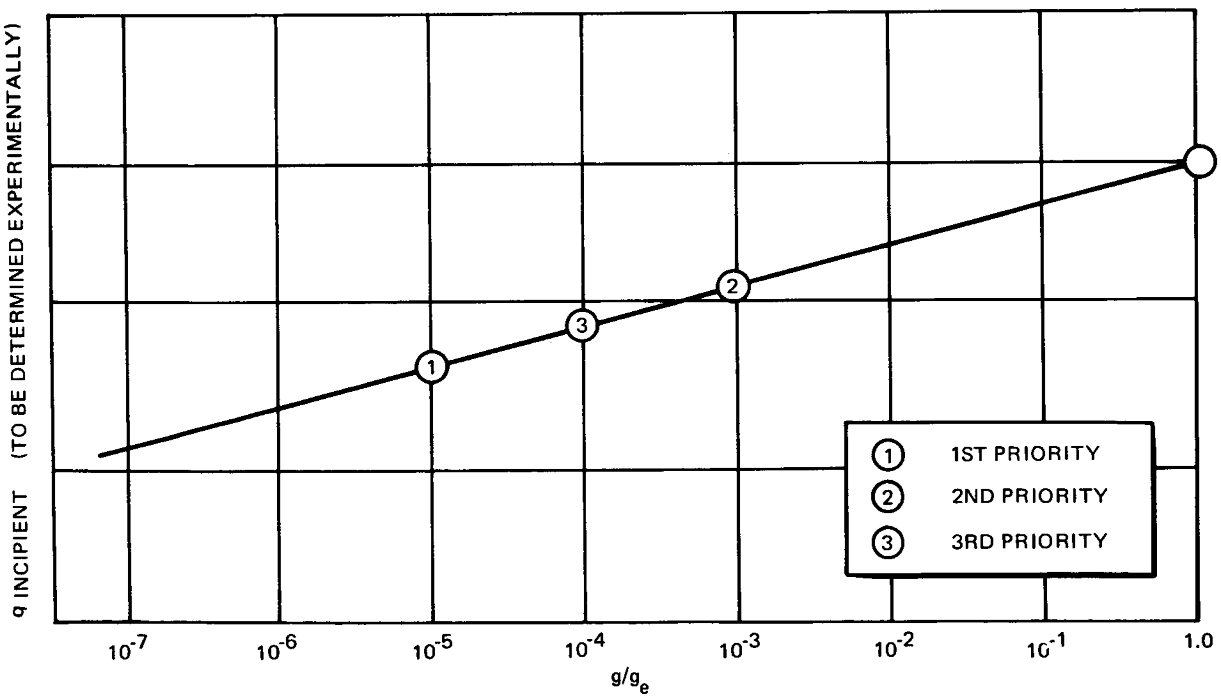

Figure 10-5. Incipient Heat Flux-Gravity Relationship

A more quantitative analysis of the data will provide information necessary for the development of an analytical model for stratification with boiling. This will come from the results of the boiling curve and the visual observations. Several two phase boundary layer models for flow over a flat vertical surface have been found in the literature (References 10-3 and 10-4). Each includes a term in its energy equation representing the fraction of vapor by volume in the boundary layer. The present models, however, have simplified their analyses by treating this fraction as a constant. It is expected however, that this value varies as a function of length along the heated wall and depends also on the heat flux and gravity level. In addition the film coefficient, obtained from the boiling curve, is required to obtain a relationship between wall shear and the heat flux. Finally a more detailed relationship between bubble and liquid velocities is required including its relationship to the vapor volume fraction. Chin et al (Reference 10-3) assumes that the slip ratio between the bubble velocity and the mean fluid velocity is constant. Petrick (Reference 10-5) has shown that the ratio of the two velocities is a function of the vapor volume fraction.

Another important relationship using the same data is the fraction of the total heat flux which goes into vapor considering the entire heated surface. The trend of this fraction with gravity will be obtained if experimentation is conducted at several gravity levels and visual coverage is available. Large fractions would indicate more rapid pressure rise rates and small fractions would result in slower rise rates. However, the effect of sub-cooling is required to determine what percentage of the vapor collapses in the bulk before reaching the surface.

Because the self-pressurized vehicle tank will likely result in thermal stratification and hence liquid subcooling, the effect of subcooling on incipient boiling should be investigated. Figure 10-6 illustrates the type of results which might be obtained. The trend of incipience with (T_{sat} - T_{bulk}) at 1 g/g_e may be sufficient for understanding the subcooling effect at lower gravity levels. However, lacking a good analytical model, it is necessary to determine experimentally whether or not this is the case.

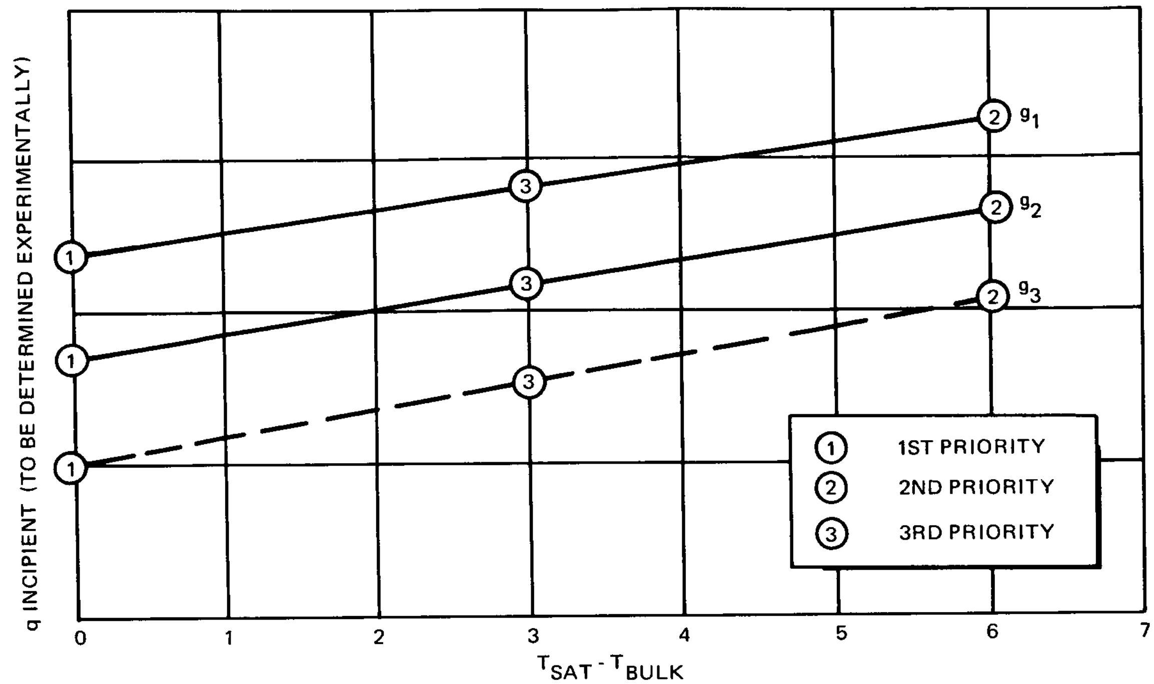

Figure 10-6. Effect of Subcooling and Gravity on Incipient Boiling

Method of Obtaining

The method of obtaining the above data relies to a large extent on television coverage. Information such as bubble breakoff sizes and bubble growth rates will depend on being able to clearly distinguish between distinct vapor forms. The determination of the vapor volume fraction or the fraction of the total heat flux going into vapor will be more difficult to achieve.

Vapor volume fractions must be made by measuring the volume of vapor in a control volume at some given location on the wall.

If the bubble sizes become as large or larger than the heater surface, which is a possibility at 10^{-5} g/g_e, then the vapor volume fraction as related to any boundary layer flow will become meaningless. On the other hand, the amount of wall heat flux going into vapor should be measurable under all conditions.

Here a control volume surrounding the entire heater surface is defined and the number and size of the vapor bubbles crossing the boundary of this system can be tabulated over a fixed time increment. The amount of vapor leaving the control volume plus the accumulation or depletion of vapor within the control volume yields the net formation of vapor at the wall. Since the wall heat flux is known, the fraction of this total heat flux which went into vapor is easily obtained. Two television cameras 90° apart are required to accurately measure all of the bubbles formed, since a wide heater surface with only a single side view camera would probably result in many bubbles being obscured. Care will also have to be taken to provide an optimum background for easy viewing of the bubbles.

Bubble velocities along the heated wall can be measured as long as the bubbles are small compared to the heater itself. Bubble size and location with respect to the heater can also be determined.

The boiling curve is obtained by measuring the difference in temperature between the heater surface and the liquid for each heat flux. The heat flux is obtained from the power input to an electrical heater placed on the non-wetted surface of the heater plate. The temperature difference will be measured with platinum resistance sensors.

Development of Correlations

The development of correlations related to the boiling phenomenon can range from bubble growth to the vapor volume fraction. Many correlations involving bubble forces not directly related to the present low gravity propellant storage problem could also be derived from the expected data.

Present bubble breakoff diameter predictions assume that breakoff occurs when the bouyancy force on a bubble exceeds the surface tension force. Others include a factor which considers the forces involved in the rapid growth of a bubble. These techniques hold for isolated bubbles where it is not clear as to whether or not the breakoff diameter is related to the heat flux. But, it appears that the mean breakoff diameter of a non-isolated bubble is both heat flux and gravity dependent (Reference 10-6).

This could be stated as follows:

$$D_{isolated} = D(g, \text{ liquid properties})$$

$$D_{non\text{-}isolated} = D(g, q, \text{ liquid properties})$$

Bubble growth rates will be difficult to measure in the early growth period due to camera resolution problems with small bubbles in a large field of view. The growth rate measurement as the bubble size increases will also be difficult if not impossible since coalescence or interference with other bubbles may occur. Individual bubbles which are observed and measurable can be used, however, to check existing correlations which do not include a gravity effect. In fact, present low gravity experiments (References 10-6 and 10-7) with water have only indicated that the growth rate has decreased as time increased for the larger bubbles. Thus, bubble growth data would provide some check on existing correlations for bubble growth rates as well as on the limited amount of existing low gravity data.

The vapor volume fraction is expected to depend on the distance along the heater surface, the heat flux and the gravity level as well as certain liquid properties. By examining the data where two of the three independent parameters (q, g, x) are held constant, the effect of the third parameter on this fraction can be assessed. Intuitively it would seem that vapor volume fraction will increase for increasing x and q and decreasing g. The precise form of this functional relationship is to be determined. A similar correlation is expected for the fraction of the heat flux which goes into vapor where the independent parameters may be plate length and q and the vapor fraction f is based on the entire heater surface.

Bubble velocity correlations along a vertical wall should differ from those in a stationary liquid. The effect of the velocity of the rising liquid will be superimposed onto the bubble velocity due to buoyancy. This can be expressed in terms of the slip ratio which is the ratio of the vapor velocity to the mean liquid velocity. Since the bubble velocity in a stationary liquid depends on the bubble size and gravity level, the slip ratio will probably depend on the size distribution of the vapor masses.

Slip ratios have been examined in closed conduits but nothing has been found in the literature for a flat vertical wall. If none exist, additional analytical and 1 g/g_e experiments must be considered in conjunction with the low g data. At present it appears that a rough estimate of the mean liquid velocity can be made assuming uncoupled single phase liquid flow with a wall heat flux of (q_{total} -$q_{vapor\ bubbles}$). An experimental method of estimating this liquid velocity for the LH_2 along the heater wall should also be considered.

10.3 CONCEPTUAL DESIGNS

Several payload weights were found to be suitable for boiling heat transfer experiments in orbit. The degree of sophistication and the quantity of data naturally increase with increasing booster payload capability. Figure 10-7 shows the expected data for each of 3 payloads. The larger payload allows several gravity levels to be selected and provides additional data concerning the effect of subcooling on boiling.

The 350 lb payload provides both incipient boiling and the boiling curve (saturated LH_2). No visual check of the incipient boiling point or bubble dynamic data will be available with this setup. There is the possibility of including one subcooling level.

The 700-lb payload provides the capability for a TV camera. This should increase the confidence level in the determination of the incipient point. Also, visual coverage of the boiling phenomenon in the nucleate boiling regime will provide information on the nature of the boiling process over a range of heat flux values. In addition, boiling curves can be obtained for 10^{-4} and $10^{-5} g/g_e$.

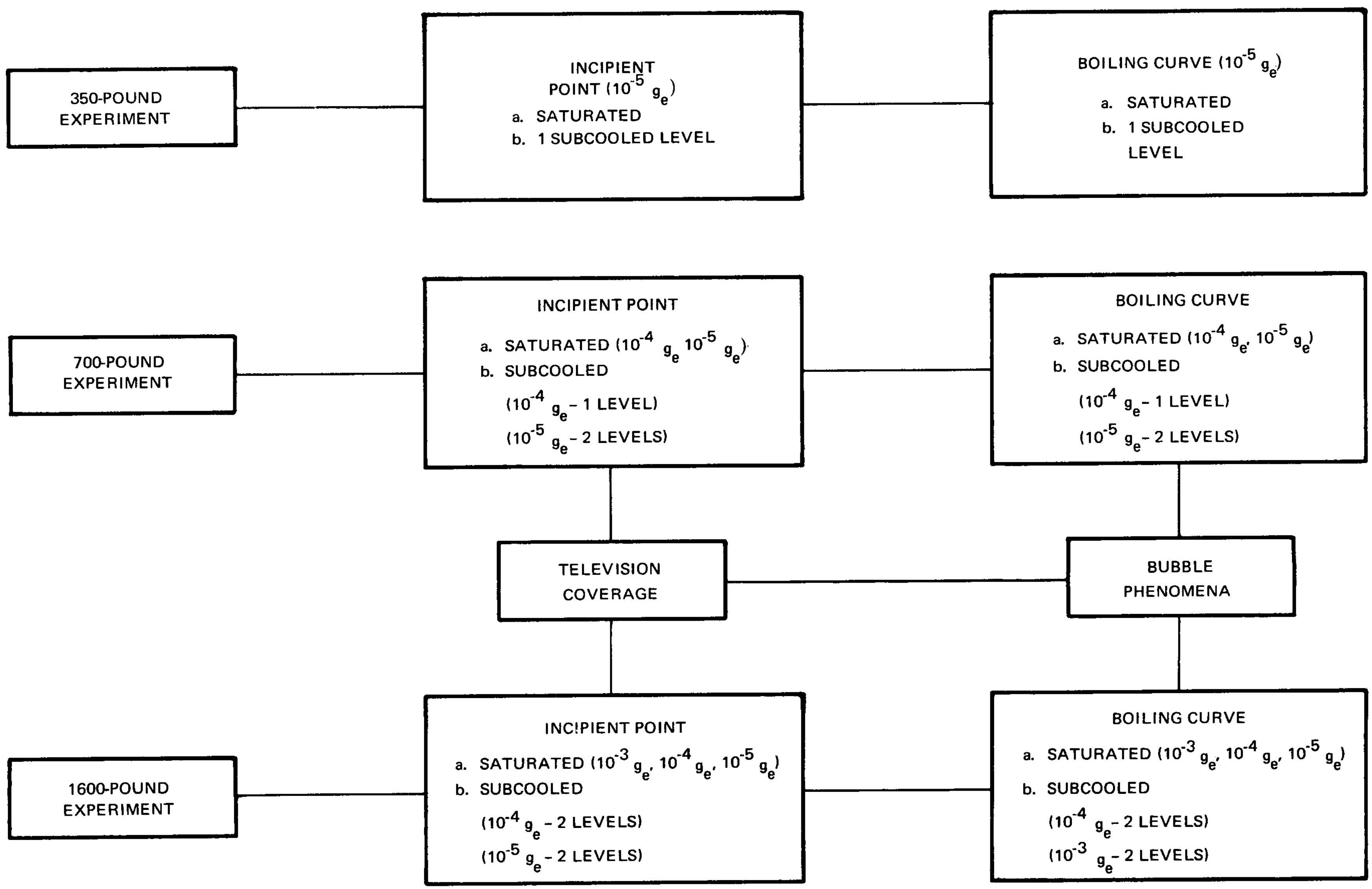

Figure 10-7. Potential Boiling Payloads

The 1,600-lb payload increases the scope of the boiling experiment considerably. Here two television cameras could be used which provides the third coordinate to view the bubble growth phenomena. Subcooled boiling can also be studied where two levels of subcooling can be included at 10^{-4} and $10^{-5} g/g_e$. At $10^{-3} g/g_e$ only the saturated condition should be considered due to APS weight limitations.

10.3.1 350-lb Payload

Figure 10-8 is a sketch of the configuration experiment tank. The experiment itself consists of a vertical heater element with temperature sensors attached to it as well as in the liquid. A gravity level of $10^{-5} g/g_e$ can be supplied by the APS system for approximately four days enabling a boiling curve to be obtained for saturated hydrogen as well as for one level of subcooling.

Data Point

This experiment determines the incipient boiling point at 10^{-5} g/g_e by finding the change of slope in the boiling curve. Table 10-1 shows the individual data points along with experiment time and power requirements.

Experiment Sequence

Because only 22 data points need to be measured, direct telemetry once every orbit is sufficient to record data. The experiment sequence should follow the list of data points (Table 10-1) since it is desirable to construct a boiling curve starting from the low heat flux values. Without considering settling periods or time periods between data points for bubbles to move out of the heater region, 72 hours are required to take the 22 data points where no more than one data point per orbit was considered. Approximately 100 hours was used for the total experiment time for boiloff estimates. Subcooling can be obtained by heating the ullage with an electrical resistance ribbon.

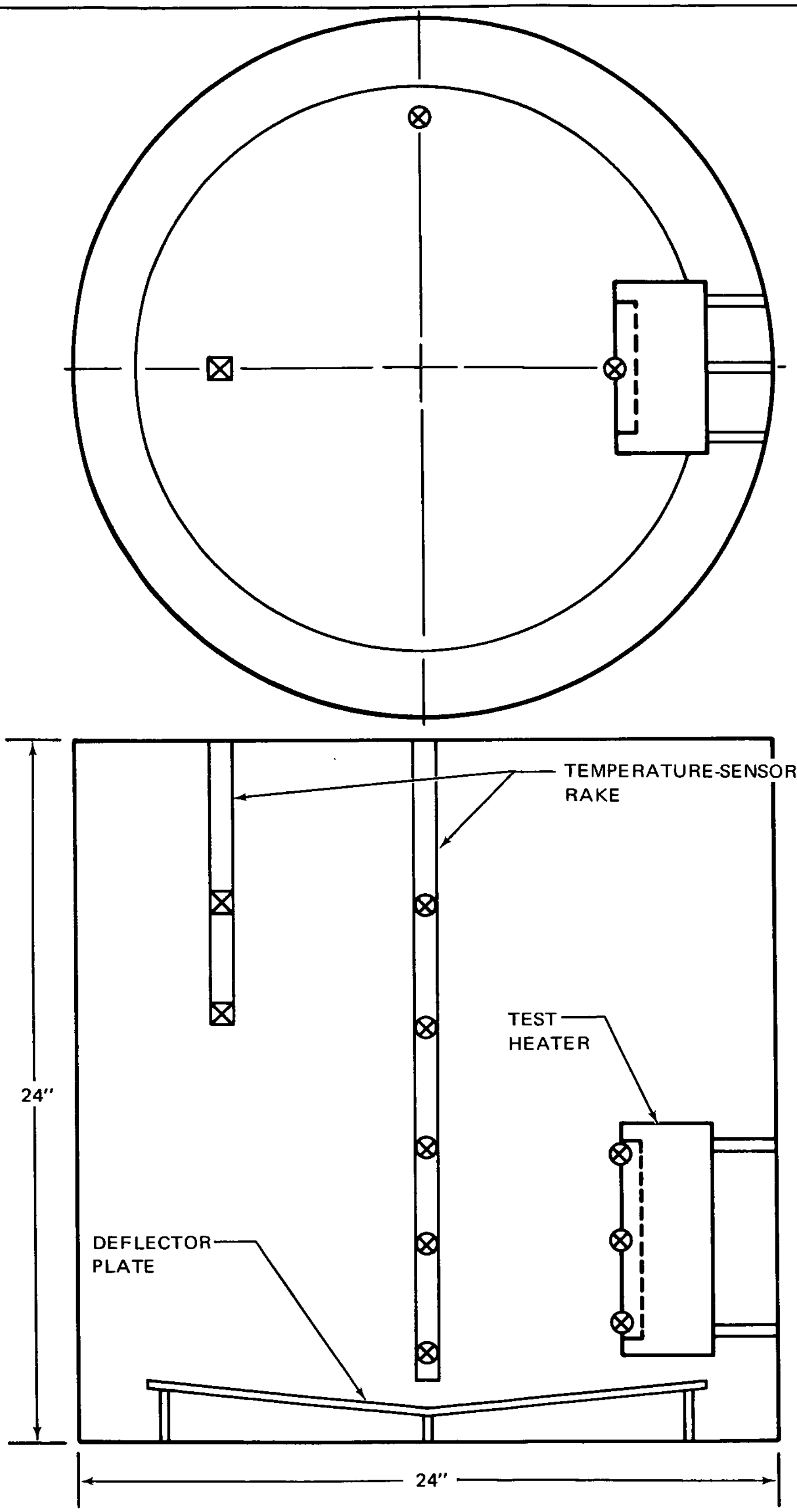

Figure 10-8. 350-lb Experiment Tank

Table 10-1

350-POUND EXPERIMENT LIST

Experiment Number	g/g_e	Heat Flux (Btu/hr-ft^2)	Total Test Time (hrs)	Heater Power (kW)	Energy Used (kW-hr)
350-1	10^{-5}	0.005	10.00	0.001	0.01
350-2		0.010	8.00	0.002	0.02
350-3		0.400	1.80	0.080	0.02
350-4		2.000	1.50	0.400	0.60
350-5		10.000	1.20	2.000	2.90
350-6		100.000	0.33	20.600	6.90
350-7		320.000	0.33	65.000	21.70
350-8		1,000.000	0.33	206.000	68.70
350-9		1,500.000	0.33	300.000	100.00
350-10		320.000	0.33	65.000	21.70
350-11		10.000	0.33	2.000	0.67
350-11	10^{-5}	1.000	1.60	0.200	0.30
			26.08		223.50

*350-S-12 through 350-S-22 for 6° subcooled.

Data Acquisition

The principle instrumentation is the heater surface temperature sensors and those in the liquid itself. A pressure sensor is also required to measure the absolute pressure inside of the tank. Some method of measuring the acceleration level will be necessary. The simplest method may be to use the thrust from the APS system although accelerometers which could be calibrated down to 10^{-5} g/g_e would be a more desirable method.

The heater surface is approximately 3 in. wide by 8 in. long and has temperature sensors mounted in the plate at the top, center and bottom of the plate. One temperature sensor is used for the range between 0 to 1.0°R to minimize error in the vicinity of incipient boiling. As shown in Figure 10-8, two temperature sensor rakes will be required to provide the liquid temperature. These are offset to minimize the chance of impeding bubble motion.

Heater Design

A heater design similar to that used in the Project THERMO pilot test program (See Reference 2-7 for discussion) is a likely candidate. Heat loss errors are larger in the low heat flux regime with this design. If thermal conductivity values for foam insulation are of the same order of magnitude as hydrogen gas, then errors will be within an acceptable range. If this is not the case, then an alternative heater design as listed in Reference 2-7 will be necessary.

Power

The electrical energy requirements are approximately 4 Kw Hrs. Based on the available batteries (Section 3) this power requirement lies between the lighter fractional Kw Hr. batteries and the heavier 12 Kw Hr. battery weighing 155 pounds. Unless a battery of intermediate power and weight can be found, the 155 pound battery will be required. However, its excessive weight and unnecessary energy supply severely penalizes the experiment.

Summary

Table 10-2 lists the necessary items for the experiment payload. Included are the power and energy requirements. Note that the total weight is approximately 80 pounds over the 350 pound limit. However, as discussed above further investigation of available battery power supplies is required before refinements in the total weight of the package can be made. For example, if a 6Kw Hr. battery that is approximately one half of the weight of the 12 Kw Hr. battery were available, then the package weight could be reduced to the 350-lb limit. In addition, it is expected that further investigation into the power requirements of the additional components will show that the present values may be conservative.

10.3.2 700-lb. Payload

The 700-lb experiment package conceptual design is somewhat similar to the preferred 1,600-lb package (Section 10.3.3). The major difference is a shorter mission period where no 10^{-3} g/g_e data is obtained and only one level of subcooling is studied, at 10^{-4} g/g_e. Only one television camera is available which detracts from complete visual coverage of the boiling phenomenon.

Many of the components of this package are the same as that for the 1,600-lb package. The heater, itself, is one foot in height so that the experiment tables for the 1,600-lb experiment apply. Figure 10-9 is a sketch of the proposed tank for this boiling experiment. Table 10-3 provides the list of experiment components, their weights and the energy required for the mission. Note that the electrical energy consumption is about the same as that produced by one 155-lb battery. This was based on a mission period of 100 hours. The available energy thus appears to be marginal as is the weight at 733 pounds. However it appears compatible with the Atlas E and F based on conceptual design calculation. However more precise weight and energy estimates along with a detailed design of the package are necessary.

Table 10-2

350-POUND PAYLOAD EXPERIMENT COMPONENTS

Item	Weight (lb)	Power (watts)	Energy (watt-hr)
Guidance Sensor and Computer	20	30	3,000
Sequencer	5	0.45	45
Antenna	4		
TM Command Receiver	3	6	600
Batteries	155		
Tank (including LH_2 and fittings)	60		
50 Channel TM--no recorder	34	95	285
50 Transducers	25		
ACS	65		
APS (10^{-5} gc for 100 hr)	50		
Heater	5	300 (maximum)	634
Beacon	4	3.9	390
	430		4,954

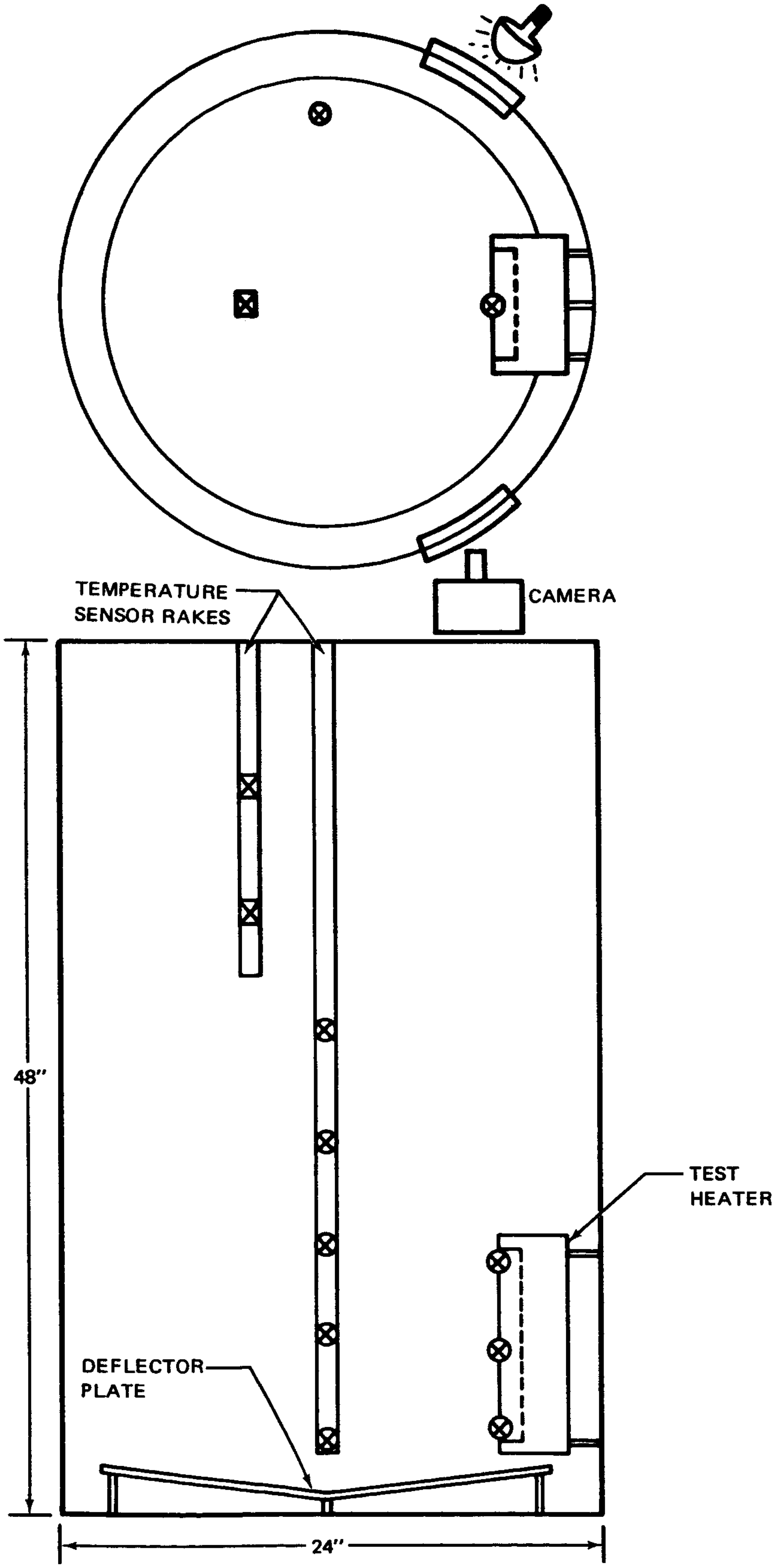

Figure 10-9. 700-lb Experiment Tank

Table 10-3

700-POUND EXPERIMENT COMPONENTS LIST

Item	Weight (lb)	Power (watts)	Energy (watt-hr)
Guidance Sensor and Computer	20	30	3, 000
Sequencer	10	0. 45	45
Antenna Beacon	4	3. 9	390
TM Command Receiver	3	6	600
Tank (entire)	190		
50 Channel Recorder (8 hrs)	43	122	976
50 Transducers	25	55	55
ACS	130		
APS	110		
Heater	10		2, 411
Battery	155		
TV System			
Transmitter	18	50	500
Power Amplifier	2	140	1, 400
Camera and Controls	10	12	120
Light	3	100	1, 000
	733		10, 897

10.3.3 1,600-lb Payload

Most of the experiment goals listed for the Project THERMO Phase B boiling experiment can be met with this size experiment. However, only a vertical heater surface is included here.

Of the three experiment packages, this one is preferred and recommended because it offers the most comprehensive experiment. Figure 10-10 presents a conceptual design.

Experiment

Boiling curves for saturated hydrogen can be obtained at 10^{-3}, 10^{-4}, and 10^{-5} g/g_e. In addition, subcooled boiling curves can be obtained at 10^{-4} and 10^{-5} g/g_e for two subcooled levels. These results will yield the incipient point both as a function of gravity and degree of subcooling. Television coverage provides an additional check on the determination of the incipient point.

The boiling mechanism itself can be recorded with the cameras. This provides information on bubble size, bubble motion, and the amount of energy which goes directly into vapor bubbles. The two cameras will provide additional accuracy for bubble measurements. The subcooling experiments will provide information concerning vapor formation where condensation may limit the net rate of production. The second camera provides the coverage necessary to measure this rate. Table 10-4 shows the data points which can be measured in this experiment.

Sequence

Experimentation should begin with the lowest gravity level, 10^{-5} g/g_e since this gravity level is considered to have the highest priority. Then the 10^{-3} g/g_e and 10^{-4} g/g_e experiments follow in that order. The subcooled liquid experiments for each gravity level begin immediately after the saturated boiling experiment at that level. The tank pressure rise which is necessary to subcool the liquid can be achieved by heating the ullage with a resistance heater. If further investigation indicates that this approach is unsuitable, a pressurization system will be required.

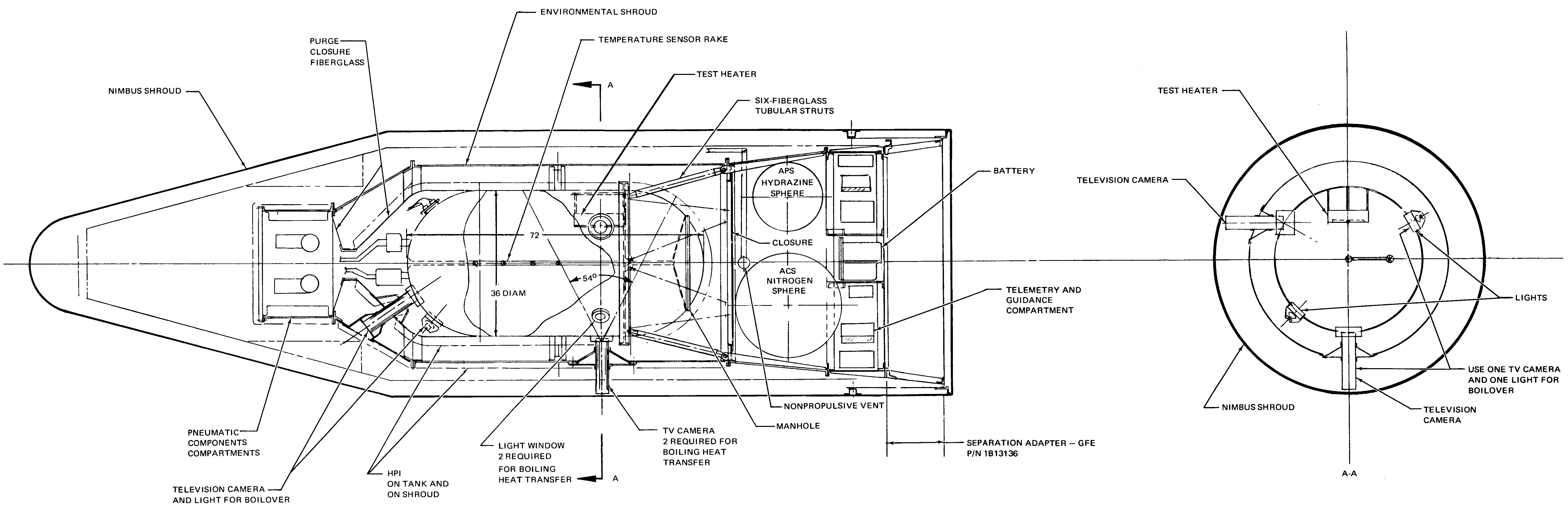

Figure 10-10. Boiling Heat Transfer Experiment and Boilover Entrainment Experiment

IC-22-2 IC-22-3

Table 10-4 (Page 1 of 2)

700- AND 1600-POUND EXPERIMENT DATA POINTS

Experiment Number	g/g_e	Heat Flux Btu/hr ft^2	Total Test Time (hrs)	Heater Power (watts)	Energy Used watt-hrs
1600-1	10^{-3}	0.03	0.90	0.006	0.005
1600-2		0.10	0.50	0.03	0.02
1600-3		1.0	0.33	0.29	0.10
1600-4		10.0	0.33	2.4	0.97
1600-5		100	0.33	29	9.67
1600-6		1000	0.33	290	96.7
1600-7	10^{-3}	5000	0.33	1470	490
			3.05		687.47
1600-8	10^{-4}	0.01	3.00	0.003	0.009
1600-9		0.10	1.30	0.03	0.04
1600-10		1.00	0.50	0.29	0.15
1600-11		10.0	0.33	2.9	0.97
1600-12		100	0.33	29	9.67
1600-13		320	0.33	94	31.3
1600-14		1000	0.33	290	96.7
1600-15		2000	0.33	580	193
1600-16		3000	0.33	870	290
1600-17		1000	0.33	290	96.7
1600-18		100	0.33	29	9.67
1600-19	10^{-4}	10	0.33	2.9	0.97
			9.37		729.17

Table 10-4 (Page 2 of 2)

700- AND 1600-POUND EXPERIMENT DATA POINTS

Experiment Number	g/g_e	Heat Flux Btu/hr ft^2	Total Test Time (hrs)	Heater Power (watts)	Energy Used watt-hrs
1600-44	10^{-5}	0.005	10.0	0.002	0.015
1600-45		0.01	8.00	0.003	0.023
1600-46		0.40	1.80	0.12	0.216
1600-47		2.0	1.50	0.6	0.9
1600-48		10.0	1.20	2.9	0.97
1600-49		100	0.33	29	9.67
1600-50		320	0.33	94	31.3
1600-51		1000	0.33	290	96.7
1600-52		1500	0.33	435	145
1600-53		320	0.33	0.4	31.3
1600-54		10	0.33	2.9	0.97
1600-55	10^{-5}	1	1.60	0.29	0.48
			26.08		317.54

Instrumentation

The instrumentation for this package is essentially the same as that for the 350-lb experiment with the exception of the television cameras. Platinum resistance thermometers in the liquid and the heater, pressure sensors and other instrumentation basic to a boiling experiment are required.

To conserve power it may be necessary to record data for only a fraction of each experiment period. This can be accomplished by turning the recorder off except at the beginning and end of the experiment. However, it will probably be necessary to check the time it takes to reach steady state in the boiling regime since these times have not been determined analytically. This can be done by monitoring one or two experiment points in orbit until an approximate time scale is determined. This would be accomplished by direct telemetry.

Heater Design

The previous discussion on heater design also applies for this payload. The only difference is that an increased heater length can be accommodated by the larger tank. A heater, one foot in length, is proposed.

Power

Two batteries (Saturn type, 12 Kw Hrs each) are required for the experiment package. Table 10-5 shows a power consumption of 17.8 Kw Hr.

Summary

Table 10-5 summarizes the 1,600-lb payload experiment package components. The 1,369-lb payload weight appears quite reasonable and the electrical energy requirement can be met by two batteries. Additional sequencing will be required to efficiently record and telemeter the data.

10.4 EXPERIMENT ANALYSIS

The experiment limitations determined in Project Thermo Phase B were necessarily considered in developing the conceptual designs for the three payloads. As a result much of the experiment analysis was taken directly from this work (Reference 2-7). The following discussion summarizes the results of the analysis for the present study.

Table 10-5

1,600-POUND PAYLOAD EXPERIMENT COMPONENTS

Item	Weight (lb)	Power (watts)	Energy (watt-hrs)
Guidance Sensor and Computer	20	30	5040
Sequencer	10	0.45	75
Antenna Beacon	4	3.9	672
TM Command Receiver	3	6	1008
Tank (all)	400		
94 Channel Recorder (TM)	73	210 (record) 105 (playback)	2100
94 Transducers	47		
ACS	190		
APS	250		
Heater	10	1470 (maximum)	3828
Battery (2)	310		
TV System			
Transmitter	18	50	1400
Power Amplifier	2	140	1400
Camera and Controls (2)	20	24	240
Lights (2)	6	200	2000
Multiplexer	6	9	90
	1369		17,765

10.4.1 Propellant Utilization

The propellant consumption rate for the boiling heat transfer tank was estimated using the same basic approach as in Phase B. The wall heat flux was assumed to be 0.2 Btu/hr-ft^2 using HPI. However, for the early part of the mission where helium gas still remains in the insulation, an integrated heat input is used. Values for this energy input as well as that for the heat shorts and electrical leads were taken from Section 6 since they are also representative of the boiling tank. Here an input of 7.5 Btu/hr was used. The heat leak estimated through a 4-in. window of 3 Btu/hr from Project Thermo was also used. The heat from the windows used for illumination was assumed to be equal to the energy output of the light. The electrical energy of the test heater was included in estimating the total boiloff. These values were taken directly from the tables of experiments which include the energy consumption. Figure 10-11 summarizes the results, by illustrating the liquid level drop as a function of time for each of the three payloads.

10.4.2 Photographic Limitations

Although a rough order of magnitude analysis is necessary when considering photographic techniques, an actual test arrangement usually is necessary to verify a photographic design. The pilot test of Project Thermo illustrated this fact where due to the restrictions of 1-in. windows, the lighting became a serious problem.

Standard depth of field and resolution calculations were made to check the feasibility of the present design. A thousand lines for a television screen indicates that there is a 0.012-in. space between lines for a 12-in. field of view. This suggests that a bubble diameter less than 0.05 in. in diameter will be difficult to resolve. Also, the depth of field should be of the order of the heater width which will be approximately 6 inches. If a 12-in. field of view is required with a 24-in. camera to object distance, then a 0.75-ft depth of field is obtained with an f:4 opening. Lighting requirements will have to be verified by test.

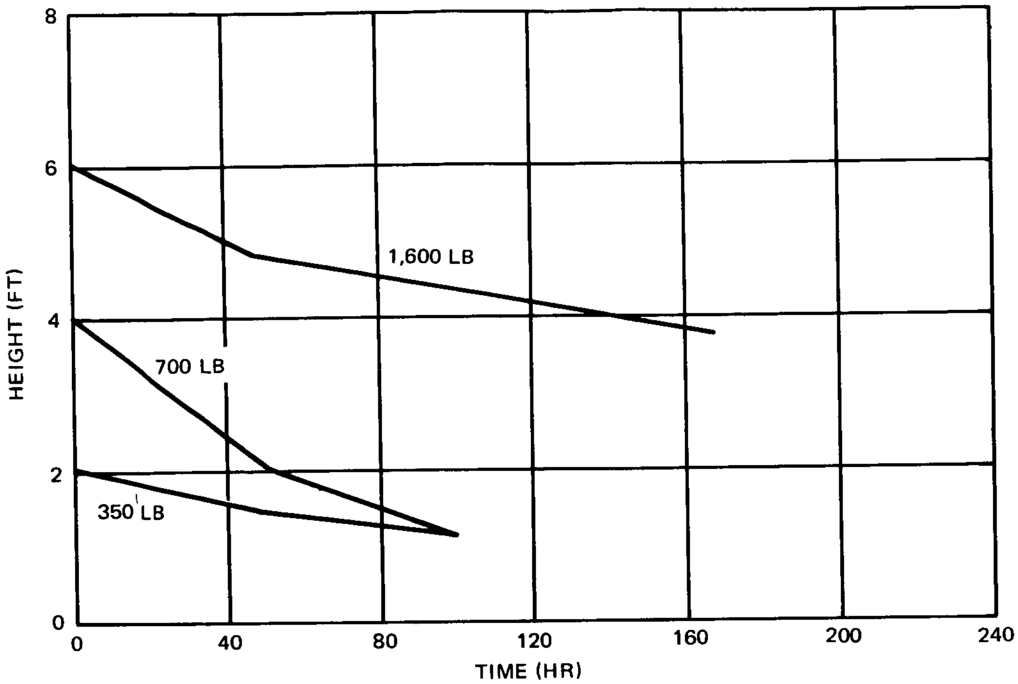

Figure 10-11. Boiloff Losses

10.4.3 Error Analysis

The following discussion supplements the error analysis performed during Phase B.

One possible form of a boiling correlation is

$$q = C\Delta T^{b} (g/g_{e})^{n} \tag{10-1}$$

where

$$\frac{\Delta q}{q} = 1 - \left(\frac{g_2}{g_1}\right)^{n} \tag{10-2}$$

for a fixed ΔT. This indicates the spacing between boiling curves at g_1 and g_2 as a function of n.

The error in q or $\frac{\Delta q}{q}$ can arise from measurement errors in q or from measurement errors in ΔT which can be expressed in terms of $\frac{\Delta q}{q}$ using equation (10-1). Assuming that the error in ΔT is $\pm\delta$, then $\left(\frac{\Delta q}{q}\right)_{\Delta T\text{-error}}$ is $\left(\frac{\delta b}{\Delta T}\right)$

Figure 10-12 shows both values of $\left(\frac{\Delta q}{q}\right)_{error}$ as dotted lines. Since $\left(\frac{\Delta q}{q}\right)_{\Delta T\text{-error}}$ is a function of b, several curves are drawn where b is an experimentally determined value which usually varies between 2 and 4. Values for $\delta/\Delta T$ were taken from the instrumentation list (Section 10.5). The curves, based on equation (10-2), show the minimum value of n above which an effect of gravity on boiling can be observed. Note that the above approach is conservative since $\left(\frac{\Delta q}{q}\right)_{\Delta T\text{-error}}$ only provides the spread in the data. Hence, data for two different curves could overlap and yet each curve may statistically be considered distinct from one another.

10.5 INSTRUMENTATION LIST

The instrumentation list of Table 10-6 is that required for the 1,600-lb experiment package. The instruments called out are similar to those in the Project Thermo B Phase study. Six heater temperature sensors are listed to cover the ΔT range from 0 to 50°R. Some testing will probably be required to insure that six sensors can be installed and operated in a single heater. Direct telemetry of ΔT values requires one or two additional sensors. Liquid sensors are used to indicate the amount of subcooling in the liquid as a function of location.

Two television cameras are required for two fields of view. The previous photographic discussion has considered fixed lenses with a 12-in. field of view. A zoom lens capability, if it would not introduce serious technical problems, would improve the resolution capabilities considerably. Then small bubble phenomena could be observed. Furthermore, more latitude for matching the field of view to the relevant occurrence would be available.

One other instrument, not listed here, which would be of considerable importance to the boiling experiment is an accelerometer. Correlation of measured ACS perturbations or vibrations to the observed bubble phenomena

Table 10-6

INSTRUMENTATION REQUIREMENTS FOR BOILING HEAT TRANSFER EXPERIMENTS

Measurement Title	No. Required	System Range/Accuracy		Frequency Response	Environment at Point of Measurement	
					Media	Temperature
Temperature LH_2 Liquid	6	35-45 ± 0.3°R	(±3%)	1 cps (4 sps)	LH_2, GH_2	37 to 630°R
Temperature LH_2 Ullage	2	30-230 ± 6°R	(±3%)	1 cps (4 sps)	LH_2, GH_2	37 to 620°R
Temperature Htr Surf/ Liq Diff	1(2)	0-1 ± 0.03°R	(±3%)	1 cps (4 sps)	LH_2, GH_2	37 to 620°R
Temperature Htr Surf/ Liq Diff	3	1-5 ± 0.12°R	(±3%)	1 cps (4 sps)	LH_2, GH_2	37 to 620°R
Temperature Htr Surf/ Liq Diff	1	5-10 ± 0.12°R	(±3%)	1 cps (4 sps)	LH_2, GH_2	37 to 620°R
Temperature Htr Surf/ Liq Diff	1	10-50 ± 1.2°R	(±3%)	1 cps (4 sps)	LH_2, GH_2	37 to 620°R
Pressure LH_2 Boil Ht Trans Ullage	2	0-50 ± 0.25 psia	(±1/2%)	1 cps (4 sps)	GH_2, LH_2	37 to 620°R(1)
Level Liq (Loading)	6	Liq/Vapor Indicator	(±3%)	1 cps (4 sps)	LH_2, GH_2	37 to 620°R
Level Liq Continuous(3) (RF)	1	TBD	(±4%)	1 cps (4 sps)	LH_2, GH_2	37 to 620°R
TV	2	TBD				

Note:

(1) Sensing line must isolate transducer to provide -60 to +165°F environment.

(2) Relative differential temperature resolution is primary accuracy requirement--absolute temperature accuracy is not as critical.

(3) Experimental Measurement.

(4) Heater power varies from 0.001 to 1400 watts in steps.

would no doubt result in easier interpretation of the photographic results. Additional instrumentation required to provide values of the tank pressure, the liquid level and the heat flux are also indicated.

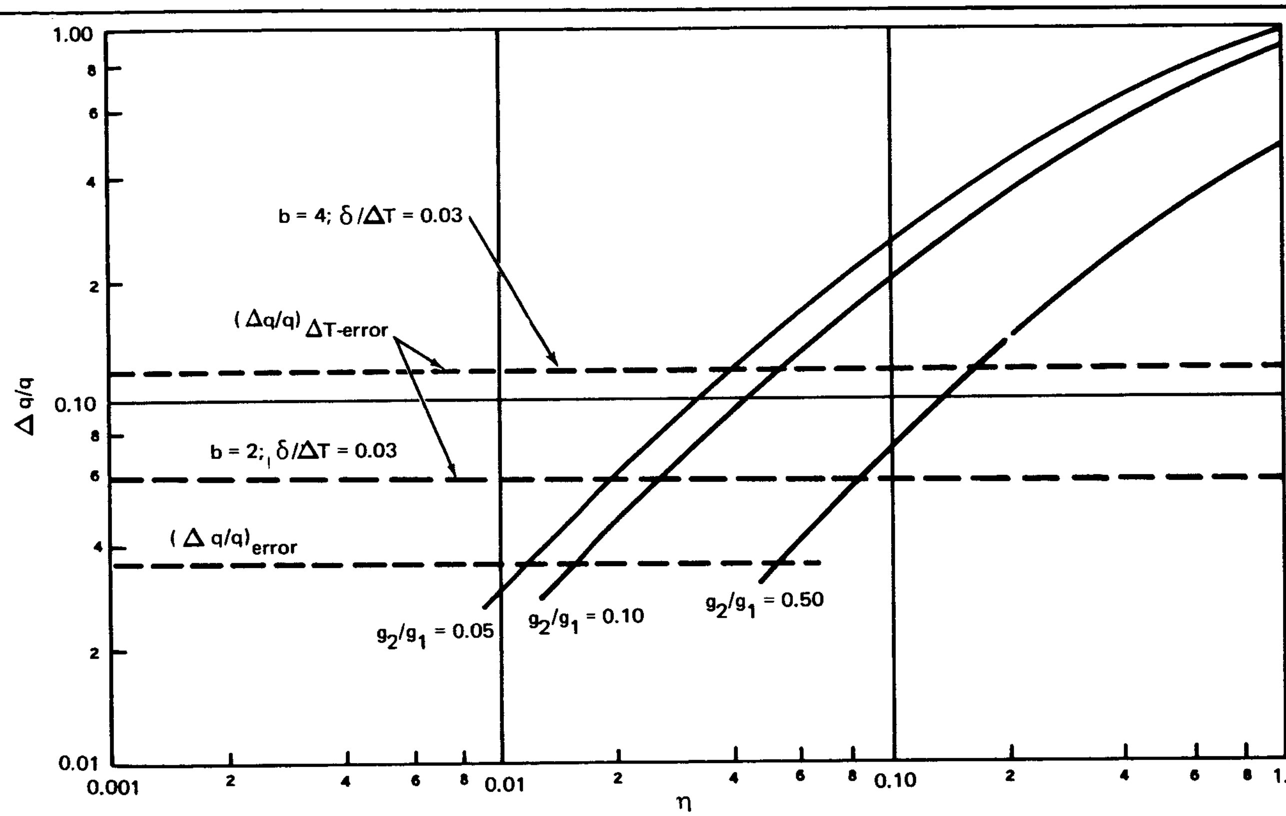

Figure 10-12. Comparison of $\Delta q/q$ with $(\Delta q/q)_{error}$ and $(\Delta q/q)_{\Delta T\text{-}error}$ Based on $\Delta q/q = 1 - (g_2/g_1)^n$

Section 11
EXPERIMENT COSTS AND SCHEDULE

11.1 EXPERIMENT COST

The definition of cost effective individual experiment packages rested upon the utilization of available flight-qualified equipment, wherever possible. Also, during the experiment conceptual design effort, commonality of experiment subsystems, between experiment packages, was emphasized to provide a foundation program. The conceptual design drawings (Section 5 through 10) graphically demonstrate the resulting subsystem similarities.

It is estimated that each recommended experiment conceptual design shown in the respective technological sections will cost about $6.5 million to design, develop, and fly two articles plus a ground test article. This one figure, independent of experiment, is meaningful due to system similarities. The only differences between experiments are basically the tankage and instrument sensors, a relatively small perturbation on the cost shown.

A two-year design-to-flight program was assumed with 2-1/2 units of each package fabricated; two flight units and a partial ground test unit. Booster and fairing costs were excluded.

A great reduction in total experimentation costs will be achieved through consideration and design of each experiment package as part of an overall program. Extensive benefits will accrue to NASA through the cost trade-offs involved by taking advantage of the "built-in" system similarities.

Much of the basic engineering expended for one experiment is directly applicable to the others. This is particularly true for the design of the equipment section and booster-spacecraft interface adapters and separation system. The propulsion, telemetry, power distribution, insulation, basic spacecraft structure, LH_2 manhole cover seals, and guidance systems design efforts are also essentially common and applicable to each experiment. Electronic checkout, GSE, and launch support servicing hardware will also be similar in many cases. Tankage-tooling similarities are also inherent in the designs.

In the area of development and qualification, the basic spacecraft commonality also provides extensive program cost reduction benefits. Much of the development and testing for the following items need be accomplished only once: APS, ACS, attitude sensors, basic guidance electronics, programmer, telemetry, transmitters, power distribution system, antenna, thermal shroud, some valving and plumbing, windows and the vent system. In short, most of the electronic equipment, propulsion and basic structural packages.

In light of the above, it is recommended that a further study be accomplished with the objective of ascertaining the details of a plug in-plug out spacecraft equipment and propulsion section which may be readily modified for individual experimentation. This work should also result in the definition and costing of a total overall flight program which includes all the experimentation shown necessary herein for the Mars vehicle development and design programs.

11.2 PROGRAM SCHEDULE

Table 11-1 presents a typical schedule to design, develop, test, fly, and evaluate an orbital experiment. This schedule is believed to be applicable to all of the experiments, since the schedule is constrained by engineering and manufacturing, and all of the experiments are similar in complexity. The development of new hardware has been minimized, which results in a flight in 20 months with data reduction complete in 24 months.

Table 11-1

TYPICAL PROGRAM SCHEDULE FOR THERMO EXPERIMENTS

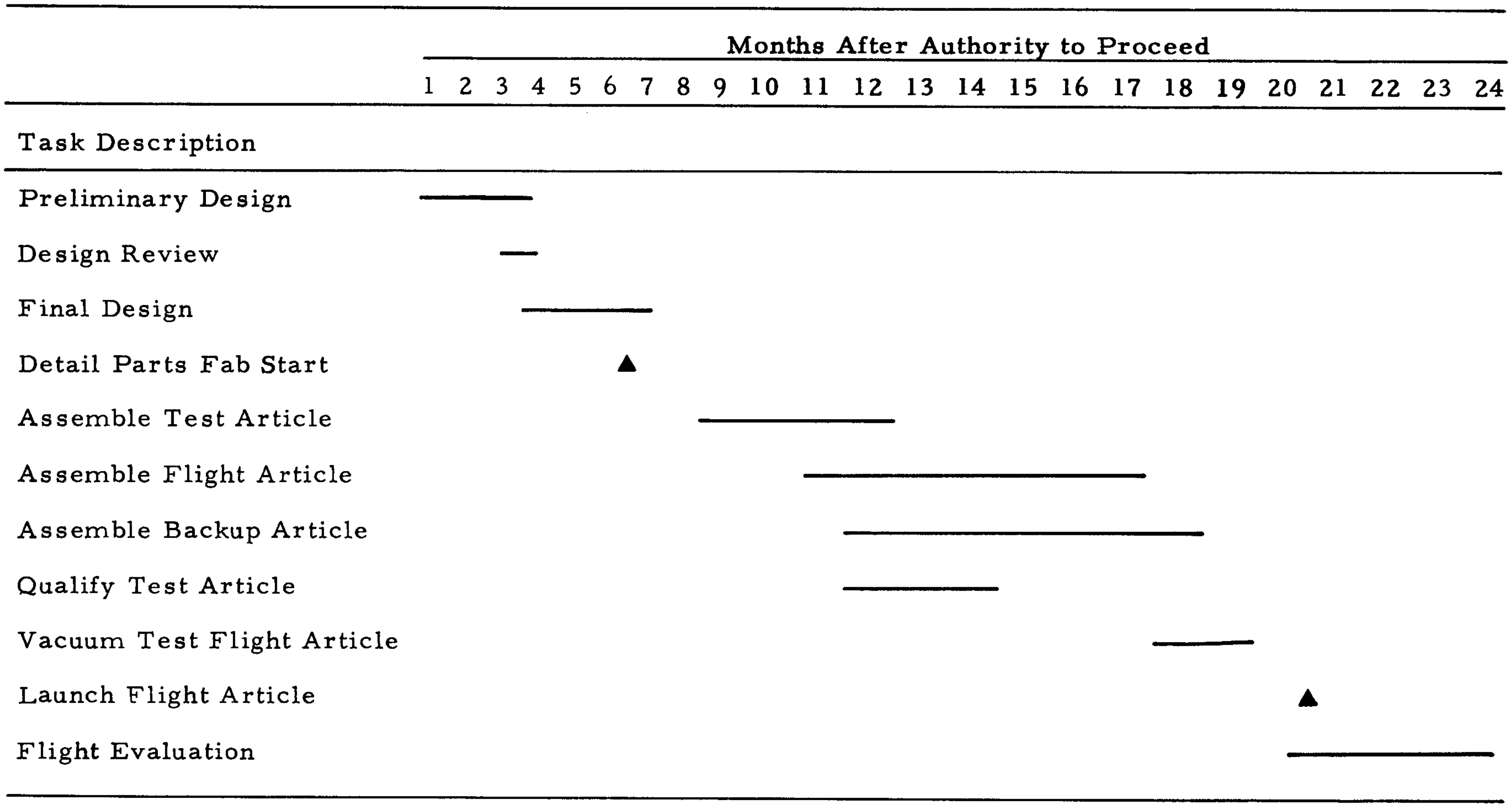

Section 12

REFERENCES

Section 2

2-1 W. J. Normyle. Manned Mars Flights Studied for 1970's. Aviation Week & Space Technology, March 27, 1967, pp 62-67.

2-2 NAA Mission Study Briefing, June 1967.

2-3 Feasibility of Modifying the S-IVB Stage as an Injection Stage for Manned Planetary Flyby Missions. Douglas Aircraft Company, Douglas Report DAC-57997, April 1967.

2-4 Nuclear Stage Design Study. Douglas Aircraft Company, Douglas Report DAC-57976, January 1967.

2-5 Modification of S-IIB Stage as an Injection Stage. North American Aviation, Inc., Report No. SID 67-275-6, April 1967.

2-6 R. B. Carpenter, Jr. Reliability and Maintainability, Part 5 — Space: Manned Interplanetary Travel, Mechanical Engineering, June, 1966.

2-7 Thermo and Hydrodynamic Experiment Research Module in Orbit, Final Report, Contract NAS 8-18053, Douglas Aircraft Company Report DAC-60594, March 1967.

2-8 L. R. Koval and P. G. Bhuta. An Analytical Study of Liquid Outflow from Cylindrical Tanks during Weightlessness, NASA CR-54974, June 1, 1966.

2-9 M. A. Saad and D. A. Oliver. Linearized Time-Dependent Free Surface Flow in Rectangular and Cylindrical Tanks. Proceedings of the Heat Transfer and Fluid Mechanics Institute, 1964.

2-10 D. F. Gluck, et al., Distortion of the Liquid Surface During Tank Discharge under Low-g Conditions. Presented at AIChE 55th Annual Meeting, Houston, Feb. 1965.

Section 3

3-1 The Scout; August 1966 Revision. LTV Astronautics Division, Ling-Tempo-Vought Aerospace Corporation, Dallas, Texas.

3-2 Delta Payload Planner's Guide. Douglas Aircraft Company, Inc., Santa Monica, California.

3-3 1 on the Side, 2 on Top, 3 in Orbit; October 1965. The Convair Division of General Dynamics Corporation, San Diego, California.

3-4 Convair Fairing Systems. The Convair Division of General Dynamics Corporation, San Diego, California.

3-5 Atlas Launch Vehicle Family for Spacecraft Contractor Planning, Report No. GDC-BJG 67-002. The Convair Division of General Dynamics Corp., San Diego, California, April 1967.

3-6 Burner II General Description, The Boeing Company, Report D2-82601-1, August 1966.

3-7 Burner II Performance Handbook, The Boeing Company, Report D2-82601-2, August 1966.

3-8 Burner II--A Versatile Upper Stage, The Boeing Company, Report D2-82678-2, November 1966.

3-9 DSV-2L Space Booster--Payload Planners Guide, Douglas Aircraft Co., Report SM 44155, revised December 1966.

3-10 Smithsonian Institute Astrophysical Observatory Special Report 170, 30 December 1964.

3-11 Journal Atmospheric Sciences, Vol. 22, Pages 462-463, 29 March 1965.

3-12 Lockheed Report LMSC-448514, October 1961.

Section 4

4-1 Saturn S-IVB-203 Stage Flight Evaluation Report, Volume II (DAC Report SM-46988).

Section 6

6-1 E. D. Marion. High-Performance Insulation System Development. Douglas Report No. SM-48806, October 1965.

6-2 N. R. Folkman and T. G. Lee. Thermodynamic Design Fundamental of High Performance Insulation. Douglas Paper No. 4169, April 1967.

6-3 J. C. Cody and E. H. Hyde. Thermal Problems Associated With the Development of a Flight Configured Cryogenic Insulation System. Proceedings of the Conference on Long-Term Cryo-Propellant Storage in Space, October 1966.

Section 7

7-1 Holmes, L. A., and Schwartz, S. H., "The Thermodynamics of Space Storage of Liquid Propellants," presented at the 13th Annual Technical Meeting, Institute of Environmental Sciences, Washington, D. C., April 10-12, 1967.

7-2 Stevens, R. A., Westerheide, D. E., and Poth, L. J., "Study of Cryogenic Propellant Stratification Reduction Techniques," Quarterly Progress Report, 1 August 1966 through 31 October 1966. Report FPR-027-6, General Dynamics, Fort Worth Division, 15 November 1966.

7-3 Sterbentz, W. H., "Liquid Propellant Thermal Conditioning System," Interim Report, Contract NAS3-7942, April 20, 1967.

7-4 Neff, B. D., "Free Convection in a Container of Cryogenic Fluid," M.S. Theses, Denver University, 1965.

7-5 Evans, L. B., Reid, R. C., and Drake, E. M., "Transient Natural Convection in a Vertical Cylinder," presented at the 61st National Meeting, AIChE, Houston, Texas, February 19-23, 1967.

Section 8

8-1 G. C. K. Yeh and N. Zuber. On the Problem of Liquid Entrainment. Report ANL-6244, Argonne National Laboratory, Argon, Illinois, 1960.

8-2 L. S. Sterman. The Generalization of Experimental Data Concerning the Bubbling of Vapor Through Liquid. Soviet Physics--Technical Physics, Vol. 1, 1957, Page 1479.

8-3 L. S. Sterman. The Theory of Steam Separation. Soviet Physics, Technical Physics, Vol. 3, 1959, Page 1440.

8-4 S. J. Kline and F. A. McClintock. The Description of Uncertainties in Single Sample Experiments. Mech. Engr., Vol. 75, January 1953.

Section 9

9-1 Study of Cryogenic Container Thermodynamics During Propellant Transfer, Lockheed Missile & Space Company Report No. A820996, Contract No. NAS8-20362, October 15, 1966.

Section 10

10-1 Siegel, R., "Transient Free Convection from a Vertical Flat Plate," Trans. ASME, Vol. 80, 1958, pp. 347-359.

10-2 Fritz, W., "Berechnung des Maximalvolumens von Dampfblasen," Physik Zeitschrift, Vol. 36, p. 379, 1935.

10-3 Chin, J.H., et al., Progress Reports, Contract NAS8-11525, "Analytical and Experimental Study of Liquid Ullage Coupling and Low Gravity Interface Stability," 1963-1966.

10-4 Hirata, M., and Nishiwaki, N., "Skin Friction and Heat Transfer for Liquid Flow Over a Porous Wall with Gas Injection," Int. Journal Heat Mass Transfer, Vol. 6, 1963, pp. 941-949.

10-5 Petrick, M., "Investigation of Two-Phase Air-Water Flow Phenomena," ANL 5787, 1958.

10-6 Schwartz, S.H., "Saturated Pool Boiling of Water in a Reduced Gravity Environment," Ph. D. Dissertation, University of Southern California, 1966.

10-7 Siegel, R., and Keshock, E. G., "Effects of Reduced Gravity in Nucleate Boiling, Bubble Dynamics in Saturated Water," Presented at AIChE, 51st Natial Meeting, San Juan, Puerto Rico, 1963.